CHARLES UNIVERSITY IN PRAGUE
FACULTY OF SCIENCE

PhD. study program: Molecular and Cellular Biology, Genetics and Virology

Mgr. Jiří Pergner

Evolution of light detection in chordates

Evoluce vnímání světla u strunatců

PhD. Thesis

Supervisor: RNDr. Zbyněk Kozmik, Csc.

Prague 2018

Statement/Prohlášení

I hereby declare that I did not use this PhD. thesis to acquire another academic degree. Furthermore, I declare that I have worked on my PhD. thesis independently, under the supervision of Dr. Zbyněk Kozmik and that I have cited correctly all used information sources and publications.

Svým podpisem stvrzuji, že jsem předloženou dizertační práci nepoužil k získání jiného akademického titulu. Dále prohlašuji, že jsem na vypracování této dizertační práce pracoval samostatně pod vedením školitele RNDr. Zbyňka Kozmika, Csc. a správně jsem uvedl všechny použité informační zdroje a literaturu.

In Prague/v Praze …… ……

Jiří Pergner

Acknowledgements

In the first place I would like to thank to my supervisor Dr. Zbyněk Kozmik, for all the time he spent with me discussing my projects, providing numerous ideas that helped with pushing my work forward and getting funding for my research.

Besides my supervisor I would like to thank to all my lab mates (and almost friends) from the Department of Transcriptional Regulation, with whom I spent days and nights working on moving the knowledge of the mankind forward. Namely, I would like to express my thanks to Peter Fabian, Jan Mašek and Bára Antošová my PhD. fellows and Vladimír Soukup, my fellow during work with amphioxus. Next, I would like to thank to Pavel Vopálenský, Michaela Liegertová, Chrysoula N. Pantzartzi, Iryna Kozmiková, Antonio R. Pombinho (former member of the Department of Cell Differentiation), Jan Pačes, Hynek Strnad, Čestmír Vlček (all three members of Dpt. of Genomics and Bioinformatics), Petr Bartůněk (Dpt. of Cell Differentiation) and Matteo Bozzo (visiting student from Italy), with whom I had the honor to work on preparation of scientific papers during my PhD. studies.

Next, I would like to thanks to Veronika Nosková, Jitka Láchová, Anna Zitová, Veronika Kovácsová and Katarína Kováčová who provided technical support for my work.

I am also grateful to Radim Žídek, Simona Macháčová, Simona Mršťáková and Miroslava Kolková for help with amphioxus maintenance.

I would like to acknowledge Vladimír Soukup and Chrysoula N. Pantzartzi for reading and improving the first version of this thesis.

Last but not least, I cannot thank enough to my family, mainly my wife Tereza Pergnerová and my son Jiří Pergner, for supporting me during my almost never-ending PhD. studies.

Work on this thesis was supported by grants P305/10/2141, P305/10/J064, 17-15374S, 15-21285J awarded by the Czech Science Foundation; grants nr. LO1220, LQ1604 NPU II and BIOCEV-CZ.1.05/1.1.00/02.0109 awarded by the Ministry of Education, Youth and Sports of the Czech Republic and IMG institutional support RVO 68378050. I acknowledge the Microscopy Centre - Light Microscopy Core Facility, IMG ASCR, Prague, Czech Republic, supported by grants (Czech-Bioimaging – MEYS LM2015062), “Centre of Model Organisms” OPPK (CZ.2.16/3.1.00/21547) and “Biomodels for health” (LO1419), for their support with the confocal imaging.

Abstract

Light detection is one of the crucial abilities of all animals. The light cues are important e.g. for maintaining of circadian rhythms, regulation of spawning cycles, changes of pigmentation and arguably most importantly for vision. Most animals detect light by opsins, members of the G protein coupled receptors superfamily.

Amphioxus belongs to earliest branching chordate clade, cephalochordates. Thanks to their phylogenetic position, physiology and morphology, cephalochordates became the most relevant model organism for understanding the evolutionary origins of vertebrate specific traits. Amphioxus evince various reactions to light throughout its development.

In the presented thesis light detecting systems of amphioxus were studied thoroughly. More specifically characterization of the opsin gene repertoire of two amphioxus species *Branchiostoma floridae* and *Branchiostoma lanceolatum* and their comparison with opsins from other animals is presented. In addition, remarkable similarity on the gene expression level between one of amphioxus visual organs, so called frontal eye, and neurons and retinal pigmented epithelium in vertebrate retina was shown. These data confirm the long time ago proposed homology between amphioxus frontal eye and vertebrate lateral eyes.

Taken together all the presented data help with getting insights into the evolution of light detection in vertebrates and more broadly in putative chordate ancestor.

Abstrakt

Vnímání světla je jednou ze základních vlastností živočichů. Světelné signály jsou pro ně důležité např. pro udržování cirkadiárních rytmů, regulaci rozmnožovacích cyklů, provedení změn v pigmentaci a pravděpodobně nejdůležitěji ze všeho pro vidění. Většina zvířat vnímá světlo za pomocí opsinů, členů proteinové superrodiny G protein spřažených receptorů.

Kopinatec je zástupcem bezlebečných, nejbazálnějšího podkmene strunatců. Díky jejich fylogenetické pozici, morfologii a fyziologii se bezlebeční stali nejlépe použitelným modelovým organizmem pro porozumění evoluce obralovců a jejich specifických znaků. Během svého vývoje kopinatec vykazuje mnoho různorodých reakcí na světlo.

Tato dizertační práce se zabývá studiem světločivných orgánů a opsinů v kopinatci. Do větší hloubky je zde probrán repertoár opsinových genů ve dvou druzích kopinatce, kopinatci floridském (*Branchiostoma floridae*) a kopinatci plžovitém (*Branchiostoma lanceolatum*) a jejich porovnání zejména s opsiny v obratlovcích. Dále jsou prezentována data ukazující pozoruhodnou podobnost na úrovni genové exprese mezi vizuálním orgánem kopinatce, tzv. předním okem, a neurony a pigmentovým epitelem v oku obratlovců. Tato data potvrzují dlouho předpokládanou homologii mezi předním okem kopinatce a okem obratlovců.

Celkově předložená data napomáhají s vhledem do evoluce vnímání světla u obratlovců a šířeji vzato u předka všech strunatců.

Contents

1. Preface

Light detection is one of the crucial abilities of most organisms on earth. Light cues are used by animals e.g. for regulation of circadian rhythm, spawning cycles and arguably most importantly for vision guided behavior.

Most animals use for light detection specially adapted neuronal cell type – photoreceptor cell. Photoreceptor cells usually have enlarged cell membrane with incorporated photosensitive pigment to achieve higher sensitivity by increasing the probability of catching photon. Two main photoreceptor types can be distinguished based on their cellular ultrastructure: ciliary photoreceptors (expanding their surface by modifying a cilium) and rhabdomeric photoreceptors (expanding their surface by microvilli). Almost complete dichotomy exists in employment of these photoreceptor cell types in animal visual organs. Ciliary photoreceptors serve as visual photoreceptors in the vertebrate eyes (with some exceptions, e.g. jellyfish, fan worms or molluscs eyes), while rhabdomeric photoreceptors are used in the eyes of invertebrates.

Various types of eyes can be found throughout the animal kingdom, from the most simple ones consisting of one photoreceptor cell and adjusting shielding pigment cell (in extreme cases both functions can be found in one cell) to very sophisticated eyes, e.g. the compound eyes of insect, or vertebrate camera eyes. The huge diversity of eyes as well as their complexity was always puzzling scientists since the Darwin´s times. It was proposed that eyes evolved independently at least 40 or even 65 times in various animal lineages (reviewed by Fernald[1]). On the other hand discoveries in the early 1990´s showed that Pax6 gene is crucial for the development of vertebrate[2] as well as invertebrate eyes[3] and its ectopic expression can induce development of ectopic eyes both in invertebrates[4] and in vertebrates[5]. This started the discussion about possible monophyletic origin of various eye types or at least the photoreceptor cells found in diverse eyes and the role of Pax6 as a "master control gene of eye development" (proposed by Gehring and Ikeo[6]). Later several cases of Pax6 independent photoreceptor development were documented, e.g. the rhabdomeric photoreceptors of amphioxus[7], the adult eyes of marine annelid *Platynereis*[8] or the eyes of horse-shoe crab *Limulus*[9]. The view on eye evolution was thus revised and nowadays the generally accepted view is that it is impossible to argue for mono- or polyphyletic origin of eyes, since gene sharing, convergence and parallelism can be found in development of various eye types[10].

Branchiostoma species (alternatively called amphioxus or lancelets) are representatives of cephalochordates, the most basally branching chordate subphylum. Amphioxus possesses four types of visual organs – frontal eye and lamellar body formed by ciliary photoreceptors and Joseph cells and dorsal ocelli formed by rhabdomeric photoreceptors. For the purpose of this thesis, the frontal eye is the most interesting. The frontal eye has always been considered as being the homolog of vertebrate lateral eyes, mainly due to its position at the tip of the neural tube and ciliary morphology (even though the frontal eye is not a paired organ as the vertebrate eyes).

The aim of this PhD. thesis was to gain new data about photoreceptive organs in amphioxus (with special attention to amphioxus frontal eye) and amphioxus opsins and thus provide some insights into evolution of vertebrate photoreceptors. This thesis is based on four

published/accepted original scientific publications, one review (with original data included) accepted for publication and one submitted manuscript:

1. Molecular analysis of the amphioxus frontal eye unravels the evolutionary origin of the retina and pigment cells of the vertebrate eye.
   Vopalensky P, Pergner J, Liegertova M, Benito-Gutierrez E, Arendt D, Kozmik Z.
   Proc Natl Acad Sci U S A. 2012 Sep 18; 109(38):15383-8. Epub 2012 Sep 4.

2. Cubozoan genome illuminates functional diversification of opsins and photoreceptor evolution.
   Liegertová M*, Pergner J*, Kozmiková I, Fabian P, Pombinho AR, Strnad H, Pačes J, Vlček Č, Bartůněk P, Kozmik Z.
   Sci Rep. 2015 Jul 8;5:11885.
   * Equal contribution

3. The opsin repertoire of the European lancelet: a window into light detection in a basal chordate.
   Pantzartzi CN*, Pergner J*, Kozmikova I, Kozmik Z
   Int. J. Dev. Biol. 61: 763-772 (2017)
   * Equal contribution

4. Novel polyclonal antibodies as a useful tool for expression studies in amphioxus embryos.
   Bozzo M*, Pergner J*, Kozmik Z, Kozmikova I
   Int. J. Dev. Biol. 61: 793-800 (2017)
   *Equal contribution

5. Photoreceptors of amphioxus - insights into evolution of vertebrate opsins, vision and circadian rhythmicity. (review)
   Pergner J, Kozmik Z
   Int. J. Dev. Biol. 61: 665-681 (2017)

6. Opsin genes in the genus *Branchiostoma*: lost and found in transposition
   Pantzartzi CN, Pergner J, Kozmik Z
   Manuscript in revisions in Scientific Reports

2. List of abbreviations

2RWGD	two rounds of whole genome duplication
aa	amino acid
BMP	bone morphogenetic protein
CNG	cyclic nucleotide-gated (channels)
CNS	central nervous system
DNA	deoxyribonucleic acid
DO/DOs	dorsal ocellus/dorsal ocelli
dpf	days post fertilization
EM	electron-microscopical
evo-devo	evolutionary developmental biology
FE	frontal eye
GPCR	G-protein coupled receptor
hpf	hours post fertilization
ipRGCs	intrinsic photosensitive retinal ganglion cells
ISH	RNA *in situ* hybridization
JCs	Joseph cells
LB	lamellar body
MHB	midbrain-hindbrain boundary
mya	million years ago
PDE	phosphodiesterase
PigmC	pigment cell
PRCs	photoreceptor cells
ProjN	projecting neurons
RNA	ribonucleic acid
TRP	transient receptor potential (channels)
ZLI	zona limitans intrathalamica

3. Literature overview

3.1. Amphioxus – the best extant proxy for a chordate ancestor

Cephalochordates are the most basally branching group of chordates[11], consisting of three genera, *Branchiostoma*, *Asymmetron* and *Epigonichthys*. Cephalochordates can be found worldwide, inhabiting shallow sea waters. Amphioxus embryos and larvae are planktonic, while adults are benthic, spending most of their live buried in the sand burrow with only the anterior part facing out, enabling filter feeding. Amphioxus body exhibit characteristics typical for extant as well as extinct chordates, e.g. perforated pharynx, hollow through gut, segmented muscles and gonads, dorsally located notochord and neural tube and tail fin[12]. On the other hand, amphioxus lacks typical vertebrate-specific structures, e.g. paired sensory organs (image forming eyes, ears), paired appendages, neural crest cells and placodes[12].

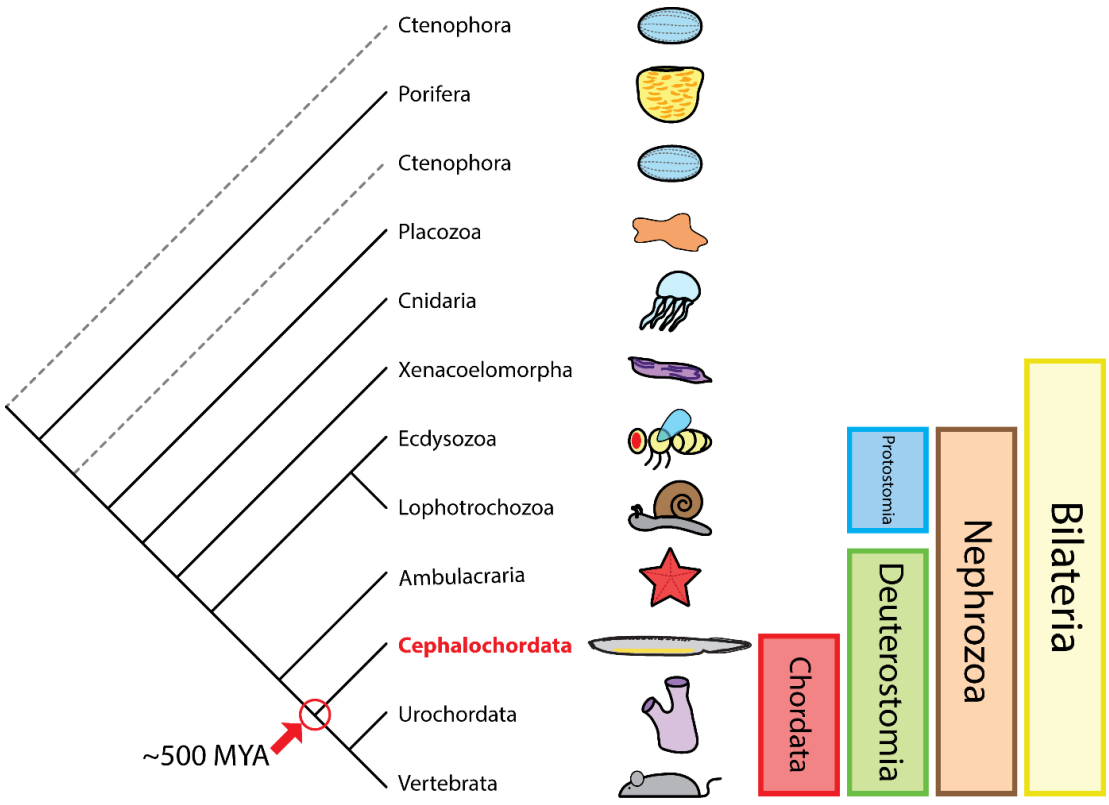

Fig.1 Simplified phylogenetic tree of Metazoa

Cephalochordates represent the most basally branching chordate phylum. Cephalochordates and vertebrates split from common ancestor about 500 million years ago (mya).

Due to its unique phylogenetic position (see Fig.1 for simplified phylogenetic tree) amphioxus served as a proxy for chordate ancestor already in the 19th century[13]. More recently studies of amphioxus morphology, development, genome and molecular biology have provided many important results, giving insights into the evolution of various vertebrate traits, e.g. head structures[14], the two rounds of whole genome duplications (2RWGD) shaping the genome of vertebrates[15,16], the evolution of Hox genes cluster and its regulation[17] or the V(D)J recombination of B and T cell receptor[18].

Historically, application of amphioxus for studies in the field of evolutionary-developmental biology (evo-devo) was limited. Lack of reliable laboratory culturing protocols, established methods for genetic manipulations (transgenesis, knock-outs and gain of function experiments) and absence of assembled genome were main obstacles for broader implementation of amphioxus as a model organism. Most of these difficulties in amphioxus research have been overcome recently. Several labs succeeded in establishing reproducibly reliable protocols for obtaining gametes and raising embryos of various amphioxus species (*Branchiostoma lanceolatum*[19], *Branchiostoma belcheri*[20], *Branchiostoma floridae*[21,22] and *Asymmetron lucayanum*[23]). Later, the expansion of possible genetic manipulations in amphioxus followed (reviewed by Kozmikova and Kozmik[24]). Moreover, the first complete amphioxus genome was released in 2008 for *B. floridae*[16]. Currently, transcriptomic, EST and genomic data are available for other amphioxus species – *B. belcheri* (genome[25], EST[26], transcriptome[27]), *A. lucayanum* (transcriptome[28]) *or B. lanceolatum* (transcriptome[29]).

In total it is generally accepted that amphioxus serves as irreplaceable model organism for getting insights into evolution of vertebrate-specific characters. It is, nevertheless, necessary to complement amphioxus studies with studies of other non-vertebrate chordates like hemichordates or urochordates to avoid wrong interpretations of possible amphioxus specific body plan modifications.

3.1.1 Amphioxus development

Amphioxus early development is relatively fast – *B. floridae* gastrulation begins at 4 hours post fertilization (hpf), neurulation starts about 8 hpf and larval stage at 24 hpf (see Fig.2 for an overview of amphioxus development). The timing of early development is comparable with the one observed in zebrafish. Metamorphosis takes place about 25 days post fertilization (dpf) (*B. floridae*) to 3 months post fertilization (mpf) (*B. lanceolatum*). The amphioxus sexually maturates at the age of one year (*B. floridae*) or two years (*B. lanceolatum*). In laboratory conditions, sexually mature *B. floridae* adults were obtained already after 6 months (Linda Holland, personal communication). This is a very promising result for possible establishment of amphioxus transgenic lines and broadening of the future use of amphioxus as model organism.

Studies of amphioxus early development, showed, that many important developmental processes are probably ancestral to all chordates. For example BMP-Chordin interactions during establishment of dorso-ventral patterning of embryo seems to be conserved in all chordates[30]. Next the role of Nodal signaling in establishment of left-right asymmetry is important in both amphioxus and vertebrates[31,32]. In contrast, study of neural induction in amphioxus disrupted previously accepted model that BMP inhibition is sufficient for neural induction in all chordates, showing some discrepancies between vertebrates and amphioxus. It seems, that in amphioxus activation of Nodal and FGF signaling is more important than in vertebrates and BMP inhibition alone is insufficient for neural induction[33]. The authors however admit, that BMP inhibition, FGF and Nodal signaling play role in neural induction in all chordates, but their contribution varies among different species. Interestingly, despite being thoroughly studied, conflicting results exist for example for role of Wnt signaling and the presence of Spemann organizer in amphioxus (reviewed by Kozmikova and Yu[34]). Sometimes opposing results come from studies done on different amphioxus species. As was, for example, documented for the role of BMP in mouth development. In *B. floridae*, *B. lanceolatum* and Chinese population of *Branchiostoma japonicum* BMP was shown not to be expressed in area of future mouth[35,36], while in Japanese population of *B. japonicum*, the

BMP expression was detected at the rim of developing oral opening[37]. The amphioxus can thus serve for both for identification of conserved as well diverse chordate characters.

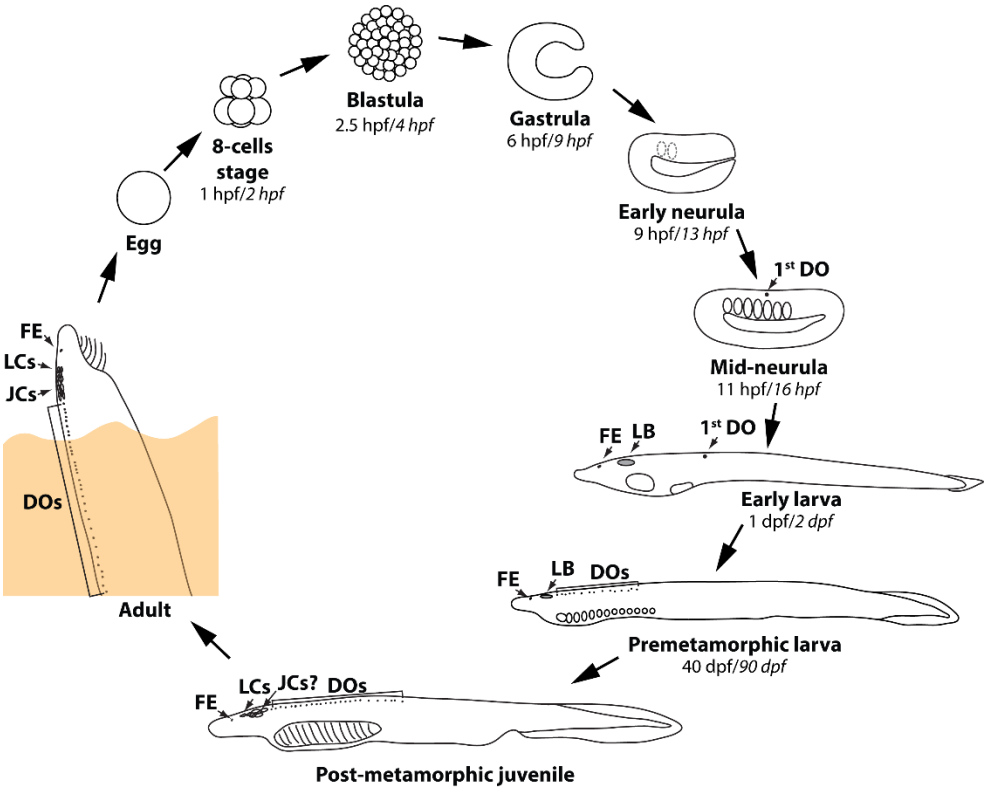

Fig.2 Scheme of amphioxus development

Scheme of chosen amphioxus developmental stages is presented. Time after fertilization necessary for reaching given stage is written for B. floridae (standard format) – development at 25°C, and for B. lanceolatum (in italics) – development at 19°C. Time data were taken from study by Fuentes, et al.[19]. Presence of photoreceptive organs in particular developmental stages is stressed. Time of the first appearance of Joseph cells was not determined so far. 1st DO – first dorsal ocellus; FE – frontal eye; LB – lamellar body; DOs – dorsal ocelli; LCs – lamellate cells (dissociated lamellar body); JCs – Joseph cells.

3.2. Landmarks of amphioxus central nervous system

3.2.1. Amphioxus central nervous system

Amphioxus neural system consists of central nervous system (CNS), peripheral nerves and neural plexuses (reviewed in Wicht and Lacalli[38]). CNS is composed of dorsally located neural tube running along the whole body, with slightly enlarged anterior part forming so called cerebral vesicle (a putative homolog of vertebrate dien-/mesencephalon[39]). The neural tube develops by closure of the neural plate. This happens quite early in the development, about 12-16 hours post fertilization.

The amphioxus CNS consists of about 20 thousand neurons in the neural tube and several hundreds of neurons in the cerebral vesicle[40]. Studies of the development and morphology of amphioxus CNS revealed its rather simple organization. It seems, for example, that putative visual processing center or putative balance organ is composed of only several cells[38]. Processing of most sensory stimuli and reactions to them seems to take place in the

neural tube, since decerebrated animals were shown to be light sensitive or were able to react to chemical stimuli[41].

In the past, several studies tried to define homology between amphioxus cerebral vesicle and vertebrate brain with various results[42-45]. The estimated homologies were mostly based on expression patterns of amphioxus orthologs of vertebrate genes, known to be involved in development and patterning of brain. It was for example shown, based on expression of amphioxus gene *Pax2/5/8*, that amphioxus probably lacks midbrain hind-brain boundary (MHB)[46]. MHB is a signalling center that is necessary for formation of midbrain and hindbrain. Amphioxus also appears to lack a proper zona limitans intrathalamica (ZLI), necessary for the development of the thalamus and the prethalamus[47]. Some studies even argued that cephalochordates underwent secondary simplification after the split from lineage leading to vertebrates, based on the fact that gene regulatory network (GRN) similar to that in vertebrate MHB and ZLI can be found in hemichordate *Saccoglossus kowalevskii*[48]. On the other hand hemichordates´ CNS is not as elaborate as the one in cephalochordates and vertebrates. Hemichordate CNS for example lacks any morphological sign of cerebral vesicle and its posterior part is formed by two neural tubes (dorsal and ventral). Tunicates appear to lack MHB and ZLI just as cephalochordates. Nevertheless, it was recently proposed that cephalochordates might still have some kind of MHB and ZLI, but in a reduced form, which is connected to the simplicity of its CNS[47]. Moreover vertebrates could benefit in the evolution from the 2RWGD that appeared after the split of cephalochordates´ and urochordates´ ancestors from the lineage leading to vertebrates. Vertebrates thus could have added new genes into the brain patterning GRN already present in chordate ancestor. It thus seems that proper MHB and ZLI are probably vertebrate specific characteristics but build upon an ancestral chordate GRN[47] (Fig.3).

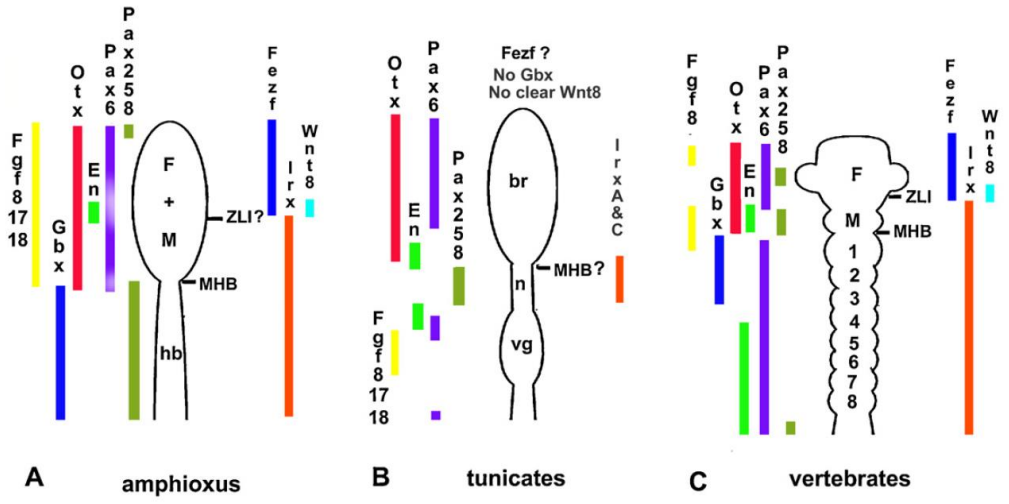

Fig.3 Scheme of expression patterns of genes involved in patterning of anterior CNS in amphioxus, tunicates and vertebrates (scheme from Holland[47])

Expression patterns of amphioxus and urochordate orthologs of genes involved in vertebrate brain patterning are depicted. The spatial and/or temporal expression in amphioxus and urochordates is not the same as in vertebrates, but the core of the GRN appears to be present already in chordate ancestor. Vertebrate specific brain patterning was enabled by adding new genes or functional specification of genes already present in the ancestral GRN. This probably happened thanks to the expansion of the gene toolkit after 2RWGD (e.g. Fgf8 that evolved from the ancestral Fgf8/17/18).

3.2.2. Amphioxus photoreceptive organs

Amphioxus demonstrates various reactions to light during its life cycle (summarized in Table 1 on next page). Positive phototaxis was observed at mid-neurula stage of *B. floridae*[21], but not in the same stage of *B. lanceolatum* (observation done in our lab) or *A. lucayanum*[23]. Planktonic larvae of various amphioxus species stay close to the bottom during the day and migrate to water surface levels during sunset[49,50]. Such typical diurnal migration can be observed also in other marine organisms. Amphioxus adults are photophobic and when exposed to light, swim away from the light source and try to hide in the burrow[51]. Moreover adults were shown to be more active (moving in the burrow) during the night[52].

Spawning of amphioxus is also light dependent. In nature *B. floridae*, *B. lanceolatum* and *B. belcheri* spawn usually within one hour after sunset[19-21]. This can be also mimicked in the lab, were the animals spawn within 1-2 hours after switching off the lights[19-21]. Spawning of *A. lucayanum* occurs also shortly after sunset both in the field and in the lab[53]. Additionally *A. lucayanum* spawning is dependent on the phase of moon, since it usually spawns one or two days before new moon[53].

Amphioxus possesses four distinct photoreceptor organs: two of them, the frontal eye and the lamellar body, consisting of ciliary photoreceptors (expanding their membrane surface by a modified cilium and two, Joseph cells and dorsal ocelli, are formed by rhabdomeric photoreceptors (expanding their cell surface by membranous protrusions) (Fig.4). Frontal eye and dorsal ocelli are directional photoreceptors, due to the presence of closely associated pigment cell. In contrast lamellar body and Joseph cells serve for non-directional photoreception. The frontal eye is situated at the very tip of the cerebral vesicle. The lamellar body develops in the dorso-posterior part of the cerebral vesicle. Joseph cells appear at the border of cerebral vesicle and neural tube, right behind the lamellar body. Dorsal ocelli are located longitudinally along the whole neural tube.

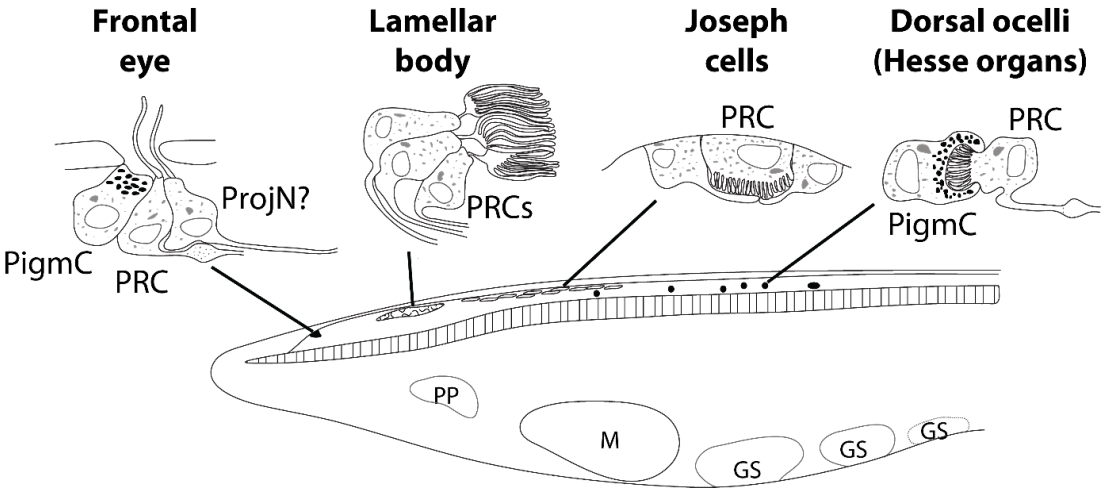

Fig.4 Overview of amphioxus photoreceptive organs

Schematic drawing of juvenile premetamorphic amphioxus with stressed position and morphology of particular photoreceptive organs. Four different photoreceptive organs can be found in amphioxus in depicted stage. Two of them – frontal eye and lamellar body are of ciliary character, while Joseph cells and dorsal ocelli are rhabdomeric. PigmC – pigment cell; PRC/PRCs – photoreceptor cell/cells; ProjN? – putative visual projecting neurons. Some anatomical landmarks are shown: PP – preoral pit, M – mouth, GS – gill slit.

Table 1. Overview of reactions to light stimuli in individual amphioxus developmental stages

Developmental stage	Species	Response to light		References
Neurula	*B. floridae*	Accumulation at surface level facing to the direction of the light source		Holland and Yu, 2004[21]
	B. lanceolatum	No response		Pergner and Kozmik, 2017[54]
	A. lucayanum	No response		Holland and Holland, 2010[23]
Larva	*B. floridae*	During hovering in water column orientation with FE facing from the light source		Stokes and Holland, 1995[55]
	B. belcheri	Diurnal migration - close to the bottom during day, close to the surface level during and after sunset		Chin, 1941[50]; Wickstead and Bone, 1959[49]
	B. lanceolatum	Diurnal migration - close to the bottom during day, close to the surface level during and after sunset		Wickstead and Bone, 1959[49]
		Swimming to surface and then catching the food sinking down with mouth open		Webb, 1969[56]
Adult	*B. lanceolatum*	Negative phototaxis		Costa, 1834[57]; Willey, 1894[13]; Hesse, 1898[58]
		Increased locomotor activity in the burrow during the night (suppressed by light)		Schomerus *et al.*, 2008[52]
	B. caribbaeum	Negative phototaxis		Parker, 1908[51]
Adult – spawning behavior	*B. floridae*	Short term	Spawning 1h after sunset	Holland and Yu, 2004[21]
	B. lanceolatum		Spawning 1h after sunset	Fuentes *et al.*, 2007[19]
	B. belcheri		Spawning 1h after sunset	Li *et al.*, 2013[20]
	A. lucayanum		Spawning 1h after sunset	Holland, 2011[53]
	A. lucayanum	Long term	Spawning one day before the new moon	Holland, 2011[53]

The first amphioxus photoreceptive organ to develop is the first dorsal ocellus at the region of the 5th somite at mid-neurula stage (already depicted in Fig.2). Next, the frontal eye develops and was shown to be differentiated already at early larval stage[59]. Later follows differentiation of the lamellar body in early larva[60]. In mid-larval stage the differentiation of other dorsal ocelli begins. At first, dorsal ocelli develop anteriorly from the first dorsal ocellus (from 3rd to 5th somite) and later also posteriorly towards the caudal end of the body. At the same time, the differentiation of Joseph cells commences. While frontal eye and lamellar body seems to be terminally differentiated in early larval stages, number of Joseph cells and dorsal ocelli increases to the adult stage. Dorsal ocelli (sometimes called Hesse organs after Prof. Hesse who described them thoroughly for the first time in 1898[58]) are the most abundant photoreceptor organ – about 1500 of them can be found in adult amphioxus.

Not much is known about participation of particular amphioxus photoreceptive organs to amphioxus light guided behavior. Currently, it is generally accepted that dorsal ocelli control how good the amphioxus body is hidden in the sand[61]. Frontal eye seems to be involved in orientation of larvae during feeding[55] and also in regulation of switching between slow migratory and fast startle movements of larva[38]. The lamellar body probably serves as a circadian rhythm controller similarly as the pineal organ in vertebrates[38]. The role of Joseph cells in amphioxus photoreceptive behavior is up to date enigmatic.

3.2.3. Amphioxus frontal eye – a putative homolog of vertebrate eyes

The evolution of the vertebrate eye was puzzling scientists already from Darwin´s time. Even Charles Darwin himself dedicated a chapter to the problem of evolution of complex vertebrate organs by means of natural selection. To the topic of the evolution of vertebrate eye Darwin stated: “To suppose that the eye, ..., could have been formed by natural selection, seems, I freely confess, absurd in the highest possible degree. Yet reason tells me, that if numerous gradations from a perfect and complex eye to one very imperfect and simple, ..., can be shown to exist; ..., then the difficulty of believing that a perfect and complex eye could be formed by natural selection, though insuperable by our imagination, can hardly be considered real.“[62]. Since those times, the search for possible candidates that would show how the ancestral chordate eye could have looked like have begun. Currently, amphioxus frontal eye seems to be a pretty reasonable candidate.

Amphioxus frontal eye was proposed as a possible homolog to the vertebrate eye already at the turn of the 20th century[63,64]. Only scarce data, however, supported this homology. First of all the frontal eye develops at the tip of the cerebral vesicle, which was recently shown to be putative homolog of vertebrate dien-/mesencephalon[39]. Similarly the neural retina of vertebrate eye develops as an extension of diencephalon. Next frontal eye photoreceptors are ciliary-type and so are also the photoreceptors in the vertebrate retina. On the other hand, the ultrastructure of frontal eye photoreceptors is not as elaborate as that of rods and cones of vertebrate retina. The function of the frontal eye as a photoreceptive organ was, however, doubted in several studies. As previously mentioned, decerebrated amphioxus is able to react to light[51]. Additionally, no trace of putative neuronal projection from the region of frontal eye was detected in the past (Lacalli, personal communication). Scientists also discussed the fact, that amphioxus frontal eye is not a paired organ as are the vertebrate eyes. Two hypotheses were raised to explain this fact. Either a single non-image forming photoreceptive organ was the chordate ancestral state[65] or ancestral chordates possessed paired image forming eyes and the amphioxus frontal eye is a result of

simplification after adaptation of amphioxus for life as borrower[65]. Due to the lack of fossil records and experimental data both scenarios must still be taken into account.

In conclusion, amphioxus cerebral vesicle can be, in general, considered as presumptive homolog of vertebrate Di- and Mesencephalon. The problem that scientists face now is finding solid grounds for proposed homologies of particular landmarks of amphioxus CNS with their vertebrate counterparts. These are for example the balance organ, olfactory neurons and, most importantly for the purpose of this thesis, homologies of particular amphioxus and vertebrate photoreceptive organs.

3.3. Opsins – key molecular components of light detection in Metazoa

Three different light detecting systems were described in multicellular animals depending on the protein molecule used – opsins[66], cryptochromes[67,68] and LITE-1[69]. Cryptochromes are utilized in visual organs of larval sponges[67,68] and are potentially involved in regulation of circadian rhythms in other animals[70]. Interestingly sponges lack opsin genes in their genome. LITE-1 is a special photoreceptive protein derived from taste receptor so far found only in *Caenorhabditis elegans*[69] (which appears to lack opsin genes in its genome). From all current data, opsins seem to be the most important light sensing molecules in animals, since they are used as main visual systems in most Metazoa even in Ctenophora, with the already mentioned exception of sponges[71].

3.3.1. Biochemical characteristics of opsins

The opsins belong to the superfamily of G-protein coupled receptors (GPCRs), seven-transmembrane domain proteins signaling through heterotrimeric G proteins. The GPCR superfamily consists of about 800 genes (in human genome) divided in five different families marked by letters A-E[72]. Defects in GPCRs and their downstream signaling cascades were shown to be connected with various diseases, e.g. diabetes, obesity or neurological disorders[73]. GPCRs are thus nowadays considered as the most promising drug targets and belong amongst the most intensively studied proteins of any kind.

The most abundant GPCRs are those of the family A, or sometimes called “The Rhodopsin family”. This family includes not only opsins, but also various other receptors, e.g. the prostaglandin receptor, the neuropeptide FF receptor, the arginine vasopressin receptors, etc. There are three main differences between opsins and other GPCRs: 1. A physical elementary particle, the photon, serves as a ligand for opsins while other GPCRs are activated by chemical molecules (hormones, odorants, peptides, etc.)[74]. 2. Opsin consists of the apoprotein and the chemical cofactor retinal (mostly 11-*cis*-retinal, less often *all-trans* retinal and in experimental conditions also 9-*cis*-retinal). The retinal is covalently bound to the opsin apoprotein. Other GPCRs usually don´t have any cofactor and if so, it is not covalently bound[74]. 3. Opsins can be distinguished from other GPCRs by the presence of a highly conserved lysine residue in the seventh transmembrane domain (in bovine rhodopsin at position 296) (Fig.5). Retinal is bound to the apoprotein right through this K296[66].

The first GPCR with solved crystal structure was the bovine rhodopsin[75]. The bovine rhodopsin serves as model for studies dealing with opsin structural, biochemical and signaling properties, for example identification of several important amino acid (aa) residues in opsin structure (shown in Fig.5)[76]. One of them is so called counterion, a negatively charged aa (mostly glutamate (E) and theoretically also aspartate (D))[66,77]. Counterion serves as

a stabilizer of protonated Schiff base linkage between opsin´s lysine and retinal. Protonation of the Schiff base linkage enables shift of the retinal absorption peak to visible spectrum. Without stabilization of the Schiff base, the retinal absorption peak would be shifted to the UV part of the spectrum. In most opsins, the counterion is found at the position 181 (numbering according to the bovine rhodopsin), located in opsin´s 2nd extracellular loop[66]. Interestingly in vertebrate visual opsins, glutamate at position 113 (in 3rd transmembrane domain) serves as the counterion[78]. Recent analysis proposed, that E or D at position 83 can also function as counterion[77].

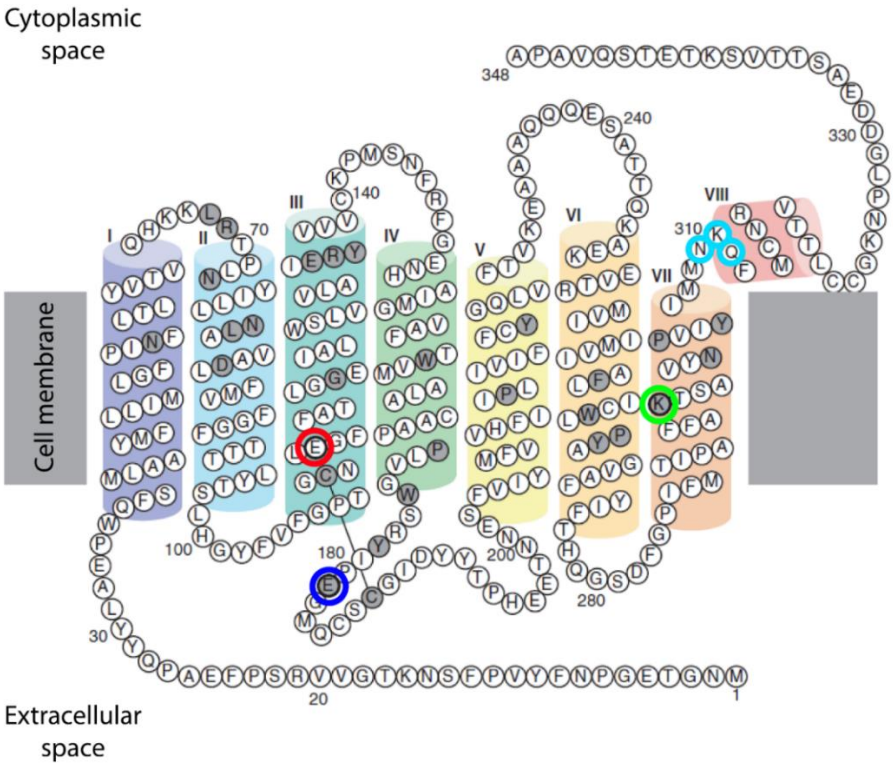

Fig.5 Overview of an opsin protein structure highlighting amino acids important for opsin function (adapted from Terakita[66])
Scheme of opsin structure presented on the example of bovine rhodopsin. Position of K296 (green circle), counterions E113 (red circle) and E181 (blue circle) and NKQ tripeptide (cyan circles) is marked. Other highly conserved aa are marked in grey. See text for more details.

A group of three adjacent aa in the fourth cytoplasmic loop, the so called tripeptide, was shown to be important. Mutational analysis of the bovine rhodopsin tripeptide NKQ showed that it is crucial for activating downstream signaling, more specifically for contact with trimeric G protein[79]. Rhodopsin with mutated tripeptide was not able to transduce signal when stimulated by light[79].

Several other aa were shown to be highly conserved in the structure of most opsins (highlighted in grey in Fig.5). The function of some of them is known, e.g. E/DRY in the 3rd transmembrane domain – a motif of three aminoacids (glutamate or aspartate, arginine, tyrosine) is found also in other GPCRs and is important for downstream signaling[80]. So is also the NPxxY(x)$_{5,6}$F (asparagine-prolin-5 or 6 different aa-phenylalanin) motif in the 7th

transmembrane domain[80]. The function of most of the other highly conserved aa within the opsin family remains, however, elusive.

After excitation of the opsin by a photon the phototransduction cascade continues through activation of a trimeric G protein. Generally, GPCRs signal transduction cascade can utilize either G_α subunit and/or $G_{\beta\gamma}$ dimer. Employment of various G subunit then continues through diverse second messengers and leads to different cellular responses. So far, it is accepted, that opsins mainly signal through G_α subunits. Vertebrate visual c-opsins were shown to signal through G_αt subunit (that evolved from G_αi by tandem duplication[81,82]). The cascade then continues through cGMP decrease, closure of cyclic nucleotide gated (CNG) channels and cell hyperpolarization[83]. R-opsins signal through G_αq subunit, leading to Ca^{2+} increase and cell depolarization[84]. Next, example of opsin signaling through G_αo was also identified[85]. Opsin found in the eyes of the cubozoan jellyfish *Carybdea rastoni* was shown to signal through G_αs subunit, leading to an intracellular cAMP increase[86]. It seems that information about opsin-G_α subunit coupling might provide some clues about the evolution of opsin mediated photoreception[87]. Downstream signaling cascades of c-type (ciliary-type), r-type (rhabdomeric-type) and one representative of Cnidarian opsins are shown in Fig.6.

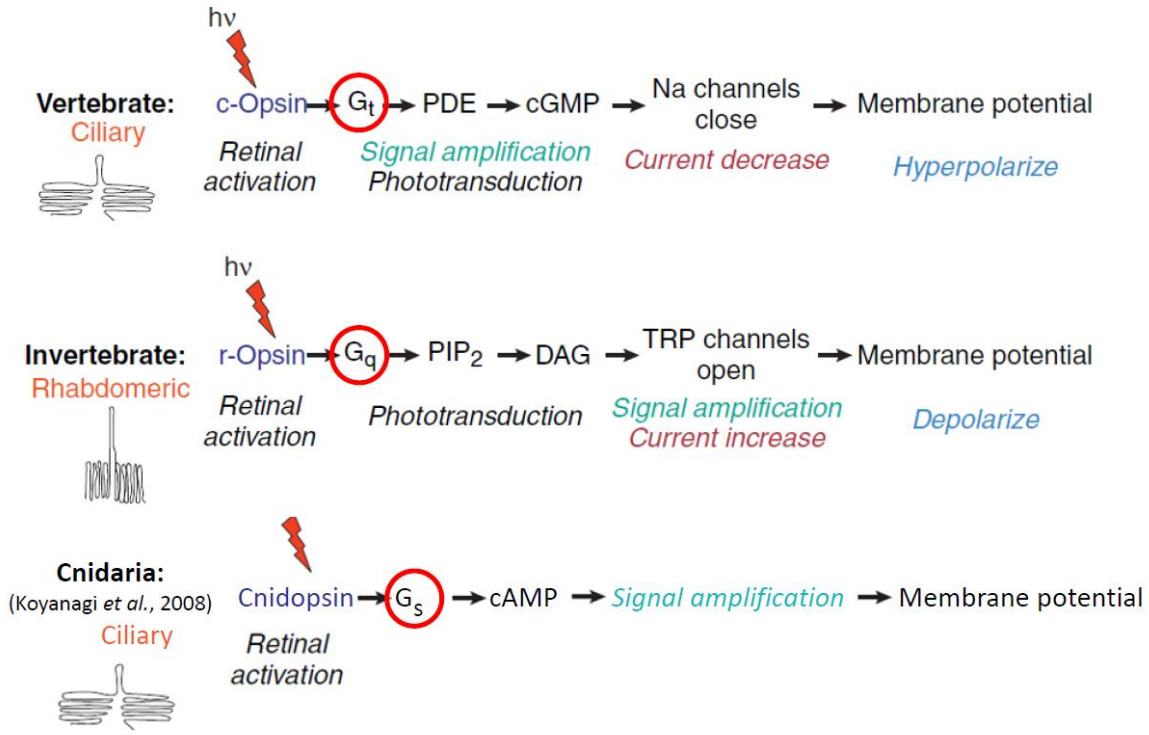

Fig.6 Examples of identified phototransduction cascades (adapted from Fernald[84])
Phototransduction cascade of c-opsin, r-opsin and one representative of Cnidopsins are shown. While the phototransduction cascades of c-opsins and r-opsins are well understood, the one utilized by Cnidopsins remains enigmatic. All known c-opsins were shown to signal through transducing (G_t) member of G_αi protein family. Cascade continues through activation of PDE, decrease in cGMP, closure of CNG channels and cell hyperpolarization. After activation of the r-opsin, the cascade continues via G_αq, phosphatidylinositol 4,5-bisphosphate (PIP_2), diacylglycerol (DAG), opening of TRP channels and cell depolarization. In 2008 it was shown by Koyanagi, et al.[86], that an opsin from the cubozoan jellyfish Carybdea rastoni *signals through G_αs leading to increase of intracellular cAMP. Next steps of the cascade are uknown.*

3.3.2. Opsins phylogeny

For the reason that the opsins are widely used as light sensing pigments in various animals, their evolution can provide insights into the evolution of animal light detection *per se*. Since the first identification of opsin gene sequences, many studies were published, describing the phylogenetic relationships between them. Almost 1000 opsin genes sequences are identified in various animals up to date. According to the first thorough analysis of opsin genes, including those from Cnidaria, the opsins can be divided into four main groups – c-opsins, r-opsins, Cnidopsins and Group4 opsins[88]. C-opsins encompass mainly opsins found in ciliary photoreceptors, r-opsins group is formed mainly by opsins from rhabdomeric photoreceptors and Group4 opsins consists of various mostly non-visual opsins found in both types of photoreceptors. The Cnidopsin group consists only of Cnidaria specific opsins. The relationships between the four groups varies among different studies. Usually the Cnidopsin group was the one, which changed its position in various studies (Fig.7).

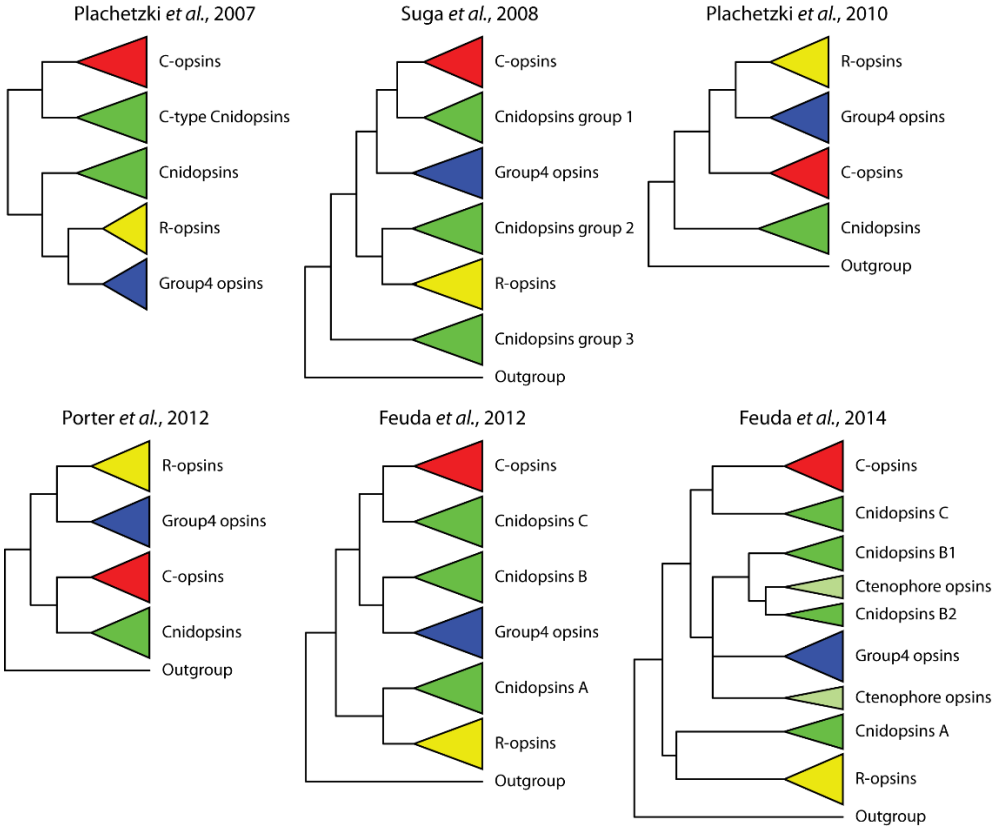

Fig.7 Schematic representation of different phylogenetic analyses of opsins
Analyses vary mainly in different approach to Cnidopsins group. In some studies the Cnidopsins were paraphyletic, while in others they form a monophyletic group. The studies differ also in relationships between c-, r- and Group4 opsins. The phylogeny of opsins is still a matter of debates and new studies either come with their own interpretation, or support one of the previously published studies. Schemes are based on studies by Plachetzki, et al.[87]; Suga, et al.[88]; Plachetzki, et al.[89]; Porter, et al.[77]; Feuda, et al.[90] and Feuda, et al.[71].

Plachetzki, *et al.*[87] divided Cnidopsins into two groups, one forming a sister group of c-opsins and the other forming a sister group to r-opsins and Group4 opsins. Next Suga, *et al.*[88] divided Cnidopsins into three groups – Group1 Cnidopsins being a sister group to c-opsins, Group2 Cnidopsins being a sister group to Group4 opsins and Group3 Cnidopsins forming

a sister group to all other opsins. In 2010 Plachetzki*, et al.*[89] revised their phylogeny and placed all Cnidopsins basally to all other opsins. Phylogenetic analysis by Porter*, et al.*[77] placed Cnidopsins as sister group to c-opsins and r-opsins and Group4 opsins as separate sister groups. Additional changes in opsins relationships were proposed in 2012 by Feuda*, et al.*[90]. They supported the division of Cnidopsins into three Groups – Group A, B and C. According to this analysis orthologs of all the other opsin groups are found in Cnidaria. Feuda*, et al.*[71] performed updated analysis in 2014 adding sequences from *Mnemiopsis leidyi* a representative of Ctenophora. This analysis, despite some difficulties in placing Ctenophores in phylogenetic tree[91,92], showed that Ctenophore opsins form two groups, one forming a sister group to c-opsins and the other to Go opsins (belonging to Group4 opsins).

3.3.3. Amphioxus opsin genes

Six amphioxus opsin gene sequences were described for *B. belcheri* in 2002[93]. Their clustering was however difficult, due to shortage of available opsin sequences from other animals. Next, in 2008 complement of about 20 opsin genes was identified in *B. floridae* genome[16]. Phylogenetic analysis revealed that members of all known opsin families except for Cnidopsin group, can be found in genome of *B. floridae*. Interestingly, a group of six *B. floridae* opsins clustering with Amphiop6 opsin from *B. belcheri* and forming a sister group to r-opsins was identified. Two of these opsins have glutamate at position 113. Whether it acts as a counterion has, however, so far not been determined. Interestingly, some of the *B. floridae* opsins lack E at position 181. Their biochemical characteristics have not been analyzed yet. Huge tripeptide variability was observed in the amphioxus opsin sequences, from tripeptide NKQ in amphioxus c-opsins (typical vertebrate opsin tripeptide), through HPK tripeptide in amphioxus melanopsin (tripeptide typical for r-type opsins) to tripeptide EKE previously not identified in any other opsin sequence.

Generally speaking, it is obvious, that opsins can provide important data that would shed new light on the evolution of photoreception. Identification of new opsin sequences is nowadays, with the expansion of genome sequencing techniques, easier than any time before. What is, however, still limiting are biochemical characteristics of opsins belonging to different opsin families. Therefore, studies of, for example, counterion position in the newly identified amphioxus opsins or studies of downstream signaling cascades of amphioxus opsins are highly warranted.

4. Aims of the study

As discussed earlier, amphioxus serves as reasonably good proxy for chordate ancestor. As such amphioxus is a cornerstone for studies dealing with the evolution of vertebrate traits such as the vertebrate-type body plan, CNS or sensory neurons. Light detection is crucial for most of the organisms on earth. Although studies of amphioxus light detecting systems were performed already at the turn of the 20th century[51,58,63], followed by thorough EM analysis of amphioxus photoreceptor organs in the second half of the 20th century[94-101], huge gaps remain in understanding the photoreception of amphioxus. The aim of this thesis was to broaden available information about light detection in amphioxus, provide data about the development of amphioxus photoreceptive organ – the frontal eye and putative visual center in amphioxus cerebral vesicle and thus provide clues about photoreception in the hypothetical chordate ancestor.

Particular aims were:

- Molecular characterization of neurons in amphioxus frontal eye with special attention to genes involved in the frontal eye development, phototransduction cascade and neuronal transmitters and comparison with the data known from development of the vertebrate eyes

- Establishment of a cell-line based assay enabling studies of opsin function and biochemical characterization of opsins landmarks

- Characterization of opsin repertoire in two amphioxus species, the Florida species *B. floridae* and the European species *B. lanceolatum*

5. List of methods

Work with nucleic acids

Genomic DNA isolation

Cloning of DNA fragments: for preparation of plasmids for heterologous peptides production; preparation of probes for ISH; sequencing of opsin genes; cloning of whole opsin genes for biochemical analysis

Total RNA isolation, preparation of cDNA

Quantitative RT-PCR – SYBR green (Roche); detection on LightCycler (Roche)

Preparation of antisense probes for *in situ* hybridization

Work with proteins

Production and purification of heterologous proteins from bacteria BL21-(DE3)-RIPL

Preparation of mouse polyclonal antibodies

SDS-PAGE and western blot

Work with animals

Tissue isolation from anesthetized animals

Immunostaining (whole mount of amphioxus embryos, cell culture)

Confocal imaging, image processing, 3D reconstructions in FIJI software

Whole mount *in situ* hybridization

Chemical manipulation of developing embryos

Work with cell cultures

Measuring of intracellular levels of cAMP using GloSensor HEK cell line (Promega)

6. Results

6.1 Molecular analysis of the amphioxus frontal eye unravels the evolutionary origin of the retina and pigment cells of the vertebrate eye.

Amphioxus frontal eye seemed to be the best reasonable candidate for a homolog of the vertebrate lateral eyes. Only limited data supporting this hypothesis were, however, present in the literature. The frontal eye develops at the tip of the cerebral vesicle and EM studies showed its ciliary character, which was in agreement with this proposition. Moreover, amphioxus orthologs of genes involved in eye development of both invertebrates and vertebrates were detected in the developing frontal eye. More specifically Pax4/6, Otx and Six3/6 were shown to be expressed in the frontal eye neurons and Pax2/5/8 was detected in the pigment cells of the frontal eye[7,46,102,103]. On the other hand, function of the frontal eye as photoreceptive organ was questioned, since no projecting neurons were spotted in EM samples and scarce behavioral studies rather casted doubts about the photoreceptive function of the frontal eye in adult[51,58] and showed its limited function in larvae[55].

In this study we performed thorough analysis of genes expressed in individual cells of the amphioxus frontal eye. Due to divergence of amphioxus and vertebrate proteins on one hand and the presence of highly conserved domains (e.g. DNA binding domains) in different developmental genes on the other hand, the usage of commercially available antibodies targeted against vertebrate (mostly mouse) antigens faced many problems. Either the antibodies did not provide any signal, or more members of particular gene family were stained in amphioxus. We thus decided to overcome this problem by preparation of amphioxus specific antibodies. To this end we cloned parts of amphioxus proteins, other than highly conserved domains (like DNA binding domains), fused them with protein tag, expressed them in bacteria and purified them from bacterial lysate. Purified proteins were then used for immunization of rabbits or mice. Blood serum was used to perform whole mount immunofluorescent staining of two days old *B. floridae* larvae, followed by subsequent analysis on confocal microscope. Amphioxus larvae are only about 1 mm in length and 60 um wide, allowing scanning through the whole larvae at standard confocal microscope.

Our analysis confirmed the presence of Otx in the developing pigment cell and photoreceptors of amphioxus frontal eye. Next, Pax4/6 was detected in developing photoreceptors, putative visual projecting neurons and neurons of putative visual processing center of amphioxus (so called primary motor center (PMC)). Amphioxus Rx, the ortholog of vertebrate RAX, was also detected in developing frontal eye. Amphioxus Pax2/5/8 and Mitf, orthologs of genes involved in the development of vertebrate retinal pigmented epithelium (RPE), were both found to be expressed in the developing pigment cells of frontal eye and in the case of Mitf also in developing pigment cells of 1st dorsal ocellus. Moreover, the pigment was experimentally shown to be melanin. One of the other highlights of our study was documenting the presence of c-opsins and $G_{\alpha}i$ subunit in the frontal eye photoreceptors, confirming their ciliary character and demonstrating their differentiated state already at two days old larvae. Search in available *B. floridae* genomic source showed, that it lacks transducin gene ($G_{\alpha}t$) and the phototransduction cascade utilized in the frontal eye photoreceptors is thus probably different than the one used in vertebrate photoreceptors. Furthermore we

succeeded in mapping the terminals of the so called Row2 neurons, putative visual projecting neurons of amphioxus frontal eye, localized immediately behind the frontal eye photoreceptors. Row2 neurons terminate in presumptive tegmentum and might therefore represent homologs of vertebrate retinal interneurons.

Our study also provided some data about amphioxus lamellar body, a putative homolog of the vertebrate pineal gland. Amphioxus Rx was not detected in the developing lamellar body while the vertebrate ortholog RAX is expressed in developing pineal gland and none of the three tested c-opsins was detected in lamellar body.

Taken together our data demonstrate that amphioxus frontal eye and vertebrate eyes, despite the huge morphological difference between them, utilize during their development the same gene repertoire – Otx, Pax6, Rx, Pax2 and Mitf and use a similar phototransduction cascade. This genetic and signal transducing machinery, therefore, represents an ancestral chordates´ trait.

My contribution to this work: I generated an antibody for amphioxus c-opsin 3. I performed staining of amphioxus larvae with this antibody and documented the expression of c-opsin 3 in the photoreceptors of frontal eye (data presented in Fig.3 of the paper). I repeated staining with antibodies raised against Otx, Pax4/6, Mitf and c-opsin 1 & 2 (some of my data are presented in Fig.2, Fig.3 and Fig.S3 of the paper), to confirm the results previously obtained by Pavel Vopalensky (first author) and Michaela Liegertova (co-author).

Molecular analysis of the amphioxus frontal eye unravels the evolutionary origin of the retina and pigment cells of the vertebrate eye

Pavel Vopalensky[a,1], Jiri Pergner[a], Michaela Liegertova[a], Elia Benito-Gutierrez[b], Detlev Arendt[b,c], and Zbynek Kozmik[a,2]

[a]Department of Transcriptional Regulation, Institute of Molecular Genetics, CZ-14220 Prague, Czech Republic; [b]Developmental Biology Unit, European Molecular Biology Laboratory, Heidelberg, 69117 Heidelberg, Germany; and [c]Animal Evolution Department, COS Heidelberg, 69120 Heidelberg, Germany

Edited by Sean B. Carroll, University of Wisconsin, Madison, WI, and approved August 3, 2012 (received for review May 10, 2012)

The origin of vertebrate eyes is still enigmatic. The "frontal eye" of amphioxus, our most primitive chordate relative, has long been recognized as a candidate precursor to the vertebrate eyes. However, the amphioxus frontal eye is composed of simple ciliated cells, unlike vertebrate rods and cones, which display more elaborate, surface-extended cilia. So far, the only evidence that the frontal eye indeed might be sensitive to light has been the presence of a ciliated putative sensory cell in the close vicinity of dark pigment cells. We set out to characterize the cell types of the amphioxus frontal eye molecularly, to test their possible relatedness to the cell types of vertebrate eyes. We show that the cells of the frontal eye specifically coexpress a combination of transcription factors and opsins typical of the vertebrate eye photoreceptors and an inhibitory Gi-type alpha subunit of the G protein, indicating an off-responding phototransductory cascade. Furthermore, the pigmented cells match the retinal pigmented epithelium in melanin content and regulatory signature. Finally, we reveal axonal projections of the frontal eye that resemble the basic photosensory-motor circuit of the vertebrate forebrain. These results support homology of the amphioxus frontal eye and the vertebrate eyes and yield insights into their evolutionary origin.

evolution | vision | cephalochordate

The evolutionary origin of vertebrate eyes is enigmatic. Charles Darwin appreciated the conceptual difficulty in accepting that an organ as complex as the vertebrate eye could have evolved through natural selection (1). Part of the problem lies in the paucity of extant phyla with useful gradations that occurred during eye evolution, thus providing a scenario that led to the emergence of the vertebrate eye. For example, the eye of the adult lamprey (a jawless vertebrate) is remarkably similar to the eye of jawed vertebrates in the overall design, retina cell types, and multiple classes of opsins (2). Given these similarities, it is likely that the last common ancestor of jawless and jawed vertebrates already possessed an elaborate camera-type lens eye. To understand the seemingly sudden origin of the vertebrate eye, its evolutionary precursor must be identified within the non-vertebrate chordates lacking elaborated eye structures. Because of its basal phylogenetic position within the chordates (3), its slowly evolving genome (4), and its ancestral morphology, the cephalochordate amphioxus represents a traditional model organism for understanding the origin of vertebrate organs. Extensive electron microscopy studies of the cerebral vesicle of the basal chordate amphioxus revealed several putative photoreceptive organs—dorsal ocelli, Joseph cells, lamellar body, and the unpaired "frontal eye" (5). The pigmented dorsal ocelli and the Joseph cells are morphologically and molecularly related to invertebrate eye photoreceptors (6, 7), whereas the frontal eye and the lamellar body traditionally have been homologized to the vertebrate eyes and pineal gland, respectively, based on their position and morphological features. However, these statements of homology have been a matter of debate (8), and the lack of adequate comparative molecular evidence has not allowed any firm conclusion to be drawn.

In this work we focus specifically on the functional molecules (c-opsin, melanin, and serotonin) and on transcription factors (Rx, Otx, Pax4/6, Mitf) playing crucial roles during vertebrate eye development. Unlike the majority of published amphioxus expression studies, we use a set of amphioxus-specific antibodies in combination with confocal microscopy to gain cellular resolution and coexpression information and to track axonal projections of the frontal eye. Our data provide evidence that the amphioxus frontal eye is an opsin-based photoreceptive organ and that the frontal eye photoreceptors and pigment cells are homologous to rods/cones and pigment cells of the vertebrate eyes, respectively.

Results

Developmental Patterning of the Amphioxus Frontal Eye. Vertebrates have two separate sets of eyes, the lateral visual eyes and the dorso-medial pineal and parietal "eyes" that play a role in the detection of ambient light and, in some groups, convey a fast response to predator shadows (9–11). Previous studies have revealed a small set of transcription factors that specify photoreceptor cells in both retina and pineal gland. Expression of retinal homeobox (*Rx*) is an early marker for the developing retina and pineal gland and is required for eye vesicle morphogenesis (12–14). We cloned the amphioxus *rx* gene (Fig. S1 for the phylogenetic tree) and determined its expression in the developing cerebral vesicle. We found that *rx* demarcates the anterior end of the cerebral vesicle from the 24-hours postfertilization (hpf) stage onwards (Fig. 1 *A*–*C*). This location is where the frontal eye will start to differentiate at later stages, as evidenced by the presence of cells with long dendrites and cilia that exit the neuropore (15) and by the presence of a spot of dark pigment (Fig. 1 *D* and *E*). However, *rx* expression has not been detected in the area of the lamellar body (Fig. 1 *D* and *F*), the previously proposed homolog of the vertebrate pineal gland (16). During differentiation stages *rx* expression becomes restricted to the cells lying behind the most anterior tip of the cerebral vesicle.

To determine further whether any of the differentiating cells of amphioxus frontal eye would resemble the vertebrate

EVOLUTION

Author contributions: P.V., D.A., and Z.K. designed research; P.V., J.P., and M.L. performed research; P.V., J.P., M.L., and E.B.-G. contributed new reagents/analytic tools; P.V., J.P., E.B.-G., D.A., and Z.K. analyzed data; and P.V., E.B.-G., D.A., and Z.K. wrote the paper.

The authors declare no conflict of interest.

This article is a PNAS Direct Submission.

Freely available online through the PNAS open access option.

Data deposition: The sequences reported in this paper have been deposited in the GenBank database [accession nos. JX101655 (Rx), JX101656 (Go-alpha); JX101657 (Gi-alpha); JX101658 (c-opsin1); JX101659 (c-opsin2); and JX101660 (c-opsin3)].

[1]Present address: Animal Evolution Department, COS Heidelberg, 69120 Heidelberg, Germany.

[2]To whom correspondence should be addressed. E-mail: Kozmik@img.cas.cz.

This article contains supporting information online at www.pnas.org/lookup/suppl/doi:10.1073/pnas.1207580109/-/DCSupplemental.

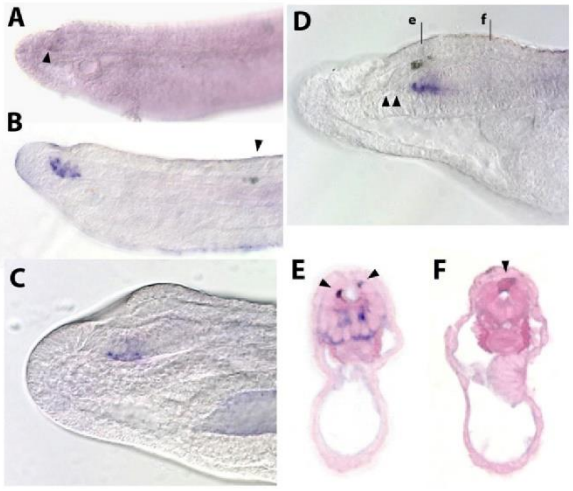

Fig. 1. Developmental expression of amphioxus *rx*. (*A*) The earliest trace of *rx* expression was detected in late neurula (24 hpf) in the anterior part of the cerebral vesicle (arrowhead). (*B*) In early larva (30 hpf), the expression becomes stronger and demarcates the anterior ventral half of the cerebral vesicle. The arrowhead points to the first Hesse eyecup. (*C*) At later stages, the expression is more restricted to the most anterior ventral part of the cerebral vesicle but excluding its very anterior-most tip. (*D*) In the 3.5-d-old larva with pigment cells and Row1 (arrowheads) cells already differentiated, the expression is restricted to the area of Row3/Row4 cells. (*E*) Plastic-embedded cross-section at the level of 'e' in *D*, showing the expression of *rx* in ventral cells of the cerebral vesicle. The arrowheads point to the posterior-most projections of the pigment deposits. (*F*) Expression of *rx* in the lamellar body was not observed at any stage of development. A more detailed inspection performed on the cross-section (at level 'f' in *D*) did not reveal the signal in cells of the lamellar body; the weak signal observed in the membrane protrusions (arrowhead) of the lamellar body is attributed to non-specific probe trapping caused by the large surface area of the structure.

photoreceptors molecularly, we produced antibodies against the amphioxus Otx, Pax4/6, and Rx transcription factors (Table S1). The antibodies showed the ability to recognize their respective antigens (Fig. S2 *A–C* and Fig. S3), recapitulated the RNA in situ expression patterns, and provided robust signal clearly distinguishable from nonspecific epidermal signal that we attribute to endogenous GFP expression (17) and secondary antibody trapping (Fig. 2*E*).

Expression of the single amphioxus *otx* and *pax4/6* orthologs has been detected previously in the anterior portion of the amphioxus cerebral vesicle (18, 19), but whole-mount RNA in situ hybridization analysis has not provided cellular resolution. Fluorescent confocal immunohistochemistry of amphioxus larvae with antibodies directed against amphioxus Otx and Pax4/6 proteins revealed colabeling of a single row of cells in the very anterior of the frontal eye (Fig. 2 *C–F*), termed "Row 1" by Lacalli et al (15). These cells are adjacent to the cells containing the dark pigment and thus are the most likely candidates for photoreceptor cells (15). Pax4/6 protein expression also was detected more posteriorly in cells scattered in the floor of the cerebral vesicle (Fig. 2 *F*) in a pattern similar to that of Rx (Fig. 2 *G–I* and Fig. S4). Interestingly, in addition to the differentiated cells bearing the apical extension, a small subset of Rx-positive cells buried deeper in the cerebral vesicle floor retained a rounded shape (Fig. 2*H*), suggesting a possible undifferentiated state.

Row1 Cells of the Frontal Eye Express *C-Opsin* Genes and the Gi-Alpha Protein Subunit. To challenge the possible photosensitive nature of Row1 cells in the amphioxus frontal eye (15), we set out to identify cells expressing the amphioxus *c-opsin* genes. Sixteen opsins have been detected in the amphioxus genome, four of which are related to the vertebrate rod, cone, and pineal opsins (20, 21). Phylogenetic analysis revealed that ancestral chordates possessed one *c-opsin* gene that by repeated and independent duplications gave rise to four paralogs in amphioxus and to numerous paralogs in the vertebrate lineage (20). We could not detect expression of any of the amphioxus *c-opsin* genes by RNA whole-mount in situ hybridization and subsequent RT-PCR analysis revealed a low mRNA expression level of these opsins, suggesting a low mRNA expression level; therefore we produced antibodies against all four c-opsin proteins (Table S1). Antibody staining indeed revealed specific expression of c-opsin1 and c-opsin3 in the Row1 (15, 22) cells of the amphioxus frontal eye (Fig. 3 *A* and *B*). The specificity of each antibody was confirmed by the loss of specific signal after preadsorption with the respective antigen (Fig. S3). We further noted that the c-opsin1 and c-opsin3 antibodies labeled morphologically distinct cells within Row 1 (compare Fig. 3 *A* and *B* and Fig. S5), consistent with possible differential responses to distinct wavelengths. None of the other rows of the frontal eye was positive for any of the other c-opsins. To characterize phototransduction in the amphioxus frontal eye further, we cloned the proteins of the amphioxus G-alpha subunit see Fig. S6 for the phylogenetic tree). The proteins of the G-alpha subunit are specific for distinct phototransductory cascades in vertebrates and invertebrates (23). In vertebrate rods and cones, transducin signals to phosphodiesterase that hydrolyses cGMP and shuts down the dark current, mediating an "off response" to light (23). The activity of such phosphodiesterase is stimulated by transducins, which arose by gene duplication of a more ancestral *Gi* gene encoding the inhibitory Gi-alpha subunit (23). Because the amphioxus genome predates the duplication events that generated transducins later in evolution, we investigated the expression of their more ancestral counterpart *Gi*. The only amphioxus *Gi* gene that we found is expressed in the most anterior cells of the amphioxus frontal eye (Fig. 3*C*). We also investigated expression of the Go-alpha subunit, which is active in the photoreceptors of vertebrate pineal eyes (11) and in the ciliary photoreceptors of mollusks (24). The amphioxus *Go* gene is expressed more broadly in the amphioxus cerebral vesicle (Fig. 3*D*); however, the most anterior portion of the frontal eye appeared to be specifically excluded from the *Go* expression domain, indicating that it is unlikely that the Row1 cells also signal via the Go-alpha subunit. Notably, the Gq-alpha subunit characteristic for invertebrate rhabdomeric photoreceptor cells has not been detected in the amphioxus frontal eye (6). This result suggests that the Row1 cells of the frontal eye couple to an inhibitory G-alpha subunit protein mediating the off response.

Pigmented Cells of the Amphioxus Frontal Eye. Cells of the vertebrate retinal pigmented epithelium (RPE) are specified by the *Mitf* transcription factor and use melanin as a shading pigment (25). We investigated expression of amphioxus *mitf* within the cerebral vesicle and found it restricted to the pigment cells of the frontal eye (Fig. 4 *A* and *B*). In addition, the vertebrate *Otx2* paralog acts in tight cooperation with *Mitf* during RPE development and differentiation (26). This might also be the case in amphioxus, where *mitf* is expressed concomitantly with *otx* in the pigment cells of the frontal eye (Fig. 2 *D–F*). Furthermore, we exposed developing amphioxus embryos and larvae to phenylthiourea (PTU), a specific inhibitor of melanin synthesis causing the absence of melanin pigment in the vertebrate eye (27). After PTU exposure, the dark pigment of the frontal eye was abolished completely (Fig. 4 *C–E*), indicating that melanin is indeed the only dark pigment of the frontal eye.

Projections. Finally, we analyzed axonal projections from frontal eye cells. Previous transmission electronic microscopy studies revealed only short projections to the laterally adjacent frontal

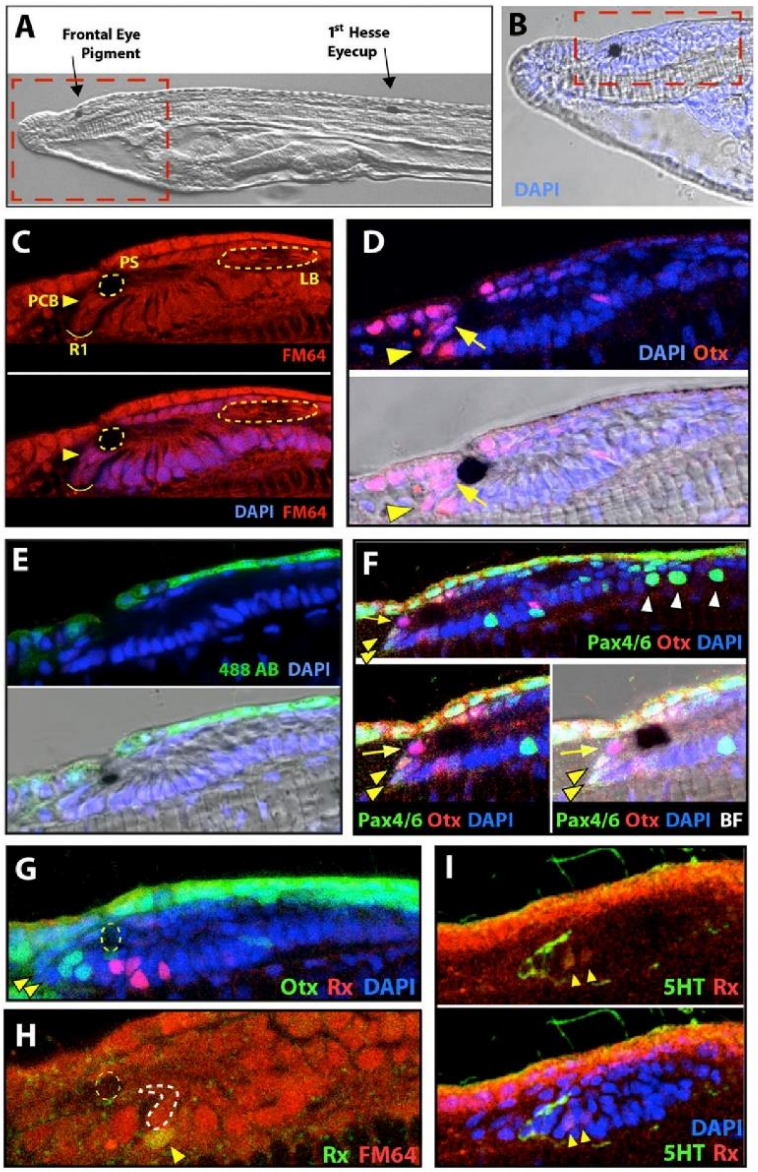

Fig. 2. Expression of *otx*, *pax4/6*, and *rx* in the amphioxus cerebral vesicle. (*A*) Overview of the anterior part of a larva at the 2.5–gill-slit stage typically used in this study. (*B*) Detailed view of the most anterior part of the larva (defined by red dashed box in *A*) with nuclei stained with DAPI. (*C–I*) The area of the cerebral vesicle defined by the red dashed box in *B*. (*C*) The cerebral vesicle was stained with FM64 stain to visualize the cell bodies and with DAPI to stain the nuclei to address the comparability of this stage with previous studies (22). The Row1 cells (R1) are positioned ventro-anteriorly to the pigment spot. Note the shapes of the cell bodies in the cerebral vesicle; the presence of apical cilium projecting to the lumen of the cerebral vesicle suggests that these cells already have differentiated at this developmental stage (compare with figure 2 in ref. 49). LB, lamellar body; PCB, pigment cell body; PS, pigment spot; R1, Row1 cells. (*D*) Otx protein is present in the nuclei of the most anterior cells of the cerebral vesicle, including the Row1 cells (arrowhead) and the more dorso-posteriorly positioned pigment cells (arrow). (*E*) Endogenous amphioxus GFP expression (17) and nonspecific trapping of the secondary antibody causes the presence of epidermal signal when green-fluorescent secondary antibodies are used (Alexa 488 is shown). For easy orientation, the *Lower* panel shows the same image including the brightfield. (*F*) (*Upper*) The broad *pax4/6* expression in the amphioxus cerebral vesicle and epidermis (19) includes Row1 cells, in which *pax4/6* is coexpressed with *otx* (yellow arrowheads). Furthermore, Pax4/6 is observed in scattered cells within the ventral floor of the cerebral vesicle (Fig S4C), in cells of the lamellar body, and the large cells of the PMC (white arrowheads). A detailed view of the frontal eye region is shown in the *Lower Left* panel and the brightfield channel for easy orientation is included in the *Lower Right* panel. (*G*) Consistent with the RNA in situ hybridization result (Fig. 1*D*), the antibody raised against Rx protein stained several nuclei positioned posterior to Row1 cells (arrowheads), and *rx* expression did not overlap with the most posterior nuclei expressing *otx*. The dashed circle demarcates the pigment spot. (*H*) A subset of *rx*-positive nuclei (yellow arrowhead) belonged to cells lacking apical projections and positioned deeper in the cerebral vesicle floor. Yellow dashed circle demarcates the pigment spot, and the white dashed line follows the cell shape of a cell possessing the apical projection. (*I*) To see whether *rx*-positive nuclei might belong to serotonergic Row2 cells (22), we performed coimmunolabeling with Rx and anti-serotonin antibody. The Rx signal (yellow arrowheads) was posterior to Row2 cells, suggesting possible expression in Row3 or Row4 cells. The high background staining in the red channel comes from the double sequential protocol used to perform staining with two primary antibodies raised in the same species (rabbit). The *Lower* panel includes the DAPI staining to visualize the extend of the cerebral vesicle.

nerves (22). We took advantage of the serotoninergic nature of the Row2 cells of frontal eye, which are in direct contact with the Row1 cells (22, 28), and detected long basal axonal projections from the frontal eye Row2 cells toward the posterior cerebral vesicle (Fig. 5 *A* and *B*), where we observed massive serotonin varicosities within the tegmental neuropil (22).

Discussion

The thorough immunohistochemical study presented in this work defines, at least in part, a molecular fingerprint for the amphioxus frontal eye at cellular resolution (summarized in Fig. 5*C*) and thus provides important insight into the evolutionary origin of the vertebrate eyes. The expression profile of vertebrate eye-specific regulatory (*Rx*, *Otx*, *Pax4/6*, and *Mitf*) genes and differentiation markers (c-opsins, Gi, melanin) in the amphioxus cerebral vesicle strongly supports the homology of photoreceptor and pigmented cells of the amphioxus frontal eye and the corresponding cell types in the vertebrate retina and retinal pigmented epithelium, respectively.

Regulatory Signature. The early developmental patterning of the amphioxus frontal eye is performed by the same set of transcription factors (Otx, Rx, and Pax4/6) as the vertebrate retina. In vertebrates, *Otx2* controls the development of both the retina and the pineal gland (29) and another vertebrate paralogue of *Otx*, cone rod homeobox (*Crx*) transcription factor, is crucial for

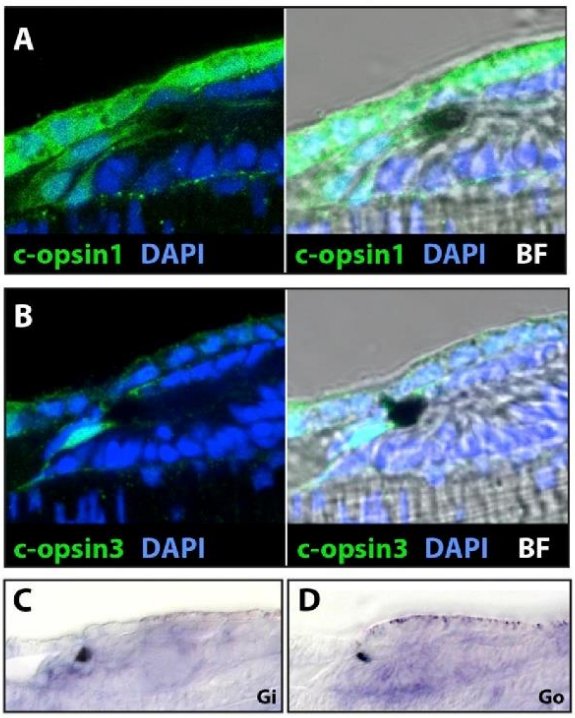

Fig. 3. Expression of amphioxus c-opsins and G-alpha subunits in the cerebral vesicle. Amphioxus larvae were stained with mouse polyclonal sera raised against the C-terminal portion of amphioxus c-opsins. For easy orientation, the bright-field (BF) images of the confocal plane are included on the right in *A* and *B*. (*A*) The expression of *c-opsin1* in several cells positioned at the most anterior tip of the frontal eye, corresponding to Row1 cells (22). (*B*) *c-opsin3* is expressed most dorsally, in the *Row1* cells ventrally adjacent to the pigment-producing cells (compare with figure 17 in ref. 22). (*C*) Expression of the Gi-alpha subunit in the cerebral vesicle revealed by RNA in situ hybridization. The cells with the strongest labeling are localized in the very anterior tip of the vesicle in the position corresponding to the photoreceptor cells. (*D*) The Go-alpha subunit is expressed throughout the cerebral vesicle, except in the very anterior tip, suggesting that it is excluded from the Row1 cells.

the terminal differentiation of the rods and cones (30). Likewise, vertebrate *Pax6* is necessary for proper eye development (31, 32), and the expression of *pax4* is characteristic for differentiated rods and cones (33, 34). During later stages, *otx* and *pax4/6* remain expressed in the differentiated Row1 photoreceptors, albeit at lower levels that suffice for maintenance of the differentiated state of the given cell type. This situation exemplifies the division of labor of the chordate single-copy orthologs (such as amphioxus *pax4/6* and *otx*) after gene duplication in the vertebrates, where *Pax6* and *Otx2* are active during early eye/pineal gland development, and their paralogs *Pax4* and *Crx* act during the terminal differentiation stages. Although the transient expression of *rx* in the precursors of ciliary photoreceptors (Fig. 1*B*) seems to be evolutionarily conserved (35), the absence of *rx* in the differentiated photoreceptors of Row1 cells contrasts with its expression in vertebrate differentiated photoreceptors and its involvement in the regulation of phototransduction genes (36). The overlapping expression of *rx* and ci-opsin1 in the ciliary photoreceptor of tunicates (37, 38) suggests either the acquisition of *rx* for the direct regulation of photoreceptor genes such as opsins at the base of Olfactores or amphioxus-specific loss of *rx* role for maintaining the differentiated ciliary photoreceptor program. The small population of *rx*-positive cells lacking the apical cilium might represent, as in vertebrates (39–41), a progenitor subpopulation needed for further growth of the frontal eye later in development. The absence of expression of *otx* and *rx* in the lamellar organ challenges its proposed homology with the vertebrate pineal gland, but the currently available data are too sparse to allow any conclusions. To resolve this issue, further molecular characterization of the lamellar organ will be rewarding.

Evolutionary Precursor of the Vertebrate Phototransduction Cascade. The expression of two ciliary opsins and the proteins of the G_i-alpha subunit in the amphioxus frontal eye provides molecular evidence of the photosensory nature of Row1 cells and corroborates the homology of these amphioxus cells and vertebrate rods, cones, and/or pinealocytes. Because c-opsin and Gi-alpha also are coexpressed in tunicate ciliary photoreceptors (38, 42), the amphioxus frontal eye photoreceptors using ciliary opsin

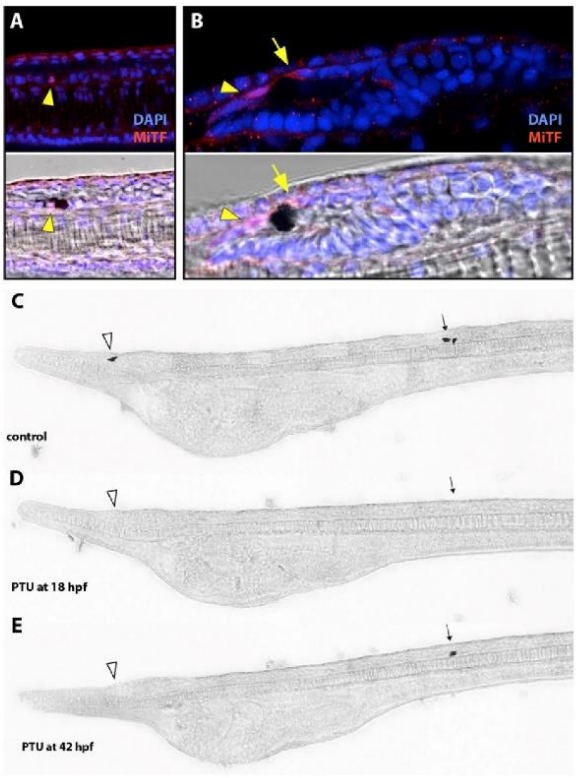

Fig. 4. Characterization of the frontal eye pigment cells. The *Lower* panels in *A* and *B* include the brightfield channel to visualize the pigment spot. (*A*) The specificity of Mitf antibody has been confirmed by specific nuclear staining (yellow arrowhead) in the pigment cell of the Hesse eyecup in which *mitf* expression was reported previously (57). (See also Fig. S2*E* for Western blot and Fig. S3 *E* and *F* for loss of signal after antigen preadsorption.) (*B*) The Mitf antibody labeled the nuclei (yellow arrowhead) and cytoplasm (yellow arrow) of the frontal eye pigment cells. The cytoplasmic localization of Mitf also was observed in vertebrates (58). (*C–E*) PTU treatment blocks pigment synthesis in both frontal eye and first Hesse eyecup in *B. lanceolatum*. (*C*) Control animals treated only with ethanol developed both pigmented structures, the first Hesse eyecup (black arrow) and pigment of the frontal eye (arrowhead). (*D*) Animals treated with 0.22 mM PTU from 18 hpf (before developing the first Hesse eyecup pigment) lack both pigmented structures. (*E*) Addition of PTU at 42 hpf (after the first Hesse eyecup has developed), results in animals lacking only the frontal eye pigment. This experiment shows that the pigment in both the Hesse eyecup and the frontal eye is melanin.

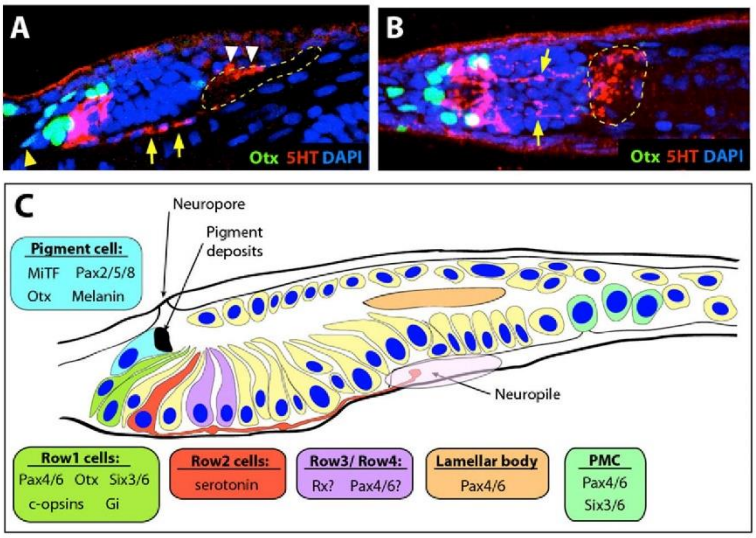

Fig. 5. The projections of the frontal eye region. (*A*) Serotonergic Row2 cells project axons to the neuropil (dashed outline), where the axons terminate by many varicosities (white arrowheads). A few varicosities are also encountered along the axons (yellow arrows). This double labeling also revealed that the Row2 cells do not express Otx, because its nuclear signal is never present in the cells expressing serotonin. Yellow arrowhead points to a Row1 cell. (*B*) Dorsal view of the same specimen showing the trajectory of the serotonergic axons with varicosities (yellow arrows) terminating in the neuropil area (dashed outline). (*C*) A schematic drawing summarizing the molecular data available for the frontal eye region at the differentiated state. The expression data for Pax2/5/8 (46) and Six3/6 (47) are based on previous studies.

coupled to Gi-alpha represent the ancestral chordate condition and an evolutionary forerunner of more sophisticated vertebrate visual photoreceptors. In early vertebrate evolution the two rounds of genome duplication giving rise to the vertebrate visual opsin subclass (by duplicating ancestral chordate ciliary opsin genes) and a new subclass of Gi-derived Gt-alpha protein subunits provided enough genetic material to allow biochemical evolution (43) to provide the highly efficient phototransductory system operating in today's vertebrate rods and cones.

Frontal Eye Pigment Cells Are Homologous to the Cells of the Vertebrate RPE. Unlike previous observations based on morphological and chemical properties (44, 45), our data provide biochemical evidence that the only shielding pigment of amphioxus pigment cells is melanin. The molecular fingerprint of the amphioxus frontal eye pigment cells, expressing *mitf*, *otx*, and *pax2/5/8* (46, 47), resembles the fingerprint of the vertebrate retinal pigmented epithelium (48). In both amphioxus and vertebrates, the pigmented cells are located directly adjacent to the ciliary photoreceptor cells (Row1 cells in amphioxus and rods and cones in the vertebrates), further corroborating the homology of amphioxus and vertebrate eyes.

Neural Circuitry of the Frontal Eye. The Row2 cells projecting axons to the tegmental neuropil provide further evidence for the homology of the frontal eye and the vertebrate retina. As projection neurons, Row2 cells would correspond to retinal ganglion cells [and to horizontal and amacrine cells, the presumed sister cell types of the ganglion cells (7)]. However, more information about Row2-specific expression will be needed to substantiate this issue and to test for any relationship to the rhabdomeric photoreceptor lineage (7). The tegmental neuropil has been compared with locomotor control regions of the vertebrate hypothalamus, where paracrine release modulates locomotor patterns such as feeding and swimming (49). Consistent with this idea, *FoxD* (50) and *Brn1/2/4* (51), whose vertebrate orthologs are expressed in the hypothalamus, also are expressed in the tissue apposed the tegmental neuropil in amphioxus. In addition, the retinohypothalamic tract in vertebrates projects to the anterior hypothalamic area involved in the control of basic behaviors (52) and also the pineal fibers connect bilaterally to the rostral hypothalamus (53). The amphioxus tegmental neuropil in the posterior cerebral vesicle receives not only projections from the frontal eye area but also bilateral afferents from the giant cells located in the primary motor center (PMC) (49). The PMC, positioned immediately beyond the caudal end of the cerebral vesicle, likewise is connected to the frontal eye region via an asymmetrical lateral dendrite of one of the abovementioned giant cells (49). Given that the PMC cells lie in the *gbx* expression region (54), and some of them also are positive for *pax4/6* (Fig. 2*F*), their molecular identity resembles that of the vertebrate interpeduncular nucleus located in the hindbrain and involved in locomotor control (55). Taken together, these findings indicate that in amphioxus the frontal eye projects to the neurosecretory/tegmental neuropil and to the locomotor center, like the eye and the pineal gland in vertebrates.

The study highlights the advantage of cellular resolution, gene coexpression, and structural analyses using molecular markers to define the neuronal circuitry in the amphioxus cerebral vesicle. Our data reveal direct innervation and indicate paracrine release of serotonin from Row2 cells in the tegmental neuropil in the posterior cerebral vesicle, reminiscent of retinohypothalamic projections in the vertebrates. Also, the frontal eye directly innervates locomotor control regions in the primary motor center, again reminiscent of more complex vertebrate circuits of the retina and pineal. The amphioxus frontal eye circuit thus represents a very simple precursor circuit that, by expansion, duplication, and divergence, might have given rise to photosensory-locomotor circuits as found in the extant vertebrate brain.

Experimental Procedures

Animals. *Branchiostoma floridae* larvae were obtained in Tampa Bay (Florida), during the spawning season in August 2010. At the 2.5–gill-slit stage, the animals were fixed with 3-(N-morpholino)propanesulfonic acid (MOPS) fixative (0.1 M MOPS, 2 mM $MgSO_4$, 1 mM EGTA, 0.5M NaCl, pH 7.5) for 30 min at room temperature and then were transferred to 100% methanol. Larvae for RNA in situ hybridization were kindly provided by Linda Z. Holland (Scripps Institution of Oceanography, University of California at San Diego, La Jolla, CA). *B. lanceolatum* larvae for the PTU experiment were provided by the amphioxus facility of the Arendt group, European Molecular Biology Laboratory, Heidelberg.

Immunohistochemistry. If not otherwise stated, all incubation steps were carried out at room temperature. Specimens were transferred to 1× PBS, 0.1% (vol/vol) Tween 20 (PBT) through 50% (vol/vol) and 25% (vol/vol) methanol in PBS. Specimens were washed three times (20 min each washing) in PBT, blocked in block solution [10% (wt/wt) BSA in PBS] for 1 h, and incubated with preadsorbed sera (dilutions are given in Table S1) overnight at 4 °C. On the next day, specimens were washed three or four times in PBT (20 min each washing) and were incubated with secondary antibodies for 2 h. Secondary antibodies were washed away with three washings in PBT (20 min

each washing). Nuclear counterstaining was carried out by incubation with 1 μg/mL DAPI in PBS and washing three times (5 min each washing). For FM4-64FX (Invitrogen) staining, the larvae were incubated in the dye (10 μg/mL) for 10 min in PBS and were washed twice with PBS.

For fluorescence/confocal microscopy, the specimens were mounted in VECTASHIELD (Vector Laboratories, Inc.) using small coverslips as spacers between the coverslip and the slide. The confocal images were taken using a Leica SP5 confocal microscope and were processed (contrast, brightness, and histogram adjustment) with FIJI free image analysis software (http://fiji.sc).

RNA in Situ Hybridization. Whole-mount RNA in situ hybridization to amphioxus larvae was performed according to a standard protocol (56). The only modification was the omission of levamisole in washes on day 3 (step vi).

PTU Treatment. *B. lanceolatum* embryos raised at 20 °C were treated in the dark with 0.22 mM PTU (stock solution 100 mM PTU in 96% EtOH) either from the 18-hpf stage onwards or from the 42-hpf stage onwards. Ethanol at the same dilution was used as a negative control. The drug was changed every 24 h. At 66 hpf the specimens were fixed and documented.

ACKNOWLEDGMENTS. We thank Nicholas and Linda Holland for providing fixed animals for whole-mount in situ hybridization and help with RNA in situ hybridization, Jitka Lachova for immunization of mice, and Cestmir Vlcek for excellent help in sequencing. This study was supported by the Grant Agency of the Czech Republic Grants P305/10/2141 and P305/10/J064 (to Z.K.) and DFG AR 387/2-1 (to D.A.) and the Grant Agency of the Charles University, Grant GAUK 91808 (to P.V.) and by IMG institutional support RVO 68378050.

1. Darwin C (1859) *On the Origin of Species by Means of Natural Selection* (Murray, London) 1st Ed.
2. Lamb TD, Collin SP, Pugh EN, Jr. (2007) Evolution of the vertebrate eye: Opsins, photoreceptors, retina and eye cup. *Nat Rev Neurosci* 8:960–976.
3. Delsuc F, Brinkmann H, Chourrout D, Philippe H (2006) Tunicates and not cephalochordates are the closest living relatives of vertebrates. *Nature* 439:965–968.
4. Putnam NH, et al. (2008) The amphioxus genome and the evolution of the chordate karyotype. *Nature* 453:1064–1071.
5. Lacalli TC (2004) Sensory systems in amphioxus: A window on the ancestral chordate condition. *Brain Behav Evol* 64:148–162.
6. Koyanagi M, Kubokawa K, Tsukamoto H, Shichida Y, Terakita A (2005) Cephalochordate melanopsin: Evolutionary linkage between invertebrate visual cells and vertebrate photosensitive retinal ganglion cells. *Curr Biol* 15:1065–1069.
7. Arendt D (2003) Evolution of eyes and photoreceptor cell types. *Int J Dev Biol* 47: 563–571.
8. Satir P (2000) A comment on the origin of the vertebrate eye. *Anat Rec* 261:224–227.
9. Solessio E, Engbretson GA (1993) Antagonistic chromatic mechanisms in photoreceptors of the parietal eye of lizards. *Nature* 364:442–445.
10. Vigh B, et al. (2002) Nonvisual photoreceptors of the deep brain, pineal organs and retina. *Histol Histopathol* 17:555–590.
11. Su CY, et al. (2006) Parietal-eye phototransduction components and their potential evolutionary implications. *Science* 311:1617–1621.
12. Rohde K, Klein DC, Møller M, Rath MF (2011) Rax: Developmental and daily expression patterns in the rat pineal gland and retina. *J Neurochem* 118:999–1007.
13. Furukawa T, Kozak CA, Cepko CL (1997) rax, a novel paired-type homeobox gene, shows expression in the anterior neural fold and developing retina. *Proc Natl Acad Sci USA* 94:3088–3093.
14. Bailey TJ, et al. (2004) Regulation of vertebrate eye development by Rx genes. *Int J Dev Biol* 48:761–770.
15. Lacalli T, Holland N, West J (1994) Landmarks in the anterior central nervous system of amphioxus larvae. *Philos Trans R Soc Lond B Biol Sci* 344(1308):165–185.
16. Ruiz S, Anadón R (1991) The fine structure of lamellate cells in the brain of amphioxus (Branchiostoma lanceolatum, Cephalochordata). *Cell Tissue Res* 263:597–600.
17. Deheyn DD, et al. (2007) Endogenous green fluorescent protein (GFP) in amphioxus. *Biol Bull* 213:95–100.
18. Williams NA, Holland PWH (1996) Old head on young shoulders. *Nature* 383:490.
19. Glardon S, Holland LZ, Gehring WJ, Holland ND (1998) Isolation and developmental expression of the amphioxus Pax-6 gene (AmphiPax-6): Insights into eye and photoreceptor evolution. *Development* 125:2701–2710.
20. Holland LZ, et al. (2008) The amphioxus genome illuminates vertebrate origins and cephalochordate biology. *Genome Res* 18:1100–1111.
21. Albalat R (2012) Evolution of the genetic machinery of the visual cycle: A novelty of the vertebrate eye? *Mol Biol Evol* 29:1461–1469.
22. Lacalli TC (1996) Frontal eye circuitry, rostral sensory pathways and brain organization in amphioxus larvae: Evidence from 3D reconstructions. *Philos Trans Roy Soc Lond B, Biol Sci* 351(1337):243–263.
23. Yau KW, Hardie RC (2009) Phototransduction motifs and variations. *Cell* 139:246–264.
24. Kojima D, et al. (1997) A novel Go-mediated phototransduction cascade in scallop visual cells. *J Biol Chem* 272:22979–22982.
25. Nguyen M, Arnheiter H (2000) Signaling and transcriptional regulation in early mammalian eye development: A link between FGF and MITF. *Development* 127: 3581–3591.
26. Martínez-Morales JR, et al. (2003) OTX2 activates the molecular network underlying retina pigment epithelium differentiation. *J Biol Chem* 278:21721–21731.
27. Karlsson J, von Hofsten J, Olsson PE (2001) Generating transparent zebrafish: A refined method to improve detection of gene expression during embryonic development. *Mar Biotechnol (NY)* 3:522–527.
28. Holland ND, Holland LZ (1993) Serotonin-Containing Cells in the Nervous-System and Other Tissues during Ontogeny of a Lancelet, Branchiostoma-Floridae. *Acta Zoologica* 74(3):195–204.
29. Nishida A, et al. (2003) Otx2 homeobox gene controls retinal photoreceptor cell fate and pineal gland development. *Nat Neurosci* 6:1255–1263.
30. Furukawa T, Morrow EM, Li T, Davis FC, Cepko CL (1999) Retinopathy and attenuated circadian entrainment in Crx-deficient mice. *Nat Genet* 23:466–470.
31. Hill RE, et al. (1991) Mouse small eye results from mutations in a paired-like homeobox-containing gene. *Nature* 354:522–525.
32. Estivill-Torrús G, Vitalis T, Fernández-Llebrez P, Price DJ (2001) The transcription factor Pax6 is required for development of the diencephalic dorsal midline secretory radial glia that form the subcommissural organ. *Mech Dev* 109:215–224.
33. Rath MF, et al. (2009) Developmental and daily expression of the Pax4 and Pax6 homeobox genes in the rat retina: Localization of Pax4 in photoreceptor cells. *J Neurochem* 108:285–294.
34. Rath MF, et al. (2009) Developmental and diurnal dynamics of Pax4 expression in the mammalian pineal gland: Nocturnal down-regulation is mediated by adrenergic-cyclic adenosine 3′,5′-monophosphate signaling. *Endocrinology* 150:803–811.
35. Arendt D, Tessmar-Raible K, Snyman H, Dorresteijn AW, Wittbrodt J (2004) Ciliary photoreceptors with a vertebrate-type opsin in an invertebrate brain. *Science* 306: 869–871.
36. Kimura A, et al. (2000) Both PCE-1/RX and OTX/CRX interactions are necessary for photoreceptor-specific gene expression. *J Biol Chem* 275:1152–1160.
37. D'Aniello S, et al. (2006) The ascidian homolog of the vertebrate homeobox gene Rx is essential for ocellus development and function. *Differentiation* 74:222–234.
38. Kusakabe T, et al. (2001) Ci-opsin1, a vertebrate-type opsin gene, expressed in the larval ocellus of the ascidian Ciona intestinalis. *FEBS Lett* 506:69–72.
39. Casarosa S, et al. (2003) Xrx1 controls proliferation and multipotency of retinal progenitors. *Mol Cell Neurosci* 22:25–36.
40. Nelson SM, Park L, Stenkamp DL (2009) Retinal homeobox 1 is required for retinal neurogenesis and photoreceptor differentiation in embryonic zebrafish. *Dev Biol* 328: 24–39.
41. Chen CM, Cepko CL (2002) The chicken RaxL gene plays a role in the initiation of photoreceptor differentiation. *Development* 129:5363–5375.
42. Yoshida R, Kusakabe T, Kamatani M, Daitoh M, Tsuda M (2002) Central nervous system-specific expression of G protein alpha subunits in the ascidian Ciona intestinalis. *Zoolog Sci* 19:1079–1088.
43. Sato K, Yamashita T, Ohuchi H, Shichida Y (2011) Vertebrate ancient-long opsin has molecular properties intermediate between those of vertebrate and invertebrate visual pigments. *Biochemistry* 50:10484–10490.
44. Franz V (1927) Morphologie der Akranier. *Ergeb Anat Entwicklungsgesch* 27:464–692.
45. Tenbaum E (1955) Polarisationsoptische Beiträge zur Kenntnis der Gewebe von Branchiostoma Lanceolatum (P). *Cell and Tissue Research* 42(3):149–192.
46. Kozmik Z, et al. (1999) Characterization of an amphioxus paired box gene, AmphiPax2/5/8: Developmental expression patterns in optic support cells, nephridium, thyroid-like structures and pharyngeal gill slits, but not in the midbrain-hindbrain boundary region. *Development* 126:1295–1304.
47. Kozmik Z, et al. (2007) Pax-Six-Eya-Dach network during amphioxus development: Conservation in vitro but context specificity in vivo. *Dev Biol* 306:143–159.
48. Martínez-Morales JR, Rodrigo I, Bovolenta P (2004) Eye development: A view from the retina pigmented epithelium. *Bioessays* 26:766–777.
49. Lacalli TC, Kelly SJ (2000) The infundibular balance organ in amphioxus larvae and related aspects of cerebral vesicle organization. *Acta Zoologica* 81(1):37–47.
50. Yu JK, Holland ND, Holland LZ (2002) An amphioxus winged helix/forkhead gene, AmphiFoxD: Insights into vertebrate neural crest evolution. *Dev Dyn* 225(3):289–297.
51. Candiani S, Castagnola P, Oliveri D, Pestarino M (2002) Cloning and developmental expression of AmphiBrn1/2/4, a POU III gene in amphioxus. *Mech Dev* 116:231–234.
52. Canteras NS, Ribeiro-Barbosa ER, Goto M, Cipolla-Neto J, Swanson LW (2011) The retinohypothalamic tract: Comparison of axonal projection patterns from four major targets. *Brain Res Brain Res Rev* 65:150–183.
53. Yáñez J, Busch J, Anadón R, Meissl H (2009) Pineal projections in the zebrafish (Danio rerio): Overlap with retinal and cerebellar projections. *Neuroscience* 164:1712–1720.
54. Castro LF, Rasmussen SL, Holland PW, Holland ND, Holland LZ (2006) A Gbx homeobox gene in amphioxus: Insights into ancestry of the ANTP class and evolution of the midbrain/hindbrain boundary. *Dev Biol* 295:40–51.
55. Lorente-Cánovas B, et al. (2012) Multiple origins, migratory paths and molecular profiles of cells populating the avian interpeduncular nucleus. *Dev Biol* 361:12–26.
56. Holland LZ, Holland PW, Holland ND (1996) *Whole Mount in Situ Hybridization Applicable to Amphioxus and Other Small Larvae*, Molecular Zoology, Advances, Strategies, and Protocols, eds Ferraris JD, Palumbi SR (Wiley-Liss Inc., New York), pp 474–483.
57. Yu JK, Meulemans D, McKeown SJ, Bronner-Fraser M (2008) Insights from the amphioxus genome on the origin of vertebrate neural crest. *Genome Res* 18:1127–1132.
58. Lu SY, Wan HC, Li M, Lin YL (2010) Subcellular localization of Mitf in monocytic cells. *Histochem Cell Biol* 133:651–658.

Supporting Information

Vopalensky et al. 10.1073/pnas.1207580109

SI Experimental Procedures

Expression and Purification of Proteins for Immunization. For overexpression of protein fragments, the pET system (Novagen) was used. Selected coding sequences were cloned into the pET42a(+) vector to create proteins containing 6xHis-GST fused to the protein fragment of interest. A total volume of 500 mL fresh LB medium without antibiotics was inoculated by culture grown overnight in LB medium supplemented with 12.5 μg/mL chloramphenicol and 30 μg/mL kanamycin. Bacteria were grown at 37 °C at 200 rpm until OD_{600} 0.6, and subsequently induced by 0.5 mM IPTG for 3 more hours. Cells were harvested at 6,000 × *g* for 20 min and the pellet wa stored at −80 °C until further processing. The pellet was resuspended in lysis buffer (6 M guanidine hydrochloride, 0.1M NaH_2PO_4, 0.01M Tris·Cl, pH 8.0, supplemented with fresh β-mercaptoethanol to a final concentration of 20 mM). The suspension was sonicated six times for 20 s and was incubated for 3 h at room temperature. The resulting lysate was centrifuged at 10 000 × *g* for 10 min, and the supernatant was mixed with Ni-NTA agarose beads (Qiagen) previously equilibrated with urea buffer (8 M urea, 20 mM Tris·Cl, 50 mM NaH_2PO_4, 100 mM NaCl, pH 8.0, supplemented with fresh β-mercaptoethanol to a final concentration of 20 mM). The suspension was incubated on a rotating platform overnight at room temperature. The beads with bound proteins were washed two times with 40 mL urea buffer and were loaded onto a disposable chromatographic column (Bio-Rad). The column was washed with urea buffer with decreasing pH (8.0–6.8), and His-tagged protein was eluted by urea buffer (pH 4.2) into several 1-mL aliquots. After elution, pH was adjusted immediately to 7.5 by 1 M Tris·Cl (pH 8). Protein concentration was estimated using Protein Assay Reagent (Bio-Rad).

Immunization of Rabbits and mice. For rabbit immunization, unbred female New Zealand White rabbits (Charles Rivers Laboratories) were used. Rabbits were immunized three or four times at 1-month intervals with 300–500 μg of purified protein mixed with Freund's Adjuvant (F5506; Sigma) in each immunization step. The final sera were tested for the ability to recognize a given antigen by Western blot. For mouse immunization, mice of the B10A-H2xBALB/CJ strain were immunized three or four times in 3-weeks interval with 30 μg purified protein mixed with Freund's Adjuvant (Sigma). Animal research complied with established protocols and was approved by the Animal Committee of the Institute of Molecular Genetics.

Preabsorbtion of Antibodies to Animal Powder. Before immunohistochemical staining, the sera were preadsorbed to amphioxus powder. Two frozen adult animals were ground in liquid nitrogen. Then 1 mL of acetone was added, and the mixture was left 30 min on ice. The powder was washed twice with acetone, dried and stored at −20 °C. To 1.5 mg powder, 1 mL of 10% BSA in 1× PBT (1× PBS, 0.1% Tween 20) was added and incubated for 30 min at 70 °C. After cooling, the crude serum was added to a final concentration of 1:100, and the solution was incubated overnight at 4 °C on a rotating platform. The next day the solution was centrifuged 5 min at 16,000 × *g*, and the supernatant containing the preadsorbed antibody was aliquoted and stored at −80 °C.

The rabbit polyclonal anti-5-HT antibody (20080; ImmunoStar) and mouse anti-acetylated β-tubulin (T6793; Sigma-Aldrich) were diluted 1:200 and 1:500, respectively.

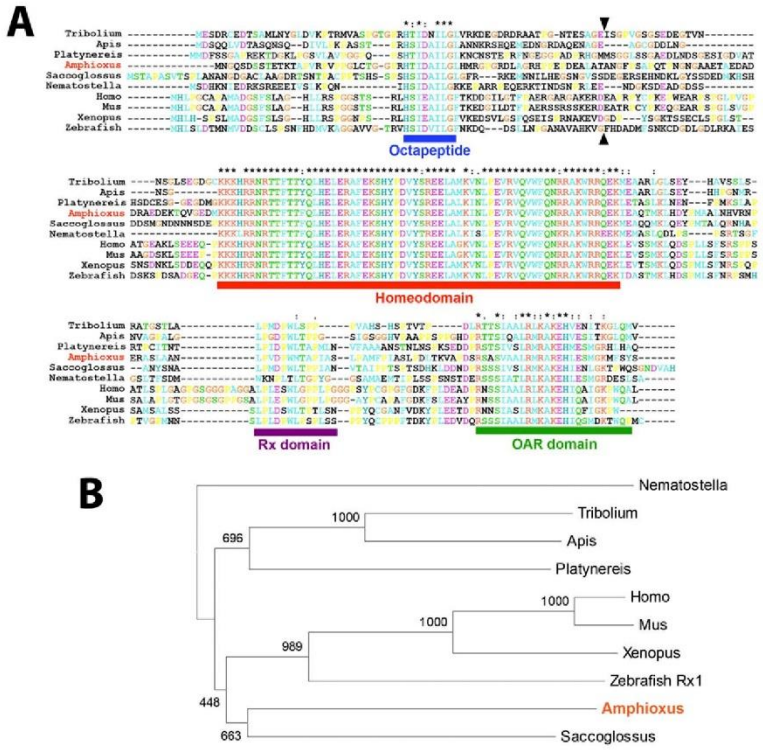

Fig. S1. Amino acid sequence alignment and phylogenetic tree of amphioxus Rx. (*A*) Amphioxus Rx contains the features characteristic for Rx proteins: the octapeptide, the Q50 homeodomain, the Rx domain, and the C-terminal otp, aristaless, and rax (OAR) domain. For brevity, a part of the amino acid sequence has been excluded (in the position of black arrowheads). (*B*) Neighbor-joining (NJ) phylogenetic tree of Rx protein sequences. The nonalignable regions have been excluded from the analysis. Numbers at the nodes represent the bootstrap support with 1,000 replicates. Accession nos.: *Nematostella*, XP_001634210.1; *Tribolium*, XP_973468.1; *Apis*, XP_001119966.1; *Platynereis*, AAU20320.1; *Homo sapiens* (Homo) Rx, NP_038463.1; *Mus* Rx, NP_038861.2; *Xenopus* Rx, AAB70267.1; Zebrafish Rx1, NP_571300.2; *Saccoglossus*, AAP79282.1.

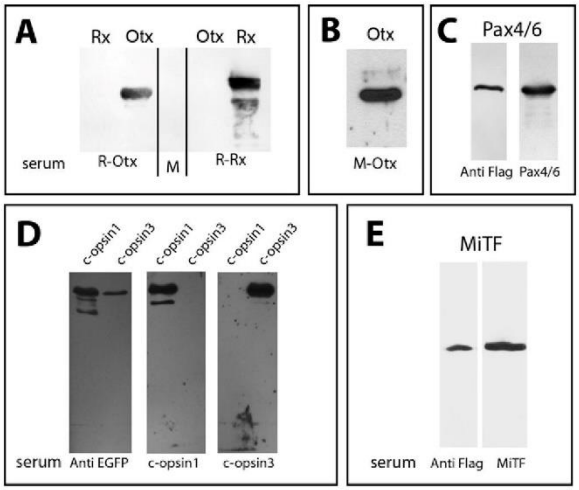

Fig. S2. Western blot analysis of antibodies generated in this work. HEK293T cell lines were transfected with an expression vector carrying Flag- (*A–C* and *E*) or EGFP-tagged (*D*) full-length coding sequences of the proteins indicated above each lane. Two days after transfection a whole-cell extract was prepared and subjected to Western blotting. The specificity of anti-Otx, -Rx, and -Pax4/6 antibodies was confirmed independently by recapitulating the whole-mount in situ hybridization patterns in immunohistochemical staining. (*A*) Rabbit antibodies against amphioxus Rx and Otx were tested on a double-lane blot containing the appropriate protein and another protein as a negative control. The lower band in the N-Rx–detected AmphiRx lane likely is caused by protein degradation. (*B*) Mouse polyclonal antibody against amphioxus Otx was generated to perform double immunohistochemical staining. (*C*) The rabbit antibody raised against amphioxus Pax4/6 recognizes the same band size as M2 anti-Flag (F1804; Sigma-Aldrich) antibody when tested with Flag-Pax4/6 fusion antigen. (*D*) Flag-tagged opsin antigens are recognized by anti-EGFP antibody as well as by mouse antibodies against amphioxus c-opsins. To exclude the possible cross-reactivity of anti–c-opsin antibodies, the antisera were tested with both c-opsin1 and c-opsin3 protein, showing specificity to the respective antigen. (*E*) Rabbit antibody raised against amphioxus Mitf recognizes the same band as M2 anti-Flag antibody when tested with Flag-Mitf fusion antigen.

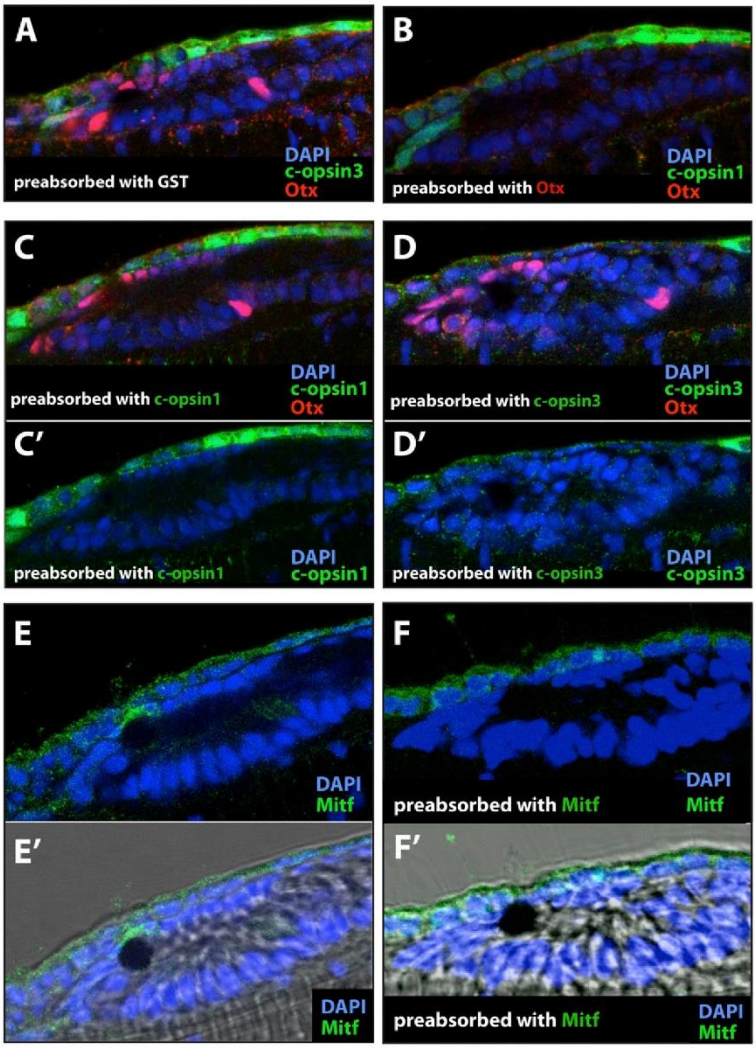

Fig. S3. Testing the specificity of c-opsin and Mitf antibodies. To test the specificity of antibodies for gene products with an unknown pattern of whole-mount in situ hybridization expression, we tested for the loss of specific signal after preadsorption of the antibody with its respective antigen used for immunization. Purified antigen was separated by SDS/PAGE, blotted to a nitrocellulose membrane, washed three times in PBT, and blocked with 10% BSA. Afterwards, the membranes with bound antigen were incubated for 4–6 h with the antibodies diluted to working concentration in 10% BSA. Following this preadsorption, the antibodies were used for immunohistochemical staining as described in *Experimental Procedures*. (*A*) As a negative control, the mixture of Otx and c-opsin3 antibodies was preadsorbed with GST not fused with any antigen. After such control preadsorption, the antibodies do not show any loss of specific immunohistochemical signal. (*B*) As a proof of principle, the preadsorption of the mixture of Otx and c-opsin1 antibodies with Otx antigen results in the specific loss of Otx but not c-opsin1 signal. (*C* and *C′*) Preadsorption of Otx/c-opsin1 antibody mixture with c-opsin1 antigen leads to specific loss of c-opsin1 staining. (*D* and *D′*) Likewise, only the signal of c-opsin3 is lost after preadsorbtion with c-opsin3 antigen. (*E–F′*) The signal of Mitf (*E* and *E′*) is lost when Mitf antibody is preadsorbed with Mitf antigen (*F* and *F′*).

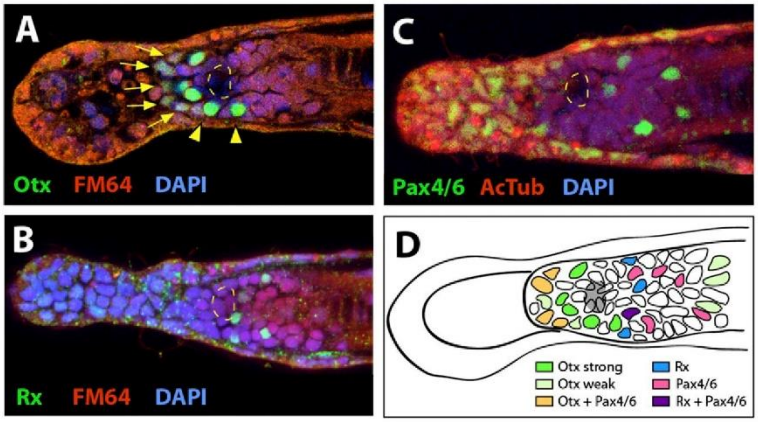

Fig. S4. Dorsal views on the cerebral vesicle floor plate. (*A*) *Otx* is expressed at two levels in the anterior tip of the cerebral vesicle: at a lower level in the very anterior row of cells (Row 1) and at a higher level in the adjacent more posterior row. The dashed yellow line demarcates the pigment spot. (*B*) *Rx* is expressed in few scattered cells in the anterior cerebral vesicle corresponding to the Row3/4 area. The mediolateral distribution of *rx*-positive nuclei varies among specimens. (*C*) Pax4/6 expression within the floor of the cerebral vesicle also is scattered, with the most anterior *pax4/6*-positive nuclei possibly overlapping some of the *rx*-positive nuclei. However, double immunohistochemistry could not be performed because the primary antibodies were from the same host species. (*D*) A schematic representation of the anterior part of an amphioxus larva showing the nuclei of the floor of the cerebral vesicle. The expression of *otx*, *rx*, and *pax4/6* is color-coded based on observations of multiple specimens. The coexpression of *rx* and *pax4/6* (purple) is only putative, based on position, and was not confirmed experimentally by double immunohistochemistry. The gray area represents the position of the pigment spot, which lies above the plane of the cerebral vesicle floor.

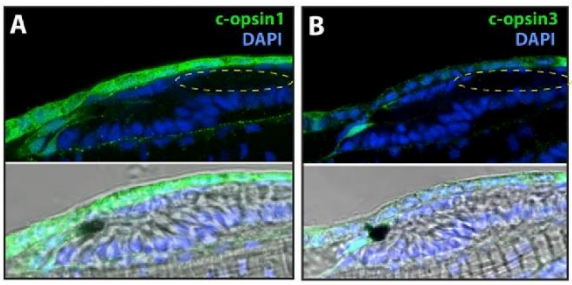

Fig. S5. Expression of *c-opsin1* and *c-opsin3* within the cerebral vesicle. The expression of *c-opsin1* (*A*) and *c-opsin3* (*B*) is restricted to Row1 cells in the anterior tip of the neural tube. No expression is observed within the lamellar body (marked with yellow dashed line). For easy orientation, the brightfield channels are included in the *Lower* panels.

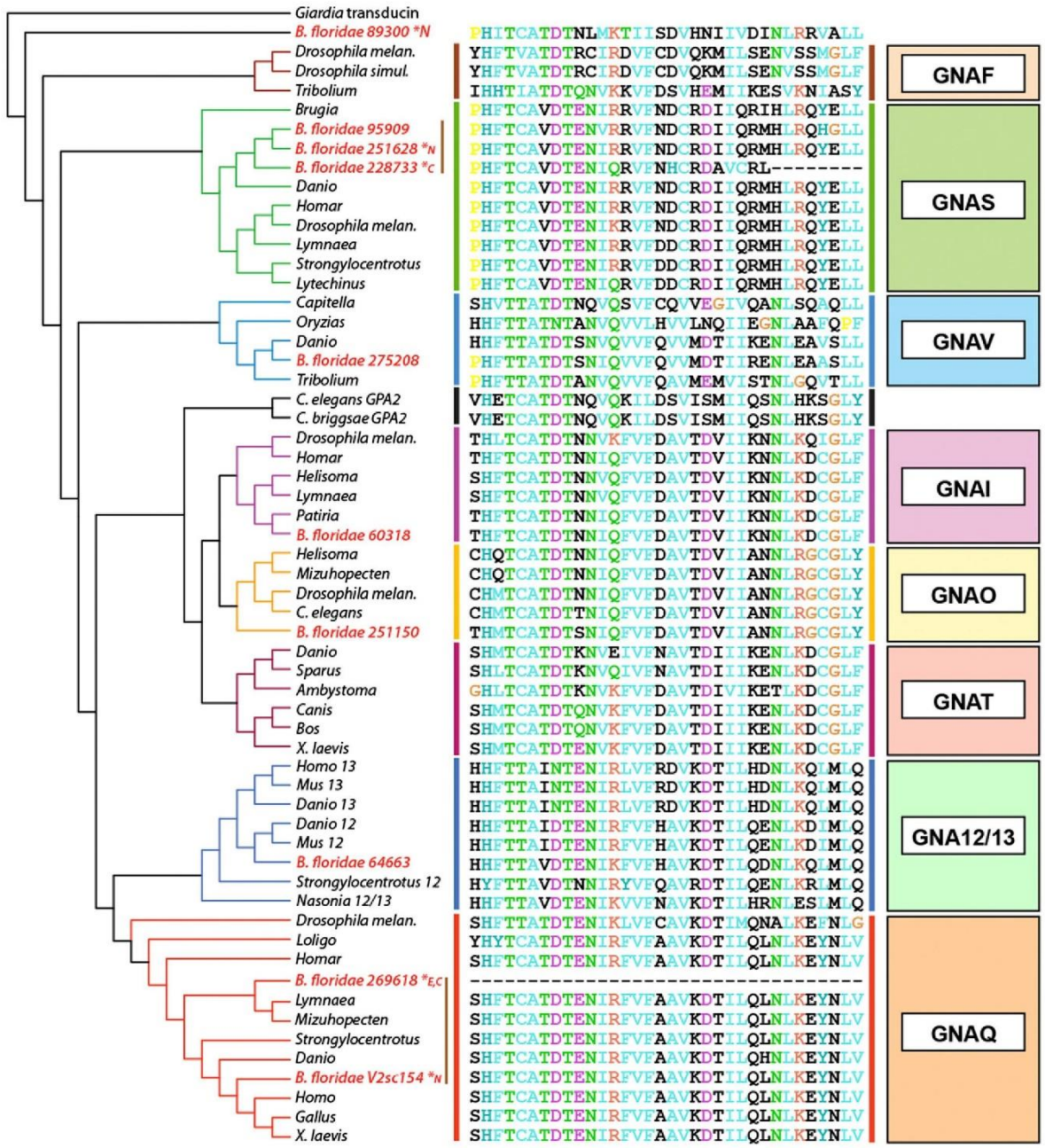

Fig. S6. Amino acid sequence alignment of Gα subunit C termini. The phylogenetic tree was inferred by the NJ method using *Giardia* transducin as an outgroup sequence. The missing sequence at either N or C termini did not allow all sequences of the phylogenetic tree to be inferred simultaneously. Therefore the tree shown here is based on two separate reconstructions. For this reason, the bootstrap support values are not shown; however, the tree reflects the topology of the two separate trees. In addition, the 12-amino acid C-terminal section is highly conserved in different subclasses and also supports the classification. Missing sequence information in the predicted amphioxus Gα subunits is marked by asterisks and a letter denoting the missing section (C, C-terminal portion; E, exon; N, N-terminal portion). The V1.0 predicted models mapping to the same genomic position in the V2.0 assembly are marked with a brown vertical bar. The gene model 251628 (GNAS subfamily) does not map to the same position; however, the overall sequence similarity suggests its identity with model ID 95909. The red-highlighted numbers of *B. floridae* sequences correspond to JGI *B. floridae* gene models V.1, except for V2sc154 referring to scaffold 154 in JGI *B. floridae* genome V2.0. Accession numbers: *Giardia* "transducin" - XP_001709656.1; *Drosophila melanogaster* GNAF - Q05337.1; *Drosophila simulans* GNAF - XP_002085174.1; *Tribolium* GNAF - XP_970742.1; *Brugia* GNAS - XP_001901198.1; *Danio* GNAS - XP_971664.2; *Homarus* GNAS - O16118.1; *Drosophila* GNAS - P20354.1; *Lymnaea* GNAS - CAA78808.1; *S. purpuratus* GNAS - NP_001001474.1; *Lytechinus* GNAS - AAS38583.1; *Capitella* GNAV - JGI Capca1:227716;

Legend continued on following page

Oryzias GNAV - (Oka et al, 2009); *Danio* GNAV - XP_699972.2; *Tribolium* GNAV - (Oka et al, 2009); *C. elegans* GPA2 - P22454.1; *C. briggsae* GPA2 - Q4VT35.1; *Drosophila* GNAI - P20353.2; *Homarus* GNAI - P41776.2; *Helisoma* GNAI - P51876.2; *Lymnaea* GNAI - P30682.3; *Patiria* GNAI - P30676.3; *Helisoma* GNAO - AAC41539.1; *Mizuhopecten* GNAO - O15976.3; *Drosophila* GNAO - P16378.1; *C. elegans* GNAO - P51875.3; *Danio* GNAT - AAL05601.1; *Sparus* GNAT - AAB41887.1; *Ambystoma* GNAT - AAC67569.1; *Canis* GNAT - NP_001003068.1; *Bos* GNAT - P04695.3; *X. laevis* GNAT - NP_001084030.1; *Homo* GNA13 - NP_006563.2; *Mus* GNA13 - NP_034433.3; *Danio* GNA13 - AAR25617.1; *Danio* GNA12 - NP_001013295.1; *Mus* GNA12 - NP_034432.1; *S. purpuratus* GNA12 - NP_001001476.1; *Nasonia* GNA12/13 - XP_001600076.1; *Drosophila* GNAQ - P23625.2; *Loligo* GNAQ - P38412.1; *Homarus* GNAQ - AAB49314.1; *Lymnaea* GNAQ - P38411.1; *Mizuhopecten* GNAQ - O15975.1; *S. purpuratus* GNAQ - NP_999835.1; *Danio* GNAQ - CAK04448.1; *Homo* GNAQ - NP_002063.2; *Gallus* GNAQ - NP_001026598.1; *X. laevis* GNAQ - AAH81126.1.

Table S1. Antibodies prepared in this work

Gene	Antigen amino acid sequence[†]	Host	Note[‡]	Dilution[§]
c-opsin1	NPLVYFAMNNQFRRYFQDLLCCGRRLFDA SASVNTCNTSAMPRHSPVFQKPDSDQYN GIQKSREPQMRTTGQNAPYRQWIEMQTIA VVVKADEVNNKFGEVKT*	Mouse	124039	1:200
c-opsin2	MNNQFRKCFLRSLNCRSQPRDPSSQQYTLK VGMSTSGSQAARTADRIKTVHVATANPQ DHRSSSGQAVEDNGGFRKSLTHSLPLN SISTLLEAEK*	Mouse	70446	1:200
c-opsin3	RVCCRQQAVPRVTPMDDNVHVRLGGEG PSQSQQFLPAGENVENVDMLEYVQE NCKPKADSLSTISE*	Mouse	74631	1:200
Otx	MAYMKSPYGMNGLSLSNPSIDLMTHHHH PGVGVSQYYNPTSAYTVTGQCPPPP*	Rabbit	275923	1:500
Otx	MAYMKSPYGMNGLSLSNPSIDLMTHHHH PGVGVSQYYNPTSAYTVTGQCPPPP*	Mouse	275923	1:500
Pax4/6	KLRNQRRSQDSDSSSPSRIPISSSFSTA TMYQPIAPPSAPVMSRSSHAGLTDSYS SLPPVPRWENFSVPGNMAPMPSMQQS RDQTSYSCMIPHSTAMTPRGYDSLALG SYNPTHAGHHVTTTHPSHMQAPSMPGH SHMSHANGGSAGLISPGVSVPVQVPG AVTEEMTSQPYWPRIQ*	Rabbit	69411	1:500
Rx	MNGQSDSSTETKTAPVRPVPPGLCT GGPRHTIDAILGLHMRGPGRDLAG RHPPEPDEALATYGDDDGQDQSEA LNLVVDILNASDDENRTVKPVTHS ANGFPSAPQTPNGNGAAETAEDADD RAEDEKT*	Rabbit	78608	1:250
MiTF	MDDVIDDIISLESSFDDSFNFLDAPM QQISSTMPLTSSLLDGFGTVGSLTP MVTANTSASCPADLTNIKKEPVQMS ESELKALAKDRQKKDNHNMNEWGYS EMVGWIGGVPEQAMALAKDRQKKDN HNIIERRRRFNINDRIKELGTLLPK TADPDMRWNKGTILKASVDYIRRLK KEHERMRHMEERQKQMEQMNRKMLLR IQELEMHCRAH*	Rabbit	247501	1:200

The asterisks in the protein sequence here denote the STOP codon, which has been always included in the plasmid.
[†]Amino acid sequence of the antigen used for immunization of the host species.
[‡]The protein ID in the JGI Amphioxus genome V1.0 (http://genome.jgi-psf.org/Brafl1/Brafl1.home.html).
[§]The dilution of antibodies for immunohistochemical staining.

6.2 Cubozoan genome illuminates functional diversification of opsins and photoreceptor evolution.

Even though the Cnidarian opsins seems to be unique in terms of biochemical properties and sequence, they were not studied in such details as opsins from the other opsin groups – c-type, r-type and Group4. This was partly due to lack of Cnidarian genomic resources and partly due to the problems with heterologous production of other than vertebrate opsins in cell culture. The phylum Cnidaria contains about 9000 species, highly variable in the sense of body plan, life cycles and habitat. First Cnidarian opsin genes were, however, identified no earlier than in 2007[87] for hydrozoan *Hydra magnipapillata* and *Nematostella vectensis* and in 2008[88] for jellyfish *Cladonema radiatum* (with eyes) and hydrozoa *Podocoryne carnea*. Phylogenetic analysis always showed, that Cnidarian opsins cluster together (despite the overall huge differences between individual Cnidaria species). In 2008 two studies documented the presence of opsins in the eyes of Cubozoan jellyfish *Tripedalia cystophora*[104] and *Carybdea rastronii*[86]. Phylogenetic analysis of the identified *Tripedalia* opsin (Tcop18) showed that it clusters closely to vertebrate c-opsins.

In our study we searched for opsin genes in the genome of *T. cystophora*. In addition to a previously characterized opsin gene (Tcop18), we identified 17 new *Tripedalia* opsins, Tcop1-Tcop17. One of them, Tcop13, was the exact homolog of a previously identified *Carybdea* opsin. We provided phylogenetic analysis of newly identified opsins (confirming their expected clustering within Cnidopsins monophyletic group) and characterization of their structural landmarks (counterion and tripeptide) – showing that D or E can be found at positions 83, 113 and 181 in various *Tripedalia* opsins as well as other Cnidopsins, while the typical vertebrate tripeptide NKQ was found in one opsin (Tcop1). Additionally we provided data about expression of *Tripedalia* opsins in various developmental stages and tissues of adult body by qRT-PCR. We showed that all Tcops were expressed at mRNA level and they manifest temporal (stage) and/or spatial (tissue) expression specificity. We checked the expression of Tcop13 and Tcop18 (shown to be expressed in eyes (rhopalia) in previous studies[86,104]) in *Tripedalia* rhopalia retina, using specific antibodies raised against each of these opsins. Interestingly two different photoreceptor types were identified (mutually expressing either Tcop13 or Tcop18). We also performed a cell line based assay for monitoring the coupling of *Tripedalia* opsins with the downstream partner $G_{\alpha}s$ subunit of a trimeric G protein and activation of a cascade leading to intracellular cAMP increase. From all tested opsins, Tcop5 and Tcop13 showed ability to signal via this cascade. Moreover, we performed tests with mutated tripeptide of Tcop13. Remarkably, we observed that mutations in the tripeptide sequences surprisingly did not abolish the ability of Tcop13 to signal, but rather modulated the sensitivity and length of Tcop13 response to light stimulus. We confirmed the role of Tcop13 as a visual opsin and utilization of opsins-$G_{\alpha}s$-cAMP cascade *in vivo* using specific reversible inhibitor of $G_{\alpha}s$ subunit. *Tripedalia* with inhibited $G_{\alpha}s$ were still able to swim, but lost phototactic behavior. After removal of the inhibitor, the animals were again able to react to light. With this experiment we, for the first time, documented usage of opsin-$G_{\alpha}s$ pathway in a visual system.

To sum up, our thorough analysis of opsin repertoire of *T. cystophora* uncovered both redundancy and specificity of opsin utilization in various developmental stages and body tissues. Our data also demonstrate easy evolvability of Cnidarian opsins, in terms of modulation of their response, by the means of simple mutations in their C terminus (tripeptide sequence).

From this study was for the aim of the thesis important the establishment of cell line based assay for opsin – trimeric G protein coupling. This assay can be used for verifying of opsin coupling to $G_{\alpha}s$ or with some modifications to $G_{\alpha}i$ pathway. Moreover we possess available system enabling verification of opsin-$G_{\alpha}q$ coupling. We expect, that this assay would be important for further studies and will have, except for opsin-G_{α} subunit coupling, also many different applications, e.g. it will enable studies of opsin´s biochemical characteristics (counterion position); it will enable measuring of opsin spectral sensitivity; it will be used for testing potential optogenetic tools based on mutated opsins, etc.

My contribution to this work: I established, in cooperation with Antonio Pombinho (co-author of the study), a cell line based assay enabling monitoring of the coupling of opsin with $G_{\alpha}s$ subunit of trimeric G protein and subsequent increase of cellular cAMP level. I performed tests of G protein coupling for all Tripedalia opsins. I performed mutational analysis of tripeptide sequences in Tcop13. I contributed to writing of the manuscript, more specifically parts of methods, results and discussion.

www.nature.com/scientificreports

SCIENTIFIC REPORTS

OPEN

Cubozoan genome illuminates functional diversification of opsins and photoreceptor evolution

Received: 10 February 2015
Accepted: 05 June 2015
Published: 08 July 2015

Michaela Liegertová[1,*], Jiří Pergner[1,*], Iryna Kozmiková[1], Peter Fabian[1], Antonio R. Pombinho[2], Hynek Strnad[3], Jan Pačes[3], Čestmír Vlček[3], Petr Bartůněk[2] & Zbyněk Kozmik[1]

Animals sense light primarily by an opsin-based photopigment present in a photoreceptor cell. Cnidaria are arguably the most basal phylum containing a well-developed visual system. The evolutionary history of opsins in the animal kingdom has not yet been resolved. Here, we study the evolution of animal opsins by genome-wide analysis of the cubozoan jellyfish *Tripedalia cystophora*, a cnidarian possessing complex lens-containing eyes and minor photoreceptors. A large number of opsin genes with distinct tissue- and stage-specific expression were identified. Our phylogenetic analysis unequivocally classifies cubozoan opsins as a sister group to c-opsins and documents lineage-specific expansion of the opsin gene repertoire in the cubozoan genome. Functional analyses provided evidence for the use of the Gs-cAMP signaling pathway in a small set of cubozoan opsins, indicating the possibility that the majority of other cubozoan opsins signal via distinct pathways. Additionally, these tests uncovered subtle differences among individual opsins, suggesting possible fine-tuning for specific photoreceptor tasks. Based on phylogenetic, expression and biochemical analysis we propose that rapid lineage- and species-specific duplications of the intron-less opsin genes and their subsequent functional diversification promoted evolution of a large repertoire of both visual and extraocular photoreceptors in cubozoans.

Many animals sense light cues for vision and nonvisual photoreception. Light is captured by an opsin-based photopigment in a photoreceptor cell and leads to a cellular light response through a G protein-mediated phototransduction cascade[1,2]. Opsins are members of the G protein-coupled receptor (GPCR) superfamily; proteins with seven transmembrane helices that are involved in a diverse set of signaling functions. Within the GPCR superfamily, the opsins form a large monophyletic subclass of proteins characterized by a lysine in the seventh transmembrane helix that serves as the attachment site for the chromophore. Functional opsin proteins covalently bind a chromophore, gaining photosensitivity. Opsins are essential molecules in mediating the ability of animals to detect and use light for diverse biological functions and have been discovered in a wide variety of tissue and cell types, signaling through multiple pathways, and carrying out functions beyond image formation[1,3].

Phylogenetic analysis has indicated that four major opsin monophyletic groups can be recognized[1,3–5]. The first group, is comprised of the c-type opsins, the vertebrate visual (transducin-coupled) and non-visual opsin subfamily, the encephalopsins, pinopsins, paprapinopsins, parietopsins and tmt-opsin subfamily and the invertebrate ciliary opsins. The second group, Cnidopsins, is a group consisting of all cnidarian opsins, except for so called Nematostella group 1 and Nematostella group 4 opsins, whose phylogenetic position is still unresolved[4,6]. Cnidopsins are exclusively found among cnidarians and not

[1]Department of Transcriptional Regulation, Institute of Molecular Genetics, Videnska 1083, Prague, CZ-14220, Czech Republic. [2]Department of Cell Differentiation, Institute of Molecular Genetics, Videnska 1083, Prague, CZ-14220, Czech Republic. [3]Department of Genomics and Bioinformatics, Institute of Molecular Genetics, Videnska 1083, Prague, CZ-14220, Czech Republic. *These authors contributed equally to this work. Correspondence and requests for materials should be addressed to Z.K. (email: kozmik@img.cas.cz)

present in any other phyla. The third so-called 'r-type' group consists of Gq-coupled invertebrate visual opsins and vertebrate and invertebrate melanopsins and Group 4 opsins contain an assortment of relatively poorly characterized opsin types including, neuropsins, peropsins, and a mixed group of RGRs (retinal G-protein coupled receptors)[7–10]. The distribution of the opsins into these four major groups is supported by analyses of intron arrangements and insertion/deletion events[3] and all groups contain genes found in multiple tissue locations (*e.g.* photoreceptor cells (PRCs) and/or other tissues). Two recently published analyses of opsin phylogeny by Feuda *et al.*[6,11] have shown that in contrast to the findings of a majority of other studies[3,5,10], Cnidarian opsins, including the Nematostella group 1 and Nematostella group 4 opsins, might not be of monophyletic origin, but rather can be divided into three groups, each more closely related to either the c-, r- or Group 4 opsins.

One of the defining characteristics of opsins are the presence of covalently bound chromophores, most commonly 11-cis retinal, that confer light sensitivity to the visual pigment. The chromophore is attached via a Schiff base linkage to a universally conserved lysine in the seventh transmembrane helix. Upon exposure to light, the chromophore undergoes a photoisomerization event to form all-trans retinal, that in turn drives the activation of the photopigment. Aside from this universally conserved lysine, other important amino acid residues can also be found in opsin primary structures. One example is the so-called 'counterion', typically a negatively charged amino acid that is required to interact with and thus raise the pKa of the protonated Schiff base linkage between retinal and lysine, stabilizing the binding of a proton at physiological pH. While vertebrate visual pigments use amino acid-113 as the counterion, position 181 can also be used by a diverse group of opsins containing photoisomerases and Gi/o-coupled pigments, whereas vertebrate melanopsins utilize amino acid position 83[3]. Multiple lines of evidence support the hypothesis that amino acid substitutions in the fourth cytoplasmic loop of duplicated opsins were involved in the origins of novel opsin-G protein interactions[5]. Residues 310-312, encompassing the so-called tripeptide region, were formerly demonstrated by site-directed mutagenesis to mediate opsin-G protein interactions in ciliary opsins[12] and these data were later supported by correlation analyses[5].

Box jellyfish belong to the phylum Cnidaria, arguably the most basal phylum containing a well-developed visual system. It is well known that light affects many behavioral activities of cnidarians, including diel vertical migration, responses to rapid changes in light intensity and reproduction[13]. Their phylogenetic position, simple nervous system and elaborate set of eyes[14] make their visual system of key importance for understanding the early evolution of vision, and also for understanding the biology of box jellyfish[15–18]. The eyes of box jellyfish share many features with those of vertebrates. Morphologically, they are similar by overall design (lens, retina, ciliary photoreceptors)[14,19], and recently, characterization of some molecular components has suggested that the box jellyfish visual system is more closely related to vertebrate than to invertebrate visual systems[20–23]. Photoreceptive organs in Cnidaria have diverse structures, not only between species[24] but within the same species. The cubozoan jellyfish investigated in this study, *Tripedalia cystophora*, has four equally spaced sensory structures called rhopalia, dangling from a stalk and situated within open cavities surrounding the bell. Each rhopalium has six separate eyes. There are two complex, lens-containing eyes (upper lens eye – ULE, and lower lens eye – LLE), one larger than the other, situated at right angles to each other, and two pairs (one pit-shaped, one slit-shaped) of simple ocelli comprising photoreceptors on either side of the complex eyes[25,26]. As the visual fields of individual eyes of the rhopalium partly overlap, *T. cystophora* (as well as other Cubomedusae) has an almost complete view of its surroundings. The lens-containing *T. cystophora* eyes have sophisticated visual optics, similar to molluscs and vertebrates[14,19]. Two opsin genes have so far been identified in cubozoans, one in *T. cystophora*[22], and one in the related species *Carybdea rastonii*[27]. Expression of both these opsins has been detected in eyes of the corresponding species[22,27]. *C. rastonii* opsin was furthermore shown to transfer the light stimulus via the Gs signaling pathway[27].

In the present work, we characterize a complement of 18 opsin genes identified in cubozoan jellyfish *T. cystophora* by the whole-genome analysis. Based on phylogenetic, expression and biochemical analysis we propose that rapid lineage- and species-specific duplications of the intron-less opsin genes and their subsequent functional diversification promoted evolution of both visual and extraocular photoreception in cubozoans.

Results

A large complement of opsin genes are present in *T. cystophora* genome. In addition to previously annotated *T. cystophora* c-opsin[22] we identified 17 other *Tripedalia* opsins (Tcops) sequences. Among those novel sequences, we were able to identify the ortholog (93% sequence identity) of the previously investigated *C. rastonii* opsin (Caryb)[27], designated here in *T. cystophora* as Tcop13 (Fig. S1). Complete coding sequences for all these opsins were obtained by Genome Walking (GenomeWalker, Clontech). All of the eighteen *T. cystophora* opsins are intron-less genes, which show overall sequence homology with other cnidarian opsins as well as to bilaterian rhodopsins. The conserved lysine to which the chromophore 11-cis-retinal binds was found in each of the cloned opsins, suggesting that they are indeed used for photoreception. Next, we investigated the three potential counterion sites at amino-acid position 83, 113, 181 (numbered according to bovine rhodopsin) within the cnidopsins (Fig. S2). Negatively charged amino acids (either glutamic acid/E or aspartic acid/ D) at position 83 was found in more than 50% of the identified cnidopsins, with more than 95% having E/D at position 181. Intriguingly, E/D residues at position 113 were only found in four of the identified *T. cystophora* opsins.

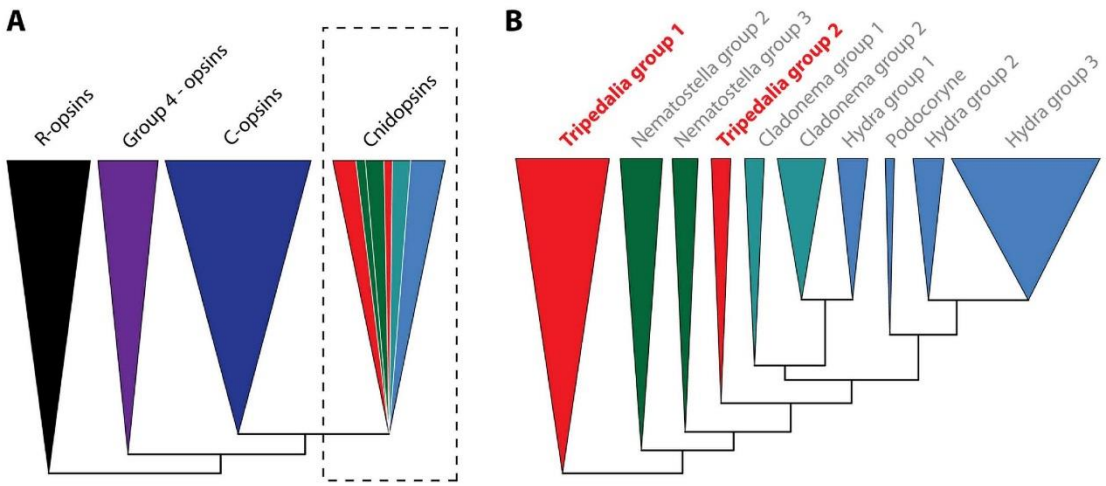

Figure 1. Schematic representation of the opsin phylogenetic analysis of a large set of opsin genes including the cubozoan dataset. A) Phylogenetic analysis performed in this study recovered previously described four major opsin lineages – r-opsins, c-opsins, group 4 opsins and cnidopsins. Herein the C-opsins and cnidopsins form sister groups. (For details see Fig. S3), **B)** Detailed inspection of cnidopsin branch indicates extensive gene duplication and lineage-specific expansion of cnidarian opsins. (For details see Fig. S4).

These were, Tcop8, Tcop12, Tcop15, and Tcop16 (Fig. S2 – red box). However, it is important to note that E/D counterions at position 113 have, to date, not been found in any opsins identified outside of chordates. Next, we investigated the identity of residues 310–312 within all the Tcop sequences. The tripeptides tended to be conserved among closely related cnidopsin groups of each species (Fig. S2) but are apparently not conserved across the cnidarian lineages. In summary, our collective data indicate that a large repertoire of diverse opsins is present in the cubozoan genome, some of which have some intriguing sequence similarities to vertebrate opsins.

Phylogenetic relationships of cubozoan opsins within the opsin gene family. To investigate the relationship between the newly identified Tcops and other known metazoan opsins, we inferred a molecular phylogenetic tree by the maximum likelihood method from a set of 779 opsin protein sequences. Our phylogenetic analysis of this large and diverse set of opsin sequences recovered the four major lineages described in earlier studies[3–5,10], *i.e.* the c-type opsins, the cnidopsins, the r-type opsins, and group 4 opsins. The relationships among the four major lineages in our analyses correlated with those proposed in other recent studies of opsin evolution[4,5,10], however, the statistical support for some of the relationships was weak. Due to such weak branch support, we were unable to exclude the possibility that group 4 and r-type opsins cluster together as sister groups, opposing the c-type opsin and cnidopsin subgroups as has been suggested by Porter *et al.*[3] (based on their phylogeny and the presence of functional unity as bistable pigments of arthropod/cephalopod visual r-type opsins and chicken group 4 neuropsin[28,29]). We found that the relationship between cnidopsins and the c-type opsin subfamily was most strongly supported. All cnidarian opsins except for *Nematostella* group 1 and *Nematostella* group 4 opsins fell within the cnidopsins, group and as was shown by Suga *et al.*[4], the phylogenetic positions of these two groups remained unclear even after more precise Maximum-Likelihood analyses. In the phylogenetic tree of the opsin family, all identified Tcops fell into the cnidopsins subfamily (Fig. 1A, Fig. S3), consistently clustering with the hydrozoan opsins[30]. The cnidopsin group, composed entirely of cnidarian opsins, is the only group lacking representation of broad taxonomic diversity from the major animal phyla. The phylogenic trees presented here (Fig. 1B, Fig. S4) and elsewhere[3,4] are indicative of extensive gene duplications (and diversifications) in each of the cnidarian lineages after their initial split. This latter point is exemplified by the case of Tcops that form two distinct phylogenetic groups: Tc-group 1 and Tc-group 2 (Fig. 1B).

In summary, our phylogenetic analysis unequivocally classifies cubozoan opsins as a sister group to c-type opsins and documents lineage-specific expansion of the opsin gene repertoire in the cubozoan genome.

Functional diversification of opsins in *T. cystophora*: evidence of an apparent dichotomy in G protein-coupled signaling. Sequence analysis and phylogenetic classification provided an important insight into the evolutionary history and possible relationships among opsins. However, these sequence-based approaches do not answer the question whether one or more signaling pathways are being used by *T. cystophora* opsins and do not permit the drawing of conclusions regarding which signaling pathway is coupled to any particular opsin. In order to get a deeper insight into the functional diversification of opsins identified in *T. cystophora* we used a GloSensor™ cAMP HEK293 cell based Gs protein-coupled signaling assay[31] to investigate biochemical properties of all Tripedalia opsins (for description see Material and methods). We used *C. rastonii* opsin (Caryb), shown to activate the Gs-cAMP pathway[27], as a positive control. As heterologous protein expression in cell lines may sometimes prove difficult or even impossible[32], we first checked the expression of the individual opsin genes in GloSensor™ cAMP HEK293 cells by immunofluorescent labeling. The staining revealed that all examined opsins were expressed in GloSensor™ cAMP HEK293 cells and at comparable levels. Moreover the sub-cellular fluorescent signal for opsin was consistently detectable on the cell membranes (Fig. S5 and data not shown), thus confirming successful expression of the Tcop genes. The luciferase activity in GloSensor™ cAMP HEK293 cells, transfected with individual opsin constructs and pre-incubated in the dark with 9-cis retinal, was determined before and after repeated light stimulations (Fig. 2). Light stimulation of cells was in specific cases immediately followed by increased luciferase activity reaching a maximum after several minutes (Tcop5) or 10 minutes (Tcop13, Caryb) and remaining constant for several minutes before decreasing to the basal levels observed prior to illumination (Tcop5) or slightly higher (Caryb; Tcop13). Comparison of the previously characterized Caryb with its ortholog from *T. cystophora*, Tcop13, revealed that both opsins show similar light responses (Fig. 2A). In contrast, medaka (*Oryzias latipes*) opsin RH1, expected to signal via a distinct G protein-coupled pathway (Gi, leading to a cGMP decrease), elicited no increase of luciferase activity in our assay (Fig. 2A), being expressed at comparable levels to those of *T.cystophora* opsins (Fig. S5). Furthermore, no light-dependent stimulation of the Gs protein-coupled assay was detected using the invertebrate r-opsin gene, expected to function via Gq signaling (data not shown). Our assay was, therefore, highly specific for opsins signaling via the Gs-cAMP pathway, but was insensitive to signaling via Gi or Gq. We performed the light response assay several times for the entire set of *T. cystophora* opsins. Of all the opsins examined, only Tcop5 and Tcop13 activated the Gs-cAMP signaling pathway (Fig. 2B–E and data not shown). No convincing light induced opsin-Gs-cAMP response, similar to that of Caryb, Tcop5 and Tcop13, was detected for other Tcops. Tcop5 and Tcop13 sustained enhancement of G protein-coupled pathway signaling after repeated light stimulation. However, we noticed a conspicuous difference in the light response between these two opsins. Tcop5 responded to light faster but with lower intensity (Fig. 2C), whereas the response of Tcop13 was considerably slower, ultimately reaching higher signaling values (Fig. 2D).

To better understand the molecular features of cnidopsins, we focused on the role of the tripeptide in cnidopsin signaling. As stated above, the tripeptide is important for the contact between bovine rhodopsin and its G protein[12]. Accordingly, we replaced the HKQ tripeptide region in Tcop13 with either the tripeptides NKQ, SKS and NRS, originally found in Tcop1 (or bovine rhodopsin), Tcop14 and Tcop18, respectively, none of which activated the Gs signaling cascade in our assay. We expected to observe a loss of Gs cascade activation resulting from the tripeptide mutation. Surprisingly, we found that the tripeptide mutation in Tcop13 did not disrupt Gs activation; rather, it influenced the dynamics of the response to the light stimulation. Specifically, the introduction of the tripeptides NKQ and SKS led to an enhanced and prolonged response, while the introduction of NRS variant caused a massive light response after both single and repeated stimulation (Fig. 2F). Our data show that tripeptide mutation in cnidopsins contributes to subtle tuning of the opsin response to light stimulation, rather than influencing Tcop-G protein coupling *per se*.

In summary, Gs-cAMP signaling characterized only a small set of *T. cystophora* opsins, indicating that the majority of cubozoan opsins likely signal by a distinct and as of yet unidentified signaling pathway. Moreover, the highly sensitive two-dimensional functional assay used here (measuring time response as well as response intensity) uncovered subtle differences among individual opsins, suggesting possible fine tuning for specific photoreceptor tasks.

Phototactic behavior of *T. cystophora* medusa is dependent on Gs signaling. Caryb opsin present in retinas of lensed eyes of *C. rastonii* was previously shown to transfer the light stimulus via the Gs signaling pathway[27]. To investigate whether Tc-group 2 (especially Tcop13), that signal via Gs (see above), serve as important visual pigments in *T. cystophora*, we performed a phototaxis behavioral assay in the absence or presence of the pharmacological compound NF449. NF449 was originally identified as a selective suppressor of the Gs signaling pathway, with limited effect on the prototypical Gi/Go- and Gq-coupled receptors pathways[33]. Positive phototaxis in *T. cystophora* medusa was significantly decreased after treatment with NF449. Although, a variable response was detected in response to white light depending on NF449 concentration and timing of the treatments (Fig. 3 + video), most probably due to reversible inhibition of the Gs signaling pathway by NF449. The number of treated animals exhibiting a phototactic response 5 minutes after the treatment was: $5 \pm 5\%$ in samples treated with 100 μM NF449 and 0% in samples treated with 1 mM. The number of responding medusae treated with 100 μM NF449 after 3 h rose to $95 \pm 5\%$ and the number of medusae treated with 1 mM NF449 rose to 10%.

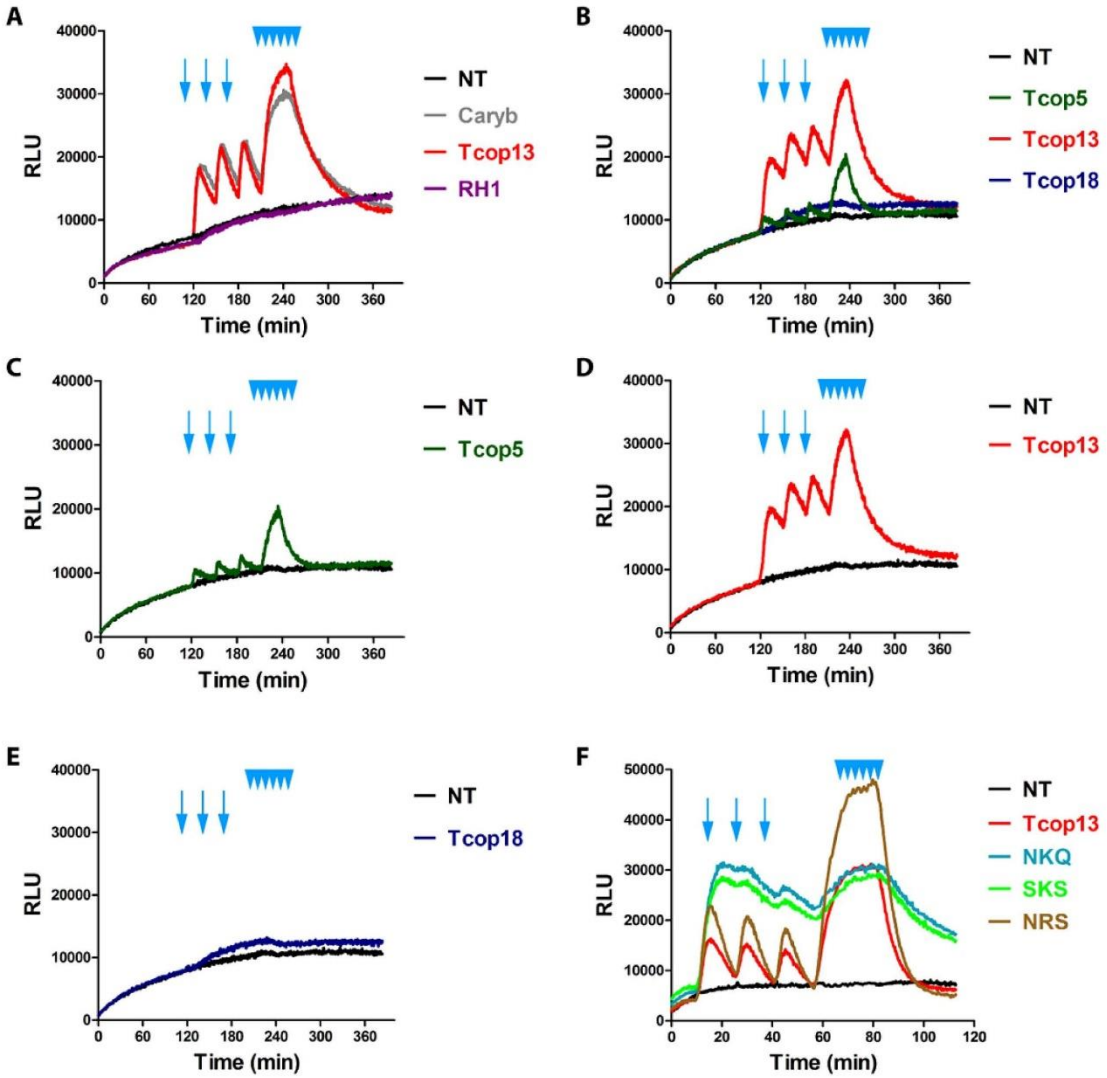

Figure 2. Opsin-Gs-cAMP assay. Light activation of opsin-Gs-cAMP pathway by selected opsins. GloSensor™-20F cAMP HEK293 cells (Promega) were transfected with expression vectors encoding genes for different opsins, treated and stimulated with light, as described in Materials and Methods. Arrows represent simple light pulses, multiple arrowheads represent repeated stimulation. Each graph represents a mean of triplicates for every sample. **A)** Previously reported Gs-cAMP pathway stimulating opsin from *C. rastonii* (Caryb)[27] showed ability to increase the cAMP level in our setup (visualized with cAMP-dependent luciferase activity). The exact homolog of Caryb from *T. cystophora* Tcop13 showed a highly similar response in our assay. Opsin RH1 from medaka, expected to signal via Gt leading to cGMP decrease, showed no change in luciferase activity. **B)–E)** Examples of different Tcop light responses. Tcop5 showed faster and weaker activation of the Gs-cAMP pathway than Tcop13. Tcop18 did not activate the Gs-cAMP pathway. **F)** Analysis of tripeptide activity in Tcop13 was performed. Tcop13 tripeptide HKQ was replaced with tripeptides NKQ, SKS and NRS (originally found in opsins Tcop1 or bovine rhodopsin, Tcop14 and Tcop18 – none of which activated the Gs cascade). Tripeptide mutation did not disrupt Gs activation by Tcop13, but influenced length or sensitivity of Tcop13 response to light stimulation. NT – non-transfected cells used as negative control; Caryb – signal for cells transfected with a vector expressing opsin from *C. rastonii*, used as positive control; RH1 – signal for cells transfected with a vector expressing opsin RH1 from medaka fish *Oryzias latipes*, used as negative control; Tcop5, Tcop13, Tcop18 – signal for cells transfected with vectors expressing opsins from *T. cystophora* - Tcop5, Tcop13 or Tcop18, respectively; NKQ, SKS, NRS – Tcop13 original tripeptide HKQ replaced with tripeptides NKQ, SKS or NRS.

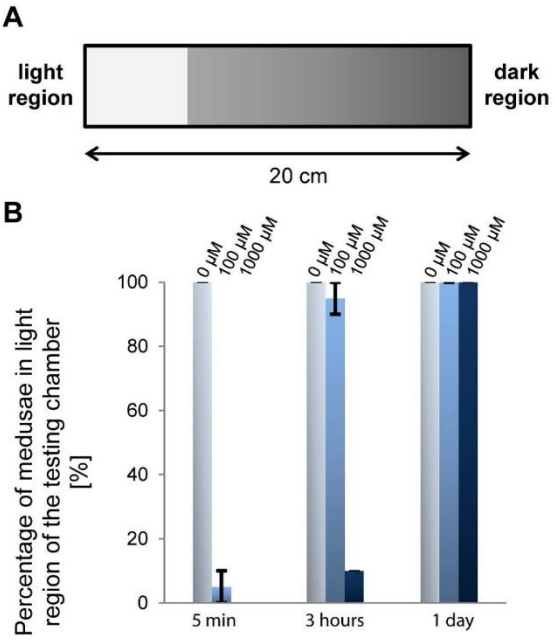

Figure 3. Test of *T. cystophora* medusa phototaxis after NF449 treatment. A) Schematic representation of the testing chamber. **B)** Statistical analysis of the light response of *T. cystophora* after NF449 (Gαs inhibitor) treatments (0 μM, 100 μM, 1 mM). Bars represent the percentage of phototactic medusae in given time point.

However, after 24 hours the decrease in photosensory response was no longer present. We observed 100% phototactic response in untreated animals (0 μM NF449) after 5 min, 3 h, 24 h intervals (Fig. 3B). Thus, the pharmacological inhibition of Tc-group 2 opsins abrogates positive phototactic movement of cubozoan medusa.

Opsin gene expression analysis reveals both redundancy and specialization. The large complement of opsins found in the *T. cystophora* genome raises the possibility of their differential tissue-specific or stage-specific utilization. To investigate the expression patterns of *T. cystophora* opsins, we first analyzed mRNA isolated from different jellyfish life stages and dissected adult tissues by real-time qRT-PCR analysis. The normalized expression levels, relative to Rpl32 levels, of specific opsin genes in each dissected adult body part was calculated relative to that observed in the rhopalium (set at 1.0) and plotted (Fig. 4). Relevant opsin expression data were also represented as a heat map showing z-score of Tcops expression in different *T. cystophora* body parts. (Fig. S6A). All Tcop genes were found to be expressed at the mRNA level in the rhopalium. Moreover, for the majority of opsins (Tcop1, Tcop3–7, Tcop9, Tcop11, Tcop13, Tcop16, Tcop18), the rhopalium was the tissue exhibiting the highest detected expression. Other opsins were most highly expressed in the male gonads (Tcop2, Tcop10, Tcop17), tentacles (Tcop12, Tcop14) or manumbrium (Tcop8, Tcop15). For a better gene-to-gene comparison within the rhopalium, the results were plotted separately (Fig. S7). The expression data in the adult tissues identified common/over-lapping sites of expression most probably reflecting a common gene origin. Nevertheless, a clear tendency for specialization was apparent as very large differences in relative expression levels and/or unique sites of expression were detected.

Next, we investigated opsin gene expression during the life cycle of *T. cystophora*. To this end, mRNAs from non-pigmented larva, pigmented larva (larval eye-containing stage), vegetatively grown polyp, four stages of a metamorphosing polyp (stages 3 and 4 containing a developing rhopalia) and medusae were isolated and subjected to qRT-PCR. The expression levels of all individual opsins for each *T. cystophora* life stage relative to the juvenile medusa expression (set as 1.0) were then calculated (Fig. 5 and Fig. S6B). The results revealed two consistent features. Firstly, opsins whose expression was detected in the adult rhopalium, sharply increased their expression during the polyp metamorphosis, coincident with the emergence of the developing rhopalia structure. Secondly, many Tc-group 1 opsins were highly expressed in the pigmented (eye-containing) larval stage, contrasting with the expression of Tc-group 2 opsins (established as Gs-coupled receptors with a major functional role in the adult lens-containing eye, see above), that were notably absent at this stage.

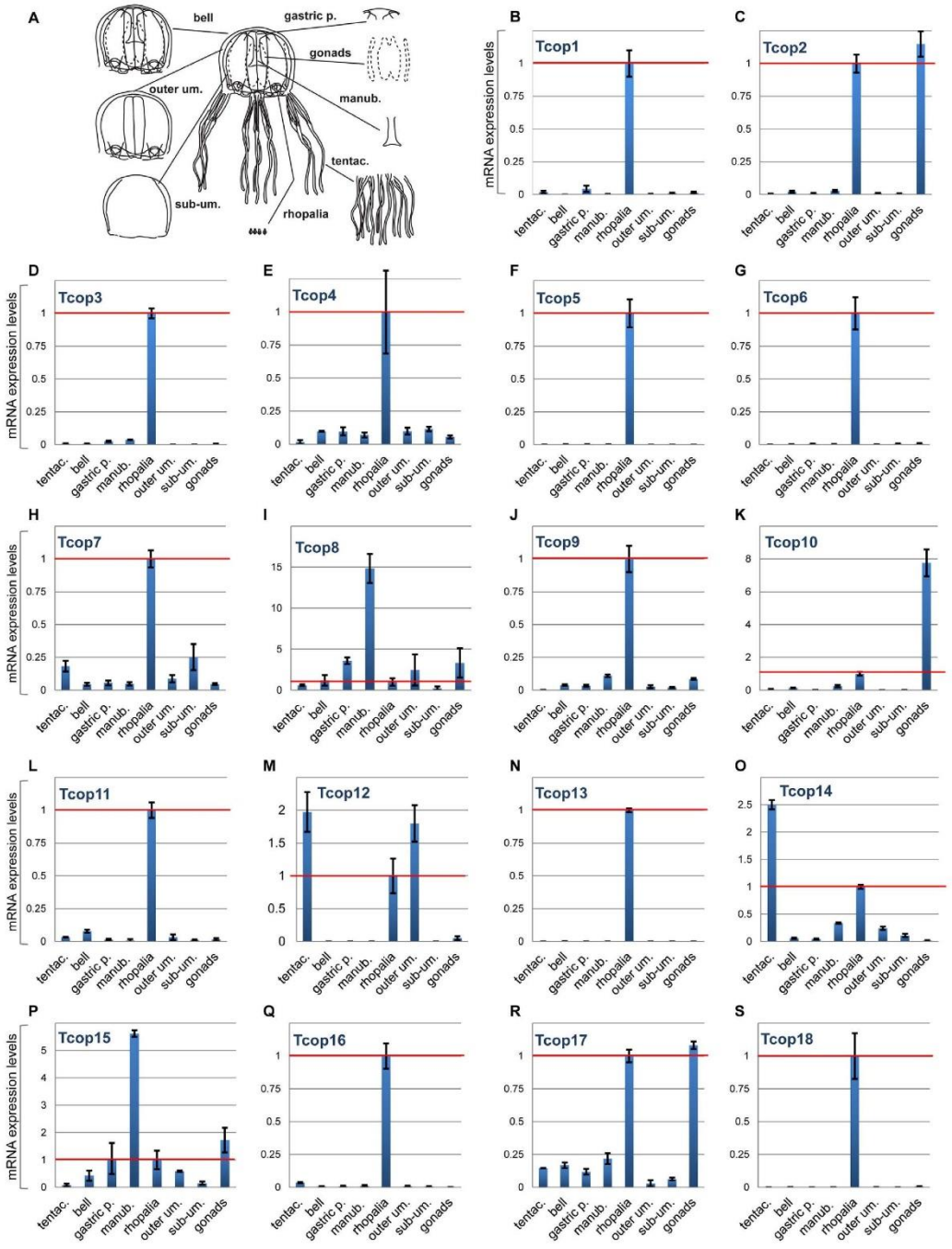

Figure 4. mRNA expression levels of *T. cystophora* opsins in dissected body parts of adult jellyfish. A) For real-time PCR analysis, medusae were dissected into eight body parts: tentacles (tentac.), manubrium (manb.), male gonads, gastric pouch (gastric p.), bell, outer umbrella (outer um.), sub-umbrella (sub-um.) and rhopalia. **B–S)** mRNA expression level of opsins for each dissected body part relative to the rhopalium expression (1.0 – red line). y – axis: relative mRNA expression level, x – axis: analyzed body parts.

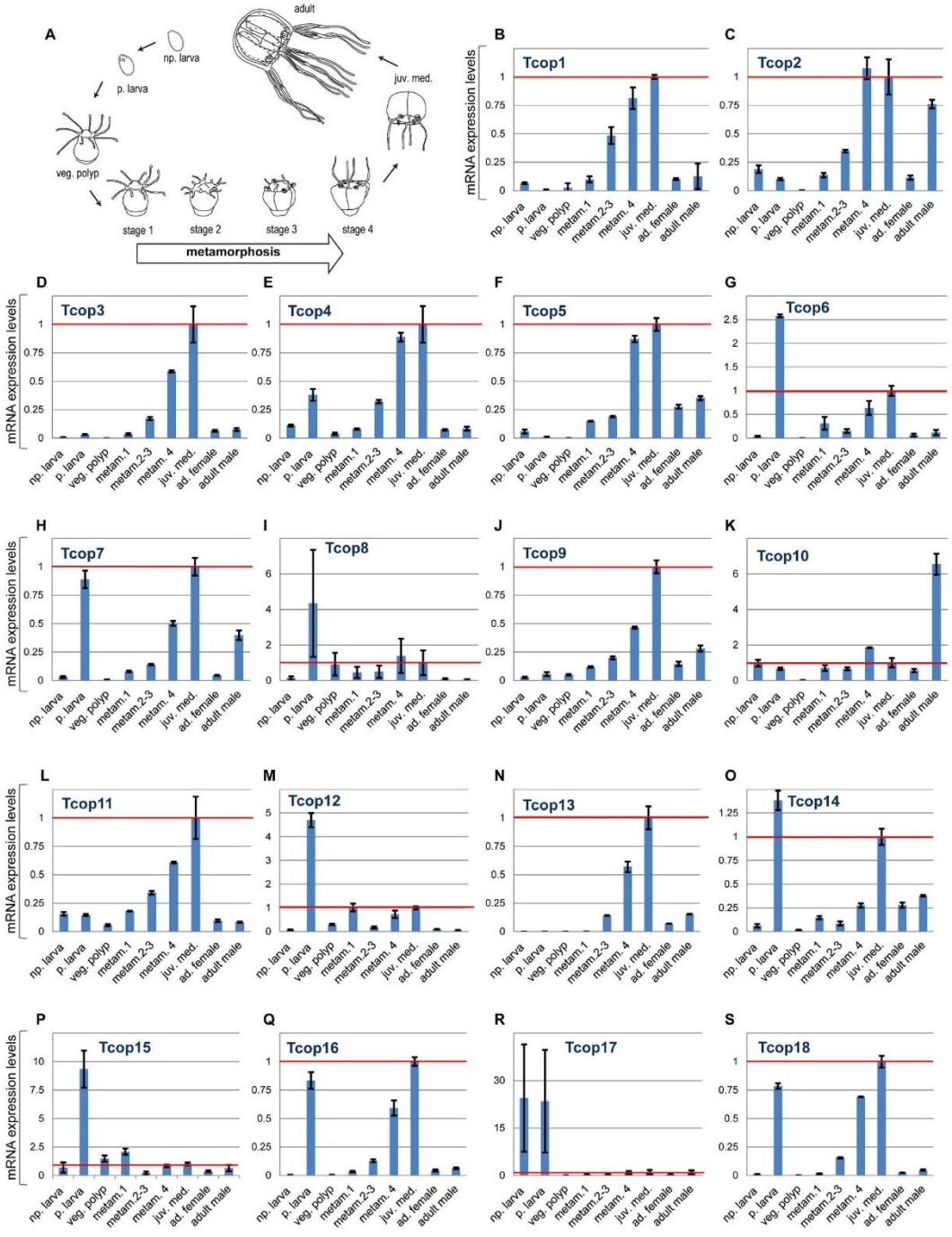

Figure 5. mRNA expression levels of *T. cystophora* opsins in different life stages . **A)** For real-time PCR analysis, animals of nine subsequent life stages were collected: non-pigmented larva (np. larva), pigmented larva (p. larva), vegetative polyp (veg.polyp), three polyp-to-medusa metamorphosing stages (metam1, 2–3, 4), juvenile medusa (juv. med.), adult female (ad. female) and adult male. **B-S)** mRNA expression levels of opsins for each life stage relative to the juvenile medusa expression (1.0 – red line). x – axis: analyzed stages, y – axis: relative mRNA expression level.

To gain further insight into the possibly diverse roles of Tc-group 1 and Tc-group 2 opsins in the various cubozoan eyes (Fig. 6A–C), we also analyzed the expression of key representatives of each opsin type by immunohistochemical staining (IHC) *in situ*. Accordingly, we generated a specific antibody against Tcop13 and performed co-staining with another antibody raised against Tcop18[22] on cryo-sectioned rhopalia. We found that both Tcop13 and Tcop18 were found to be co-expressed in the retinas of *T. cystophora* ULE and LLE in distinct patterns (Fig. 6D–P). We also discovered that *T. cystophora* retinas contain at least two distinct photoreceptor types: ciliary photoreceptor type-A that express Tcop18 not restricted only to the cilia but rather expressed more broadly within the whole cell body (Fig. S8) plus ciliary photoreceptor type-B (expressing Tcop13 in the receptor cell cilia). Both opsins were also distinctly expressed in the developing lens eyes of the newly metamorphosed *T. cystophora* medusae; however, only Tcop18 was detected in the developing eyes of another Carybdeid jellyfish, *Alatina marsupialis* (Fig. S9). Another difference in the apparent utilization of Tc-group 1 and Tc-group 2 opsins was revealed by further analysis of their expression in the two lesser eye types, slit and pit eyes, whose morphology has been thoroughly studied[26]. Only Tcop18 (but not Tcop13) was found to be expressed in the pit and slit ocelli of *T. cystophora*; both types of ocelli thus seem to be formed exclusively from type-A photoreceptors based on the opsin type expression (Fig. S10). However, some molecular features are shared by the PRCs of lesser eye types with those of complex lensed eyes. For example, all PRCs in *T. cystophora* contain two different screening pigments, dark pigment and a white pigment, first described in *Chiropsella bronzie*[24], that becomes conspicuous in polarization microscopy (Fig. S11). It is important to stress that the Tc-group 1 opsin Tcop18 is the only known opsin to be expressed in the lesser eyes thus far. All phylogenetic, biochemical and gene expression data are schematically summarized in Fig. 7.

Discussion

A Scenario for intron-less retrogene-derived cnidarian opsin expansion. The current results highlight distinct features of intron-less genes in vertebrates. It appears that many intron-less genes are evolutionary innovations, so their formation, at least in part, via reverse transcription-mediated mechanisms, could be an important route of evolution of tissue-specific functions in animals[34,35].

The lack of introns is typical for most members of the giant GPCR gene family and it has been proposed that many G-protein-coupled receptors are derived and amplified from a single intron-less common progenitor that was encoded by a retrogene (a DNA gene copied into genome by reverse transcription of an RNA transcript)[36,37]. Interestingly the vertebrate rhodopsin GPCRs, that are widespread phylogenetically and abundantly expressed, contain four introns in highly conserved positions[38]. However, most of the cnidarian opsins thus far annotated are intron-less genes, although at least one opsin in anthozoan *Acropora digitifera*, CNOP2, has been characterized with two introns[39]. Astonishingly, the first of these intron matches, in position and phase, with the first intron of bovine rhodopsin (Fig. S12). Such examples of the first introns to be located in cnidarian opsins are moderately short and have conventional GT-AG donor and acceptor splice sites and thus it appears that this intron was already present in an opsin gene present in the last common ancestor of eumetazoa. Accordingly, intron-less opsin genes appear to be a Cnidarian feature, with the original variant of the gene most probably being lost in medusozoans. Similarly, intron-less opsin genes were previously identified in two cephalopod species[40] and in genome of teleost fish[41], in both cases probably derived from introns containing opsin genes by retrotransposition. Based on these facts and our data, we propose the scenario (Fig. S13) that cnidarian intron-less opsins are retrogenes derived from an ancient eumetazoan ciliary-like opsin with introns. This hypothesis is supported by the phylogenetic relationship of c-like opsins and cnidopsins (Fig. 1A) and by the fact that both variants of the opsin gene (with or without introns) are still present in basal anthozoa (Fig. S12). Once an intron-less opsin gene was present in cnidarian genome, subsequent rapid lineage- and species-specific duplications resulted in a variety of opsins. This process provided the substrate for the evolution of cnidarian photoreception, be it either extraocularly or in sophisticated cubozoan eyes.

Gene duplications and their subsequent divergence play an important part in the evolution of novel gene functions[42]. Our data show that in *T. cystophora* genome, each of the opsins has been duplicated at least once, and several have undergone multiple rounds of duplication (Fig. S4). Theory suggests that duplicated genes can be lost rapidly[43], but the spectrally diverse aquatic environment (such as the margins of mangrove lagoons naturally inhabited by *T. cystophora*) could provide strong selective pressures on the opsin genes, and thus, photoreception evolution. Photoreception tuning through opsin sequence evolution might therefore be a result of sensory adaptation to this rich environment of spectral light.

In both medaka and zebrafish the opsin gene diversity in the genome is high, similarly as in the genome of *T. cystophora*. Subtype opsin genes in medaka and zebrafish are closely linked and are clearly products of local gene duplications[44]. Tandem duplication appears to be the most common mode of opsin gene family expansion in fishes[45]. Gene duplication followed by amino acid substitutions at key tuning sites played an important role in generating a diverse set of fish opsin genes. It is probable that similar mechanisms of opsin gene repertoire expansion occurred in the case of cnidaria (evolutionary convergence), where the opsin genes, being relatively short and intron-less, were even more rapidly duplicated and subsequently functionally diversified (see Fig. 8 for schematical representation).

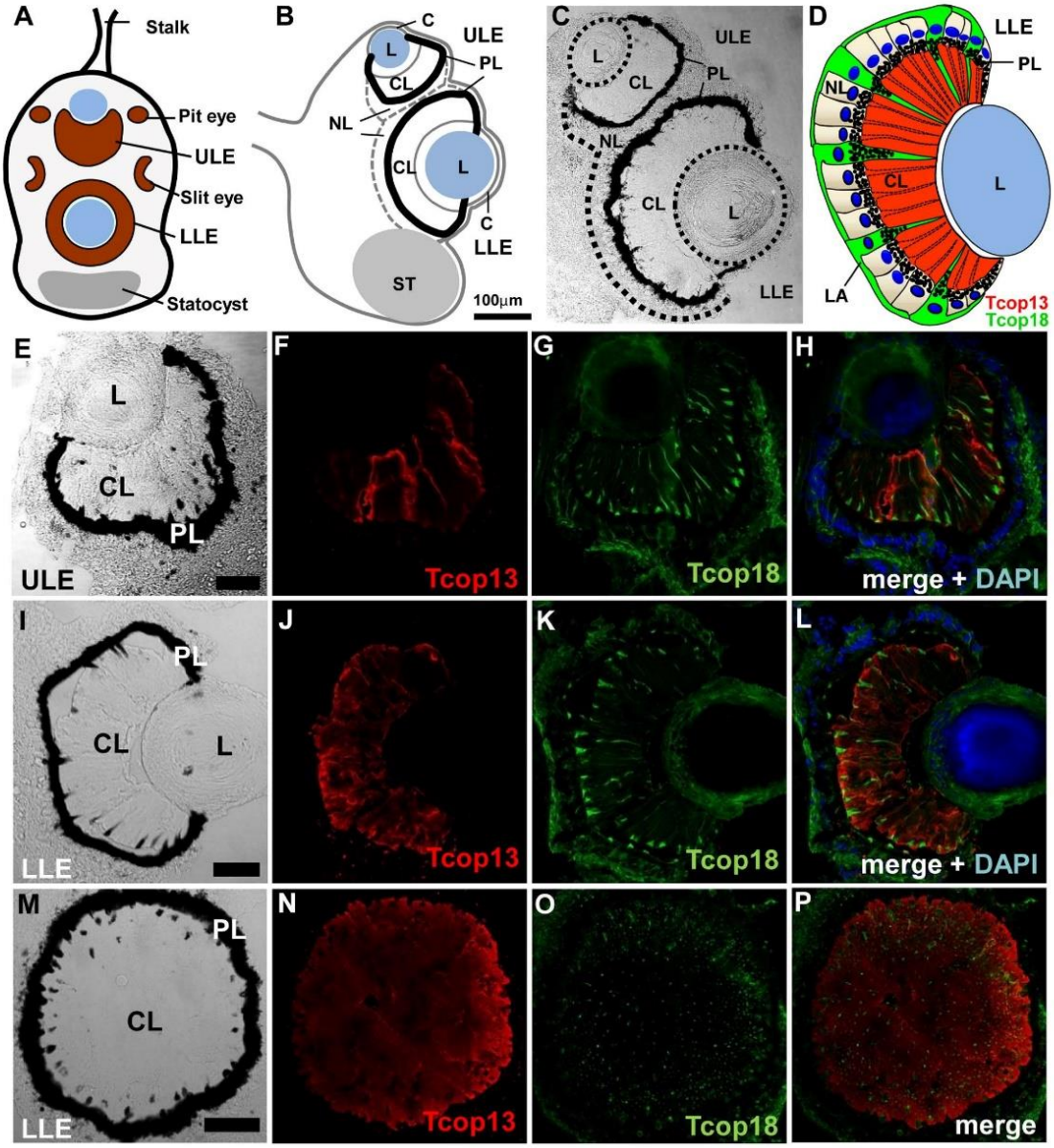

Figure 6. Visual organs of *T. cystophora* and immunohistochemical localization of Tcop13 and Tcop18. **A)** Schematic diagram of the rhopalium. The large (LLE) and small (ULE) complex eyes lie along the medial line, while the pit and slit ocelli are paired laterally. **B)** Schematic diagram of rhopalium sagittal plane (adapted from O´Connor 2009). **C)** Sagittal section through the rhopalium. Upper (ULE) and lower (LLE) lens eyes contain the typical components of camera-type eyes: a cornea (C), a lens (L), and a retina consisting of a ciliary layer (CL), a pigment layer (PL) and a neural layer (NL). St – statocyst, S – stalk. **D)** Schematic representation of the lens eye retina. The ciliary layer (CL) is dominated by the ciliary segments of type-B receptor cells (red). Scattered among the type-B receptor cells are the cone-shaped projections of type-A photoreceptor cells (green). In the neural layer (NL), both receptors types have their cell bodies with nuclei (dark blue); only type-A receptor cell bodies are positive for opsin signal. Projections of type-A photoreceptor cell bodies create a compact layer (LA) surrounding the whole retina. **E–H)** Confocal images of immuno-histochemical staining for Tcop13 (red), Tcop18 (green), DAPI (blue) in the upper lens eye (ULE). **I-L)** Large camera-type eye (LLE) retina longitudinal section. **M–P)** Large camera-type eye retina transverse section. (Scale bars: 50 µm).

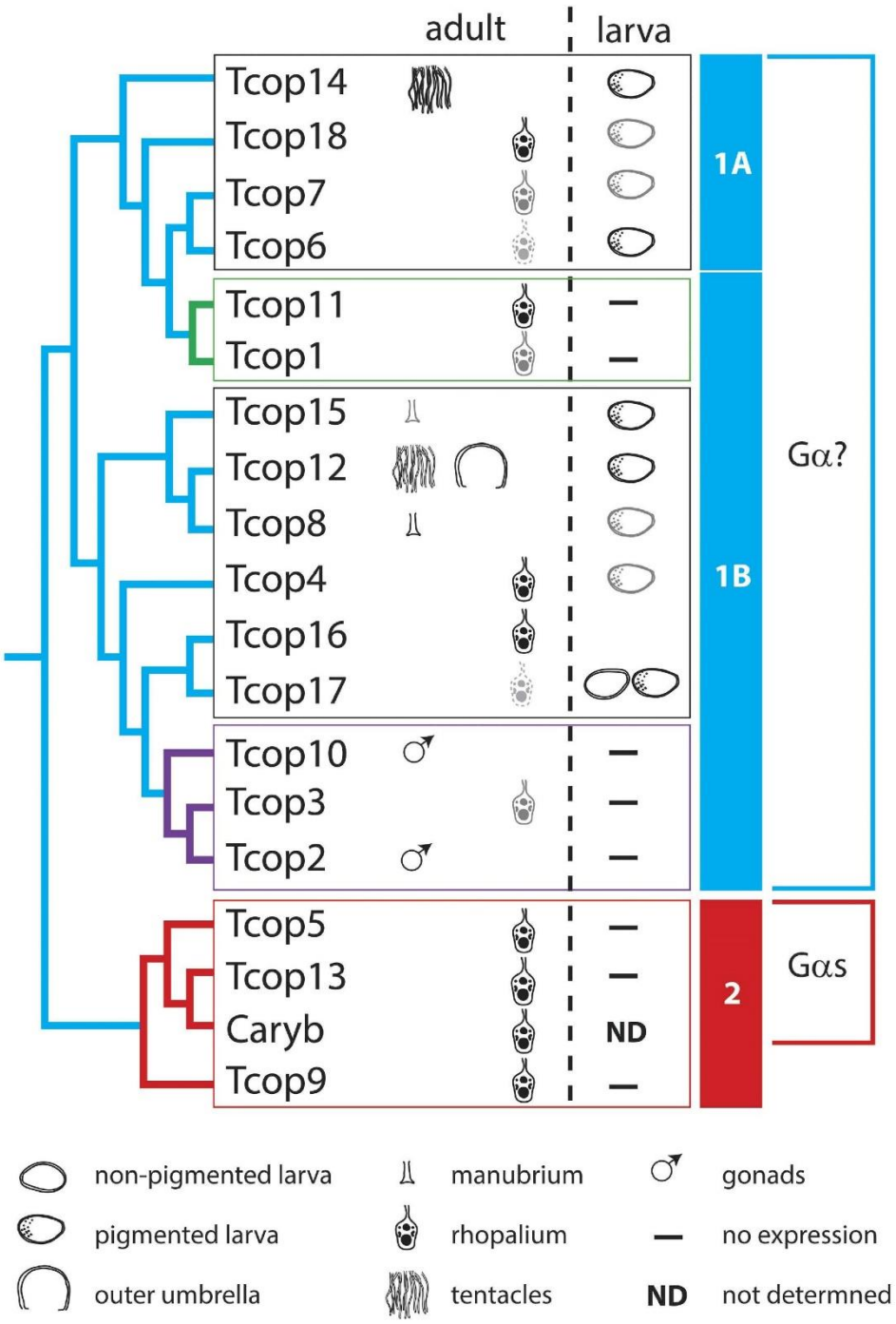

Figure 7. Schematic representation of opsin expression patterns according to their phylogenetic relationship. *T. cystophora* opsins can be classified into two groups, a probable more ancient Tc-group 1 opsin, with a broader expression pattern, and Tc-group 2 – rhopalium-specific opsins. The size and shade intensity of the symbols corresponds with the level of expression. Green coloured box and branches represent rhopalia specific Tc group 1A opsins. Purple coloured box and branches represent male specific Tc group 1B opsins. Red coloured box and branches represent rhopalia specific Tc-group 2 opsins.

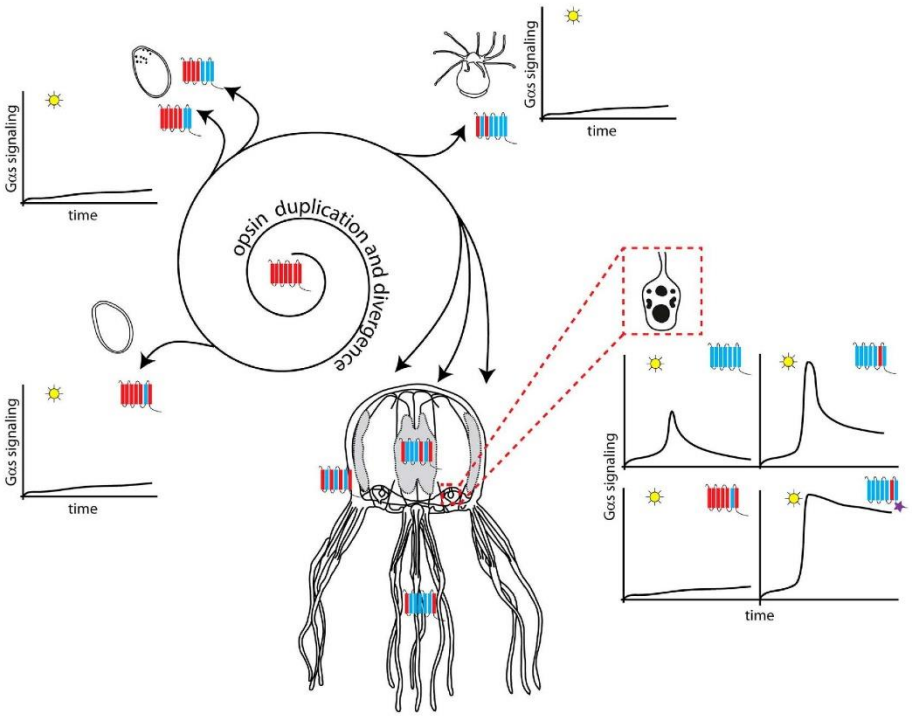

Figure 8. Possible scenario for expansion and functional diversification of opsins in *T. cystophora*. Our data and data from other studies[39,60] show that Cnidarian intron-less opsins might have been derived from an ancient eumetazoan ciliary-like opsin containing introns by retro-transposition. Once anchored in the genome the ancient cnidopsin gene underwent several rounds of duplication, diversification and sensitivity tuning. Individual opsins were thus accommodated for distinct functions in diverse tissue photoreceptors - ocular, extraocular and larval. These opsins differ in stage- or tissue-expression, primary structure and also in subsequent cellular signaling – either via Gs-cAMP pathway or other G-protein pathways. For further information see Discussion.

Rhopalia-specific opsin expression in *T. cystophora*. Cubozoa have relatively simple nervous systems consisting of a nerve net and a ring nerve. The latter has extensions forming ganglia and connections with the radial nerves and rhopalia. Morphological and electrophysiological studies have shown that a significant part of the CNS of cubomedusae is situated within the rhopalia[25,46,47]. In addition to numerous ciliated photoreceptors within the retinas of all six eyes, each rhopalium houses over 1,000 neurons of which approximately 500 are retina-associated. Each rhopalium also contains a group of pacemaker neurons that regulate swimming movements through the direct control of neuronal activity in the motor nerve net, and thus individual rhopalium facilitates various behaviors such as obstacle avoidance or light-shaft attraction enabling them to remain in close proximity to prey gathered in beams of light passing through open parts of the mangrove canopy. This behavioral regulation is most probably influenced by the visual input received by each rhopalium[48].

Based on our mRNA (Fig. 4) and protein (Fig. 6) expression profiles, many of the opsin genes identified here are expressed in rhopalia. Since it is not easy to determine the physiological relevance of a given gene just based on the level of its mRNA expression, we appreciated the finding that Tcop18, with 100 times lower level of mRNA transcripts compared to Tcop13 (Fig. S7), is significantly expressed on protein level (Fig. 6). Based on this fact, we suggest that all Tc-group 2 opsins, plus at least one opsin from each subclass of Tc-group 1 is rhopalium-specific. Moreover, the real-time PCR analysis has revealed that all of the rhopalium-expressed opsins are dramatically up-regulated when the rhopalia are formed during the polyp-to-medusa metamorphosis (Fig. 5). We thus propose that the *Tripedalia* rhopalium is a complex organ integrating and processing multiple light cues, gained though a diverse set of opsins, and transforming these signals into various behavioral responses.

Retina-specific opsin expression in *T. cystophora*. In addition to the extensive real-time PCR expression analysis, we paid special attention to the IHC analysis of retina specific opsins expression in *Tripedlia* rhopalia. The cubozoan lens-containing eyes have a thin cornea (made of monociliated

epithelial cells), a spherical cellular lens, a thin vitreous space, and a hemisphere-shaped everse retina with pigmented photoreceptors of the ciliary type, as judged from their ultra-structural morphology[24,49,50].

A previous study identified three types of photoreceptors in the lensed eyes of *T. cystophora* on the basis of differences in the morphology of their sensory cilium and microvillar organization[50]. In contrast, other studies[51–53] supported the interpretation that there was only a single basic morphological type of photoreceptor in cubozoan lensed eyes. Our IHC data support the first interpretation, showing that there are at least two types of PRC (each with markedly different opsin expression profiles) in the lensed eyes of *T. cystophora*. Both cell types have three distinct segments, giving rise to three retinal layers: 1. a thick layer of receptor-cell cilia formed from type-B PRCs (expressing Tcop13) and cone-shaped projections from type-A PRCs (expressing Tcop18), creating the ciliary layer; 2. a thin pigment layer where both receptor cells types are densely pigmented; 3. a neural layer containing nucleated cell bodies of both types of receptor cells.

The ciliary layer is dominated by the ciliary segments of type-B receptor cells. The cilia extend from the pigment layer to the vitreous space. From the ciliary membrane, microvilli extend, partly as bundles of parallel microvilli and partly as a disorganized tangle (as shown in another cubozoan jellyfish *Ch. bronzie*[24]). The microvilli make up the majority of the volume of the ciliary layer. Scattered among the type-B receptor cells are the cone-shaped projections of type-A photoreceptor cells partially filled with screening pigment granules. These cones run parallel to the ciliary trunks of the type-B sensory cells. In the neural layer, the type-A receptor cells have their cell bodies with nuclei, and they are also positive for Tcop18 protein expression (Fig. 6E–P). Projections of type-A photoreceptor cell bodies create a compact layer surrounding the whole retina.

It has been previously suggested that the lens eye photoreceptors utilize a different photopigment from those of the pit eyes and slit eyes[52]. According to dominant mRNA and protein levels and strict retinal specificity, we consider Tcop13 the main visual opsin of *T. cystophora* complex lens eyes. On the other hand, Tcop18 (also expressed in lens eyes) appears to be the main visual opsin in the lesser eyes. Our IHC data show, that retinas of both eye types (lens and lesser eyes) express different opsin combinations (various combinations of Tcop13 and Tcop18) according to their task (another level of visual tuning). The expression of rhopalium-specific opsins surely does not only involve photoreceptors of the retina, as some of the retina-associated neurons will most probably prove to be photosensitive as well, given our qRT-PCR analysis. This possibility should be resolved in the future by detailed IHC analysis assaying other Tcops expression.

Tissue-specific and larval opsins. Eyes are not the only means of photoreception in the Cnidarians, as many species lack distinct ocular structures yet exhibit specific photic behaviors. In these animals, photosensitivity is mediated through extraocular PRCs. Extraocular photosensitivity, is widespread throughout the animal kingdom, in both invertebrates and vertebrates[54,55]. The extraocular photosensitive cells are not organized into a complex organ such as ocelli or lens eyes. Instead, these cells are solitary or grouped and are scattered or localized throughout the animal body. Identification of the cells involved in extraocular photodetection has often proved difficult, but in some animals, neurons, epithelial cells, and muscle cells have been shown to be photosensitive[54,56–58]. Intriguingly, an ancient opsin-mediated phototransduction pathway and a previously unknown layer of sensory complexity in the control of cnidocyte discharge in cnidarian *Hydra magnipapillata* was reported very recently[59]. These various extraocular photoreceptors function as light detectors, informing the animal of the presence of light, measuring light intensity, and activating rhythmic behaviors as well as other physiological processes.

Our extensive qRT-PCR analysis (Figs 4, 5, S6, S7) (with support from the phylogenetic data) of different developmental stages and tissues revealed that the *T. cystophora* opsins can be classified into two groups, the probably more ancient Tc-group 1 opsins and Tc-group 2 rhopalium-specific opsins (Fig. 7). Tc-group 1 opsins tend to have broader expression. The broadest tissue- and stage-specific expression distribution is visible in Tc-group 1B, with Tcop2 and Tcop10 being male gonad-specific and other Tcops expressed in tissues such as bell, tentacles or manubrium. Both sub-groups 1A and 1B show a trend for increasing tissue/organ specificity of opsins after subsequent duplications.

More than a half of the opsins from those two subgroups were detected (at least in small amounts) in planula larvae, with Tcop17 (and probably Tcop6) being larva-specific. Such a variety of larval opsins is astonishing considering that to date only three larval opsins have been reported from reef corals[60]. Planula larvae have an extremely simple organization with no nervous system at all. Their only advanced feature is the presence of 10–15 pigment-cup ocelli, evenly spaced across the posterior half of the larval ectoderm. The ocelli are single-cell structures containing a cup of screening pigment filled with presumably photosensory microvilli. These morphologically rhabdomeric-like photoreceptors have no neural connections to any other cells, but each has a well-developed motor-cilium, appearing to be the only means by which light can control the behavior of the larva[61].

Our analysis implies that Cnidarians extensively utilize opsins not only for visual but also for extraocular photosensitivity. Revisiting the possible diversity of Tcops tissue/stage specific expression by IHC protein expression analysis and physiological studies could shed more light on their use for various behavioral tasks.

Phototransduction by cubozoan opsins. To investigate the coupling partner of *T. cystophora* opsins we performed an opsin-Gs-cAMP coupling assay. Our data revealed that the Gs-cAMP pathway[27] is used by opsin genes from Tc-group 2. Moreover our behavioral test showed for the first time that the opsin-Gs-cAMP cascade is functionally connected with vision guided behaviour. However, we were unable to obtain any light-mediated activation of signal transduction via this pathway for Tc-group 1 opsins. We propose that opsins that did not signal in our assay either use different G-protein pathways, as recently proposed in reef corals[60], act as photoisomerases or for unknown reason do not signal in our cell-line based assay, but nonetheless use Gs signaling cascade under natural conditions. The later possibility is, however, in our opinion very unlikely, because we saw comparable expression of all Tcops on the cell membranes of our test cell system and moreover not even a repeated flash stimulation lead to any response. However, we do acknowledge the possibility, that some of examined Tcops did not fold properly in mammalian cells used in the assay and thus were unable to signal. In some cases we did record slight increases in luciferase signal (like the one in Fig. 2E for Tcop18), however this phenomenon also appeared in some wells containing cells transfected with control opsins (not signaling though Gs-cAMP cascade) or non-transfected cells. This slight increase in luciferase activity was probably connected with non-opsin-specific changes in cellular metabolism during experiment (note that increase in luciferase activity in Fig. 2E starts 140 minutes from the beginning of the experiment and does not seem to be connected with light stimulation). Clearly the future identification of the actual Gα subunit coupled to Tc-group 1 opsins is going to be necessary to understanding if *T. cystophora* possess at least two independent photosystems, thus providing another level for the functional divergence of the identified opsins. Another interesting feature of our assay is the time-course of response of Tcop5, Tcop13 and Caryb transfected cells to light stimulus, reaching the peak in the order of minutes. This phenomenon is probably not caused by the slow light response of the opsins themselves, but rather indicative of the slow kinetics of the recombinant cAMP-sensitive luciferase expression in GloSensor™ cAMP HEK293 cells. In a study by Koyanagi *et al.*[62], the use of a similar assay led to peak of response in order of minutes even in the case of bovine rhodopsin, which is known to respond to light stimuli in other direct assay systems within millisecond time periods[63].

Future structure-function studies of prototypical cubozoan group 2 opsin is highly warranted. It would be interesting to find out whether any of the proposed E/D counterions are indeed used by *T. cystophora* opsins. Likewise, the significance of various tripeptide variants found among *T. cystophora* opsins awaits further experimental interrogation. Our data so far point to variable sensitivity and bleaching properties of individual opsins depending on their primary amino acid sequence. Based on their expression and conserved amino acid sequence at key positions, we assume that all Tcops described here are functional opsins, but as mentioned earlier, this remains to be confirmed by other analysis (IHC expression, identification of Tc-group 1 signalling cascade).

In summary, our data suggest that the expansion and diversification of the opsin gene family in cubozoans has allowed fine tuning and optimal photopigment function.

In summary, a detailed expression analysis uncovered both redundancy and specialization in the utilization of the opsin gene repertoire. On the one hand, multiple opsins with presumably similar molecular characteristics are apparently utilized in the same stage/tissue. On the other hand, a clear tendency to establish unique expression patterns exists both within the opsin subfamilies (Tc-group 1 and Tc-group 2) and between the two subfamilies. Remarkably, retina photoreceptors of lens-containing eyes express opsins most probably utilizing at least two distinct signaling pathways.

Materials and Methods

Jellyfish collection and culture. Adult *T. cystophora* were collected from the mangroves of La Parguerra, Puerto Rico. Laboratory cultures were established using settling larvae and artificial seawater. Settled larvae metamorphosed into young polyps. Young polyps were transformed into budding (asexually reproducing) polyps by feeding with Artemia once a week. Polyps were stimulated into metamorphosis (transformation into free swimming medusa) by incubation at 28°C. Polyps and young medusa were both maintained at 26 °C. All stages were collected for (opsin) expression pattern analysis (RT-PCR) and juvenile medusa also for rhopalium IHC.

Isolation of *Tripedalia cystophora* opsin genes. *Tripedalia cystophora* genomic DNA shotgun sequencing was performed on the GS FLX Titanium platform (454 Life Sciences, Roche). Pyrosequencing resulted in 1,952,068 reads (about 7×10^8 bases) with average read length of 360 bp. Assembly generated 134,683 of all contigs containing 790,111 (40.5%) reads. Assembly was done by program Newbler, version 2.3 (Roche). Resulting contigs were combined with singleton reads to produce a complete contig database. The database was subjected to similarity search by the FASTA[64] program using a wide range of homologous opsin proteins from other cnidarian and bilaterian species. FASTA search provided hits corresponding to short stretches of assumed Tripedalia opsin protein sequences. Full opsin genes sequences were obtained by using the Genome Walking strategy (Genome Walker, Clontech). Opsin sequences were deposited in GeneBank (accession numbers: JQ968416 -JQ968432).
(Primers in Supplement -T1)

Molecular phylogeny. To investigate the relationship between the cnidarian opsins and bilaterian opsins, we inferred a molecular phylogenetic tree by the maximum likelihood (ML) method implemented in PhyML 3.0[65] with LG substitution model[66]. Support for internal nodes was assessed using Approximate Likelihood-Ratio Test for Branches[67].

Dataset. Opsin protein sequences were acquired as described by Porter *et al.*[3]; however, incomplete sequences were discarded from the analysis and other 26 *Nematostella vectensis* annotated opsins were added to the dataset. In order to root the phylogenetic tree, 22 non-opsin GPCRs from the human genome were used as outgroups. The resulting dataset of 801 (779 opsin plus 22 non-opsin) transcripts plus genome trace opsin sequences was aligned using ClustalX[68] under default parameters and trimmed by eye in BioEdit. For phylogenetic analyses, only the 7-transmembrane region including intervening inter- and extra-cellular domains was included, as it was difficult to ascertain homology of N- and C- termini due to sequence length variation and lack of conservation across genes. The molecular phylogenetic tree of the opsin family was inferred from an alignment of 226 amino acids long (after N- and C-termini exclusion) opsin sequences. (Sequences in Supplement -T2)

Quantitative RT-PCR. RNA from indicated stages or dissected adult *T. cystophora* tissues was isolated using TRIZOL reagent (Invitrogen). Contaminating genomic DNA was removed by DNAse digestion and RNA repurification on RNeasy Micro columns (Qiagen) according to the manufacturer's protocol. The same amounts of RNA from each sample were used for reverse transcription using VILO cDNA kit (Invitrogen). Primers for qPCR were designed using Primer 3 software (see Supplementary Table 1 for sequences of primers). The qPCR was performed in LightCycler 2.0 System using LightCycler® 480 DNA SYBR Green I Master kit (Roche Diagnostics, Germany) according to the standard manufacturer's protocol. Target genes (Tcop1-Tcop18) and the housekeeping gene (Rpl32) were measured under the same conditions from the same cDNA. Results were analyzed by LightCycler software and crossing point values (Cp) were further determined as an average of Cp values from all replicates and normalized by Cp values of the housekeeping gene (so called deltaCp values). The results show relative normalized gene expression. Statistical significance of changes in the mRNA level of target genes between different samples were calculated by a Student´s t-test. For other data reproduction, heat map from z-scores (Standard scores) of deltaCp values for target genes (Tcop1-Tcop18) expression in different *T. cystophora* tissues was constructed. Z-score representation was obtained in R statistical environment with Bioconductor package.

Generation and verification of antibodies. An antibody directed against Tcop13 c-opsin was prepared by immunization of mice as follows. The C-terminal region of *c-opsin* corresponding to amino acids 281-330 (*NPIIYCFLHKQFRRAVLRGVCGRIVGGNAIAPSSTGVEPGQTLGGGAAES*; primers in Supplement -T1) was cloned into the expression vector pET42, expressed in BL21(DE3)RIPL cells (Stratagene), and purified by *Ni*-NTA Agarose Beads (QIAGEN). Purified protein was used as antigen for mouse immunization. Human kidney HEK293 cells were transfected with EGFP_C1-c-opsin (amino acids 281–330) expression vector by using FuGENE®6 reagent (Roche). Total extracts were prepared from c-opsin-transfected cells and mock-transfected cells and were analyzed by Western blotting by using anti-c-opsin mouse serum and chemiluminescent detection kit (Pierce).

Tissue collection and histology. Jellyfish were fixed in 4% paraformaldehyde (PFA), cryoprotected in 30% sucrose overnight at 4°C, and embedded and frozen in OCT (Tissue Freezing Medium, Jung). Horizontal frozen sections were prepared with a 8–12 μm thickness. The cryosections were washed three times in PBS and subsequently immuno-stained with an antibody.

Immunohistochemistry. The cryosections were refixed in 4% PFA for 10 min, washed three times with PBS, permeabilized with PBT (PBS + 0.1% Tween 20) for 15 min, and blocked in 10% BSA in PBT for 30 min. The primary antibodies were diluted in 1% BSA in PBT (1:500), incubated overnight at 4 °C, washed three times with PBS, and incubated with secondary antibodies in 1% BSA in PBT (1:500). The sections were counterstained with DAPI and mounted. Primary antibodies used were: anti-Tcop18[22], anti-Tcop13, and anti-acetylated tubulin (Sigma). The following secondary antibodies were used: Alexa Fluor 488- or 594-conjugated goat anti-mouse or anti-rabbit IgG (Molecular Probes).

Construction of opsin-expressing vectors. The expression vector pcDNA3.1 + 1D4 for opsin gene production in mammalian cells was prepared as follows. The sequence for BamHI restriction site followed by the sequence of 1D4 epitope tag from bovine rhodopsin was introduced into multiple cloning site of pcDNA 3.1+ vector (Clontech) through KpnI and EcoRI sites. Opsin cDNA of box jellyfish *C. rastonii* (GeneBank AB435549), kindly provided Dr. Koyanagi, was amplified from the vector by PCR and cloned into pcDNA3.1 + 1D4 vector using BamHI and HindIII cloning sites. The opsins of box jellyfish *T. cystophora*, which are all intron-less, were amplified by PCR from genomic DNA and cloned

into pcDNA 3.1 + 1D4 vector either via BamHI and HindIII or BamHI and KpnI cloning sites. All the constructs were verified by standard sequencing techniques before use.

Immunofluorescent staining of GloSensor™ cAMP HEK293 cells. GloSensor™ cAMP HEK293 cells (Promega) ($2.5*10^3$) were seeded onto coverslips and transfected with FuGene HD (ROCHE). The next day, cells were washed with PBS and fixed with 4% paraformaldehyde (PFA) for 10 minutes. Fixed cells were permeabilized with 0.1% Triton X-100 for 10 minutes and blocked with 10% BSA in 1x PBS with 0.1% Tween 20 for 1 hour. A mouse monoclonal antibody raised against 1D4 epitope (Millipore Chemicon MAB5356), at a concentration of 1:250, was used in conjunction with a secondary antibody conjugated with Alexa Fluor 488 to immuno-stain expressed opsins. Cells were mounted in Mowiol®. Fluorescent images were captured using a Leica SP5 confocal microscope.

Light response assays. GloSensor™ cAMP HEK293 cells (Promega) ($10*10^3$) were plated into a solid white 96-well plate in L15 CO_2-independent medium with phenol red (Gibco) and 10% serum and incubated overnight at 37 °C, 0.3% CO_2. The cells were transfected the next day with plasmids expressing opsin genes using FuGENE® HD Transfection Reagent (ROCHE). Immuno-fluorescent staining revealed a transfection efficiency of 50% using this method. All procedures following transfection of the cells with the various opsin receptors were carried out in dim red light. Six hours post transfection 9-cis retinal (Sigma-Aldrich) was added to a final concentration of 10 mM. The cells were then kept overnight in an incubator (37 °C; 0.3% CO_2). Next day the cells were removed from the incubator and left to equilibrate for 30 minutes at room temperature. Beetle luciferin potassium salt (Synchem) reconstituted in 10 mM HEPES buffer was added to the cells to a final concentration of 3 mM. The cells were then placed in a top-read Envision plate reader with ultra-sensitive luminescence model. Luciferase activity was measured for 2 hours with 0.1 second resolution and cycles of every 1 minute to determine the luciferin uptake. Cells were then subjected to three pulses of light stimulation using repeated flashes from a Nikon speed-light SB-600 electronic camera flash (5 flashes, 1 flash/ second in each pulse, ~40000 lumen/m2 per flash) followed by recovery periods of 30 minutes when Raw Luminescence Units (RLU) were recorded. After the third measurement, the cells were stimulated with seven light pulses with periods of 3 minutes (5 flashes, 1 flash/ second in each pulse). Luminescence was recorded between pulses (0.1 second resolution, 15 seconds per cycle) and another 120 minutes after the last pulse (0.1 seconds resolution, 30 seconds per cycle). The experiment for the tripeptide mutation was performed in a similar way with minor changes. The entire experiment was performed at 37 °C, which led to faster response of cells to the light stimulation. Three pulses (5 flashes, 1 flash/ second in each pulse) followed by recovery of 15 minutes were applied. The following repeated stimulation was done with 30 light pulses (1 flash) with periods of 30 seconds. Luminescence was measured another 30 minutes after the last pulse. Luminescence recordings were analyzed with Microsoft Office Excel. All experiments comprised cells plated and treated in triplicate. Prism (Graphpad) software was used for all statistical analyses.

***T. cystophora* phototaxis test.** All behavioral tests were performed at room temperature (22 °C). Phototaxis experiments were performed in an aquarium-like testing chamber (20 × 5 × 5 cm) with one illuminated side (Fig. 7a). To test the effect of suramin analog 4,4',4",4"'-(carbonylbis(imino-5,1,3-benzenetriylbis (carbonylimino)))tetrakis-benzene-1,3-disulfonic acid (NF449 - Calbiochem) on the *T. cystophora* phototactic behavior, we incubated 3-day-old medusae in 1 ml of artificial seawater with NF449 at a final concentration of either 0 μM, 100 μM, and 1 mM for 30 minutes under artificial day light. Medusae were then washed with artificial seawater, placed into the dark part of the testing chamber and tested for phototactic behavior. The number of medusae that reached the light region after 5 minutes, 3 hours and 24 hours was counted and compared to the number of animals from the untreated control group.

References

1. Terakita, A. The opsins. *Genome Biol* **6,** 213, doi: 10.1186/gb-2005-6-3-213 (2005).
2. Sakmar, T. P., Menon, S. T., Marin, E. P. & Awad, E. S. Rhodopsin: insights from recent structural studies. *Annual Review of Biophysics and Biomolecular Structure* **31,** 443-484, doi: 10.1146/annurev.biophys.31.082901.134348 (2002).
3. Porter, M. L. *et al.* Shedding new light on opsin evolution. *Proc Biol Sci* **279,** 3–14, doi: 10.1098/rspb.2011.1819 (2012).
4. Suga, H., Schmid, V. & Gehring, W. J. Evolution and functional diversity of jellyfish opsins. *Current Biology* **18,** 51–55, doi: 10.1016/j.cub.2007.11.059 (2008).
5. Plachetzki, D. C., Degnan, B. M. & Oakley, T. H. The origins of novel protein interactions during animal opsin evolution. *PLoS One* **2,** e1054, doi: 10.1371/journal.pone.0001054 (2007).
6. Feuda, R., Hamilton, S. C., McInerney, J. O. & Pisani, D. Metazoan opsin evolution reveals a simple route to animal vision. *Proceedings of the National Academy of Sciences of the United States of America* **109,** 18868–18872, doi: 10.1073/pnas.1204609109 (2012).
7. Kojima, D. *et al.* A novel Go-mediated phototransduction cascade in scallop visual cells. *Journal of Biological Chemistry* **272,** 22979–22982 (1997).
8. Koyanagi, M., Terakita, A., Kubokawa, K. & Shichida, Y. Amphioxus homologs of Go-coupled rhodopsin and peropsin having 11-cis- and all-trans-retinals as their chromophores. *FEBS Letters* **531,** 525–528 (2002).
9. Hara, T. & Hara, R. Rhodopsin and retinochrome in the squid retina. *Nature* **214,** 573–575 (1967).
10. Plachetzki, D. C., Fong, C. R. & Oakley, T. H. The evolution of phototransduction from an ancestral cyclic nucleotide gated pathway. *Proc Biol Sci* **277,** 1963–1969, doi: 10.1098/rspb.2009.1797 (2010).
11. Feuda, R., R.-S. O., Oakley, T. H. & Pisani, D. The comb jelly opsins and the origins of animal phototransduction. *Genome Biology and Evolution* **6,** 1964-*1971*, doi: 10.1093/gbe/evu154 (2014).

12. Marin, E. P. *et al.* The amino terminus of the fourth cytoplasmic loop of rhodopsin modulates rhodopsin-transducin interaction. *Journal of Biological Chemistry* **275,** 1930–1936 (2000).
13. Martin, V. J. Photoreceptors of cnidarians. *Can. J. Zool.* **80,** 1703–1722, doi: 10.1139/Z02-136 (2002).
14. Nilsson, D. E., Gislen, L., Coates, M. M., Skogh, C. & Garm, A. Advanced optics in a jellyfish eye. *Nature* **435,** 201–205, doi: 10.1038/nature03484 (2005).
15. Coates, M. M. Visual ecology and functional morphology of cubozoa (cnidaria). *Integr Comp Biol* **43,** 542–548, doi: 10.1093/icb/43.4.542 (2003).
16. O'Connor, M., Nilsson, D. E. & Garm, A. Temporal properties of the lens eyes of the box jellyfish Tripedalia cystophora. *J Comp Physiol A Neuroethol Sens Neural Behav Physiol* **196,** 213–220, doi: 10.1007/s00359-010-0506-8 (2010).
17. Garm, A., Oskarsson, M. & Nilsson, D. E. Box jellyfish use terrestrial visual cues for navigation. *Current Biology* **21,** 798–803, doi: 10.1016/j.cub.2011.03.054 (2011).
18. Petie, R., Garm, A. & Nilsson, D. E. Visual control of steering in the box jellyfish Tripedalia cystophora. *Journal of Experimental Biology* **214,** 2809–2815, doi: 10.1242/jeb.057190 (2011).
19. Land, M. F. & Nilsson, D. E. Animal eyes. *Oxford, Oxford University Press* (2002).
20. Kozmik, Z. *et al.* Role of Pax genes in eye evolution: a cnidarian PaxB gene uniting Pax2 and Pax6 functions. *Dev Cell* **5,** 773–785 (2003).
21. Piatigorsky, J. & Kozmik, Z. Cubozoan jellyfish: an Evo/Devo model for eyes and other sensory systems. *International Journal of Developmental Biology* **48,** 719-729, doi: 10.1387/ijdb.041851jp (2004).
22. Kozmik, Z. *et al.* Assembly of the cnidarian camera-type eye from vertebrate-like components. *Proceedings of the National Academy of Sciences of the United States of America* **105,** 8989–8993, doi: 10.1073/pnas.0800388105 (2008).
23. Kozmik, Z. *et al.* Cubozoan crystallins: evidence for convergent evolution of pax regulatory sequences. *Evol Dev* **10,** 52–61, doi: 10.1111/j.1525-142X.2007.00213.x (2008).
24. O'Connor, M., Garm, A. & Nilsson, D. E. Structure and optics of the eyes of the box jellyfish Chiropsella bronzie. *J Comp Physiol A Neuroethol Sens Neural Behav Physiol* **195,** 557–569, doi: 10.1007/s00359-009-0431-x (2009).
25. Parkefelt, L., Skogh, C., Nilsson, D. E. & Ekstrom, P. Bilateral symmetric organization of neural elements in the visual system of a coelenterate, Tripedalia cystophora (Cubozoa). *Journal of Comparative Neurology* **492,** 251–262, doi: 10.1002/cne.20658 (2005).
26. Garm, A., Andersson, F. & Nilsson, D. E. Unique structure and optics of the lesser eyes of the box jellyfish Tripedalia cystophora. *Vision Research* **48,** 1061–1073, doi: 10.1016/j.visres.2008.01.019 (2008).
27. Koyanagi, M. *et al.* Jellyfish vision starts with cAMP signaling mediated by opsin-G(s) cascade. *Proceedings of the National Academy of Sciences of the United States of America* **105,** 15576–15580, doi: 10.1073/pnas.0806215105 (2008).
28. Panda, S. *et al.* Illumination of the melanopsin signaling pathway. *Science* **307,** 600–604, doi: 10.1126/science.1105121 (2005).
29. Yamashita, T. *et al.* Opn5 is a UV-sensitive bistable pigment that couples with Gi subtype of G protein. *Proceedings of the National Academy of Sciences of the United States of America* **107,** 22084–22089, doi: 10.1073/pnas.1012498107 (2010).
30. Bridge, D., Cunningham, C. W., Schierwater, B., DeSalle, R. & Buss, L. W. Class-level relationships in the phylum Cnidaria: evidence from mitochondrial genome structure. *Proceedings of the National Academy of Sciences of the United States of America* **89,** 8750–8753 (1992).
31. Bailes, H. J., Z. L. & Lucas, R. J. Reproducible and sustained regulation of Gαs signalling using a metazoan opsin as an optogenetic tool. *PLOS one* **7,** doi: 10.1371/journal.pone.0030774 (2012).
32. Koyanagi, M., Kubokawa, K., Tsukamoto, H., Shichida, Y. & Terakita, A. Cephalochordate melanopsin: evolutionary linkage between invertebrate visual cells and vertebrate photosensitive retinal ganglion cells. *Current Biology* **15,** 1065–1069, doi: 10.1016/j.cub.2005.04.063 (2005).
33. Hohenegger, M. *et al.* Gsalpha-selective G protein antagonists. *Proceedings of the National Academy of Sciences of the United States of America* **95,** 346–351 (1998).
34. Shabalina, S. A. *et al.* Distinct patterns of expression and evolution of intronless and intron-containing mammalian genes. *Molecular biology and evolution* **27,** 1745–1749, doi: 10.1093/molbev/msq086 (2010).
35. Zou, M., Guo, B. & He, S. The roles and evolutionary patterns of intronless genes in deuterostomes. *Comparative and functional genomics* **2011,** 680673, doi: 10.1155/2011/680673 (2011).
36. Gentles, A. J. & Karlin, S. Why are human G-protein-coupled receptors predominantly intronless? *Trends in genetics : TIG* **15,** 47–49 (1999).
37. Brosius, J. Many G-protein-coupled receptors are encoded by retrogenes. *Trends in genetics : TIG* **15,** 304–305 (1999).
38. Fridmanis, D., Fredriksson, R., Kapa, I., Schioth, H. B. & Klovins, J. Formation of new genes explains lower intron density in mammalian Rhodopsin G protein-coupled receptors. *Molecular phylogenetics and evolution* **43,** 864–880, doi: 10.1016/j.ympev.2006.11.007 (2007).
39. UCSC, G. B. G. *Opsin evolution: update blog http://genomewiki.ucsc.edu, (Date of acces: 20/05/2012).*
40. Morris, A. B. J. & Hunt, D. M. The molecular basis of a spectral shift in the rhodopsin of two species of squid from different photic enviroments. *Proceedings of the Royal Society of London B* **254,** 233–240 (1993).
41. Fitzgibbon, J., H. A., Slobodvanyuk, S. J., Bellingham, J., Bowmaker, J. K. & Hunt, D. M. The rhodopsin-encoding gene of bony fish lacks introns. *Gene* **164,** 273–277 (1995).
42. Innan, H. & Kondrashov, F. The evolution of gene duplications: classifying and distinguishing between models. *Nature reviews. Genetics* **11,** 97–108, doi: 10.1038/nrg2689 (2010).
43. Lynch, M. & Conery, J. S. The evolutionary fate and consequences of duplicate genes. *Science (New York, N.Y.)* **290,** 1151–1155 (2000).
44. Matsumoto, Y., Fukamachi, S., Mitani, H. & Kawamura, S. Functional characterization of visual opsin repertoire in Medaka (Oryzias latipes). *Gene* **371,** 268–278, doi: 10.1016/j.gene.2005.12.005 (2006).
45. Rennison, D. J., Owens, G. L. & Taylor, J. S. Opsin gene duplication and divergence in ray-finned fish. *Molecular phylogenetics and evolution* **62,** 986–1008, doi: 10.1016/j.ympev.2011.11.030 (2012).
46. Skogh, C., Garm, A., Nilsson, D. E. & Ekstrom, P. Bilaterally symmetrical rhopalial nervous system of the box jellyfish Tripedalia cystophora. *Journal of Morphology* **267,** 1391–1405, doi: 10.1002/jmor.10472 (2006).
47. Garm, A., Ekstrom, P., Boudes, M. & Nilsson, D. E. Rhopalia are integrated parts of the central nervous system in box jellyfish. *Cell Tissue Res* **325,** 333–343, doi: 10.1007/s00441-005-0134-8 (2006).
48. Stockl, A. L., Petie, R. & Nilsson, D. E. Setting the pace: new insights into central pattern generator interactions in box jellyfish swimming. *PLoS One* **6,** e27201, doi: 10.1371/journal.pone.0027201 (2011).
49. Yamasu, T. & Yoshida, M. Fine structure of complex ocelli of a cubomedusan, Tamoya bursaria Haeckel. *Cell and Tissue Research* **170,** 325–339 (1976).
50. Laska, G., Hundgen, M. Morphologie und ultrastruktur der lichtsinnesorgane von Tripedalia cystophora Conant (Cnidaria, Cubozoa). *Zool Jb Anat* **108,** 107–123 (1982).
51. O'Connor, M. *et al.* Visual pigment in the lens eyes of the box jellyfish Chiropsella bronzie. *Proc Biol Sci* **277,** 1843–1848, doi: 10.1098/rspb.2009.2248 (2010).

52. Ekstrom, P., Garm, A., Palsson, J., Vihtelic, T. S. & Nilsson, D. E. Immunohistochemical evidence for multiple photosystems in box jellyfish. *Cell and Tissue Research* **333,** 115–124, doi: 10.1007/s00441-008-0614-8 (2008).
53. Garm, A. & Ekstrom, P. Evidence for multiple photosystems in jellyfish. *Int Rev Cell Mol Biol* **280,** 41–78, doi: 10.1016/s1937-6448(10)80002-4 (2010).
54. Yoshida, M. Extraocular photoreception. *Handbook of sensory physiology* **VII/6A**, 582–640 (1979).
55. Taddei-Ferretti, C. & Musio, C. Photobehaviour of Hydra (Cnidaria, Hydrozoa) and correlated mechanisms: a case of extraocular photosensitivity. *Journal of Photochemistry and Photobiology. B, Biology* **55,** 88–101 (2000).
56. Arkett, S. A. & Spencer, A. N. Neuronal mechanism of a hydromedusan shadow reflex. I. Identified reflex components and sequence of events *J. Comp. Physiol. A* **159,** 201–213 (1986).
57. Sawyer, S. J., D. H. B. & Shick, M. Neurophysiological correlates of the behavioral response to light in the sea anemone Anthopleura elegantissima. *Biol. Bull. (Woods Hole, Mass.)* **186,** 195–201 (1994).
58. Musio, C. *et al.* First identification and localization of a visual pigment in Hydra (Cnidaria, Hydrozoa). *J Comp Physiol A* **187,** 79–81 (2001).
59. Plachetzki, D. C., Fong, C. R. & Oakley, T. H. Cnidocyte discharge is regulated by light and opsin-mediated phototransduction. *BMC Biol* **10**, 17, doi: 10.1186/1741-7007-10-17 (2012).
60. Mason, B. *et al.* Evidence for multiple phototransduction pathways in a reef-building coral. *PLoS One* **7,** e50371, doi: 10.1371/journal.pone.0050371 (2012).
61. Nordstrom, K., Wallen, R., Seymour, J. & Nilsson, D. A simple visual system without neurons in jellyfish larvae. *Proc Biol Sci* **270,** 2349–2354, doi: 10.1098/rspb.2003.2504 (2003).
62. Koyanagi, M.T. E., Nagata, T., Tsukamoto, H. & Terakita, A. Homologs of vertebrate Opn3 potentially serve as a light sensor in nonphotoreceptive tissue. *Proceeding of the National Academy of Sciences of the United States of America* **110,** 4998–5003, doi: 10.1073/pnas.1219416110 (2013).
63. Heck, M. S. S., Maretzki, D., Bartl, F. J., Ritter, E., Palczewski, K. & Hofmann, K. P. Signaling States of Rhodopsin: FORMATION OF THE STORAGE FORM, METARHODOPSIN III, FROM ACTIVE METARHODOPSIN II. *Journal of Biological Chemistry* **278,** 3162–3169 (2003).
64. Pearson, W. R. & Lipman, D. J. Improved tools for biological sequence comparison. *Proceedings of the National Academy of Sciences of the United States of America* **85,** 2444–2448 (1988).
65. Guindon, S. *et al.* New algorithms and methods to estimate maximum-likelihood phylogenies: assessing the performance of PhyML 3.0. *Syst Biol* **59,** 307–321, doi: 10.1093/sysbio/syq010 (2010).
66. Le, S. Q. & Gascuel, O. An improved general amino acid replacement matrix. *Molecular Biology and Evolution* **25,** 1307–1320, doi: 10.1093/molbev/msn067 (2008).
67. Anisimova, M. & Gascuel, O. Approximate likelihood-ratio test for branches: A fast, accurate, and powerful alternative. *Syst Biol* **55,** 539–552, doi: 10.1080/10635150600755453 (2006).
68. Larkin, M. A. *et al.* Clustal W and Clustal X version 2.0. *Bioinformatics* **23,** 2947–2948, doi: 10.1093/bioinformatics/btm404 (2007).

Acknowledgements

We are grateful to Dr. Koyanagi for providing cDNA encoding *C. rastonii* opsin and Sarka Takacova and Dr. Alex Bruce for manuscript proofreading. This study was supported by the Grant Agency of the Czech Republic (P305/10/2141) to Z.K. by the Ministry of Education, Youth and Sports of the Czech Republic (LM2011022) to P.B. and by IMG institutional support RVO68378050.

Author Contributions

Conceived and designed the experiments: M.L., J.P., I.K., P.F., P.B., C.V. and Z.K. Performed the experiments: M.L., J.P., I.K., P.F., A.P. and Z.K. Analyzed the data: M.L., J.P., I.K., P.F., A.P., H.S., J.P.a. and Z.K. Wrote the paper: M.L., J.P. and Z.K.

Additional Information

Supplementary information accompanies this paper at http://www.nature.com/srep

Competing financial interests: The authors declare no competing financial interests.

How to cite this article: Liegertová, M. *et al.* Cubozoan genome illuminates functional diversification of opsins and photoreceptor evolution. *Sci. Rep.* **5**, 11885; doi: 10.1038/srep11885 (2015).

6.3 The opsin repertoire of the European lancelet: a window into light detection in a basal chordate.

Amphioxus opsin genes were previously described in two studies[16,93]. The work by Koyanagi*, et al.*[93] identified six opsin genes in the genome of *B. belcheri*. These opsins were representatives of c-type; r-type and Group4 opsins. In 2008 genome of *B.floridae* was published by Holland*, et al.*[16]. Authors of this study identified 20 opsin genes. Phylogenetic analysis confirmed that representatives of three main groups (c-type, r-type and Group4) can be found in the amphioxus genome. Results underlined the exceptionality of several amphioxus opsins that cluster within r-type opsins, but formed a rather separate clade, called Amphiop6 group (due to the presence of *B. belcheri* Amphiop6 in this group). Additionally, putative counterion E113 was detected in three of these opsins. This study also documented variability of tripeptide sequences of all amphioxus opsins.

In our study we focused on identification of opsin genes in the newly sequenced genome of European amphioxus *B. lanceolatum*. In total we identified 21 opsins and one putative opsin pseudogene in the genome *of B. lanceolatum*. We documented presence of D or E at position 113 in one Go opsin (belonging to Group4) and two Amphiop6 opsins. Additionally, the majority of *B. lanceolatum* opsins have a negatively charged aa D at position 83, a putative counterion site proposed in study by Porter*, et al.*[77]. *B. lanceolatum* opsins also evinced variability in tripeptide sequences as previously shown for *B. floridae* opsins. Furthermore, we monitored expression of identified opsin genes in various developmental stages and adult animal tissues of *B. lanceolatum*. All examined genes were detected at the level of mRNA transcript by qRT-PCR both at various developmental stages and in different adult tissues. The only exception was the predicted pseudogene *Bl_op17* (mRNA not detected). We also tried to monitor expression of several *B. lanceolatum* opsins by whole mount *in situ* hybridization (ISH) on embryonic and larval stages. We, however, succeeded only in three cases – *Bl_op11*, *Bl_op12a* and *Bl_op15* (melanopsin). *Bl_op11* and *Bl_op12a* showed an interesting expression pattern, being expressed in anterior structures around mouth, but also in posterior parts – tail fin (both genes) and close to anus (*Bl_op12a*). As expected, *Bl_op15* transcript was detected in the developing 1st dorsal ocellus.

Taken together we identified 21 opsin genes and 1 pseudogene in the genome of *B. lanceolatum*. We provided characteristics of important opsin landmarks (counterion, tripeptide) for all of the identified opsin genes. We added qRT-PCR expression data for all of the identified opsin genes, plus ISH data for three opsins. We hope that our data will be solid jumping-off point for further studies of amphioxus opsins.

My contribution to this work: I cloned problematic parts (not fully sequenced or mistakenly assembled sequences) of *B. lanceolatum* opsin genes. I performed qRT-PCR analysis (shown in Fig.3 and Suppl. Fig.S3). I performed ISH for ten *B. lanceolatum* opsins, only two successful trials (*Bl_op11* and *Bl_op12a*) are shown in Fig.4 (ISH for *Bl_op15* was performed by I. Kozmikova). I contributed to writing of some parts of methods and results.

Int. J. Dev. Biol. 61: 763-772 (2017)
doi: 10.1387/ijdb.170139zk

THE INTERNATIONAL JOURNAL OF DEVELOPMENTAL BIOLOGY
www.intjdevbiol.com

The opsin repertoire of the European lancelet: a window into light detection in a basal chordate

CHRYSOULA N. PANTZARTZI[1,#], JIRI PERGNER[2,#], IRYNA KOZMIKOVA[2] and ZBYNEK KOZMIK*[,1,2]

[1]Laboratory of Eye Biology, Institute of Molecular Genetics of the Czech Academy of Sciences, Prague, Czech Republic, Division BIOCEV, Vestec, Czech Republic and [2]Laboratory of Transcriptional Regulation, Institute of Molecular Genetics of the ASCR, Prague, Czech Republic

ABSTRACT Light detection in animals is predominantly based on the photopigment composed of a protein moiety, the opsin, and the chromophore retinal. Animal opsins originated very early in metazoan evolution from within the G-Protein Coupled Receptor (GPCR) gene superfamily and diversified into several distinct branches prior to the cnidarian-bilaterian split. The origin of opsin diversity, opsin classification and interfamily relationships have been the matter of long-standing debate. Comparative studies of opsins from various Metazoa provide key insight into the evolutionary history of opsins and the visual perception in animals. Here, we have analyzed the genome assembly of the cephalochordate *Branchiostoma lanceolatum*, applying BLAST, gene prediction tools and manual curation in order to predict *de novo* its complete opsin repertoire. We investigated the structure of predicted opsin genes, encoded proteins, their phylogenetic placement, and expression. We identified a total of 22 opsin genes in *B. lanceolatum*, of which 21 are expressed and the remaining one appears to be a pseudogene. According to our phylogenetic analysis, representatives from the three major opsin groups, namely C-type, the R-type and the Group 4, can be identified in *B. lanceolatum*. Most of the *B. lanceolatum* opsins exhibit a stage-specific, but not a tissue-specific, expression pattern. The large number of opsins detected in *B. lanceolatum*, the observed similarities and differences in terms of sequence characteristics and expression patterns lead us to conclude that there may be a fine tuning in opsin utilization in order to facilitate visually-guided behavior of European amphioxus under various environmental settings.

KEY WORDS: *Branchiostoma, amphioxus, opsin, expression*

Introduction

Light sensing systems have evolved to be uniquely suited to the environment and behavior of any given species. Animals detect light using sensory cells known as photoreceptors, present in the eyes or, in case of extraocular photoreceptors, outside of the eyes. Although other systems of light detection exist in the animal kingdom, such as cryptochromes (Rivera *et al.*, 2012) or LITE-1 (Gong *et al.*, 2016), opsins are dominantly utilized as visual pigments among Metazoa. Opsins are seven transmembrane domain proteins that belong to the G-Protein Coupled Receptor (GPCR) superfamily and are canonically distinguished from other GPCRs by a highly conserved lysine in the seventh helix. The number of opsin genes differs significantly among species studied so far and does not generally correlate with the overall level of body plan sophistication. Cnidaria for example, despite having a relatively simple body plan and limited number of cell types, are known to possess a large number of opsins originating by species-specific gene duplications (Koyanagi *et al.*, 2008; Kozmik *et al.*, 2008; Suga *et al.*, 2008). Opsin classification, interfamily relationships and evolution of animal vision have been the debate of numerous studies so far (D'Aniello *et al.*, 2015; Feuda *et al.*, 2012; Liegertova *et al.*,

Abbreviations used in this paper: CNS, Central Nervous System, GPCR, G-protein coupled receptor, TM, transmembrane.

***Address correspondence to:** Zbynek Kozmik. Institute of Molecular Genetics of the Czech Academy of Sciences, v.v.i., Videnska 1083, 14220, Prague, Czech Republic. Tel: +420 241062110. E-mail: kozmik@img.cas.cz - http://orcid.org/0000-0002-5850-2105

#Note: These authors contributed equally.

Supplementary Material for this paper is available at: http://dx.doi.org/10.1387ijdb.170139zk

Submitted: 21 June, 2017; *Accepted:* 11 July, 2017.

ISSN: Online 1696-3547, Print 0214-6282

2015; Peirson *et al.*, 2009; Plachetzki *et al.*, 2007; Porter *et al.*, 2012; Ramirez *et al.*, 2016; Shichida and Matsuyama, 2009; Suga *et al.*, 2008; Terakita, 2005). Opsins can be roughly clustered into four major groups, namely the ciliary opsins expressed in ciliary photoreceptors (C-type), the rhabdomeric opsins expressed in rhabdomeric photoreceptors (R-type), the Group 4 opsins, and the Cnidarian opsins. A further subdivision of the first three groups into seven subfamilies was suggested (Lamb *et al.*, 2007; Terakita, 2005), based on their sequence and on the type of the G-protein to which they are coupled: 1) the vertebrate visual and non-visual, 2) the encephalopsin/TMT, 3) the Gq-coupled/melanopsin, 4) the neuropsin, 5) the Go-coupled, 6) the peropsin, and 7) the retinal photoisomerase subfamilies. Ramirez and colleagues have proposed that a repertoire of at least nine opsin paralogs was present in the bilaterian ancestor (Ramirez *et al.*, 2016). In regard to the cnidarian opsins, there are conflicting results regarding their position in the phylogenetic tree (Feuda *et al.*, 2012; Liegertova *et al.*, 2015; Plachetzki *et al.*, 2007; Porter *et al.*, 2012; Suga *et al.*, 2008). The function of most opsins consists of two steps: light absorption and G-protein activation in both visual and non-visual systems. Isomerization of the chromophore 11-*cis*-retinaldehyde to all-*trans*-retinaldehyde due to light absorption, changes the conformation of the opsin and triggers a signal transduction cascade, the type of which is dependent on the G-protein to which the opsin binds

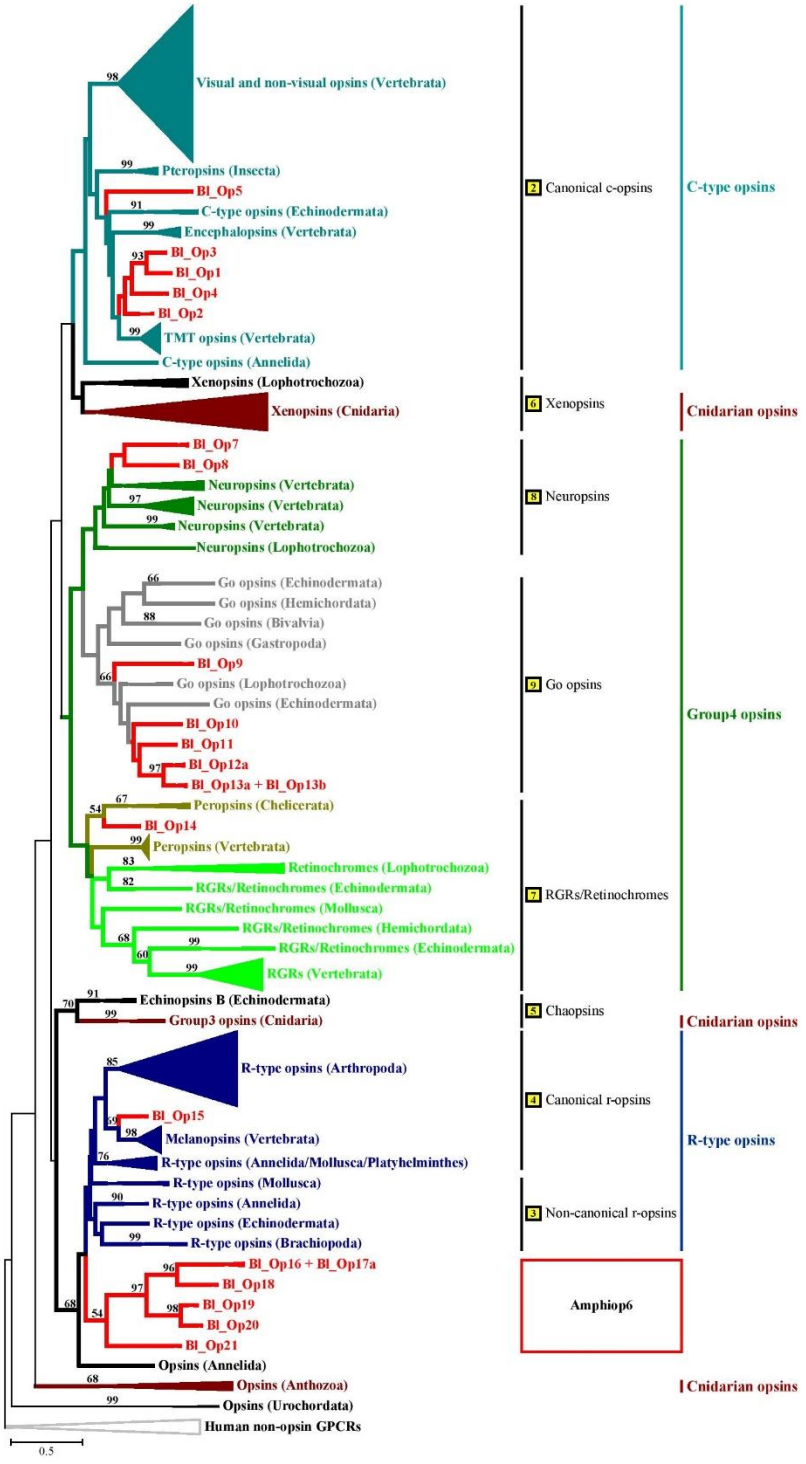

Fig. 1. Molecular phylogenetic analysis of opsins by Maximum Likelihood method. *The evolutionary history of opsin proteins was inferred by using the Maximum Likelihood method based on the Le_Gascuel_2008 model. The tree with the highest log likelihood is shown. Bootstrap values are shown (only values>50) either at the nodes or above the branches in the case of collapsed subgroups (e.g. neuropsin). A discrete Gamma distribution was used to model evolutionary rate differences among sites (2 categories). The tree is drawn to scale, with branch lengths measured in the number of substitutions per site. The analysis involved 787 amino acid sequences. There were a total of 419 positions in the final dataset (third cytoplasmic loop is excluded). Numbers in yellow boxes correspond to the bilaterian opsin paralogs identified by Ramirez* et al.*, 2016.*

TABLE 1

NOMENCLATURE FOR *BRANCHIOSTOMA* OPSIN GENES

Group	This study	*Branchiostoma floridae models**	*B. belcheri* mRNA sequences	References
C-type opsins	*Bl_op1* (MF464463)	124039	AB050610	c-opsin1 (Vopalensky et al., 2012), *Amphi*op5 (Koyanagi et al., 2002)
	Bl_op2 (MF464464)	205982		
	Bl_op3 (MF464465)	84894	AB050609	c-opsin3 (Vopalensky et al., 2012), *Amphi*op4 (Koyanagi et al., 2002)
	Bl_op4 (MF464466)	70447		
	Bl_op5 (MF464467)	84890		
Neuropsins	Not identified	210643		
	Bl_op7 (MF464468)	65045		
	Bl_op8 (MF464469)	94083		
Go opsins	*Bl_op9* (MF464470)	71561	AB050607	*Amphi*op2 (Koyanagi et al., 2002)
	Bl_op10 (MF464471)	215180		
	Bl_op11 (MF464472)	84844		
	Bl_op12a (MF464473)	91094	AB050606	*Amphi*op1 (Koyanagi et al., 2002)
	Bl_op13a (MF464474)	91095		
	Bl_op13b (MF464475)	Not identified		
Peropsins	*Bl_op14* (MF464476)	90832	AB050608	*Amphi*op3 (Koyanagi et al., 2002)
Melanopsins	*Bl_op15* (MF464477)	65960	AB205400	*Amphi*Mop (Koyanagi et al., 2005)
Amphiop6	*Bl_op16* (MF464478)	86640		
	Bl_op17a (MF464479)	201585		
	Bl_op17b (MF464480)	Not identified		
	Bl_op18 (MF464481)	Not identified		
	Bl_op19 (MF464482)	87094	AB050611	*Amphi*op6 (Koyanagi et al., 2002)
	Bl_op20 (MF464483)	110003		
	Bl_op21 (MF464484)	86195		

* Models from JGI, genome version v1.0 (http://genome.jgi.doe.gov/Brafl1/Brafl1.home.html)

(Koyanagi *et al.*, 2008; Liegertova *et al.*, 2015; Yarfitz and Hurley, 1994). The conserved lysine in the seventh helix is used to form a Schiff-base bond to the retinal chromophore (Bownds, 1967; Wang *et al.*, 1980) and in its protonated form it is stabilized by a negatively charged amino acid, called a counterion, whose position varies among different opsin subfamilies (reviewed in Porter *et al.*, 2012; Shichida and Matsuyama, 2009).

Comparative studies of opsins provide valuable insight not only into the origins of opsin diversity but also into the evolution of visual organs and light perception in animals. To help answer questions about vertebrate evolution at the key invertebrate chordate-vertebrate transition, such as "How did the vertebrate eye evolved?", one can examine opsins and visual organs of the extant and most basally divergent chordates, the cephalochordates. The subphylum Cephalochordata, a.k.a. amphioxus or lancelet, consists of approximately 29 extant species, with a worldwide distribution (Poss and Boschung, 1996). Amphioxus possesses four types of photoreceptive systems – the dorsal ocelli and the Joseph cells are rhabdomeric receptors, while the frontal eye and the lamellar body contain ciliary photoreceptors (Lacalli, 2004). Function of the first two receptors is still not clear, nevertheless, rhabdomeric receptors similar to Joseph cells are present in the cerebral eyes of tunicates (salps). Amphioxus frontal eye is considered homologous to the paired eyes of vertebrates, since its photoreceptors and pigment cells co-express a combination of transcription factors and opsins typical of the vertebrate eye photoreceptors (Vopalensky *et al.*, 2012). The lamellar body, on the other hand, is proposed as the amphioxus homolog of the pineal gland (Lacalli, 2004). Seven mRNA (*Amphi*op1-*Amphi*op6 and *Amphi*Mop) and 20 opsin genes have been previously identified in *B. belcheri* and *B. floridae*, respectively (Holland *et al.*, 2008; Koyanagi *et al.*, 2005; Koyanagi *et al.*, 2002). There are representatives from the encephalopsin/TMT, neuropsin, Go, peropsin and melanopsin subfamilies; a divergent subfamily, Amphiop6 appears to be specifically duplicated in amphioxus (Holland *et al.*, 2008). No homologs of the vertebrate visual/nonvisual opsin subfamily were detected (Holland *et al.*, 2008). Studies on expression pattern and function of the *Branchiostoma* opsins are rather limited; the biochemical data support AmphiOp1 as a typical visual pigment and AmphiOp3 as a photoisomerase (Koyanagi *et al.*, 2002), while the properties of the *B. belcheri* melanopsin homolog were found to resemble those of the visual opsins present in the intrinsically photosensitive rhabdomeric photoreceptor cells of vertebrates (Koyanagi *et al.*, 2005). In agreement with their phylogenetic placement, antibody staining revealed specific expression of two ciliary-type opsins in the ciliary photoreceptor cells of the *B. floridae* frontal eye (Vopalensky *et al.*, 2012). Here, we report for the first time the opsin repertoire of *B. lanceolatum* (Pallas, 1774) and provide information on the expression patterns of opsin genes across multiple tissues and developmental stages.

Results

Identification, classification and genome organization of opsin genes in Branchiostoma lanceolatum

To identify the opsin gene repertoire in *B. lanceolatum* we used the available genome assembly provided by the *Branchiostoma lanceolatum* genome consortium. Applying BLAST searches and *de novo* gene prediction we were able to identify 22 opsin genes in *B. lanceolatum*, out of which *Bl_op17b* is a putative non-functional gene (pseudogene), since it bears a stop codon in the first exon. Predicted transcripts and encoded proteins for newly characterized opsins in *B. lanceolatum*, details on gene organization and genomic location are provided in Supplementary file 1. In general, all predicted opsins have seven transmembrane helices and a lysine in the seventh helix. We did not detect any intronless opsins in *B. lanceolatum*.

The large scale phylogenetic relations of opsins has been the object of many studies (Albalat, 2012; Liegertova *et al.*, 2015; Porter *et al.*, 2012; Ramirez *et al.*, 2016). We wanted to classify the *B. lanceolatum* opsins and investigate their distribution over the major opsin groups. We combined the available datasets from the most recent analyses and enriched them with the 21 newly

identified homologs from *B. lanceolatum*; Bl_Op17b was omitted, for being the product of a putative pseudogene. Two different alignments were used for our phylogenetic analyses, excluding (Fig. 1 and Supplementary Fig. S1) and including (Suppl. Fig. S2) the variable third cytoplasmic loop. In both datasets, the four traditional opsin groups, i.e. the C-type, the R-type, Group4 and the Cnidarian opsins, were recovered along with some other groups, albeit supported by low bootstrap values in many cases. Clustering of *B. lanceolatum* opsins is the same in both cases. Few differences were observed between the two datasets; two of the most striking are the relative positioning of R-type and Group4 opsins and the placement of the clade containing the *CiNut* homolog (Etani and Nishikata, 2002) (Fig. 1 and Supplementary Fig. S1 and Fig. S2). In Fig. 1, the major cnidarian group together with a small set of lophotrochozoan opsins (the Xenopsin according to Ramirez *et al.*, 2016) cluster as a sister group to C-type opsins. Group4 is closer to C-type and the Xenopsin group, than the R-type group. Chaopsin (Ramirez *et al.*, 2016), consisting of Echinopsin B (D'Aniello *et al.*, 2015) and a small clade of cnidarian opsins namely Group3 (Mason *et al.*, 2012), an anthozoan and a *Ciona*-specific clade are identified in our phylogenetic trees (Fig. 1 and Supplementary Fig. S1 and Fig. S2).

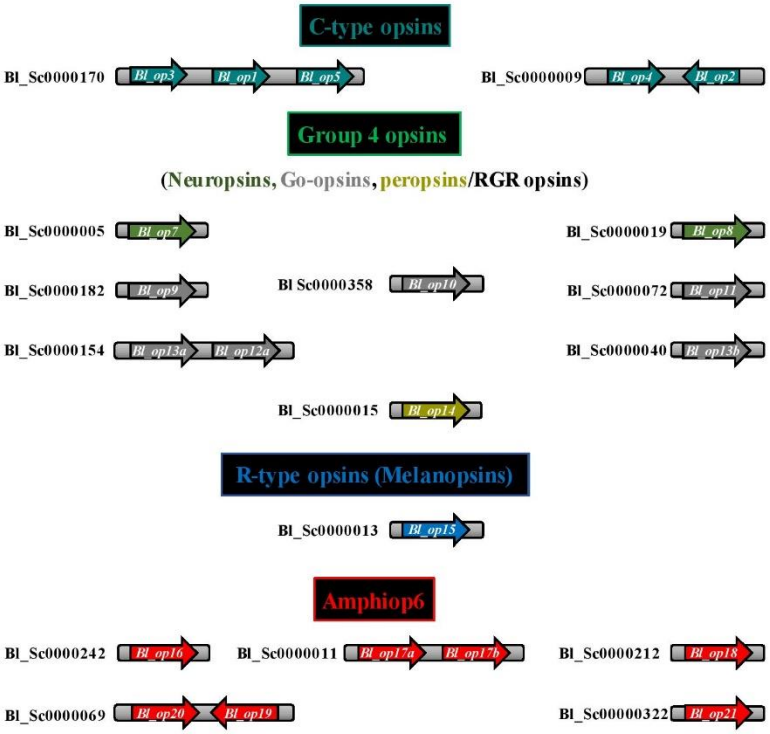

Fig. 2. Opsin containing genomic loci from *Branchiostoma lanceolatum*. *The genomic scaffolds from* Branchiostoma lanceolatum *(Bl) containing opsin genes. Groups are colored based on their phylogenetic position (see Fig. 1).*

Members from almost all opsin subfamilies have been identified for *B. lanceolatum* (Fig. 1 and Suppl. Fig. S1 and Fig. S2). Five belong to the C-type (Bl_Op1-5), two are in a clade sister to neuropsins (Bl_Op7 and Bl_Op8), six cluster with the Go opsins (Op9-Op13b), one with peropsins (Op14), one with melanopsins (Bl_Op15) and six within the Amphiop6 clade (Bl_Op16-Bl_Op21). Based on sequence similarity and genomic location, Bl_Op17b should be a member of the Amphiop6 group. No homologs of the vertebrate visual/non visual opsins have been detected. *B. lanceolatum* genes identified in this study, arranged in groups according to their phylogenetic placement, and their relation to previously identified homologs from two other *Branchiostoma* species are provided in Table 1. Next, we wanted to visualize how opsin genes are arranged in the genome of *B. lanceolatum* and whether there is some genetic linkage between opsin gene paralogs. The *B. lanceolatum* opsin-containing loci identified during our *in silico* analysis are depicted in Fig. 2. In particular, opsin genes are spread over 16 genomic regions (scaffolds) in *B. lanceolatum*, whereas in some cases, members of the same group are clustered in the same locus (scaffold), for example the Amphiop6 *Bl_op19* and *Bl_op20* (Fig. 2).

Table 2 summarizes the residues found in the three putative counterion positions, as well as the tripeptide associated with the binding to G-proteins (Arendt *et al.*, 2004; Marin *et al.*, 2000). Aspartic acid is present at position 83 of not only the melanopsin ortholog (Bl_Op15) but of most of the rest of the opsins. In almost all cases, position 113 is occupied by neutral or non-polar amino acids with the striking exception of Bl_Op11, Bl_Op19 and Bl_Op20, for which a negatively charged amino acid is present, similarly to vertebrate visual and non-visual opsins. In fact, Bl_Op11 bears aspartic acid in both positions 83 and 113, but no negatively charged amino acid residue at position 181. In the case of Bl_Op5, a negatively charged amino acid is encountered only at position 83. A really interesting case is that of Bl_Op21, in the sense that no negative amino acid is present at any of the three putative counterion positions. All of the C-type opsins, except for Bl_Op5, possess the N(N/S)Q tripeptide; the encountered motif in Bl_Op5 is EKE. Melanopsins nicely bear the R-type tripeptide HPK (Arendt *et al.*, 2004). This is not the case for Bl_Op16-Bl_Op22 (AmphiOp6); they may closely cluster with the R-type opsins but they only have the central proline, while the first position is occupied by a non-polar amino acid.

B. lanceolatum *opsin gene expression patterns*

Opsin genes are used by many animals not only for visual, but also for non-visual tasks. Their tissue specificity thus can significantly vary. Recent analyses of opsin gene expression in Cnidaria or Arthropoda documented a wide range of tissues where opsins can be detected (Liegertova *et al.*, 2015; Battelle *et al.*, 2016). Our study examined the expression pattern of opsins across multiple developmental stages (Fig. 3A and B), as well as in multiple tissue types of *B. lancelatum* adult body (Fig. 3C and D). To achieve this

we performed quantitative real-time PCR (qRT-PCR). We scanned opsin expression in developmental stages starting from late neurula (N3), where photoreceptive 1st Hesse cell is present, to adult, where frontal eye, rudiments of lamellar body, Joseph cells and series of dorsal ocelli along the neural tube are fully developed (Fig. 3A). All *B. lanceolatum* examined genes were detected at mRNA level, in at least one developmental stage (Fig. 3B and Supplementary Fig. S3A), with the sole exception of *Bl_op17b*. This is in accordance with the *in silico* prediction of this gene as a pseudogene due to a premature stop codon at the beginning of the coding region. The neuropsin *Bl_op7* and the Amphiop6 *Bl_op16* show their highest expression in N3 neurula stage; in fact *Bl_op7* is among the dominating opsins at this stage (Supplementary Fig. S3A). However, their expression is significantly reduced at later stages (Fig. 3B). Onset of several other opsin gene expression starts at L1 stage, in which frontal eye and lamellar body (ciliary photoreceptive organs) start to develop. The maximal expression of two Go opsins (*Bl_op9* and *Bl_op10*) and one Amphiop6 opsin (*Bl_op20*) was observed at this stage. We should point out that actin was used as a reference gene for normalization, a fact that could lead to a false underrepresentation of opsin genes in later developmental stages (L2/3 or adult), when compared to neurula stage, where lower total number of cells are present. Despite this fact, the majority of the opsins show most predominant expression in L2/3 stage, where most of the known amphioxus photoreceptor organs - the frontal eye, the lamellar body and the Hesse cell - are differentiated. As expected from the ciliary nature of photoreceptor cells in the frontal eye and the lamellar body, all C-type opsins reach a peak in their expression in L2/3. On the other hand, *B. lanceolatum* opsins belonging to Go coupled opsin group show broad expression across various stages. Most of the Amphiop6 opsins show elevated expression in L2/3 stage, which is true also for the single peropsin (*Bl_op14*). All of the 21 examined *B. lanceolatum* opsins could be detected in various adult tissues (Fig. 3C and D). All *B. lanceolatum* opsins but *Bl_op2*, exhibit some specificity for either the cerebral vesicle (10 opsins – *Bl_op1*, *Bl_op4*, *Bl_op5*, *Bl_op7*, *Bl_op9*, *Bl_op11*, *Bl_op12a*, *Bl_op13b*, *Bl_op17a*, *Bl_op20*) or the neural tube (7 opsins – *Bl_op3*, *Bl_op8*, *Bl_op13a*, *Bl_op14*, *Bl_op15*, *Bl_op18*, *Bl_op21*); on the contrary, *Bl_op5*, *Bl_op17a*, *Bl_op21* are expressed in both tissues (Fig. 3D and Supplement Fig. S3B). These findings show that most of the photoreceptive cells in amphioxus reside in the central nervous system, however, the cerebral vesicle and the neural tube probably exhibit a strong specialization for various photoreceptive tasks. Expression of one neuropsin (*Bl_op7*) was documented in female gonads, whereas a Go and an Amphiop6 (*Bl_op13a* and *Bl_op16*, respectively) showed noticeable expression in male gonads (Fig. 3D). Interestingly, one of the C-type opsins (*Bl_op2*) displays its highest level of expression in the most posterior part of the tail. Expression of four other opsins was significantly increased in tail. In contrast to analysis of opsin expression across various developmental stages (Fig. 3B), we were not able to observe any preference in tissue-specific usage of opsins belonging to different groups (Fig. 3D). The only exceptions were the peropsin (*Bl_op14*) and the melanopsin (*Bl_op15*), being highly expressed only in neural tube.

To investigate expression during larval development (prior to metamorphosis), we performed whole mount *in situ* hybridization. We analyzed expression of *Bl_op1, Bl_op2, Bl_op8, Bl_op10, Bl_op11, Bl_op12a, Bl_op14, Bl_op15, Bl_op17a, Bl_op19 and Bl_op20.* Of these, we have observed specific expression patterns only for *Bl_op11, Bl_op12* and *Bl_op15* (Fig. 4). *Bl_op11* is expressed in L1 stage in the area of developing preoral pit and 1st gill slit. In L2/3 the signal was detected in pharyngeal region and tail fin (Fig. 4 A,B). For *Bl_op12a* no specific signal was detected in L1 stage. In L2/3 stage the signal was detected in preoral pit, oral papilla, cells around mouth, 1st gill slit and tail fin (Fig. 4C, D). *In situ* hybridization of *Bl_op15* in L1 and L2/3 stage identified specific expression in 1st dorsal ocelli, in agreement with previous findings in *B. belcheri* (Koyanagi *et al.*, 2005).

In summary, our analysis confirms expression of all but one *B. lanceolatum* opsin genes and documents their stage and/or tissue specificity.

TABLE 2

AMINO ACIDS OBSERVED AT PUTATIVE COUNTERION POSITIONS AND THE TRIPEPTIDE AT THE FORTH CYTOPLASMIC LOOP FOR *B. LANCEOLATUM* OPSINS

		Counterion			Tripeptide		
		83	113	181			
C-type opsins	Op1	D	Y	E	N	S	Q
	Op2	D	Y	E	N	S	Q
	Op3	D	Y	E	N	N	Q
	Op4	G	Y	E	N	N	Q
	Op5	D	Y	V	E	K	E
Neuropsins	Op7	D	Y	E	N	N	R
	Op8	D	Y	E	N	D	S
Go opsins	Op9	D	Y	E	S	E	V
	Op10	D	Y	E	H	K	K
	Op11	D	D	Q	N	Q	R
	Op12a	D	Y	E	S	K	A
	Op13a	D	Y	E	N	S	K
	Op13b	D	F	E	N	S	K
Peropsins	Op14	D	Y	E	N	R	R
Melanopsins	Op15	D	Y	E	H	P	K
Amphiop6	Op16	G	F	D	L	P	V
	Op17a	D	F	D	L	P	A
	Op18	Q	A	D	L	P	A
	Op19	D	E	D	I	P	S
	Op20	D	E	D	I	P	S
	Op21	N	T	Q	M	P	D

Polar negative | Polar positive | Polar neutral

Non-Polar aromatic | Non-polar aliphatic | Special cases

Amino acids are colored based on their physicochemical properties

Discussion

We sought to characterize the opsin gene family in the genome assembly of the cephalochordate *Branchiostoma lanceolatum* and study the expression patterns of opsin genes from this species in different tissue types and across various developmental stages. We identified a total of 22 opsin genes in *B. lanceolatum*, one of which is a putative pseudogene. There is less than 20% amino acid similarity between vertebrate opsin subfamilies but more than 40% among members of a single family (Peirson *et al.*, 2009; Shichida

and Matsuyama, 2009; Terakita, 2005). Given these low similarity levels, *de novo* prediction of opsin genes could be largely hampered. Therefore, BLAST results should be carefully filtered and used in combination with synteny analyses since true positive results could be obscured by low similarity scores. In addition, manual curation of the genome assembly was needed in some cases.

Discrepancies between different phylogenetic studies have been noted before and could be attributed to the dataset used, the alignment method, the substitution model, and the tree constructing method applied. In our study, we show how sensitive the outcome of the phylogenetic analysis can be to the exclusion or inclusion of the highly variable third cytoplasmic loop (Fig. 1 and Supplementary Fig. S2, respectively). Among the observed differences, two of the most striking are the relative positioning of R-type and Group4 opsins and the placement of the Urochordate opsins clade containing the *CiNut* homolog (Etani and Nishikata, 2002), for which inconsistencies were previously observed (Albalat, 2012; Porter *et al.*, 2012; Ramirez *et al.*, 2016). A new clade – "bathyopsin" – was recently introduced (Ramirez *et al.*, 2016), consisting of one brachiopod and three echinoderm opsins. We excluded these sequences from our analysis either due to an incorrect number of transmembrane domains, based on TOPCONS and HMMTOP predictions (4 TM in the case of *Strongylocentrotus purpuratus* and 8 in the case of *Lingula anatina*) or because of their extremely small size (as in the case of *Eucidaris tribuloides*). It is obvious that there are still obstacles to reconstructing the complete evolutionary history of opsins. Sampling from specific taxonomic groups is still poor, mainly due to lack of data at the level of whole genome and missing functional data that could greatly facilitate the opsin classification. Collectively, our phylogenetic analysis ascribes *B.*

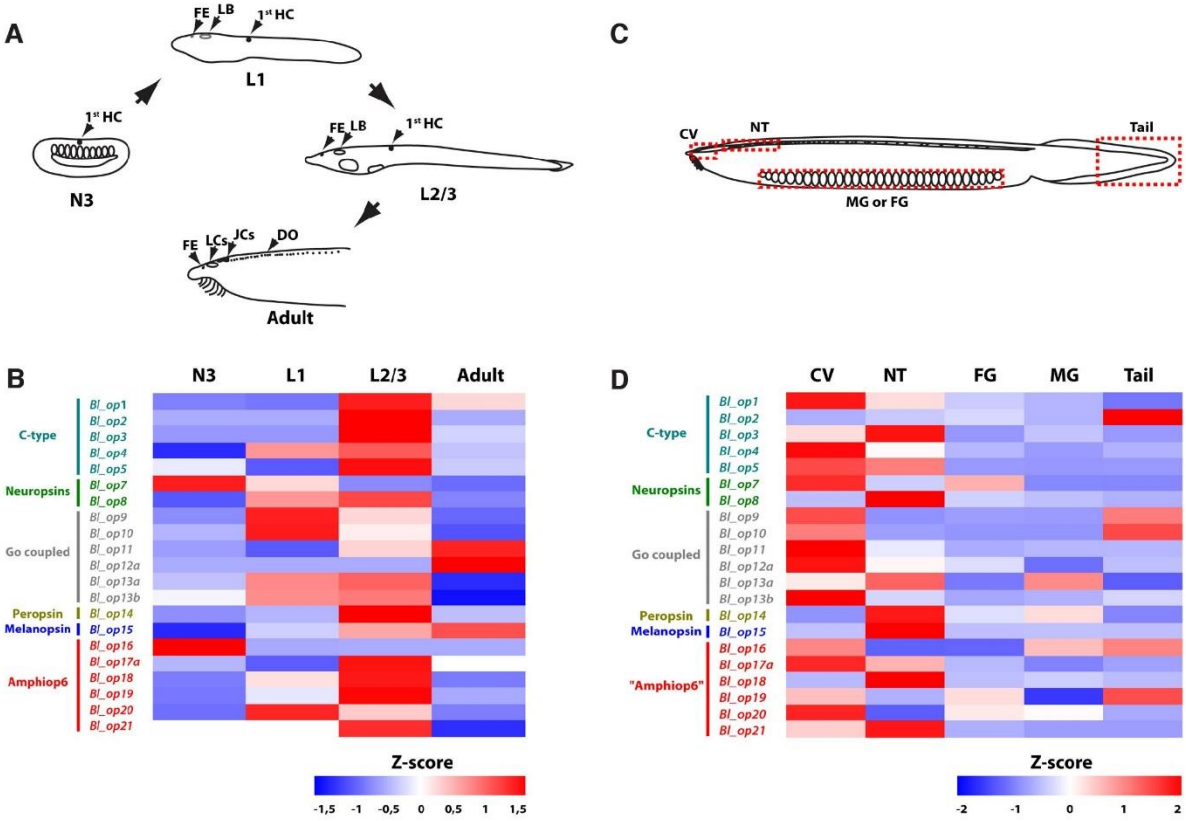

Fig. 3. mRNA expression levels of individual *B. lanceolatum* opsins across different developmental stages and various tissues of the adult body. (A) *Schematic drawing of developmental stages (N3, L1, L2/3, adult), in which detection of opsin genes expression was performed. Staging was determined according to Hirakow and Kajita (1994) (see Materials and Methods). 1st HC: 1st Hesse cell, FE: frontal eye, LB: lamellar body, DO: dorsal ocelli, JCs: Joseph cells, LCs: lamellate cells (rudiment of larval lamellar body).* **(B)** *Heat map displaying expression of opsin genes across different developmental stages. Each row represents particular opsin gene expression in various developmental stages.* **(C)** *Schematic drawing of amphioxus adult body parts in which detection of opsin genes expression was performed. CV: cerebral vesicle, NT: the most anterior third of neural tube including Joseph cells and dense clusters of dorsal ocelli, FG: female gonads, MG: male gonads, Tail: most posterior part of adult tail without dorsal ocelli.* **(D)** *Heat map displaying expression of opsin genes in various parts of* B. lanceolatum *adult body. Opsin expression was detected by qRT-PCR and normalized to expression of actin. Each row represents particular opsin gene expression in various parts of amphioxus adult body. Blue color represents expression below row average, white color represents average row expression, red color expression above row average.*

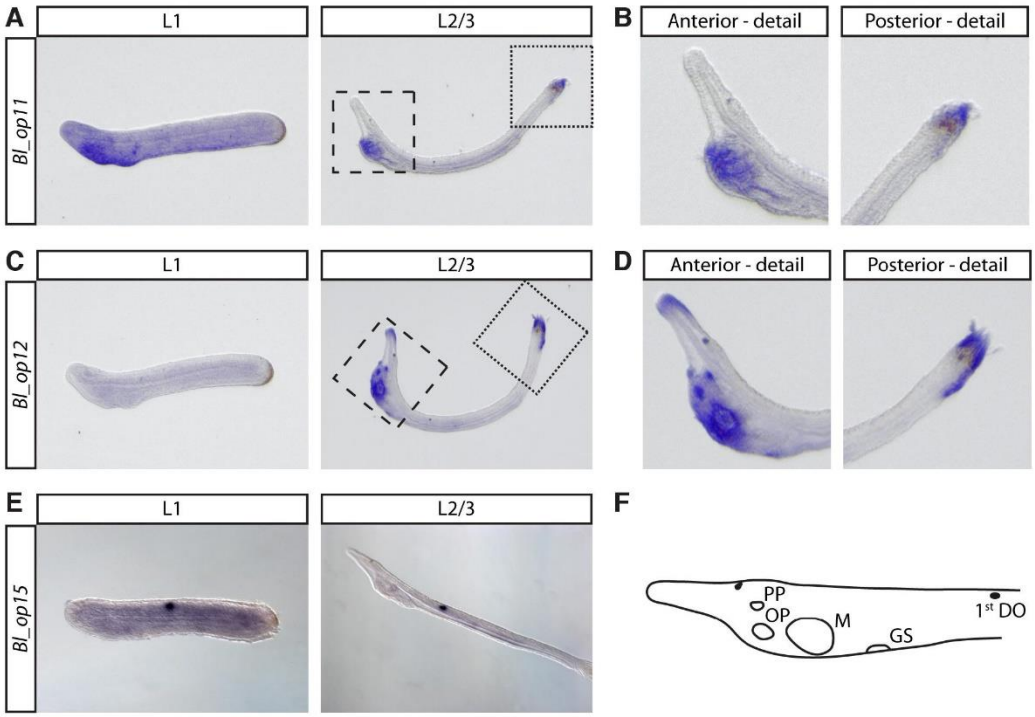

Fig. 4. *In situ* hybridization analysis of *B. lanceolatum Bl_op11, Bl_op12a* and *Bl_op15* in developing larvae (L1 and L2/3 stages). (A) *Expression of* Bl_op11. *In stage L1 the signal was detected in the area of developing preoral pit and 1st gill slit. In L2/3 the signal was detected in pharyngeal region and tail fin.* **(B)** *Detail of anterior and posterior region of the larvae (dashed and dotted framed regions in (A)).* **(C)** *Expression of* Bl_op12a. *In L1 stage no specific signal was detected. In L2/3 the signal was detected in preoral pit, oral papilla, cells around mouth, 1st gill slit and tail fin.* **(D)** *Detail of anterior and posterior region of the larvae (dashed and dotted framed regions shown in (C)).* **(E)** *Expression of* Bl_op15. *Specific signal was detected in 1st dorsal ocelli.* **(F)** *Scheme of anterior part of L2/3 larvae with marked landmarks. PP, preoral pit; OP, oral papilla; M, mouth; GS, gill slit; 1st DO, first dorsal ocelli.*

lanceolatum opsins in the three of the four traditionally recognized opsin lineages, in particular C-type, R-type and Group4 (neuropsins, RGRs and peropsins), with no differences between the two sequence datasets used in this study. The number of genes in each subfamily, including a putative pseudogene, varies from one (melanopsins and peropsins) to a maximum of seven (Amphiop6). The expansion of three opsin subfamilies in the cephalochordate lineage (Amphiop6, C-type and Go-opsins) was previously (Holland *et al.*, 2008) correlated to the diversity of photoreceptor organs in amphioxus, including both ciliary and rhabdomeric photoreceptors (Lacalli, 2004). The large size of the Go group suggests extensive redundancy and/or could be an indication of possible fine tuning of molecular properties among these opsins in order to achieve distinct photoreceptive properties.

In general, *B. lanceolatum* Go opsins exhibit a preferential expression in either the cerebral vesicle or the neural tube (parts of the Central Nervous System - CNS), with two interesting exceptions: *Bl_op13a* in male gonads and *Bl_op9-op10* in tail. A CNS-specific pattern is observed for the C-type opsins as well, with *Bl_op2*, however, being expressed almost solely in the tail. Similar is the expression in the horseshoe crab *Limulus polyphemus*, where various opsins have been detected in the tail (Battelle *et al.*, 2016), proposed to be a circadian photoreceptor organ. Photoreceptors located in the tail mediate light avoidance in larval lampreys (Binder and McDonald, 2008). Light sensitivity in the tail of amphioxus has been reported as early as 1908 (Parker, 1908), yet no study so far has documented any photoreceptor cells there. In regard to opsin expression in gonads, it has also been observed in the gonads of the cnidarian species *Cladonema radiatum* (Suga *et al.*, 2008) and *Tripedalia cystophora* (Liegertova *et al.*, 2015), and the oyster *Crassostrea gigas* (Porath-Krause *et al.*, 2016). The role in opsin-mediated light-controlled release of gametes was proposed (Liegertova *et al.*, 2015; Suga *et al.*, 2008). In agreement with data regarding the *B. belcheri* melanopsin (Koyanagi *et al.*, 2005), an orthologous *Bl_op15* is expressed in the neural tube where rhabdomeric dorsal ocelli are located. Nevertheless, it is not the unique opsin expressed in this tissue. The *B. lanceolatum* peropsin (*Bl_op14*), two C-type opsins, namely *Bl_op3* (ortholog of *B. belcheri Amphi*op4) and *Bl_op5* (not previously analyzed in *B. belcheri*), neuropsin (*Bl_op8*) and two Amphiop6 opsins (*Bl_op18* and *Bl_op21*) were all found to be expressed in the neural tube of adult *B. lanceolatum*.

Examination of amino acid residues at key positions (namely, the counterion and the tripeptide on the fourth cytoplasmic loop) may provide insight into molecular function of individual opsins. Nevertheless, there are instances of a non-typical pattern in re-

gard to these positions (Plachetzki *et al.*, 2007). The presence of negative residues at position 113, typical for vertebrate opsins, is also evident in three *Branchiostoma* (this study) as well as in four *Tripedalia* (Liegertova *et al.*, 2015) opsins. Among them is Bl_Op11, which further lacks a negative residue at position 181, thus raising questions about its role and expression domain. This opsin could also provide some insight in regard to the timepoint that counterion replacement occurred during the molecular evolution of vertebrate opsins (Terakita *et al.*, 2004). Slightly differentiated from the rest of C-type opsins is Bl_Op5, for which the sole negatively charged residue is located at position 83. Another thing that should be highlighted is the absence of a negatively charged residue in any of the three putative counterion positions of the Amphiop6 Bl_Op21. The type of signaling cascade activated by various opsins is summarized by Porter *et al.*, 2012 and an *in silico* attempt has been made to correlate the motif present in the N-terminal of the fourth cytoplasmic loop (a.k.a. the tripeptide) with the target G-proteins. As shown before, the NKQ motif of the rhodopsin holds an important role in the activation of the G-protein transducin (Marin *et al.*, 2000). In regard to this position, some of our results are rather conventional, but some should attract more attention in the future. For example, Bl_Op5 again stands out from the rest of the C-type opsins, since it contains the rather unique EKE motif. Amphiop6 genes possess only the central proline of the R-opsin HPK fingerprint, therefore their ability to couple to any downstream phototransduction cascades remains an open question. Apart from the conserved proline, there is no clear pattern for the tripeptide in Amphiop6 subgroup, except for the fact that a non-polar aliphatic residue occupies the first position. This group clusters closely with Gq opsins, however its members also differ in regard to motifs characteristic of Gq opsins, necessary for structural integrity maintenance and binding to the chromophore (Porath-Krause *et al.*, 2016).

In summary, our genome-wide analysis identifies the complement of opsin genes in *B. lanceolatum*, confirms expression of all but one genes and documents their stage and/or tissue specificity. Studies of opsin diversity can offer clues to how separate lineages of animals have repurposed different opsin paralogs for different light-detecting functions. To gain a deeper insight into the function of amphioxus photoreceptive organs, more detailed expression analysis of individual opsins (e.g. by *in situ* hybridization or immunohistochemistry staining) in conjunction with light-mediated behavioral tests of animals is of key importance. In addition, studies aimed to dissect the biochemical properties of individual amphioxus opsins and the nature of the downstream phototransduction cascade are highly warranted. Such further studies may provide evidence for fine tuning of molecular properties within the pool of available opsins that were necessary to adapt visually guided behavior of amphioxus to changing habitats.

Materials and Methods

Genome assembly and de novo *gene prediction*

B. lanceolatum opsin genomic loci were detected through tBLASTn searches against the European amphioxus (v. Bl71nemh 20/11/13) Assembly (BraLan2). The previously characterized (Holland *et al.*, 2008; Koyanagi *et al.*, 2005; Koyanagi *et al.*, 2002) *Branchiostoma* opsin homologs were used as queries. Additional BLAST searches were performed using various visual and non-visual homologs from vertebrate and protostome species. *De novo* prediction of *B. lanceolatum* opsin genes was accomplished combining results from Genscan (Burge and Karlin, 1997) and exon-intron borders predictions by SpliceView (Rogozin and Milanesi, 1997). In the case of discrepancies between database gene models and our *in silico* analysis, PCR amplification of the "suspicious" regions was performed, followed by cloning and sequencing (see paragraph "Cloning and Sequencing of Opsin Gene Fragments/Transcripts").

Prediction of membrane protein topology and functional domains

Newly identified *B. lanceolatum* opsin homologs were run in ScanProsite (de Castro *et al.*, 2006), in order to identify protein family domains/motifs, more specifically "the G Protein Coupled Receptor (GPCR) signature/profile" and the "Visual pigments (opsins) retinal binding site". In addition, TOPCONS (Tsirigos *et al.*, 2015) and CCTOP (Dobson *et al.*, 2015) were used to detect the protein topology in general and the exact position of the seven transmembrane (TM) helices, characteristic of the GPCRs in particular. In order for the proteins to be considered reliable opsin homologs they had to meet the following three criteria: 1) exhibit similarity to known opsins, 2) bear seven TM domains and 3) possess a lysine residue at the seventh TM domain.

Sequence collection, alignments and phylogenetic analysis

Given the fact that the datasets used in the most recent large scale analyses (D'Aniello *et al.*, 2015; Liegertova *et al.*, 2015; Porter *et al.*, 2012; Ramirez *et al.*, 2016) had included significant number of opsins representative of a large number of taxonomic groups, we first tried to combine the available datasets from them. Sequences of poor quality (large gaps, missing the K296, not bearing all seven TM domains) were omitted, predicted *de novo* or replaced by orthologs from relative species. We then enriched this dataset with the 21 newly identified homologs from *B. lanceolatum*.

Multiple sequence alignments were produced with the Clustal algorithm, incorporated in MEGA v7 (Kumar *et al.*, 2016), and PROMALS3D (Pei *et al.*, 2008). The latter constructs alignments for multiple protein sequences and/or structures using information from sequence database searches, secondary structure prediction, available homologs with 3D structures and user-defined constraints (Pei *et al.*, 2008), therefore, it should be more reliable in the case of such a diverse group as opsins. Ambiguously aligned regions of the sequences, i.e. parts of the N-terminal and C-terminal ends were trimmed off in the MEGA7 alignment editor, leaving only the TM domains and the connecting extra-cellular and cytoplasmic loops. TOPCONS and CCTOP predictions were taken into consideration during the trimming process. We then created another subset in which the third cytoplasmic loop was removed from the alignment; the size of this loop is rather conserved within members of the same subfamily but it is highly variable between different families; it can fluctuate from 18aa in vertebrate RGRs, to 20aa in molluscan retinochromes, 30aa in human short-wave opsins and up to 73aa in echinopsins B. High degree of sequence dissimilarity is also observed, which renders alignment rather problematic.

Maximum Likelihood (ML) trees were constructed for both datasets. LG, gamma distributed (Le and Gascuel, 2008) was indicated as the best substitution model by the "Find Best DNA/Protein Models" tool incorporated in MEGA7 (Kumar *et al.*, 2016). ML trees were built in MEGA7 and tree topologies were evaluated with the bootstrap test (100 pseudoreplicates). *B. lanceolatum* sequences are included in Supplementary file 1, accession numbers (ACs) for the rest of the protein sequences (or genomic scaffold in case of newly predicted sequences) used in the phylogenetic analysis are included in Supplementary Fig. 1. All trees were rooted with the 22 human non-opsin GPCRs used in previous studies as well (Liegertova *et al.*, 2015).

Animal collection

B. lanceolatum adult animals were collected in Argeles-sur-Mer (France) and preserved in the lab in a day/night cycle of 14h/10h until spawning, which was induced by a shift in temperature (Fuentes *et al.*, 2007). Staging of all collected embryos was performed according to Hirakow and Kajita (1994). Specimens from late neurula (N3), larvae (L1-L2/3) and adult stage were collected and frozen in RNAlater® Stabilization Solution (ThermoFisher

Scientific), under light conditions. In N3, 1st Hesse cell is present, in L1 the developing frontal eye and lamellar body are present, in L2/3 the 1st gill slit and the mouth are open, frontal eye and lamellar body have differentiated. In adult, frontal eye, rudiments of lamellar body, Joseph cells and series of dorsal ocelli are present.

B. lanceolatum adults were anesthetized with Tricaine methane sulfonate and dissected in order to obtain the required tissue types, specifically the cerebral vesicle, the most anterior third of neural tube including Joseph cells and dense clusters of dorsal ocelli, the female and the male gonads and finally the most posterior part of tail without dorsal ocelli. Tissues were stored in RNAlater® Stabilization Solution (ThermoFisher Scientific) and frozen.

RNA isolation / cDNA preparation

Total RNA was isolated from *B. lanceolatum* embryos or adult tissues stored in RNAlater® Stabilization Solution using the Trizol reagent (Ambion). To avoid genomic DNA contamination, isolated RNA was treated with DNaseI and purified on RNeasy Mini Kit (Qiagen) column. Random-primed cDNA was prepared from 250ng or 150 ng of RNA (for analysis of the different developmental stages or adult tissue types, respectively) in a 20 μl reaction using SuperScript VILO cDNA Synthesis kit (Invitrogen).

Cloning and sequencing of opsin gene fragments/transcripts

For validation of the *in silico* predicted gene models, cloning of opsin gene fragments and complete transcripts from *B. lanceolatum* was performed. Primers were designed in Primer3 software (Supplementary Table 1). PCR was performed on cDNA from neurula N3, larvae L2/3 or adult stages, using DreamTaq polymerase (ThermoFisher Scientific) according to the manufacturer´s protocol. Amplified fragments were blunted and cloned into pCR™-Blunt II-TOPO® (ThermoFisher Scientific). Plasmid DNA was isolated using GeneJET Plasmid Miniprep Kit (ThemoFisher Scientific). Sequencing was performed by the standard Sanger sequencing procedure (GATC Biotech).

qRT-PCR

Primers were designed in Primer3 software (Supplementary Table 1). The qRT-PCR was performed in the LightCycler 2.0 System using the LightCycler® 480 DNA SYBR Green I Master kit (Roche Diagnostics, Germany), according to the manufacturer's standard protocol. For each cDNA sample, both target and housekeeping genes were measured under the same conditions. Results were analyzed using the LightCycler software. Crossing point values (Cp) were determined as an average of triplicates for each gene and normalized by Cp values of the housekeeping gene (actin). Results were analyzed in R software and plotted in the form of a Z-score heat map.

Whole-mount* in situ *hybridization in amphioxus embryos

Whole-mount *in situ* hybridization with digoxigenin-labeled RNA probes was done as previously described (Kozmikova *et al.*, 2013). For better interpretation of the signal, *in situ* hybridization with Vector Blue substrate was performed in some cases, followed by subsequent confocal microscopic analysis. Primers used to generate probes are summarized in Supplementary Table 1.

Acknowledgments

This work was funded by the Czech Science Foundation (GACR, 17-15374S); Ministry of Education, Youth and Sports (LO1220 CZ-OPENSCREEN, LQ1604 NPU II, BIOCEV-CZ.1.05/1.1.00/02.0109) and the Institute of Molecular Genetics institutional support (RVO 6878050). This work was supported by the Branchiostoma lanceolatum *genome consortium that provided access to the* B. lanceolatum *genome sequence.*

References

ALBALAT R (2012). Evolution of the genetic machinery of the visual cycle: a novelty of the vertebrate eye? *Mol Biol Evol* 29: 1461-1469.

ARENDT D, TESSMAR-RAIBLE K, SNYMAN H, DORRESTEIJN A W, WITTBRODT J (2004). Ciliary photoreceptors with a vertebrate-type opsin in an invertebrate brain. *Science* 306: 869-871.

BATTELLE B A, RYAN J F, KEMPLER K E, SARAF S R, MARTEN C E, WARREN W C, MINX P J, MONTAGUE M J, GREEN P J, SCHMIDT S A *et al.*, (2016). Opsin repertoire and expression patterns in horseshoe crabs: evidence from the genome of *Limulus polyphemus* (Arthropoda: Chelicerata). *Genome Biol Evol* 8: 1571-1589.

BINDER T R, MCDONALD D G (2008). The role of dermal photoreceptors during the sea lamprey (*Petromyzon marinus*) spawning migration. *J Comp Physiol A Neuroethol Sens Neural Behav Physiol* 194: 921-928.

BOWNDS D (1967). Site of attachment of retinal in rhodopsin. *Nature* 216: 1178-1181.

BURGE C, KARLIN S (1997). Prediction of complete gene structures in human genomic DNA. *J Mol Biol* 268: 78-94.

D'ANIELLO S, DELROISSE J, VALERO-GRACIA A, LOWE E K, BYRNE M, CANNON J T, HALANYCH K M, ELPHICK M R, MALLEFET J, KAUL-STREHLOW S *et al.*, (2015). Opsin evolution in the Ambulacraria. *Mar Genomics* 24, Part 2: 177-183.

DE CASTRO E, SIGRIST C J A, GATTIKER A, BULLIARD V, LANGENDIJK-GENEVAUX P S, GASTEIGER E, BAIROCH A, HULO N (2006). ScanProsite: detection of PROSITE signature matches and ProRule-associated functional and structural residues in proteins. *Nucleic Acids Res* 34: W362-W365.

DOBSON L, REMENYI I, TUSNADY G E (2015). CCTOP: a Consensus Constrained TOPology prediction web server. *Nucleic Acids Res* 43: W408-412.

ETANI K, NISHIKATA T (2002). Novel G-protein-coupled receptor gene expressed specifically in the entire neural tube of the ascidian *Ciona intestinalis*. *Dev Genes Evol* 212: 447-451.

FEUDA R, HAMILTON S C, MCINERNEY J O, PISANI D (2012). Metazoan opsin evolution reveals a simple route to animal vision. *Proc Natl Acad Sci USA* 109: 18868-18872.

FUENTES M, BENITO E, BERTRAND S, PARIS M, MIGNARDOT A, GODOY L, JIMENEZ-DELGADO S, OLIVERI D, CANDIANI S, HIRSINGER E *et al.*, (2007). Insights into spawning behavior and development of the European amphioxus (*Branchiostoma lanceolatum*). *J Exp Zool B Mol Dev Evol* 308: 484-493.

GONG J, YUAN Y, WARD A, KANG L, ZHANG B, WU Z, PENG J, FENG Z, LIU J, XU X Z (2016). The *C. elegans* Taste Receptor Homolog LITE-1 Is a Photoreceptor. *Cell* 167: 1252-1263 e1210.

HIRAKOW R, KAJITA N (1994). Electron microscopic study of the development of amphioxus, *Branchiostoma belcheri tsingtauense*: the neurula and larva. *Kaibogaku Zasshi* 69: 1-13.

HOLLAND L Z, ALBALAT R, AZUMI K, BENITO-GUTIERREZ E, BLOW M J, BRONNER-FRASER M, BRUNET F, BUTTS T, CANDIANI S, DISHAW L J *et al.*, (2008). The amphioxus genome illuminates vertebrate origins and cephalochordate biology. *Genome Res* 18: 1100-1111.

KOYANAGI M, KUBOKAWA K, TSUKAMOTO H, SHICHIDA Y, TERAKITA A (2005). Cephalochordate melanopsin: evolutionary linkage between invertebrate visual cells and vertebrate photosensitive retinal ganglion cells. *Curr Biol* 15: 1065-1069.

KOYANAGI M, TAKANO K, TSUKAMOTO H, OHTSU K, TOKUNAGA F, TERAKITA A (2008). Jellyfish vision starts with cAMP signaling mediated by opsin-G(s) cascade. *Proc Natl Acad Sci USA* 105: 15576-15580.

KOYANAGI M, TERAKITA A, KUBOKAWA K, SHICHIDA Y (2002). Amphioxus homologs of Go-coupled rhodopsin and peropsin having 11-*cis*- and all-*trans*-retinals as their chromophores. *FEBS Lett* 531: 525-528.

KOZMIK Z, RUZICKOVA J, JONASOVA K, MATSUMOTO Y, VOPALENSKY P, KOZMIKOVA I, STRNAD H, KAWAMURA S, PIATIGORSKY J, PACES V *et al.*, (2008). Assembly of the cnidarian camera-type eye from vertebrate-like components. *Proc Natl Acad Sci USA* 105: 8989-8993.

KOZMIKOVA I, CANDIANI S, FABIAN P, GURSKA D, KOZMIK Z (2013). Essential role of Bmp signaling and its positive feedback loop in the early cell fate evolution of chordates. *Dev Biol* 382: 538-554.

KUMAR S, STECHER G, TAMURA K (2016). MEGA7: Molecular Evolutionary Genetics Analysis Version 7.0 for Bigger Datasets. *Mol Biol Evol* 33: 1870-1874.

LACALLI T C (2004). Sensory systems in amphioxus: a window on the ancestral chordate condition. *Brain Behav Evol* 64: 148-162.

LAMB T D, COLLIN S P, PUGH E N, JR. (2007). Evolution of the vertebrate eye: opsins, photoreceptors, retina and eye cup. *Nat Rev Neurosci* 8: 960-976.

LE S Q, GASCUEL O (2008). An improved general amino acid replacement matrix.

Mol Biol Evol 25: 1307-1320.

LIEGERTOVA M, PERGNER J, KOZMIKOVA I, FABIAN P, POMBINHO A R, STRNAD H, PACES J, VLCEK C, BARTUNEK P, KOZMIK Z (2015). Cubozoan genome illuminates functional diversification of opsins and photoreceptor evolution. *Sci Rep* 5: 11885.

MARIN E P, KRISHNA A G, ZVYAGA T A, ISELE J, SIEBERT F, SAKMAR T P (2000). The amino terminus of the fourth cytoplasmic loop of rhodopsin modulates rhodopsin-transducin interaction. *J Biol Chem* 275: 1930-1936.

MASON B, SCHMALE M, GIBBS P, MILLER M W, WANG Q, LEVAY K, SHESTOPALOV V, SLEPAK V Z (2012). Evidence for Multiple Phototransduction Pathways in a Reef-Building Coral. *PLoS One* 7: e50371.

PARKER G H (1908). The sensory reactions of amphioxus. *Proc Am Acad Arts Sci* 43: 415-455.

PEI J, KIM B H, GRISHIN N V (2008). PROMALS3D: a tool for multiple protein sequence and structure alignments. *Nucleic Acids Res* 36: 2295-2300.

PEIRSON S N, HALFORD S, FOSTER R G (2009). The evolution of irradiance detection: melanopsin and the non-visual opsins. *Phil Trans R Soc B* 364: 2849-2865.

PLACHETZKI D C, DEGNAN B M, OAKLEY T H (2007). The origins of novel protein interactions during animal opsin evolution. *PLoS One* 2: e1054.

PORATH-KRAUSE A J, PAIRETT A N, FAGGIONATO D, BIRLA B S, SANKAR K, SERB J M (2016). Structural differences and differential expression among rhabdomeric opsins reveal functional change after gene duplication in the bay scallop, *Argopecten irradians* (Pectinidae). *BMC Evol Biol* 16: 250.

PORTER M L, BLASIC J R, BOK M J, CAMERON E G, PRINGLE T, CRONIN T W, ROBINSON P R (2012). Shedding new light on opsin evolution. *Proc Biol Sci* 279: 3-14.

POSS S G, BOSCHUNG H T (1996). Lancelets (Cephalochordata: Branchiostomatidae): How many species are valid? *Isr J Zool* 42: S13-S66.

RAMIREZ M D, PAIRETT A N, PANKEY M S, SERB J M, SPEISER D I, SWAFFORD A J, OAKLEY T H (2016). The last common ancestor of most bilaterian animals possessed at least 9 opsins. *Genome Biol Evol* 8: 3640-3652.

RIVERA A S, OZTURK N, FAHEY B, PLACHETZKI D C, DEGNAN B M, SANCAR A, OAKLEY T H (2012). Blue-light-receptive cryptochrome is expressed in a sponge eye lacking neurons and opsin. *J Exp Biol* 215: 1278-1286.

ROGOZIN I B, MILANESI L (1997). Analysis of donor splice sites in different eukaryotic organisms. *J Mol Evol* 45: 50-59.

SHICHIDA Y, MATSUYAMA T (2009). Evolution of opsins and phototransduction. *Phil Trans R Soc B* 364: 2881-2895.

SUGA H, SCHMID V, GEHRING W J (2008). Evolution and functional diversity of jellyfish opsins. *Curr Biol* 18: 51-55.

TERAKITA A (2005). The opsins. *Genome Biol* 6: 213.

TERAKITA A, KOYANAGI M, TSUKAMOTO H, YAMASHITA T, MIYATA T, SHICHIDA Y (2004). Counterion displacement in the molecular evolution of the rhodopsin family. *Nat Struct Mol Biol* 11: 284-289.

TSIRIGOS K D, PETERS C, SHU N, KALL L, ELOFSSON A (2015). The TOPCONS web server for consensus prediction of membrane protein topology and signal peptides. *Nucleic Acids Res* 43: W401-W407.

VOPALENSKY P, PERGNER J, LIEGERTOVA M, BENITO-GUTIERREZ E, ARENDT D, KOZMIK Z (2012). Molecular analysis of the amphioxus frontal eye unravels the evolutionary origin of the retina and pigment cells of the vertebrate eye. *Proc Natl Acad Sci USA* 109: 15383-15388.

WANG J K, MCDOWELL J H, HARGRAVE P A (1980). Site of attachment of 11-cis-retinal in bovine rhodopsin. *Biochemistry* 19: 5111-5117.

YARFITZ S, HURLEY J B (1994). Transduction mechanisms of vertebrate and invertebrate photoreceptors. *J Biol Chem* 269: 14329-14332.

6.4 Novel polyclonal antibodies as a useful tool for expression studies in amphioxus embryos.

Classical evo-devo studies are based on the comparison of expression of important developmental genes between various organisms. Since non-traditional model species are often used, the expression is compared mostly by ISH. In some cases, it is, nevertheless, worthy to get also information about protein expression. Use of commercially available antibodies for staining of non-vertebrate species, however, faces several problems. The antibodies are either too specific for vertebrates´ antigens or they are raised against highly conserved protein domains resulting in the simultaneous staining of more members of a given protein family. Studies of amphioxus relied so far only on the use of antibody raised against acetylated tubulin[31,59] or polyclonal antibodies raised against neurotransmitters[59,105].

In our paper, we presented a simple protocol for obtaining polyclonal antibodies raised against amphioxus proteins. The amount of obtained sera was about 200 – 500 µl, which was enough for performing hundreds of immunofluorescent staining. In this study, we show results obtained with antibodies raised against five amphioxus proteins, namely FoxA, Lhx1, Lhx3, β-catenin and Pax4/6. We compared our immunofluorescent staining with data from literature and showed that all antibodies recapitulate previously published expression patterns obtained by ISH. We also documented the reproducibility of signal yield by immunofluorescent staining on batches of differently fixed embryos. We used our antibodies to demonstrate the advantages of whole mount immunofluorescent staining and confocal microscopy on the example of mapping various neuronal populations in amphioxus frontal eye and cerebral vesicle on single cell resolution. We also included data showing cross-species reactivity of our antibodies within cephalochordate subphylum, documented by use for staining of *B. lanceolatum*, *B. floridae* and *A. lucayanum* embryos.

We expect that our pilot study will encourage other evo-devo labs to produce antibodies usable for immunofluorescent staining in other non-model organisms. We feel that with the rapid burst of microscopical techniques available now, it is necessary to concentrate not only on the big picture obtained by ISH but also on obtaining more information on single cell resolution. Additionally, we expect that our antibodies might enable further FACS sorting of specific cell populations or might be used for chromatin immunoprecipitation (ChIP) experiments.

My contribution to this work: I performed immunofluorescent staining documenting the advantages of our antibodies for studying neuronal populations in amphioxus CNS (presented in Fig.2 and Fig.4). I performed immunofluorescent staining documenting species cross-reactivity of our “home-made” antibodies (Fig.5). I contributed to writing of some parts of methods, results and discussion sections of the manuscript.

Int. J. Dev. Biol. 61: 793-800 (2017)
doi: 10.1387/ijdb.170259ik

THE INTERNATIONAL JOURNAL OF DEVELOPMENTAL BIOLOGY
www.intjdevbiol.com

Novel polyclonal antibodies as a useful tool for expression studies in amphioxus embryos

MATTEO BOZZO#, JIRI PERGNER#, ZBYNEK KOZMIK and IRYNA KOZMIKOVA*

Laboratory of Transcriptional Regulation, Institute of Molecular Genetics of the Czech Academy of Sciences, Prague, Czech Republic,

ABSTRACT Cephalochordates, commonly called amphioxus or lancelets, are widely regarded as a useful proxy for the chordate ancestor. In recent decades, expression patterns of important developmental genes have been used extensively to infer homologies between cephalochordate and vertebrate embryos. Such comparisons provided important insight into cephalochordate biology and the origin of vertebrate traits. Most of the developmental expression data are collected using whole-mount *in situ* hybridization that allows the distributions of specific transcripts to be detected in fixed embryos. Here, we describe an experimental pipeline for production of small amounts of functional antibodies directed against amphioxus antigens for use in immunohistochemical labelling. In this pilot study, we generated antibodies against β-catenin and the transcription factors FoxA, Lhx1, Lhx3 and Pax6. We demonstrate the usefulness of antibodies by performing immunostainings on fixed specimens of *B. lanceolatum* and *B. floridae*. We anticipate that amphioxus-specific antibodies will provide a useful tool for high-resolution labelling of individual cells within the embryo and for determining the subcellular localization of the corresponding proteins.

KEY WORDS: *Branchiostoma, amphioxus, antibody, expression pattern*

Cephalochordates, commonly called amphioxus or lancelets, are regarded as a key animal group for understanding the origin of vertebrates, and a useful proxy to the ancestral chordate condition. This position has recently been affirmed especially thanks to the access to genome sequence data (Holland *et al.*, 2008; Huang *et al.*, 2014; Putnam *et al.*, 2008), introduction of novel techniques (Acemel *et al.*, 2016; Kozmikova and Kozmik, 2015; Li *et al.*, 2017; Yue *et al.*, 2016), and establishment of amphioxus as a model species for evolutionary developmental studies (for review see Bertrand and Escriva (2011)). Cephalochordates include three genera, namely *Branchiostoma*, *Asymmetron* and *Epigonychtys*. The phylogenetic relationships within the extant amphioxus lineage were recently investigated providing divergence time estimates and suggesting a rather recent diversification (Igawa *et al.*, 2017). For example, the estimated divergence times among species within the *Branchiostoma* genus (22.6 +/- 2.3 Mya for *B.lanceolatum* - *B. floridae* split) are comparable to those among rodents belonging to Muridae family (such as mouse and rat). Close phylogenetic relationship is mirrored by a high degree of coding sequence identity (Holland *et al.*, 2008; Huang *et al.*, 2014; Putnam *et al.*, 2008; Yue *et al.*, 2014) and by evidence for stasis in developmental expression patterns (Somorjai *et al.*, 2008).

Expression patterns of important developmental genes have been used extensively to infer homologies between cephalochordate and vertebrate embryos. Such comparisons provided important insight into cephalochordate biology and the origin of vertebrate traits. Most of the expression data were collected using whole mount *in situ* hybridization (WMISH) that allows the distributions of specific transcripts to be detected in fixed embryos. A plausible alternative for analysis of gene expression is based on protein detection by immunohistochemical staining in sections or whole mount preparations. In principle, immunostaining is easy to perform, provided that there are antibodies which specifically recognize the antigen of interest. Unfortunately, the current antibody repertoire for non-model invertebrates such as amphioxus is

Abbreviations used in this paper: TH, tyrosine hydroxylase; WMISH, whole mount in situ hybridization.

***Address correspondence to:** Iryna Kozmikova. Institute of Molecular Genetics of the Czech Academy of Sciences, v.v.i., Videnska 1083, 14220, Czech Republic. Tel: +420 241062110. E-mail: kozmikova@img.cas.cz #Note: The indicated authors contributed equally to this work.

Supplementary Material (2 figures + 1 table) for this paper is available at: http://dx.doi.org/10.1387/ijdb.170259i

Submitted: 11 October, 2017; *Accepted:* 25 October, 2017.

ISSN: Online 1696-3547, Print 0214-6282

rather limited. Both monoclonal and polyclonal antibodies can be made against a protein of interest. Polyclonal antibodies have the advantage of typically being of higher affinity, whereas the monoclonal antibodies have higher specificity since they recognize a single epitope. A clear disadvantage of polyclonal antibodies is the fact that they are a non-renewable resource. On the other hand, monoclonal antibodies are costly and are not within the reach of a typical lab working in the area of evolutionary developmental biology. Commercially available antibodies produced for vertebrate research can in principle be used if directed against a highly conserved epitope shared by vertebrate and amphioxus protein. Currently, only antibodies against acetylated tubulin are routinely used (Le Petillon *et al.*, 2017; Lu *et al.*, 2012; Soukup *et al.*, 2015; Vopalensky *et al.*, 2012). A fairly small number of antibodies (all polyclonal) has so far been generated that specifically recognize amphioxus proteins in developing embryos (Vopalensky *et al.*, 2012; Wu *et al.*, 2011).

Here, we describe an experimental pipeline established for the production of small amounts of functional antibodies directed against amphioxus antigens. The procedure is based on cloning of cDNA fragments of the corresponding protein into an expression vector allowing production and hexa-histidine-tagged mediated purification of protein from *E. coli* lysates followed by immunization of mice to obtain polyclonal antibodies. Antibodies recognizing five *B. floridae* proteins (β-catenin, FoxA, Lhx1, Lhx3 and Pax6) were generated. We demonstrate the usefulness of antibodies generated in this way by performing immunostainings on fixed embryo specimens of *B. lanceolatum*, *B. floridae* and *A. lucayanum*.

Results and Discussion

We set out a pilot project to develop antibodies against a panel of amphioxus regulatory proteins. Our main aim was to design and evaluate a generalized scheme of antibody production that could routinely be used in the lab for generation of functional antibodies at a reasonable cost. We opted primarily to create polyclonal antibodies due to the simplicity of production, modest cost and higher chance to cross-react with protein of interest in different amphioxus species. We chose mice as the host since they represent a cost-effective alternative to the more widely used rabbits. The amount of serum obtained is relatively small (200-400 μl per mouse) but appears to be sufficient to perform hundreds of immunostainings that are clearly enough to accomplish a focused study. It is of note that smaller amounts of purified antigen are necessary for immunization of mice compared to rabbits. Choice of mice as hosts for antibody production allows us to routinely immunize three mice with low animal cost. In the cases described in this study at least one functional antibody was obtained by immunizing three mice. However, if necessary, more mice can be immunized with minimal additional costs to increase the chance of obtaining a functional antibody and to overcome differences in immunological responses of individual mice. Although short synthetic peptides (15 to 20 amino acids) are often used for immunization, the functionality of the resulting antibodies is highly variable. Production and purification of fusion proteins encoding portions of an antigen is labor intensive. However, the use of longer peptide sequences from the antigen should in principle increase the chance of possessing an immunogenic epitope. When choosing *B. floridae* peptide sequences for immunization in our pilot study, we avoided sequences highly conserved among Metazoa, such as DNA-binding domains. In addition, in order to obtain antibody specific for a given protein, sequences with a high degree of identity among possible *B.floridae* paralogues were also omitted.

To generate antigens for immunization we expressed part of the selected proteins (ranging from 130 to 177 amino acids) in *E. coli* with hexa-histidine tags. After purification under denaturing conditions, the antigens were injected into mice for the generation of polyclonal antibodies. We standardized our procedure to

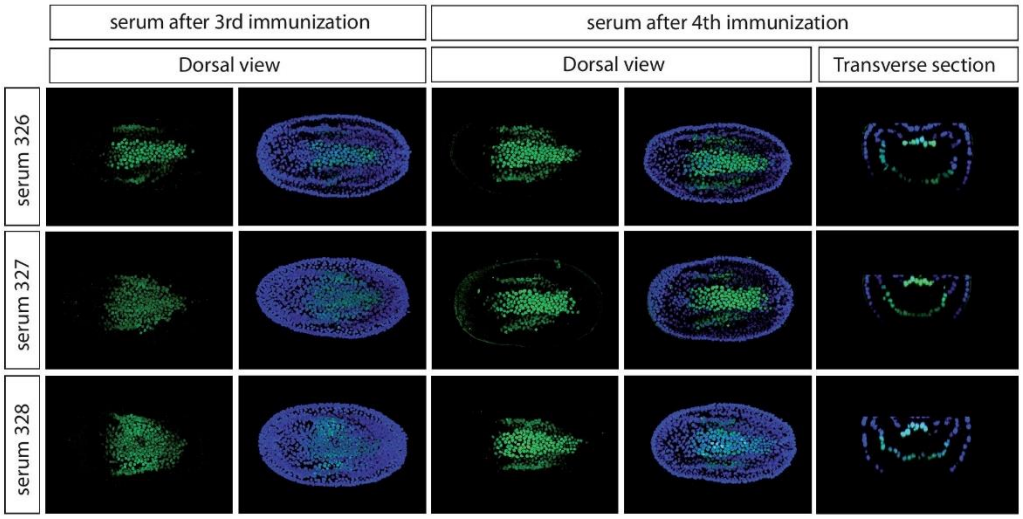

Fig. 1. Immunostaining of FoxA in the neurula stage of amphioxus. *Sera collected after 3rd and 4th immunizations of three individual mice were used for immunolabelling of FoxA (green signal). All three sera (mice 326 – 328) were able to specifically detect nuclear FoxA in the presumptive endoderm and notochord of the* B. lanceolatum *neurula. A transverse section through the embryo is shown in the right-most panel. Blue represents a nuclear DAPI signal.*

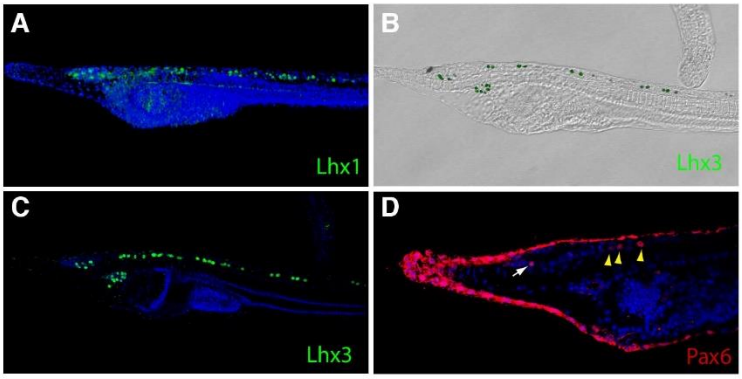

Fig. 2. Immunostaining of Lhx1, Lhx3 and Pax6 in amphioxus larvae. *Larvae of* B. lanceolatum *were immunostained with sera 249* **(A)**, *330* **(B,C)**, *and 925* **(D)**. *Lhx1* **(A)** *and Lhx3* **(B,C)** *are detected in cells of the dorsal nerve cord (green signal). In addition, nuclear signal for Lhx3 is present in the preoral pit* **(B)**. *A composite of a bright field and fluorescent image is shown in* **(B)**. **(D)** *The red nuclear signal represents Pax6 expression in the amphioxus primary motor centre (yellow arrowheads mark three pairs of Pax6-positive neurons) and in the frontal eye (white arrow). The conspicuous ectodermal signal represents unspecific labelling. Blue represents nuclear DAPI signal.*

routinely perform a series of four immunizations. A sample of the serum was taken from the tail vein after the 3rd immunization to monitor efficacy and specificity of the serum by immunostaining. Table 1 provides a summary of amphioxus-specific antibodies we produced. Antibodies recognizing five *B. floridae* proteins, namely FoxA, Lhx1, Lhx3, Pax6 and β-catenin, were generated in the current study. Below we describe each reagent that we produced and characterized by immunostaining of appropriate stages of amphioxus embryos and larvae.

The *FoxA* gene (alternative name *Hnf3*) encodes a forkhead transcription factor. Amphioxus has two *HNF3* class genes, named *AmHNF3-1* (*FoxAa*) and *AmHNF3-2* (*FoxAb*), with apparently identical expression pattern in the presumed organizer, endoderm, and notochord at the neurula stage (Shimeld, 1997). Molecular phylogenetic analysis revealed that these paralogues derive from an independent duplication in the cephalochordate lineage (Shimeld, 1997). Antibodies directed against FoxA were made by immunizing mice with a C-terminal part of *B. floridae* FoxAa. As shown in Fig.1, all three sera 326 - 328 were able to specifically detect nuclear FoxA in presumptive endoderm and notochord of *B. lanceolatum* neurula, in a pattern matching the one obtained by *in situ* hybridization (Shimeld, 1997; Terazawa and Satoh, 1997). Sera obtained after the 3rd immunization showed high specificity and good signal to noise ratio. However, a stronger signal was detected using sera 326-328 collected after the 4th immunization (Fig. 1). A similar trend regarding 3rd and 4th sera was observed for antibodies generated against other antigens as well.

Amphioxus *Lhx1* (*Lim1*) encodes a LIM-homeobox gene orthologous to vertebrate *Lhx1* and *Lhx5*. During amphioxus development, *Lhx1* is first detected in the ectoderm of the blastula (Langeland *et al.*, 2006). Then, in the gastrula, in addition to the ectoderm *Lhx1* expression appears in the mesendoderm just within the dorsal lip

TABLE 1

SUMMARY OF AMPHIOXUS-SPECIFIC ANTIBODIES DESCRIBED IN THIS STUDY

Gene	Antibody name (serum number)	Efficacy of the antibody in staining	Species tested	Fixation and storage	Comment	Reference
β-catenin	*097*	-	*Bl*	*a*	*Nonspecific staining of most nuclei.*	This study
β-catenin	*393*	++	*Bl*	*a, b*	*Functional on ethanol-stored samples.*	This study
β-catenin	*394*	++	*Bl*	*a*		This study
FoxA	*326*	+++	*Bl, Bf, Al*	*a*		This study
FoxA	*327*	+++	*Bl, Bf*	*a*		This study
FoxA	*328*	++	*Bl, Bf*	*a*		This study
Lhx1	*249*	+++	*Bl, Bf*	*a, b, c, d*	*Functional on ethanol-stored samples albeit with slightly worse signal/noise ratio.*	This study
Lhx1	*250*	+	*Bl, Bf*	*a, b, c, d*	*Signal undetectable in ethanol-stored samples.*	This study
Lhx1	*325*	++	*Bl, Bf*	*a, b, c, d*	*Diffused nonspecific staining of epidermal nuclei, together with specific signal in the neural tube. Nonspecific signal is dominant in ethanol-stored samples.*	This study
Lhx3	*329*	++	*Bl, Bf*	*a*		This study
Lhx3	*330*	+++	*Bl, Bf*	*a*		This study
Lhx3	*331*	+	*Bl, Bf*	*a*		This study
Pax6	*925*	++	*Bf, Bl, Al*	*a*		This study
Pax6	*926*	-	*Bf, Bl, Al*	*a*		This study
Pax6	*927*	+	*Bf, Bl, Al*	*a*		This study
Otx	*72*	+++	*Bf, Bl, Al*	*a*		*Vopalensky et al., 2012*
Ops3	*52*	+	*Bf, Bl*	*a*	*Non-functional for B. lanceolatum*	*Vopalensky et al., 2012*

Abbreviations: +++, easily detected; ++, detected; +, detectable; -, not detected; Bf, Branchiostoma floridae, Bl, Branchiostoma lanceolatum, Al, Asymmetron lucayanum.

a Embryos or larvae fixed 15 minutes on ice and stored in 100% methanol; *b* Embryos or larvae fixed ON 4°C and stored in 100% methanol; *c* Embryos or larvae fixed 15 minutes on ice and stored in 70% ethanol; *d* Embryos or larvae fixed ON 4°C and stored in 70% ethanol.

of the blastopore. By the mid-neurula stage *Lhx1* is expressed in the anterior part of the central nervous system, in the hindgut, in Hatschek's right diverticulum, and in the wall of the first somite on the left side (Langeland *et al.*, 2006). At the larval stage, Lhx1 expression remains in lateral and ventral cells along the anterior third of the dorsal nerve cord, in Hatschek's nephridium, in the wall of the rostral coelom, in the epidermis of the upper lip, and in mesoderm cells near the opening of the second gill slit (Langeland *et al.*, 2006). Antibodies directed against amphioxus Lhx1 were made by immunizing mice with a C-terminal part of *B. floridae* protein. We tested three anti-Lhx1 antibodies (sera 249, 250 and 324) on amphioxus larvae and obtained nuclear staining in cells of the dorsal nerve cord (Fig. 2A, Supplementary Fig. S1A), matching previously described expression domain of the gene (Langeland *et al.*, 2006). Notable differences were observed for the three sera, with the best signal/noise ratio obtained for serum 249 (Supplementary Fig. S1A, Table S1).

The amphioxus *Lhx3* gene encodes a LIM-homeobox gene. Its expression was studied in *B. belcheri* by WMISH (Wang *et al.*, 2002). Expression of *Bblhx3* first appeared in the vegetal and future dorsal side of the gastrula and became restricted to the endoderm during gastrulation. At the neurula and early larva stage, *Bblhx3* was expressed in the developing neural tube, the notochord and preoral pit. We generated three antibodies (sera 329, 330, and 331) directed against amphioxus *Lhx3* by immunizing mice with a C-terminal part of the *B. floridae* protein. All three antibodies detected Lhx3 in dorsally located cells of the nerve cord and in the preoral pit of *B. lanceolatum* larvae (Fig. 2 B,C, Supplementary Fig. S1B), i.e. in areas characteristic for the expression pattern of amphioxus *Lhx3* (Wang *et al.*, 2002). As in the case of the Lhx1 antibody, notable differences were, however, observed for the three sera with the best signal/noise ratio obtained for serum 330 (Supplementary Fig. S1B, Table S1).

Pax6 encodes a paired and homeobox gene which constitutes a member of the Pax-Six-Eya-Dach network in amphioxus (Kozmik *et al.*, 2007). *Pax6* is expressed in the anterior ectoderm from the early neurula stage until the early larval stages (Glardon *et al.*, 1998). Expression is also detectable in Hatschek's left diverticulum as it forms the preoral ciliated pit. Regional expression in the anterior neural plate of early embryos continues later in the cerebral vesicle, most conspicuously in the lamellar body, in some cells of the frontal eye and in the primary motor center (Glardon *et al.*, 1998; Vopalensky *et al.*, 2012). We have previously generated antibodies specifically recognizing *B. floridae* Pax6 by immunizing rabbits with a C-terminal part of the corresponding protein (Vopalensky *et al.*, 2012). Here, we used the same antigen to immunize mice in order to produce mouse polyclonal antibodies (sera 925, 926 and 927). Serum 925 was the most efficient one in labelling Row 1 cells of the frontal eye and cells of the primary motor center whereas serum 926 did not yield a positive signal (Fig. 2D, Supplementary Fig. S1C). In addition to specific labeling of individual neurons all Pax6 sera produced a very conspicuous (unspecific) ectodermal signal (Fig. 2D; see also Figs. 4C, 5B).

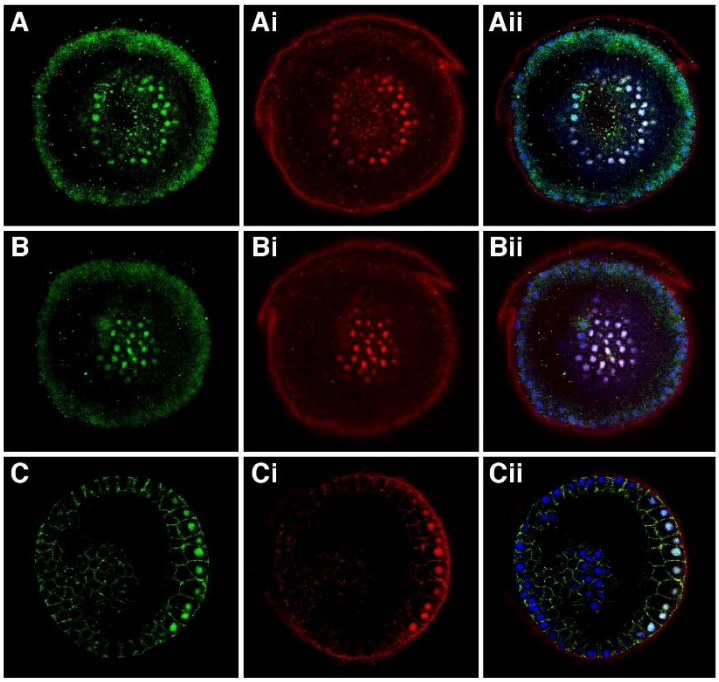

Fig. 3. Double immunostaining of β-catenin with amphioxus-specific and commercially available cross-reacting antibodies. (A,B,C) *The signal of amphioxus-specific β-catenin antibody;* **(Ai, Bi, Ci)** *the signal of commercial anti-human β-catenin antibody (Sigma C2206).* **(Aii, Bii, Cii)** *Overlapping signals of DAPI (blue), amphioxus-specific (green signal) and commercial anti-human antibody (red signal).* **(A-Aii, B-Bii)** *Two z-stacks at different positions of the same embryo at mid-gastrula stage; optical z-sectioning was taken from a blastopore view.* **(A-Bii)** *β-catenin is detected in the mesendoderm.* **(C-Cii)** *A z-stack of the embryo at the late blastula stage. The embryo in* **(A-Bii)** *was stained with serum 393, whereas the embryo in* **(C-Cii)** *was with serum 394.*

One of the hallmarks of canonical Wnt signaling activation is the nuclear accumulation of β-catenin, which interacts with Tcf/Lef family members to activate transcription of target genes. Thus, monitoring the distribution of nuclear β-catenin in the cells of the embryo permits the detection of regions in which the canonical Wnt signaling is active. Indeed, antibody labeling with immunohistochemical detection of β-catenin in *B. floridae* and *B. belcheri* embryos has previously been performed (Holland *et al.*, 2005; Yasui *et al.*, 2002). Surprisingly, the two studies demonstrated inconsistent differences in the distribution of nuclear β-catenin during early development in these two species. This could be due to the use of distinct antibody reagents derived against β-catenin of vertebrates (chicken and human) (Yasui *et al.*, 2002) or sea urchin (Holland *et al.*, 2005). We generated three antibodies (sera 097, 393, and 394) directed against amphioxus β-catenin by immunizing mice with a C-terminal part of *B. floridae* protein. To check the specificity of individual sera and to validate previously used commercially available anti-human β-catenin antibody (Yasui *et al.*, 2002) we performed double

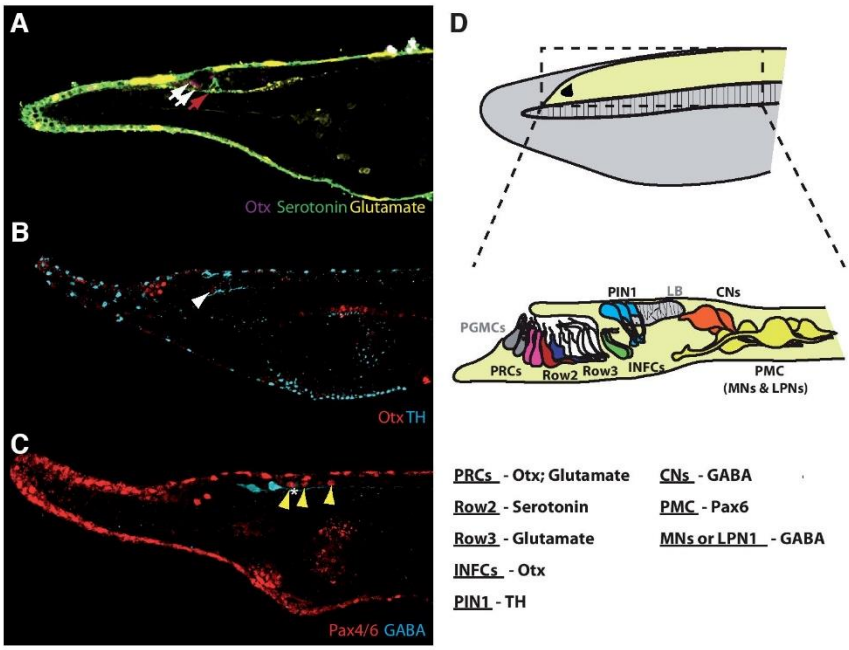

Fig. 4. High-resolution detection of specific neurons in the cerebral vesicle by double immunostaining with amphioxus-specific and commercial antibodies. *Amphioxus-specific antibodies were used to localize neuronal populations of interest and commercial antibodies were used to localize specific neuronal populations in the cerebral vesicle of* B. lanceolatum *larvae.* **(A)** *Co-staining of* B. lanceolatum *larvae with mouse polyclonal antibody generated against amphioxus Otx and commercial polyclonal antibodies against neurotransmitters serotonin (raised in goat) and glutamate (raised in rabbit). White arrows mark Row1 cells of the frontal eye (Otx positive). The red arrow points to Row2 cells (serotonin positive). Glutamate serves as a neurotransmitter in Row1 cells and Row3 cells (positive signal posterior to Row2 cells).* **(B)** *Otx was used to mark infundibular cells (white arrowhead). Projections of tyrosine hydroxylase (TH)-positive neurons can be traced from the dorsolateral region of the cerebral vesicle to infundibular organ.* **(C)** *Yellow arrowheads mark the Pax6-positive three pairs of neurons in the amphioxus primary motor centre. The first pair of neurons is GABA positive. Note, that two other pairs of GABA-positive neurons (the so-called commissural neurons) were stained more anteriorly. The conspicuous ectodermal signal represents unspecific labelling.* **(D)** *Schematic diagram of the anterior part of amphioxus neural tube indicating labelling of individual neuronal populations in cerebral vesicle. Cells populations stained in A – C are highlighted by colors and described by black letters. Other important landmarks are depicted and described in grey. PGMCs – pigment cells of the frontal eye; PRCs – photoreceptors cells of the frontal eye; Row2 – so called "Row2 cells" of the frontal eye (potential visual projecting interneurons); Row3 – so called "Row3 cells" of the frontal eye (potential projecting interneurons); INFCs – infundibular cells (possible homolog of vertebrate balance organ); PIN1 - type 1 parainfundibular neurons; LB – lamellar body (possible homolog of vertebrate pineal gland); CNs – commissural neurons (possibly involved in regulation of amphioxus larval movement); PMC – primary motor center; MNs – motoneurons; LPNs – large paired neurons. Antigen positivity shown in this study is highlighted for each of the neuronal populations. More data are necessary to decipher the identity of Pax6 positive motoneurons in PMC. Scheme adapted after Lacalli (2008).*

immunostainings (Fig. 3, Supplementary Fig. S1D). Two of the three sera (serum 393 and serum 394) labeled nuclear β-catenin at the blastula and mid-gastrula stage in the same pattern as the commercial anti-human β-catenin antibody. At mid-gastrula stage, both commercial and amphioxus-specific antibodies detected nuclear β-catenin throughout the mesendoderm (Fig. 3 A-Bii). At late blastula stage double immunostaining revealed asymmetrical distribution of nuclear β-catenin (Fig. 3 C-Cii). The immunostaining with one of the sera (serum 097) did not show any specific pattern and, in contrast to the commercially available antibody, which labeled β-catenin throughout the mesendoderm at the mid-gastrula stage, detected nuclear β-catenin in all nuclei of the embryo (Supplementary Fig. S1D). It is of note that we observed a variable degree of staining for β-catenin to adherens junctions among individual embryos. This was the case for amphioxus-specific sera 393 and 394, as well as for commercial anti-human β-catenin antibody (Fig. 3, Supplementary Fig. S1D, and data not shown). The reason for inconsistent detection of β-catenin in adherens junctions is currently unclear. Combined, we not only generated functional antibody reagents against amphioxus β-catenin, but also validated the use of cross-reacting antibody originally developed against the human protein.

Next, we tested the usefulness of the newly generated homemade antibodies for high-resolution mapping of individual cells in the amphioxus larva. We performed double immunolabelling using mouse polyclonal antibody generated in this study and a commercial antibody made in another host to obtain single-cell resolution of specific neuronal populations in the cerebral vesicle (e.g. Row1 cells, primary motor centre, infundibular cells). This approach allowed a more precise characterization of individual neurons within the cerebral vesicle with respect to their anatomical position (Fig. 4), a task which is otherwise very difficult to perform. For example, to obtain similar results Lacalli and Candiani (2017) had to deduce their conclusion from a combination of data from *in situ* hybridization experiments and detailed electron microscopy analysis (analyses had to be, however, performed on larvae from different batches). By using the approach presented here, one can localize individual cell types within a single larva and easily obtain the information about their relative positions.

All immunostainings were initially performed on specimens fixed in 4% PFA for 15-45 min on ice (alternatively at 4°C overnight). Fixed samples were subsequently transferred to 100% methanol and stored at -20°C until use. For selected sera, we also tested the efficacy of immunostainings on embryos and larvae prepared

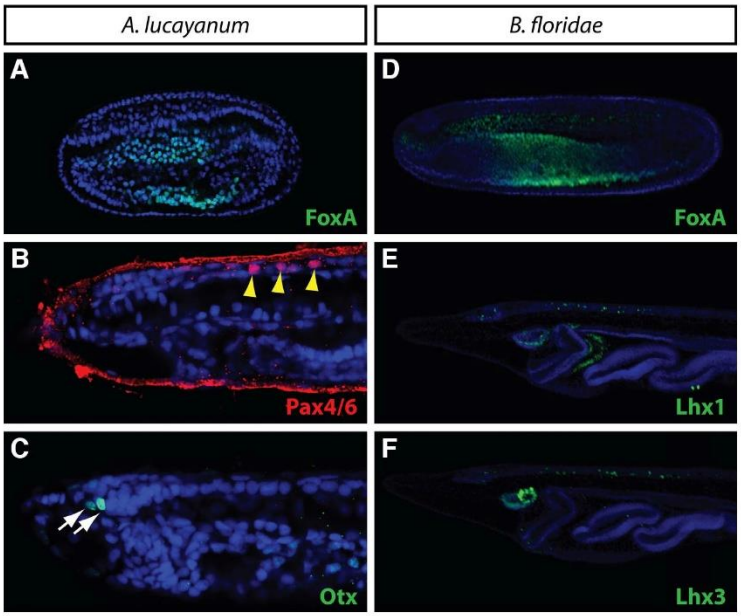

Fig. 5. Immunostaining of B. floridae and A. lucayanum specimens. *Embryos and larvae of* A. lucayanum **(A-C)** *and* B. floridae **(D-F)** *were immunostained with FoxA serum 326* **(A,D)**, *Pax6 serum 925* **(B)**, *Otx serum 72* **(C)**, *Lhx1 serum 249* **(E)** *and Lhx3 serum 330* **(F)**. *The conspicuous ectodermal signal in (B) represents unspecific labelling.*

for *in situ* hybridization (fixed in 4% PFA at 4ºC overnight and stored in 70% ethanol). We found that some polyclonal antibodies are functional on such specimens making the logistic of embryo harvest simpler – the same sample can in principle be used for *in situ* hybridization and immunostaining (see Table 1).

We presume that an apparently high success rate of obtaining functional antibodies against amphioxus proteins by the procedure described here is largely due to sequence divergence of selected peptides between amphioxus and mice and choice of long peptide antigens. At the time of commencing the project, the complete genome sequence of *B. floridae* was available. Hence the antigens used in this study are of *B. floridae* origin but due to the high degree of sequence identity among different amphioxus species, we expected that most of the antibodies would allow cross-species detection. In general, interspecies cross-reactivity for home-made polyclonal antibodies was indeed observed (Table 1). All antibodies generated against *B. floridae* antigens, except for one, appear to be functional in detecting the corresponding orthologous protein in the European lancelet (*B. lanceolatum*). Some of the antibodies were even successfully validated in the more distantly related *A. lucayanum* (Fig. 5). However, in the case of Ops3 no positive immunostaining was observed in species other than the one from which the epitope was derived from, even though 45 out of 67 amino acids of the epitope were conserved (Supplementary Fig. S2). Combined, our data suggest that high degree of sequence identity typical for transcription factors and other regulatory proteins increases the likelihood of producing an antibody cross-reacting with proteins of different amphioxus species. We anticipate that in the near future the access to genomes of individual lancelet species will allow cross-species homology analyses and a more rational choice of antigenic peptides with the aim of generating universal anti-amphioxus antibodies even for faster evolving genes, such as opsins.

Conclusions

We developed novel mouse polyclonal antibodies for use in immunostainings on amphioxus embryos. Our pilot study shows the feasibility of the experimental procedure that reliably yields functional antibodies at modest cost. Such antibodies can be used for elucidating embryonic gene expression at a single-cell resolution, for co-labelling using other antibodies or for investigating the sub-cellular localization of endogenous proteins in the developing embryo. Immunostaining can potentially be combined with WMISH (Lu *et al.*, 2012) or transgenic fluorescent reporter proteins (Kozmikova and Kozmik, 2015), allowing double labeling of cell types or of embryological structures of interest. Polyclonal antibodies often allow detection of the same protein in different amphioxus species, such as *B. floridae*, *B. lanceolatum* and *A. lucayanum*. In summary, we anticipate that a panel of antibodies such as those generated by us here and by others in the future will represent a useful toolkit in amphioxus research.

Materials and Methods

Generation of antibodies

For overexpression of protein fragments, the pET system (Novagen) was used. Selected coding sequences were cloned into the pET42a(+) vector to create proteins containing 6xHis-GST fused to the protein fragment of interest. Amino acid sequences of antigens are shown in Supplementary Table 1. Expression vectors were introduced into the bacterial production strain of bacteria BL21 (DE3) RIPL (Stratagene). A total volume of 500 ml fresh LB medium without antibiotics was inoculated with an overnight culture grown in LB medium supplemented with 12.5 μg/ml chloramphenicol and 30 μg/ml kanamycin. Bacteria were grown at 37°C at 200 RPM until OD_{600} reached 0.6, then induced by 0.5 mM IPTG for 3 hours. Cells were harvested at 6000 x g for 20 minutes and the pellet stored at -80°C until further processing. The pellet was resuspended in Lysis buffer (6M guanidine hydrochloride, 0.1M NaH_2PO_4, 0.01M Tris.Cl, pH 8.0, supplemented with fresh β-mercaptoethanol to a final concentration of 20 mM). The suspension was sonicated 6 x 20 s and incubated for 3 hours at room temperature. The resulting lysate was centrifuged at 10,000 x g for 10 minutes and the supernatant mixed with Ni-NTA agarose beads (Qiagen) previously equilibrated with Urea buffer (8 M urea, 20 mM Tris.Cl, 50 mM NaH_2PO_4, 100 mM NaCl, pH 8.0, supplemented with fresh β-mercaptoethanol to a final concentration of 20 mM). The suspension was incubated on a rotating platform overnight at room temperature. The beads with bound proteins were washed two times with 40 ml Urea buffer and loaded onto a disposable chromatographic column (Bio-Rad). The column was washed with Urea buffer with decreasing pH (8.0 – 6.8) and His-tagged protein was eluted by Urea buffer at pH 4.2 into several 1 ml aliquots. After elution, pH was immediately increased to 7.5 with 1 M Tris.Cl, pH 8. Protein concentration was estimated using Protein Assay Reagent (Bio-Rad). Three mice of the B10A-H2xBALB/CJ strain were immunized four times in monthly intervals with 30 μg purified protein mixed

with Freund's Adjuvant (Sigma). An aliquot of serum was collected ten days after the 3rd and 4th immunization.

Animal collection and immunohistochemistry

B. lanceolatum adults were collected in Argeles-sur-Mer (France), transported to Institute of Molecular Genetics (Prague, Czech Republic) and preserved in the lab in a day/night cycle of 14h/10h until spawning, which was induced by a shift in temperature (Fuentes *et al.*, 2007). Adults of Florida amphioxus (*B. floridae*) were collected from Old Tampa Bay, Florida, during the summer breeding season. Adults were induced to spawn by electrostimulation as described (Yu and Holland, 2009). Ripe adults of *A. lucayanum* were collected in Bimini and allowed to spawn naturally in the laboratory (Holland and Holland, 2010). Embryos were raised in the laboratory on site. Embryos for immunohistochemistry were fixed with 4% PFA/MOPS (0.1 M 3-(N-morpholino)propanesulfonic acid, 2 mM MgSO4, 1 mM EGTA, 0.5M NaCl, pH 7.5) for 15 minutes on ice and stored in 100% methanol. Some specimens were fixed with 4% PFA/MOPS overnight at 4°C and stored in 70% EtOH. Specimens were transferred to 1× PBS 0.1% Tween-20 (PBT) through 70% and 30% methanol in PBS. Following four 15-minute washes in PBT, samples were blocked in blocking solution (10% BSA in PBT) for (at least) 1 h and incubated with primary antibodies overnight at 4°C. Amphioxus-specific antibodies were diluted 1:200 to 1:500 in blocking solution. The following commercial primary antibodies were used: β-catenin (Sigma C2206, rabbit polyclonal, dilution 1:500), GABA (Sigma A2052, rabbit polyclonal, 1:500), tyrosine hydroxylase (TH, Abcam ab112, rabbit polyclonal, 1:1000), glutamate (Sigma G6642, rabbit polyclonal, 1:500), serotonin (Abcam ab66047, goat polyclonal, 1:1000). On the following day, samples were washed five times in PBT (20 minutes each wash) and were incubated with secondary antibodies and 1 μg/mL DAPI for 3 hours at room temperature. Alexa Fluor 488 or 594 anti-mouse, anti-rabbit or anti-goat were used as secondary antibody at 1:500 dilution. For confocal microscopy, the samples were mounted in VECTASHIELD (Vector Laboratories, Inc.) using three layers of Scotch tape as spacers between the slide and the coverslip. The confocal images were taken using a Leica SP5 or SP8 confocal microscope and were processed (brightness and contrast) with FIJI image analysis software. Images were further processed (rotation) and assembled in tables with Adobe Photoshop CS4.

Acknowledgements

This work was funded by the Czech Science Foundation (15-21285J to IK). We acknowledge the Microscopy Centre - Light Microscopy Core Facility, IMG ASCR, Prague, Czech Republic, supported by grants (Czech-Bioimaging – MEYS LM2015062), "Centre of Model Organisms" OPPK (CZ.2.16/3.1.00/21547) and "Biomodels for health" (LO1419), for their support with the confocal imaging presented herein. We are indebted to Hector Escriva and Stephanie Bertrand from OOB in Banyuls-sur-Mer, France, for providing Branchiostoma lanceolatum *adults and to Nicholas Holland for help in collecting adults of* Branchiostoma floridae *and* Asymmetron lucayanum. *We are grateful to Jitka Lachova, Veronika Noskova, Veronika Kovacsova and Vladimir Soukup for technical assistance and Sarka Takacova for proofreading.*

References

ACEMEL, R.D., TENA, J.J., IRASTORZA-AZCARATE, I., MARLETAZ, F., GOMEZ-MARIN, C., DE LA CALLE-MUSTIENES, E., BERTRAND, S., DIAZ, S.G., ALDEA, D., AURY, J.M. *et al.,* (2016). A single three-dimensional chromatin compartment in amphioxus indicates a stepwise evolution of vertebrate Hox bimodal regulation. *Nat Genet* 48: 336-341.

BERTRAND, S. and ESCRIVA, H. (2011). Evolutionary crossroads in developmental biology: amphioxus. *Development* 138: 4819-4830.

FUENTES, M., BENITO, E., BERTRAND, S., PARIS, M., MIGNARDOT, A., GODOY, L., JIMENEZ-DELGADO, S., OLIVERI, D., CANDIANI, S., HIRSINGER, E. *et al.,* (2007). Insights into spawning behavior and development of the European amphioxus (Branchiostoma lanceolatum). *J Exp Zool B Mol Dev Evol* 308: 484-493.

GLARDON, S., HOLLAND, L.Z., GEHRING, W.J. and HOLLAND, N.D. (1998). Isolation and developmental expression of the amphioxus Pax-6 gene (AmphiPax-6): insights into eye and photoreceptor evolution. *Development* 125: 2701-2710.

HOLLAND, L.Z., ALBALAT, R., AZUMI, K., BENITO-GUTIERREZ, E., BLOW, M.J., BRONNER-FRASER, M., BRUNET, F., BUTTS, T., CANDIANI, S., DISHAW, L.J. *et al.,* (2008). The amphioxus genome illuminates vertebrate origins and cephalochordate biology. *Genome Res* 18: 1100-1111.

HOLLAND, L.Z., PANFILIO, K.A., CHASTAIN, R., SCHUBERT, M. and HOLLAND, N.D. (2005). Nuclear beta-catenin promotes non-neural ectoderm and posterior cell fates in amphioxus embryos. *Dev Dyn* 233: 1430-1443.

HOLLAND, N.D. and HOLLAND, L.Z. (2010). Laboratory spawning and development of the Bahama lancelet, Asymmetron lucayanum (cephalochordata): fertilization through feeding larvae. *Biol Bull* 219: 132-141.

HUANG, S., CHEN, Z., YAN, X., YU, T., HUANG, G., YAN, Q., PONTAROTTI, P.A., ZHAO, H., LI, J., YANG, P. *et al.,* (2014). Decelerated genome evolution in modern vertebrates revealed by analysis of multiple lancelet genomes. *Nat Commun* 5: 5896.

IGAWA, T., NOZAWA, M., SUZUKI, D.G., REIMER, J.D., MOROV, A.R., WANG, Y., HENMI, Y. and YASUI, K. (2017). Evolutionary history of the extant amphioxus lineage with shallow-branching diversification. *Sci Rep* 7: 1157.

KOZMIK, Z., HOLLAND, N.D., KRESLOVA, J., OLIVERI, D., SCHUBERT, M., JONASOVA, K., HOLLAND, L.Z., PESTARINO, M., BENES, V. and CANDIANI, S. (2007). Pax-Six-Eya-Dach network during amphioxus development: conservation *in vitro* but context specificity in vivo. *Dev Biol* 306: 143-159.

KOZMIKOVA, I. and KOZMIK, Z. (2015). Gene regulation in amphioxus: An insight from transgenic studies in amphioxus and vertebrates. *Mar Genomics* 24 Pt 2: 159-166.

LACALLI, T. and CANDIANI, S. (2017). Locomotory control in amphioxus larvae: new insights from neurotransmitter data. *Evodevo* 8: 4.

LACALLI, T.C. (2008). Basic features of the ancestral chordate brain: a protochordate perspective. *Brain Res Bull* 75: 319-323.

LANGELAND, J.A., HOLLAND, L.Z., CHASTAIN, R.A. and HOLLAND, N.D. (2006). An amphioxus LIM-homeobox gene, AmphiLim1/5, expressed early in the invaginating organizer region and later in differentiating cells of the kidney and central nervous system. *Int J Biol Sci* 2: 110-116.

LE PETILLON, Y., LUXARDI, G., SCERBO, P., CIBOIS, M., LEON, A., SUBIRANA, L., IRIMIA, M., KODJABACHIAN, L., ESCRIVA, H. and BERTRAND, S. (2017). Nodal/Activin Pathway is a Conserved Neural Induction Signal in Chordates. *Nat Ecol Evol* 1: 1192-1200.

LI, G., LIU, X., XING, C., ZHANG, H., SHIMELD, S.M. and WANG, Y. (2017). Cerberus-Nodal-Lefty-Pitx signaling cascade controls left-right asymmetry in amphioxus. *Proc Natl Acad Sci USA* 114: 3684-3689.

LU, T.M., LUO, Y.J. and YU, J.K. (2012). BMP and Delta/Notch signaling control the development of amphioxus epidermal sensory neurons: insights into the evolution of the peripheral sensory system. *Development* 139: 2020-2030.

PUTNAM, N.H., BUTTS, T., FERRIER, D.E., FURLONG, R.F., HELLSTEN, U., KAWASHIMA, T., ROBINSON-RECHAVI, M., SHOGUCHI, E., TERRY, A., YU, J.K. *et al.,* (2008). The amphioxus genome and the evolution of the chordate karyotype. *Nature* 453: 1064-1071.

SHIMELD, S.M. (1997). Characterisation of amphioxus HNF-3 genes: conserved expression in the notochord and floor plate. *Dev Biol* 183: 74-85.

SOMORJAI, I., BERTRAND, S., CAMASSES, A., HAGUENAUER, A. and ESCRIVA, H. (2008). Evidence for stasis and not genetic piracy in developmental expression patterns of Branchiostoma lanceolatum and Branchiostoma floridae, two amphioxus species that have evolved independently over the course of 200 Myr. *Dev Genes Evol* 218: 703-713.

SOUKUP, V., YONG, L.W., LU, T.M., HUANG, S.W., KOZMIK, Z. and YU, J.K. (2015). The Nodal signaling pathway controls left-right asymmetric development in amphioxus. *Evodevo* 6: 5.

TERAZAWA, K. and SATOH, N. (1997). Formation of the chordamesoderm in the amphioxus embryo: Analysis with Brachyury and fork head/HNF-3 genes. *Dev Genes Evol* 207: 1-11.

VOPALENSKY, P., PERGNER, J., LIEGERTOVA, M., BENITO-GUTIERREZ, E., ARENDT, D. and KOZMIK, Z. (2012). Molecular analysis of the amphioxus

frontal eye unravels the evolutionary origin of the retina and pigment cells of the vertebrate eye. *Proc Natl Acad Sci USA* 109: 15383-15388.

WANG, Y., ZHANG, P.J., YASUI, K. and SAIGA, H. (2002). Expression of Bblhx3, a LIM-homeobox gene, in the development of amphioxus Branchiostoma belcheri tsingtauense. *Mech Dev* 117: 315-319.

WU, H.R., CHEN, Y.T., SU, Y.H., LUO, Y.J., HOLLAND, L.Z. and YU, J.K. (2011). Asymmetric localization of germline markers Vasa and Nanos during early development in the amphioxus Branchiostoma floridae. *Dev Biol* 353: 147-159.

YASUI, K., LI, G., WANG, Y., SAIGA, H., ZHANG, P. and AIZAWA, S. (2002). beta-Catenin in early development of the lancelet embryo indicates specific determination of embryonic polarity. *Dev Growth Differ* 44: 467-475.

YU, J.K. and HOLLAND, L.Z. (2009). Amphioxus (Branchiostoma floridae) spawning and embryo collection. *Cold Spring Harb Protoc* 2009: pdb prot5285.

YUE, J.X., KOZMIKOVA, I., ONO, H., NOSSA, C.W., KOZMIK, Z., PUTNAM, N.H., YU, J.K. and HOLLAND, L.Z. (2016). Conserved Noncoding Elements in the Most Distant Genera of Cephalochordates: The Goldilocks Principle. *Genome Biol Evol* 8: 2387-2405.

YUE, J.X., YU, J.K., PUTNAM, N.H. and HOLLAND, L.Z. (2014). The transcriptome of an amphioxus, Asymmetron lucayanum, from the Bahamas: a window into chordate evolution. *Genome Biol Evol* 6: 2681-2696.

6.5 Photoreceptors of amphioxus - insights into evolution of vertebrate opsins, vision and circadian rhythmicity. (*Review*)

Amphioxus arguably represents an excellent proxy for getting insights into the evolution of vertebrates and more broadly ancestral chordate traits. Even though studies of photoreceptive organs and light guided behavior of amphioxus took place already in the second half of the 19th century, review gathering all relevant data about light detection by amphioxus was missing in the literature. In our review we focused right on this topic. We put together all relevant studies beginning with the first study by Costa[57] from 19th century, mentioning amphioxus rapid reactions to light. Then we continued with studies of photoreceptive organs held on the turn of 20th century and we further summarized EM studies of amphioxus CNS and photoreceptive organs from second half of 20th century. Our synthesis finished with modern molecular analysis of amphioxus photoreceptive organs. We also aimed on comparison of amphioxus photoreceptive organs and their putative vertebrates´ counterparts and put forward several hypotheses (either previously mentioned by other authors or raised by us) about photoreceptive organs in the chordate ancestor. Moreover, we added some original data that were missing in the literature and were necessary for getting the complete picture of studied topic. We also proposed several future directions that could be followed to obtain more information about evolution of vertebrate eyes, circadian regulators and opsins.

My contribution to this work: I provided all original scientific data (in Fig.3 and Fig.7 of the manuscript). I prepared all figures and wrote majority of the manuscript´s text.

Int. J. Dev. Biol. 61: 665-681 (2017)
doi: 10.1387/ijdb.170230zk

THE INTERNATIONAL JOURNAL OF DEVELOPMENTAL BIOLOGY
www.intjdevbiol.com

Amphioxus photoreceptors - insights into the evolution of vertebrate opsins, vision and circadian rhythmicity

JIRI PERGNER and ZBYNEK KOZMIK*

Laboratory of Transcriptional Regulation, Institute of Molecular Genetics of the Czech Academy of Sciences, Prague, Czech Republic,

ABSTRACT Studies on amphioxus, representing the most basal group of chordates, can give insights into the evolution of vertebrate traits. The present review of amphioxus research is focused on the physiology of light-guided behavior as well as on the fine structure, molecular biology, and electrophysiology of the nervous system, with special attention being given to the photoreceptive organs. The amphioxus visual system is especially interesting because four types of receptors are involved in light detection – dorsal ocelli and Joseph cells (both rhabdomeric photoreceptors) and the frontal eye and lamellar body (both ciliary photoreceptors). Here, we consider how the available information on photoreceptive organs and light-guided behavior in amphioxus helps generate hypotheses about the history of these features during chordate and subsequently vertebrate evolution.

KEY WORDS: *chordate, opsin evolution, photoreceptor, eye evolution, phototransduction*

Introduction

Light is a crucial environmental signal for most of the organisms on earth. Light sensing systems have evolved to be uniquely suited to the environment and behavior of any given species. Light cues are necessary for mediating biological processes such as circadian rhythms, reproductive cycles and most importantly visually guided behavior. Animals detect light using sensory cells known as photoreceptors, present in the eyes or, in the case of extraocular photoreceptors, outside of the eyes. Although other systems of light detection exist in the animal kingdom, such as cryptochromes (Rivera *et al.*, 2012) or LITE-1 (Gong *et al.*, 2016), opsins, the seven-pass transmembrane proteins that belong to the G-Protein Coupled Receptor (GPCR) superfamily, are dominantly utilized as visual pigments among Metazoa (Feuda *et al.*, 2014). A simple eye can be defined as a photoreceptor cell neighboring a shielding pigment cell, or, in extreme cases, both photoreceptive and pigment function can be combined together in one cell. At the other end of the sophistication spectrum, complex eyes with advanced optics can be found in various animals. For example the vertebrate-style camera eye is one of the most elaborate types of animal eye. The huge diversity, as well as the extreme complexity, of eyes in different animals was already puzzling scientists in Darwin´s time (Darwin, 1859).

Recent studies have shown that cephalochordates may serve as a valuable model providing useful insight into photoreception in ancestral chordates as well as into evolution of the vertebrate eye. Cephalochordates (common name amphioxus or lancelets) represent the most basal branch of chordates (which also includes vertebrates), live worldwide in sandy shallow seashores and can be divided into three genera, *Asymmetron*, *Branchiostoma*, and *Epigonichthys* (Bertrand and Escriva, 2011).

The amphioxus body plan resembles the body plan of most extant as well as extinct chordates, having a dorsally located notochord and neural tube, a ventral gut, a perforated pharynx with gill slits, segmented muscles and gonads and a tail fin. The amphioxus central nervous system comprises a dorsal neural tube running through the whole length of the body. The anterior part of the neural tube is slightly expanded, forming a so-called cerebral

Abbreviations used in this paper: 2RWGD, two rounds of whole genome duplication; cAMP, cyclic adenosine monophosphate; cGMP, cyclic guanosine monophosphate; CNG channel, cyclic nucleotide gated channel; CV, cerebral vesicle; DAG, diacylglycerol; DO, dorsal ocellus; EM, electron microscopical; FE, frontal eye; GNA, guanine nucleotide-binding protein alpha subunit; GPCR, G protein coupled receptor; IP3, inositol trisphosphate; ipRGC, intrinsic photosensitive ganglion cell; JC, Joseph cell; LB, lamellar body; PDE, phosphodiesterase; PIP2, phosphatidylinositol 4,5-bisphosphate; PKC, protein kinase C; PLC, phospholipase C; PMC, primary motor center; PUFA, polyunsaturated fatty acid; RDGN, retinal determination gene network; RPE, retinal pigmented epithelium.

***Address correspondence to:** Zbynek Kozmik, Institute of Molecular Genetics of the Czech Academy of Sciences, v.v.i., Videnska 1083, 14220, Czech Republic. Tel: +420 241062110. E-mail: kozmik@img.cas.cz http://orcid.org/0000-0002-5850-2105

Submitted: 9 September, 2017; *Accepted:* 22 September, 2017.

ISSN: Online 1696-3547, Print 0214-6282

vesicle (CV). Based on morphological and molecular analysis, the cerebral vesicle is considered to be a homolog of the vertebrate diencephalon or di- plus mesencephalon with indistinguishable borders (Albuixech-Crespo *et al.*, 2017; Holland, 2017).

Amphioxus possesses four distinct photoreceptive organs – the frontal eye (FE), lamellar body (LB), Joseph cells (JCs) and dorsal ocelli (DO) (Fig. 1). Amphioxus development, from fertilization to metamorphosis, takes about several weeks to several months depending on species. Amphioxus larvae are planktonic, while after metamorphosis, adult amphioxus spend most of their life burrowed in the sand with just the anterior part of the body projecting outside, in order to allow feeding by filtering food particles. Associated with such a dramatic changes in the way of life are also changes in response to light stimuli.

Amphioxus responses to light stimuli

The rapid reactions of amphioxus to light had been discovered by Costa (1834), and thorough study of amphioxus sensory reactions was performed at the beginning of the 20th century. Parker (1908) described sensory reactions of amphioxus to various physical and chemical stimuli, including light. Parker´s observation about amphioxus photoresponses were in agreement with previous studies (Hesse, 1898; Willey, 1894), showing negative phototactic responses in adult amphioxus (Parker, 1908). Moreover, it was shown that amphioxus adults evince higher burrowing activity during the night (Schomerus *et al.*, 2008). Several later studies added more information about larval amphioxus reactions to light. Chin (1941) documented collections of planktonic larvae of *Branchiostoma belcheri* in different times of the day and night. During the day, amphioxus larvae were found close to the bottom, while with decrease in light intensity during sunset, most larvae were found close to the surface. Comparable observations were made two decades later by Wickstead and Bone (1959), who found an increase in concentration of amphioxus larvae close to the surface shortly before and after sunset for *B. belcheri* as well as *Branchiostoma lanceolatum*. Various amphioxus species thus demonstrate typical diurnal migration. Additionally, Webb (1969) showed that amphioxus larvae actively swim to the surface and passively sank down, with mouth open, catching food. This behavior is also light dependent. Moreover, it was shown that the FE might be important for larval light guided behavior. During feeding, amphioxus larvae adopt a vertical posture in the water column in such a way that the FE pigment cells screen off most of light coming towards the FE photoreceptor cells (Stokes and Holland, 1995). Larvae are able to change their orientation in the order of minutes, when the light direction is changed. Such an orientation to incoming light might be important for minimizing the overhead illumination and improving the ability to discriminate between levels of light intensity (Lacalli, 1996). Amphioxus reacts to light as early as the neurula stage. For *Branchiostoma floridae* it was shown that, when kept in Petri dishes, neurulae swim up to the surface of the water in the direction towards the highest light intensity (Holland and Yu, 2004). No such behavior occurs in the same developmental stage in *B. lanceolatum* (our observations) or representative of another amphioxus genus *Asymmetron lucayanum* (Holland and Holland, 2010). Whether light attraction in *B. floridae* neurula is connected with ongoing development of the first dorsal ocellus is unclear. Why this phototactic behavior of neurulae was not observed in other amphioxus species remains a mystery.

Of special interest is the dependence of amphioxus spawning on light conditions. *Branchiostoma* species kept in laboratory conditions (*B. floridae*, *B. lanceolatum* and *B. belcheri*) spawn within 1 hour after switching off the light (1h after simulated sunset) (Fuentes *et al.*, 2007; Holland and Yu, 2004; Li *et al.*, 2013). Spawning of *Branchiostoma* shortly after sunset likely occurs in nature as well. The same light dependency for spawning is also found for *A. lucayanum*. Moreover most individuals of *A. lucayanum* usually spawn one day before the new moon (Holland,

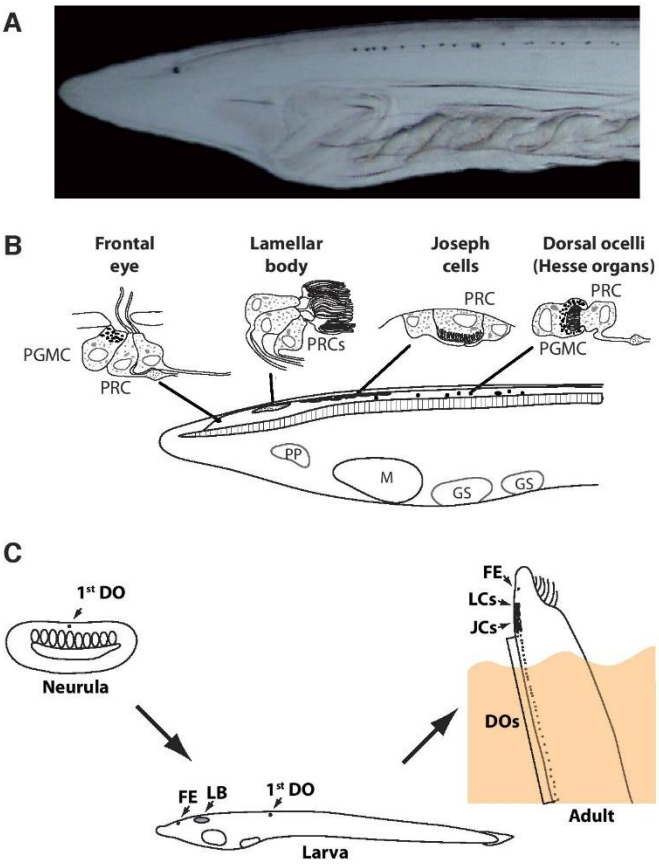

Fig. 1. Overview of amphioxus photoreceptive organs. (A) *Detail of anterior part of 3 weeks old larvae of* Branchiostoma floridae*;* **(B)** *Scheme of particular photoreceptive organs developed in larvae presented in (A). Important morphological landmarks of developing amphioxus larvae are shown (adapted after Lacalli (2004)). PRC, photoreceptor cell; PGMC, pigment cell; PP, preoral pit; M, mouth; GS, gill slit.* **(C)** *Simplified scheme of picked developmental stages of amphioxus (mid-neurula; early larva; adult - shown in typical vertical position in the sand burrow). The presence of individual photoreceptive organs is stressed. FE, frontal eye; LB, lamellar body; LC, lamellate cell; JC, Joseph cell; DO/DOs, dorsal ocellus/ocelli.*

2011) proving another piece of evidence for the key role of light for animal behavior.

Taken together, amphioxus manifests various light dependent behavioral responses. These include positive phototaxis in early developmental stages, vertical diurnal migration in larval stages, and negative phototaxis in benthic adult stage with light dependent spawning cycles (summarized in Table 1). The observed behavior is in concordance with the behavior of many marine organisms, including vertebrates.

Opsins as key molecular determinants of light detection in amphioxus

For light detection, animals use opsins and/or cryptochromes. Opsins are utilized as visual pigments in all *Eumetazoa* (Porter *et al.*, 2012), while cryptochromes function as a photosensitive pigment in sponges (Muller *et al.*, 2013; Rivera *et al.*, 2012). In vertebrates, the role of cryptochromes as functional pigments has not been proven to date, but their role in circadian rhythmicity is highly probable (Kume *et al.*, 1999; Kutta *et al.*, 2017; Shearman *et al.*, 2000). Although three cryptochrome genes have been identified in the *B. floridae* genome (Haug *et al.*, 2015), their expression was not determined and their function remains elusive. For now it thus seems likely that opsins are more important than cryptochromes for photoreception in amphioxus, a situation analogous to that in vertebrates (Haug *et al.*, 2015; van der Schalie and Green, 2005).

The opsins are members of a large family of G protein coupled receptors (GPCRs). An opsin consist of a protein moiety and a non-protein chromophore, usually 11-*cis* retinal, less often all-*trans* retinal (a photoproduct of 11-*cis*-retinal) (Terakita, 2005). The opsins can be distinguished from other GPCRs by the presence of a highly conserved lysine residue K296 (amino acid position 296 in bovine rhodopsin), that serves for covalent binding of retinal. Based on their primary structure, opsins are usually divided to four main groups: 1. c-opsins present in ciliary photoreceptors (typical visual photoreceptors in vertebrates); 2. r-opsins present in rhabdomeric photoreceptors (typical visual photoreceptors in protostome invertebrates); 3. Cnidopsins, a group consisting exclusively of Cnidarian opsins and 4. group of nonvisual opsins, called Group4 (Liegertova *et al.*, 2015; Porter *et al.*, 2012). Recently opsins were divided into up to ten groups (Ramirez *et al.*, 2016) – nine subgroups originating from subtle division of the c-, r- and Group4 opsins, plus a group of Cnidopsins.

Aquatic animals usually display higher variability than terrestrial animals in their opsin gene repertoire (Biscontin *et al.*, 2016; Liegertova *et al.*, 2015; Ramirez *et al.*, 2016) and amphioxus is no exception to this rule. Approximately twenty functional opsin genes have been identified in each of the amphioxus genomes completed so far: 21 opsin genes in *B. floridae*, 21 opsin genes plus one opsin pseudogene in *B. lanceolatum* and 20 opsin genes in *B. belcheri* (Holland *et al.*, 2008; Pantzartzi *et al.*, 2017). Transcripts of all of the identified *B. lanceolatum* opsins were detected in various developmental stages and/or in tissues of adult specimens (Pantzartzi *et al.*, 2017). Representatives of all major opsin groups (except the Cnidopsin group) can be found in the genomes of *B. floridae*, *B. lanceolatum* and *B. belcheri*. More specifically, the recently assembled genome of *B. lanceolatum* contains five amphioxus opsins that cluster with c-opsins; nine amphioxus opsins clustering with Group4 and seven amphioxus opsins clustering with r-opsins (Fig. 2A). Of the five amphioxus c-type opsins, none clusters in phylogenetic tree within the group of the vertebrate visual and non-visual c-opsins (Pantzartzi *et al.*, 2017). This is in agreement with the proposed evolution of genes involved in vertebrate phototransduction cascade after two rounds of whole genome duplication (2RWGD) that occurred after the split of amphioxus lineage and lineage leading to vertebrates (Lamb and Hunt, 2017; Lamb *et al.*, 2016; Larhammar *et al.*, 2009). Group4 amphioxus opsins representing neuropsins and putative Go-coupled opsins (a group of opsins signaling through the Gαo subunit of trimeric G proteins) are of special interest. Several gains and losses of amphioxus opsin genes in this subgroup, even between closely related species *B. floridae* and *B. lanceolatum*, have recently been identified. This indicates possible specific adjustment of the Go opsin repertoire in connection with different light conditions in habitats of particular *Branchiostoma* species. All amphioxus genomes examined so far contain a single melanopsin gene, an orthologue of the r-type opsin (melanopsin) expressed in vertebrates in intrinsically photosensitive Retinal Ganglion Cells (ipRGCs) (Provencio *et al.*, 1998). The rest of the putative r-type amphioxus opsins (six opsins) cluster together to form a specific so called "Amphiop6" group (Koyanagi *et al.*, 2002) that has not been found outside the *Branchiostoma* genus.

TABLE 1

OVERVIEW OF REACTIONS TO LIGHT STIMULI DURING INDIVIDUAL AMPHIOXUS DEVELOPMENTAL STAGES

Developmental stage	Species	Response to light	References
Neurula	*B. floridae*	Accumulation at surface level facing to the direction of the light source	Holland and Yu, 2004
	B. lanceolatum	No response	This study
	A. lucayanum	No response	Holland and Holland, 2010
Larva	*B. floridae*	During hovering in water column orientation with FE facing from the light source	Stokes and Holland, 1995
	B. belcheri	Diurnal migration - close to the bottom during day, close to the surface level during and after sunset	Chin, 1941; Wickstead and Bone, 1959
	B. lanceolatum	Diurnal migration - close to the bottom during day, close to the surface level during and after sunset	Wickstead and Bone, 1959
		Swimming to surface and then catching the food sanking down with mouth open	Webb, 1969
Adult	*B. lanceolatum*	Negative phototaxis	Costa, 1834; Willey, 1894; Hesse, 1898
		Increased locomotor activity in the burrow during the night (suppressed by light)	Schomerus *et al.*, 2008
	B. caribbaeum	Negative phototaxis	Parker, 1908
Adult – spawning behavior	*B. floridae*	Spawning 1h after sunset[a]	Holland and Yu, 2004
	B. lanceolatum	Spawning 1h after sunset[a]	Fuentes *et al.*, 2007
	B. belcheri	Spawning 1h after sunset[a]	Li *et al.*, 2013
	A. lucayanum	Spawning 1h after sunset[a]	Holland, 2011
	A. lucayanum	Spawning one day before the new moon[b]	Holland, 2011

Abbreviations: a, short term light effect; b, long term light effect

Due to the key phylogenetic position of amphioxus, their opsins provide a unique model for understanding vertebrate opsin evolution and mechanisms of opsin signaling. Since retinal has its peak absorption in UV region of the spectrum, tuning of opsin structure is necessary, to shift the absorption maximum into the visible range. To achieve this and to stabilize the Schiff base linkage between retinal and K296, the presence of a negatively charged amino acid (usually glutamate), the so-called counterion, is important. In most vertebrate opsins E113 (glutamate at position 113) serves as the counterion, while in other opsins it is usually E181 (Terakita *et al.*, 2004). It thus appears that E181 was the ancestral counterion position, and that evolution of new features of vertebrate opsins was connected with the switch to counterion position E113. Terakita *et al.*, (2004) studied the counterion in two *B. belcheri* Group4 opsins (Op12a and Op14), both having their counterion at position 181 and not 113. It was shown that switch of counterion from position E181 to E113 enhanced efficiency of G protein activation by vertebrate opsin and was also a key step for emergence of red-sensitive opsins in vertebrates (Terakita *et al.*, 2004) (Fig. 2B). From all examined *B. lanceolatum* opsins, only two (Op19 and Op20) have glutamate (E) at position 113, while one (Op11) has a different negative amino acid aspartate (D) at that position (for details see Pantzartzi *et al.*, (2017)). Whether D/E113 in any of these amphioxus opsins serves as a counterion still needs to be determined. Another important feature in opsin structure is the so-called tripeptide – a triptych of amino acids in the C-terminal part of opsin protein, responsible for contact between opsin and trimeric G protein (Marin *et al.*, 2000; Plachetzki *et al.*, 2007). Amphioxus opsins show a highly variable tripeptide sequence including the well-known tripeptide NKQ found in c-type opsin Op4 (a tripeptide typical of vertebrate visual opsins) and characteristic rhabdomeric-type HPK tripeptide identified in melanopsin (Op15) (for more details see Pantzartzi *et al.*, (2017)). It was shown that amphioxus Op12a can bind 11-*cis*-retinal as well as all-*trans*-retinal (Tsukamoto *et al.*, 2005). Vertebrate opsins have negligible affinity for all-*trans*-retinal. In vertebrate opsins, after light mediated conversion of 11-*cis*-retinal to all-*trans*-retinal, the all-*trans*-retinal is released, and replaced with 11-*cis*-retinal. The decrease in affinity

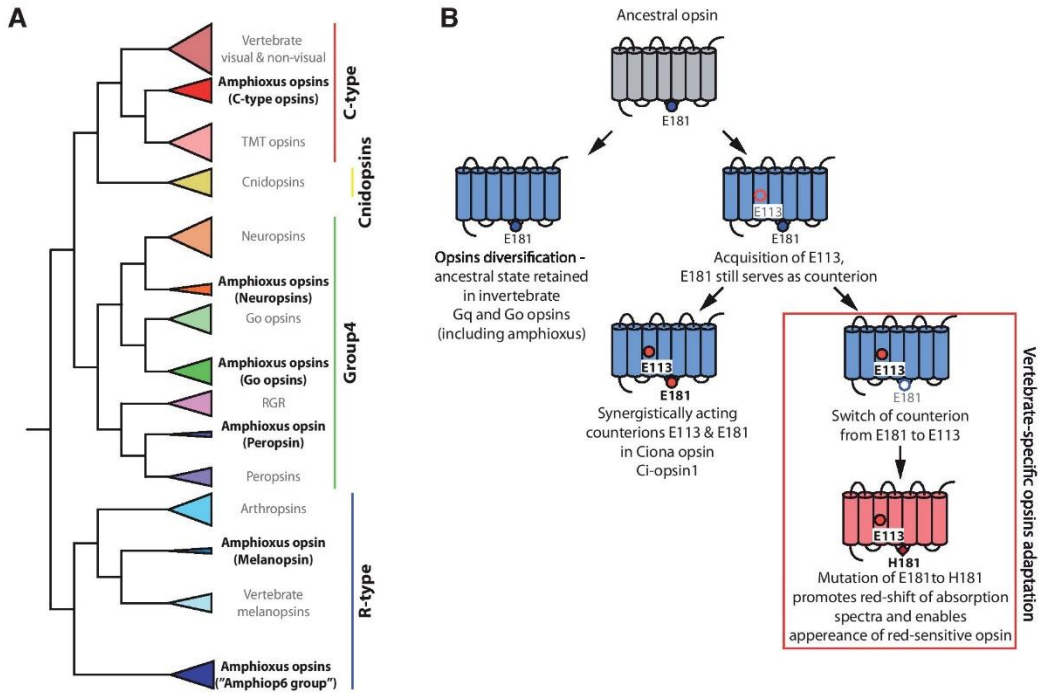

Fig. 2. The opsins in amphioxus – phylogenetic tree and evolution. (A) *Simplified phylogenetic tree of opsins, with stressed position of amphioxus opsins. Except for Cnidopsins, representantatives of each opsin family can be found in the amphioxus genome. Notable is expansion of several opsin families in amphioxus, namely Group4 opsins and R-type opsins. For detailed phylogenetic tree see Pantzartzi* et al., *(2017).* **(B)** *Scheme of proposed evolution of vertebrate specific opsin characteristics (mainly counterion). In ancestral opsin glutamate (E) at position 181 served as counterion. This counterion was retained in opsins of many invertebrate species, including amphioxus. During evolution, opsin of common ancestor of urochordates and vertebrates (commonly called "olfactores") attained glutamate at position 113. Due to subsequent changes in opsin structure, E113 became new counterion. In urochordate opsin both E113 and E181 act as synergistical counterions. In vertebrates function of E181 as counterion was lost and E113 retained as the only counterion present. Lower constraints on aminoacid present in position 181 led in vertebrates to acquisition of histidine (H) at this position and enabled a switch of opsin absorbance to red-spectrum. Scheme adapted from Terakita* et al., *(2012). Ciona opsin data based on Kojima* et al., *(2017).*

for all-*trans*-retinal enabled complete reduction of dark noise as well as faster exchange of all-*trans*-retinal for 11-*cis*-retinal during recovery period of vertebrate opsins. Rearrangements in opsin primary structure during evolution were therefore connected with enhanced affinity of vertebrate visual opsin for 11-*cis*-retinal and decreased affinity for all-*trans*-retinal. Additionally, amphioxus opsins have been shown to be less efficient in activating the downstream signaling cascade compared with vertebrate opsins (Terakita *et al.*, 2004). Vertebrate opsins thus underwent additional improvement to achieve higher activating potential, and consequently gained better signal yield per captured photon, when compared with ancestral opsins.

Several genomic and biochemical studies of amphioxus opsins confirm that amphioxus is the best proxy to gain insight into evolution of vertebrate opsins and their specific properties. With a complete list of amphioxus opsin genes published recently (Pantzartzi *et al.*, 2017), it will be worthwhile performing further biochemical studies (mainly to resolve the position of possible counterions and the nature of the tripeptides) to broaden knowledge about vertebrate opsin evolution.

Amphioxus photoreceptive organs

Four different photoreceptive organs, namely the frontal eye (FE), lamellar body (LB), Joseph cells (JCs) and dorsal ocelli (DO), respectively, have been described in amphioxus. Two of them, the FE and LB, consist of photoreceptor cells with ciliary morphology. Ciliary photoreceptors expand their membrane by modifying a non-motile cilium (with typical 9+0 microtubule structure) (Satir and Christensen, 2008), enabling incorporation of more molecules of photopigment in membrane and thus leading to higher efficiency for capturing photons. Ciliary photoreceptors serve as visual photoreceptors in vertebrates (Lamb, 2013; Lamb *et al.*, 2007) and as non-visual photoreceptors in invertebrates (Arendt *et al.*, 2004) (ciliary photoreceptors were, however, found also in eyes of some invertebrates, e.g. jellyfish or fan worms (Eakin and Westfall, 1962b; Lawrence and Krasne, 1965)). On the other hand, JCs and DO are formed of rhabdomeric photoreceptors (the typical visual photoreceptors in most protostomes) that utilize surface microvilli to attain expanded cell membrane. The presence of pigment cells makes the FE and DO directional photoreceptors. In contrast, the LB and JCs, lacking adjacent pigment, are non-directional photoreceptors. The homology between amphioxus photoreceptive organs and their possible vertebrate counterparts was enigmatic for a long time. In the subsequent sections we aim to summarize all relevant data regarding each of the photoreceptive organs in amphioxus. In addition, we present a current view about possible homologies between amphioxus and vertebrate photoreceptive organs.

Frontal eye

Due to its location at the anterior tip of the CV and the presence of pigment cells, the FE was already considered as a photoreceptive organ homologous to the vertebrate lateral eye by scientists in the 19th century (Joseph, 1904; Kemna, 1904; Kohl, 1890). Early studies dealing with photoreception of amphioxus, nevertheless, pushed the FE to the sidelines, showing, that the DO are more important for adult amphioxus light-guided behavior (Hesse, 1898; Parker, 1908). Parker (1908) (and later more precisely Crozier (1917)) confirmed an observation made by Hesse (1898), that the adult amphioxus photoresponse is connected with the presence of DO and he rejected the proposal of Krause (1888) that amphioxus can sense light with the whole neural tube. Parker also repeated experiments done by Nagel and Hesse, showing that upon removal of the anterior body end with the frontal eye, the rest of the body of the amphioxus still responded to the light in the same way as in intact animals (Hesse, 1898; Nagel, 1896). This cast doubt on the role of the FE in amphioxus photoresponses. Moreover no trace of optic nerve projecting from the FE posteriorly to the CV was observed at that time, which also questioned FE functionality as a possible photoreceptive organ. Yet Parker (1908) showed that when adult amphioxus was transversely cut in two parts, the anterior half was able to react to light, while the posterior half lost its light sensitivity, retaining its ability to be stimulated with addition of weak acid to the water. His results thus showed, that the anterior part of the neural tube (and probably also the FE) must be necessary for processing the photo-response, and that there is probably no direct connection between the dorsal ocelli and motor neurons. Although connections between the dorsal ocelli and the FE to motoneurons in adult amphioxus are still unknown, observations in *B. floridae* larvae show, contrary to Parker´s proposal, direct connection between 1st dorsal ocellus and motoneurons (Lacalli, 2002). Later, it was postulated that FE plays some role in regulation of the startle response after light illumination in adult amphioxus (Guthrie, 1975). Animals with the CV removed reacted more strongly to sudden illumination, and their reactions were more stereotyped and reliable compared to untreated animals (Guthrie, 1975). Additionally, as mentioned earlier, the importance of the frontal eye for larval vertical orientation, possibly necessary for feeding, has been documented (Stokes and Holland, 1995).

Electron microscopical (EM) examination of the CV in adult amphioxus showed that cells in the anterior tip of that region are arranged in layers (rows) transverse to the longitudinal axis of the neural tube (Meves, 1973). The cells in the row right behind the pigment cells of the FE were shown to be ciliated (as one would expect if they were homologous to vertebrate retinal photoreceptors). On the contrary, other neurons in the CV also have cilia (Meves, 1973). Moreover, the ciliary morphology was not as complex as the structure of ciliary photoreceptors in the vertebrate retina. Detailed anatomy of the FE was described in 12.5 day old *B. floridae* larvae using reconstructions of EM data of the CV (Lacalli, 1996; Lacalli. *et al.*, 1994). In spite of the scarcity of data, it is likely that the structure of the FE in young larvae or in adult amphioxus does not differ much. The only observed change was enlargement of the FE pigment spot during larval growth (Wicht and Lacalli, 2005). Detailed studies performed on larvae of *B. floridae* 12.5 day old larvae provided strong evidence for possible homology between the FE and vertebrate lateral eyes (Lacalli, 1996; Lacalli. *et al.*, 1994). This homology was based on the assumption that cells posteriorly adjacent to pigment cells are photoreceptors, even though their ultrastructure is not as elaborate as for some other ciliary photoreceptors. The pigment cup was shown to be formed of 3 rows, each consisting of 3 pigment cells. The cells located dorsally from the pigment cells form a series of morphologically slightly distinct transverse rows. They were numbered from anterior to posterior by numbers 1 – 4. Five Row1 cells were described as putative ciliary photoreceptors. Row2 cells (10 in total) were also shown to bear cilia, but they probably serve as interneurons

instead of acting as photoreceptors. Row3 and Row4 cells evinced a neuronal character, possibly serving as interneurons (see Fig. 3 for summary). Since the photoreceptor cells in amphioxus FE are arranged in single row, their receptor field is one dimensional.

Despite the difficulties in defining homology between amphioxus CV and vertebrate brain (Albuixech-Crespo *et al.*, 2017), the homology between FE and vertebrate eyes appears simpler. Amphioxus orthologues of transcription factors important for development of vertebrate retinal neurons and retinal pigmented epithelium (RPE) were found to be expressed in the developing FE (Vopalensky *et al.*, 2012). Molecular analysis uncovered distinct gene expression fingerprints for pigmented cells of the FE, for putative FE photoreceptors (Row1 cells) and for FE interneurons (Rows2-4). More specifically Otx was shown to be expressed in Row1 photoreceptors and in pigment cells; Pax4/6 was detected in Row1 photoreceptors and Row3 and 4 cells, Rx is probably expressed in Row1 photoreceptors and later in developing Row3 and Row4 cells and Pax2/5/8 and Mitf expression was documented in pigment cells (Fig. 3) (Glardon *et al.*, 1998; Kozmik *et al.*, 1999; Vopalensky *et al.*, 2012; Williams and Holland, 1996). Otx and Pax4/6 expression

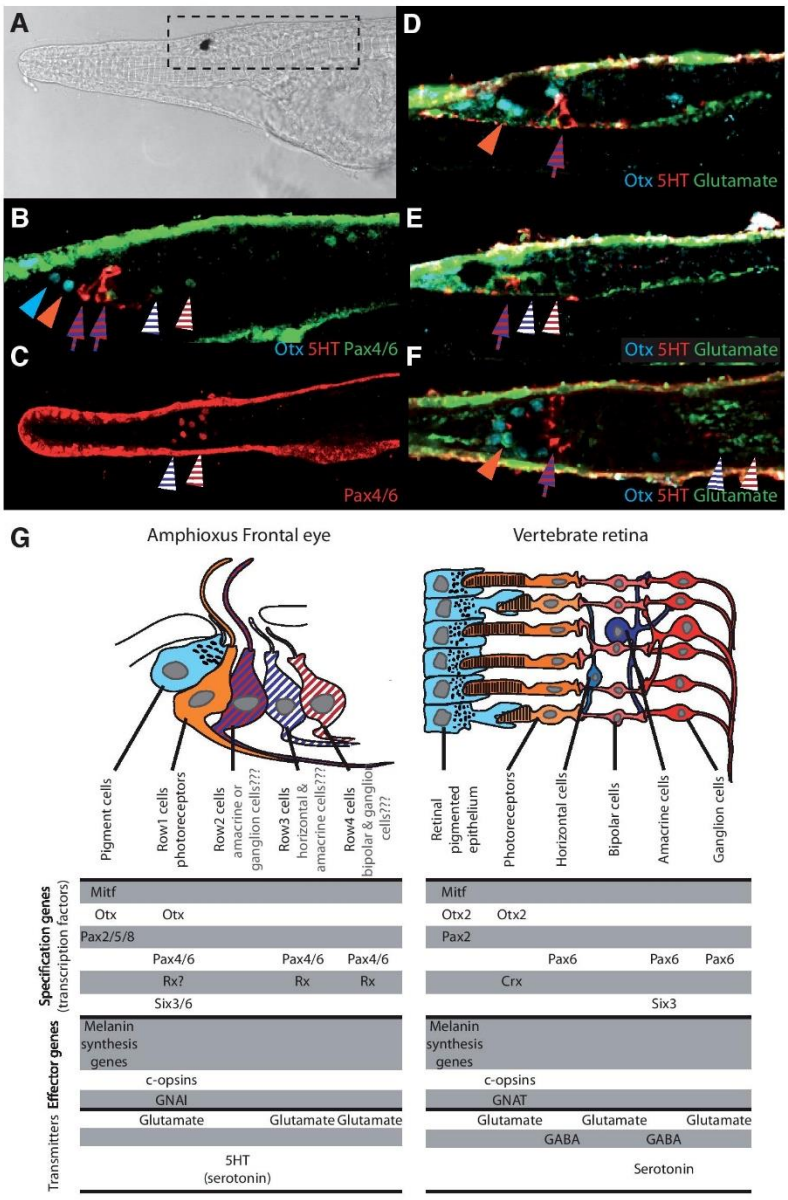

Fig. 3. Molecular fingerprint of amphioxus frontal eye cells and scheme of their proposed homology to vertebrate retinal cell types. (A) *Anterior part of 4 days old larvae of* B. lanceolatum. *Dashed rectangle marks region depicted in detail in (B-F).* **(B)** *Lateral view of larvae stained with antibodies against amphiOtx, amphiPax4/6 and 5HT. Cyan arrowhead points to Pigment cell; orange arrowhead points to Row1 photoreceptor cells; red-blue hatched arrow points to Row2 cells; blue-white hatched arrowhead points to Row3 cells; red-white hatched arrowhead points to Row4 cells.* **(C)** *Dorsal view of area marked in (A). Larvae was stained with anti Pax4/6 antibody. Pax4/6 positive Row3 and Row4 cells are highlighted.* **(D)** *Lateral view of larvae stained with antibodies against amphiOtx, 5HT and glutamate.* **(E)** *Lateral view of larvae stained with antibodies against amphiOtx, 5HT and glutamate. Different optical section than in D was chosen to show Glutamate reactivity of Row3 cells.* **(F)** *Dorsal view of larvae stained with antibodies against amphiOtx, 5HT and glutamate.* **(G)** *Scheme of proposed homologies between particular cell types in amphioxus FE and vertebrate retina. For vertebrate retinal cell types specifying transcription factors, only selection of homeodomain transcription factors is depicted, to simplify the comparison with expression pattern of amphioxus FE cell types (expression of only homeodomain transcription factors was mapped in FE on single cell resolution, for details see Vopalensky* et al., *(2012)). Rx expression in Row1 photoreceptors cells was not confirmed with antibody staining and is therefore marked with a "?". The proposed homology between amphioxus Row2, 3 & 4 cells and vertebrate retinal interneurons includes also data from EM analysis, which were mapping the projections of amphioxus FE neurons (Lacalli, 1996). Data about vertebrate cell types come from Bassett and Wallace (2012), Kolb (2011) and Swaroop* et al., *(2010). Anti amphiOtx and amphiPax4/6 antibodies were used from study by Vopalensky* et al., *(2012). Anti-5HT antibody - Abcam ab66047; Anti-Glutamate antibody – Abcam ab120049.*

starts early in amphioxus development (at mid-neurula), being important for the development of major parts of the CV (Glardon *et al.*, 1998; Williams and Holland, 1996). Later in development, expression of both genes becomes more restricted to particular cells of the developing FE (Vopalensky *et al.*, 2012). The earliest expression of Rx starts at late neurula stage in the anterior tip of the CV, probably in developing Row1 photoreceptor cells. During the course of development, the expression of Rx and Pax4/6 shifts more posteriorly to Row3 and Row4 cells. Next, expression of Six3/6, the amphioxus orthologue of the vertebrate Six3 and Six6 genes involved in eye development, was documented in the developing FE (Kozmik *et al.*, 2007). Six3/6 and Pax4/6 were shown to be expressed in neurons of the primary motor center (PMC) – anterior-most motoneurons, probably reacting to signals coming from the FE (Kozmik *et al.*, 2007; Vopalensky *et al.*, 2012). Based on BrdU staining, so-called dorsal compartment motoneurons (probably responsible for control of muscular movements during swimming (Bardet *et al.*, 2005; Wicht and Lacalli, 2005)), located posteriorly to the CV, seem to be differentiated early in development (at mid-neurula stage), while the neurons of FE are still developing (Holland and Holland 2006). The expression of Pax6 was shown to be exclusive to parts of the CV weakly stained with BrdU, confirming the role of Pax6 in neuronal differentiation in the FE (Kozmik *et al.*, 2007). Our data provide evidence for glutamate immunoreactivity of FE photoreceptors (Fig. 3) and confirmed prediction made by Lacalli and Candiani (2017). Vertebrate photoreceptors display the same glutamate immunoreactivity (Connaughton, 2005).

Based on expression of c-opsins and presence of neurotransmitters, the differentiation of FE photoreceptors seems to be completed as soon as the larvae begin to feed (Vopalensky *et al.*, 2012). This, combined with data from behavioral studies (Stokes and Holland, 1995), supports the possible role of the FE in feeding behavior. Expression of two amphioxus c-opsins (Op1 and Op3) was detected in FE photoreceptors, corroborating their ciliary character. In addition, expression of each of the opsins was detected in morphologically distinct cells, pointing to possible spectral diversity of amphioxus FE photoreceptors (Vopalensky *et al.*, 2012). As stated above, amphioxus c-opsins form a sister group to vertebrate c-opsins. The origin of vertebrate specific c-opsins is still not resolved. It is, however, clear that the primary structure of vertebrate opsins underwent several optimizations to achieve higher activation potential, different spectral sensitivity and higher affinity for 11-*cis* retinal (Terakita *et al.*, 2004; Tsukamoto *et al.*, 2005). The downstream phototransduction cascade also appears to have been modified in the course of evolution. Transducin (Gαt or GNAT), the Gα subunit of trimeric G proteins, mediating phototransduction cascade in vertebrate rods and cones, was not found in the amphioxus genome (Vopalensky *et al.*, 2012). Its role in ciliary-like phototransduction in amphioxus FE is replaced by action of the GNAI subunit (Vopalensky *et al.*, 2012). It was shown that GNAT can be found only in the genomes of vertebrates, and it most likely originated by tandem duplication of the GNAI gene. Ancient GNAT then underwent quadruplication during the 2RWGD (Lamb and Hunt, 2017; Lamb *et al.*, 2016; Larhammar *et al.*, 2009). In vertebrates two different GNATs (GNAT1 and GNAT2) participate in rod and cone phototransduction, respectively. A third gene, gustducin (GNAT3), is utilized in taste receptor cells. Interestingly GNAT3/X (lamprey homolog of vertebrate GNAT3) is probably involved in phototransduction cascade of lamprey photoreceptors (Lamb and Hunt, 2017). The appearance of GNAT gene in vertebrates also led to changes in the phototransduction cascade. Vertebrates use cGMP as a second messenger in both rods and cones. After light absorption, GNAT activates a phosphodiesterase that is responsible for decreasing the cGMP level, cGMP-sensitive CNG channels are closed, leading to hyperpolarization of the photoreceptor cell. This cascade is the same for all vertebrate ciliary photoreceptors examined to date (Fig. 4A) (Lamb, 2013). Recently, the existence of a distinct phototransduction cascade for amphioxus FE photoreceptors was proposed, based on gene inventory (Lamb and Hunt, 2017). Phototransduction starts with GNAI that inhibits adenylate cyclase which is responsible for synthesis of cAMP. Inhibition of synthesis of cAMP together with continuous activity of PDE leads to a decrease in cAMP, closure

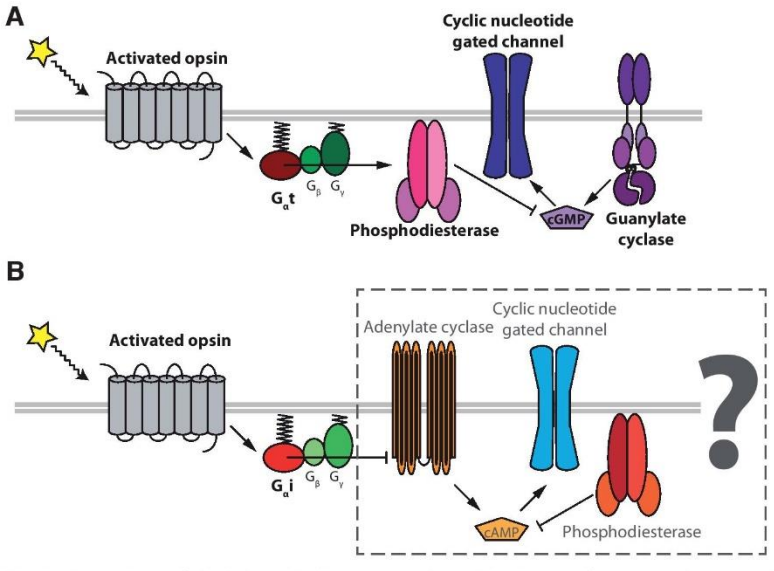

Fig. 4. Comparison of phototransduction cascade in vertebrate rods & cones and proposed phototransduction cascade in amphioxus frontal eye (FE) photoreceptors. (A) *Phototransduction cascade in vertebrate photoreceptors. The cascade starts with stimulation of opsin and continues with activation of GNAT. Next GNAT stimulates phosphodiesterase (PDE), which degrades cGMP. Decrease of cGMP intracellular level leads to closure of CNG channels.* **(B)** *Recently proposed phototransduction cascade for amphioxus FE photoreceptors (Lamb and Hunt, 2017). The cascade starts with stimulation of opsin and continues with activation of GNAI. GNAI inhibits adenylate cyclase, which leads, in combination with continuous activity of PDE, to decrease in the level of intracellular cAMP. Subsequently CNG channels are closed and the cell hyperpolarize. Identified members of cascade are written in bold black, while proposed members are written in grey and framed by dashed rectangle.*

of CNG channels, and hyperpolarization of the FE photoreceptor cell (Fig. 4B). Experimental support of this hypothetical cascade has not yet been provided, and only the expression of GNAI in the FE photoreceptors has been confirmed.

The proposed homology of amphioxus pigment cells and Row1 photoreceptors cells with vertebrate RPE and photoreceptors respectively is relatively well supported. However, the homology between putative amphioxus interneurons within the FE and particular classes of vertebrate retinal interneurons remains elusive. Differentiated Row2 cells were shown to be serotonin positive (Candiani *et al.*, 2012; Vopalensky *et al.*, 2012). In the vertebrate retina, a distinct class of amacrine cells is serotonin positive, but the role of serotonin as a neurotransmitter has not been confirmed (Kolb, 2011). On the other hand, Row2 cells send terminals to the presumptive "visual processing" center of the CV (Vopalensky *et al.*, 2012), pointing to homology with vertebrate retinal ganglion cells. The Row2 cell projections are, however, ipsilateral (Lacalli, 1996), while most ganglion cells in the vertebrate optic nerve project contralaterally. Moreover Row2 fibers seem to form irregular terminals and do not show any sign of definitive neuronal synapses (Lacalli, 1996). Contralateral projections in amphioxus are instead sent by Row4 cells (Lacalli, 1996). This would suggest homology between Row4 and retinal ganglion cells. Additional insight supporting the formerly proposed homology between Row2 and vertebrate retinal ganglion cells has been obtained by comparison of amphioxus and lamprey visual processes (Suzuki *et al.*, 2015). In lamprey, there is a fundamental difference between larval and adult eyes. The larval eyes have a simple bi-layered retina and lack a lens, being covered with translucent skin. Lamprey larval eyes are thus reminiscent of the eyes of hagfish. During metamorphosis, lamprey eyes become more complex anatomically and physiologically, coming to resemble those of higher vertebrates. Comparison of neural circuits and brain patterning between amphioxus and larval and adult lamprey (*Lethenteron camtschaticum*) has pointed to similarities and probably evolutionarily conserved characters (Suzuki *et al.*, 2015). In both amphioxus and lamprey, the photoreceptors develop in Otx- and Pax6-positive regions in the presumptive prosencephalon. Next, the signal is transmitted by neurons sending processes to integrative neurons in Pax6-positive presumptive prosencephalic region in amphioxus and larval lamprey. This seems to be the ancestral state from which, by additional modification, the current vertebrate visual circuitry evolved. This improved circuitry can be found in adult lamprey and jawed vertebrates, where the signal is transmitted to a tectum, localized in a mesencephalic region defined by Pax2 and Engrailed expression. New data, however, show that the amphioxus CV exhibits characteristics typical of both diencephalon and mesencephalon without clear distinguishable borders (Albuixech-Crespo *et al.*, 2017). This would also be supported by the proposed visual circuitry in amphioxus, where the projecting Row2 neurons send their processes to the Di-Mesencephalic part of CV. It would, however, change the view on evolution of vertebrate visual circuitry presented earlier (Suzuki *et al.*, 2015). In the more-recently proposed scenario, projection to the mesencephalon would be the evolutionarily-conserved state,

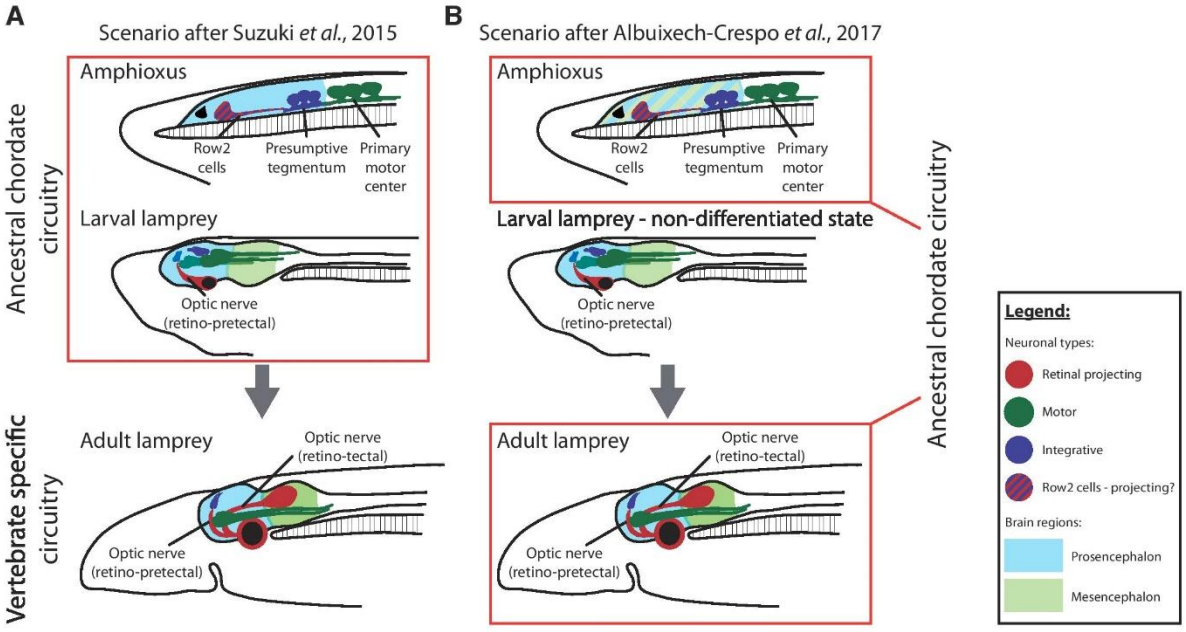

Fig. 5. Possible scenarios for evolution of vertebrate specific visual circuitry. (A) *First scenario was proposed by Suzuki* et al., *(2015). According to this scenario ancestral state for visual circuitry in all chordates would be transmission of signal from photoreceptors to visual processing center localized in prosencephalic-like Pax-6 positive part of the brain. On the other hand,* **(B)** *new data showed, that developing CV of amphioxus displays characteristics common for both prosencephalon (more specifically diencephalon) and mesencephalon in the same time (Albuixech-Crespo* et al., *2017). This would suggest, that ancestral chordate state of visual circuits is transmission of signal from photoreceptors to mesencephalic part of the brain. The situation in larval lamprey would thus represent not fully differentiated state.*

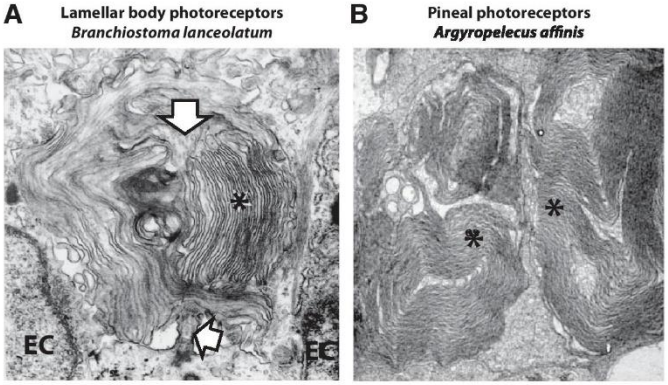

Fig. 6. Ultrastructure of photoreceptors of amphioxus lamellar body and vertebrate pineal gland. *Electron microscopical photography of amphioxus lamellar body photoreceptors* **(A)** *and photoreceptors of pineal organ in fish* Argyropelecus affinis **(B)**. *Asterisks (*) mark the membranous lamellae that are conspicuously similar in both photoreceptor types. Arrows in* **(A)** *mark cilium from which lamellae in amphioxus lamellate cells arise. EC, ependymal cells adjacent to lamellate cells. Photo of amphioxus lamellate cells used with permission of the publisher from Ruiz and Anadon (1991b). Photo of* Argyropelecus affinis *pineal photoreceptors used with permission of the publisher from Bowmaker and Wagner (2004).*

being present already in the chordate ancestor (Albuixech-Crespo *et al.*, 2017), while the nerve projection of eyes in larval lamprey would represent an incompletely-developed state (see Fig. 5 for comparison of the two proposed scenarios).

In conclusion, it seems that the homology that was proposed long ago between the amphioxus FE and vertebrate lateral eyes (Kemna, 1904), receives additional support from newly-available molecular data. Based on expression profiles, and despite their simple ultrastructure, amphioxus FE photoreceptors seem to be homologs of vertebrate rods and cones, and might represent a form of photoreceptor found in a common chordate ancestor. The difference in ultrastructure between FE photoreceptors and rods and cones is, however, striking. It seems evident that the expansion of membrane in rods and cones lead to improved photon absorption and thus enabled progress of high spatial resolution (Nilsson, 2013). This was arguably one of the crucial steps in the arms race between predators and prey during evolution. The expanded surface area of photoreceptors, as well as the above mentioned changes in opsin structure and in the phototransduction cascade, enabled higher sensitivity and resolution in the eyes of an ancestor of vertebrates. To confirm this hypothesis, more experimental data is required about physiology and the phototransduction cascade in the photoreceptors of the amphioxus FE.

Lamellar body

Of the four known amphioxus photoreceptive organs, the LB is the one with the least information about its development, molecular markers and physiology. On the other hand, relatively strong morphological evidence supports homology between the LB and its putative vertebrate counterpart, the pineal organ. The function of the LB as a possible photoreceptive organ was noted for the first time by Satir in 1958 (unpublished results mentioned in Eakin and Westfall, 1962a). The ultrastructure of lamellate cells was, at that time, confusing, because it did not show similarity with vertebrate retinal photoreceptors. While rod and cones membrane processes are perpendicular to the cilium they arise from, the membranous processes of lamellate cells are parallel with the cilium (Eakin and Westfall, 1962a). This arrangement is typical for vertebrate pineal photoreceptors (Ruiz and Anadon, 1991b) and the lamellar body was (and still is) thus considered as a homolog of the vertebrate pineal organ (Lacalli. *et al.*, 1994; Nakao, 1964). The similarity of photoreceptor ultrastructure between pineal and LB photoreceptors is indeed striking (see Fig. 6). The ciliary structure of the lamellate cells was, however, questioned after observations arguing that the membranous folds of lamellate cells come directly from the cell membrane and not from the modified cilium (Meves, 1973). Detailed EM analysis, nonetheless, confirmed the ciliary character of the membranous appendages of the lamellate cells, showing that the main cilium they arise from contains a 9+2 microtubule structure (Ruiz and Anadon, 1991b) (interestingly this structure is typical for motile cilia, for review about cilia structure see Satir and Christensen (2008)). Moreover each of the membranous appendages is supported by accessory microtubules that are not derived from the basal axonema.

Almost nothing is known about the gene regulatory network involved in development of the LB in amphioxus. Development of the LB starts probably at mid-neurula stage from the posterior part of a Pax6-positive domain of the CV (Glardon *et al.*, 1998). Pax6 is expressed in the lamellar body region at least to the two and half gill slit larvae stage in *B. floridae* (Vopalensky *et al.*, 2012). In vertebrates, Crx was shown to be involved in development of both lateral eyes and pineal organ. Expression of amphioxus Otx, the homolog of vertebrate Crx, was however not detected in the developing LB (Vopalensky *et al.*, 2012). Of the four amphioxus c-opsins examined, none was found to be expressed in the LB (Vopalensky *et al.*, 2012). It is therefore difficult to determine when the cells of the LB become photosensitive or if they ever become photoreceptors.

Recent data showed that lamellate cells can be detected as early as in the first gill slit larvae of *B. floridae* (Bozzo *et al.*, 2017). The number of cells forming the lamellar body increases during larval development from about 6 cells in 1 gill slit larvae, through 8 cells in 2 gill slits larvae to about 40 in 12.5 days old larvae of *B. floridae* (Bozzo *et al.*, 2017; Lacalli. *et al.*, 1994). The development of the LB correlates strikingly with the appearance of photosensitive behavior in larvae and is thus most likely responsible for initial light response of amphioxus larvae (Lacalli. *et al.*, 1994). Moreover lamellate cells in larvae probably send processes to the amphioxus tegmentum, and are involved in modifying the switch between different modes of swimming (for information about current views on locomotory circuits in amphioxus see Lacalli and Candiani (2017)). It seems that the LB processes might repress the startle reaction and contribute to the hovering of larvae during swimming. Later in development compact LB disaggregates (possibly due to forward expansion of JCs), since only scattered lamellate cells were detected in adults (Castro *et al.*, 2015; Meves, 1973). As described earlier, amphioxus larvae display a typical circadian rhythm guided behavior (diurnal migration), while adults live mostly borrowed in the sand during both day and night. Presence of compact LB in amphioxus larvae

(and not in adults) supports its proposed homology with the pineal organ. The pineal organ in vertebrates is important for maintaining the circadian rhythm and so is probably the LB in amphioxus larvae. Amphioxus adults still exhibit higher activity during the night, but the photoreceptors responsible for circadian rhythm control are more likely JCs than the LB (see section about JCs for more details). We hypothesize that the LB is thus more needed and therefore more developed in larvae than in adults.

Of special interest is the close proximity of lamellate cells and Joseph cells. In later developmental stages the JCs grow over the lamellate cells and cover them. The connection between JCs and lamellate cells (rhabdomeric and ciliary photoreceptors in close proximity) puzzled scientists for long time. It led to proposals about similarity with vertebrate retina where rods and cones (ciliary photoreceptors) and ipRGCs (rhabdomeric-like photoreceptors) are closely associated (Ruiz and Anadon, 1991b). Lamb (2013) came with a hypothesis, that close proximity of ciliary and rhabdomeric photoreceptors led to synaptic transmission between them, and in due course the rhabdomeric cells became projecting neurons (ganglion cells). Close spatial association was noted also between distinct photoreceptors of some ascidians. In this case, the ciliary and rhabdomeric photoreceptors are however present at different stages of development (Ruiz and Anadon, 1991b). Due to limited data regarding both LB and JCs, their possible functional cooperation remains elusive.

Taken together, the features of the LB (photoreceptor ultrastructure, development correlated with light-guided larval behavior and localization in the posterior part of the CV) strongly support its homology with vertebrate pineal organ. It is interesting that while in vertebrates the pineal gland is retained for the entire life, the LB in amphioxus disaggregates (and might thus loose some of its photoreceptive function) in adults. The striking similarity between photoreceptors of the LB and the vertebrate pineal organ led to the proposal that their ultrastructure (optimized for maximizing light absorption) was retained during the course of evolution, probably due to their optimal anatomy to function in dim light (Lacalli, 2008). This is more remarkable when one compares the changes in ultrastructure undergone by the ancestral chordate photoreceptors on the way to more elaborate ciliary photoreceptors in vertebrate retina during the course of evolution. The homology between the amphioxus LB and vertebrate pineal organ suggested by morphology should be examined further with additional data from developmental genetics and physiology.

Rhabdomeric photoreceptors

Two photoreceptive organs with rhabdomeric morphology develop in amphioxus – the dorsal ocelli (DO, sometimes also called organs of Hesse) and Joseph cells (JCs). Rhabdomeric photoreceptors (with microvilli membrane protrusions) are typical visual photoreceptors in invertebrates. In vertebrates the ipRGCs, which are considered as remnants of ancestral chordate rhabdomeric-like photoreceptors, do not have microvilli at their surface. To date, there is still an ongoing debate whether the DO and JCs are more closely homologous to vertebrate ipRGCs (which have been shown to be involved in circadian rhythm and pupillary reflex) or invertebrate photoreceptors. The DO and JCs share some common features. Nevertheless some important differences exist in their development, physiology and morphology, so when appropriate we will deal with the DO and the JCs separately. The first obvious difference between the JCs and the DO is that each dorsal ocellus consists of one photoreceptor cell and one pigment cell, and is thus directional photoreceptor, while the JCs lack pigment and are thus non-directional photoreceptors. Due to the presence of pigment, the DO were already connected with photoreceptive behavior at the turn of 20th century (Hesse, 1898; Parker, 1908). Boveri (1904) even proposed a scenario, saying that DO were evolutionary precursors of vertebrate lateral eyes, which would arise from DO by their aggregation into complex organ. This suggestion was however soon negated by Kemna (1904) (and later also by Jelgersma (1906)), showing that DO were missing along the cerebral vesicle in the right place to give rise to vertebrate lateral eyes. A description of the JCs had also been provided early in the 20th century (Joseph, 1904), but due to lack of pigment, they were neglected from studies dealing with photoreceptive behavior in amphioxus.

The first DO is already developing at mid-neurula stage, as the first photoreceptive organ in amphioxus. The role of this first DO in phototaxis is, however, unknown. Development of additional DO follow soon after the development of other photoreceptive organs at mid-larval stages. Intriguingly there is an anatomical difference between the first DO and all of those that develop subsequently. The first DO consists of two photoreceptor cells, with one pigment cell intercalated between them (Fig. 7A-C), while the subsequently developing DO are formed by one photoreceptor cell and one adjacent pigment cell (Fig. 7D). The reason for this difference is not known. The DO are located along the entire length of the neural tube, beginning from the border between the neural tube and the CV at approximately the third myotome (Nakao, 1964). The fact that the DO are not present in much of the CV was the reason for aforementioned dispute between Boveri (1904) and Kemna (1904) about possible role of the DO in evolution of vertebrate lateral eyes. The DO are located laterally or ventrally from the central canal on each side of the neural tube (Hesse, 1898). Amphioxus body segments on the right side are shifted by half of one segment posteriorly relative to those on the left side, and a corresponding shift is observed for the DO on the right side relative to those on the left side. Longitudinally the distribution of the DO varies along the neural tube, being highest in the anterior, lowest in the middle part of neural tube and increasing in numbers again in the most posterior part. They are arranged in clusters along the neural tube, with the first cluster consisting of only two DO on each side of the neural tube, and gradually increasing from the fourth myotome to about 25 on each side of the neural tube. In total, about 1500 DO can be found on each side of the neural tube in the adult amphioxus (Nakao, 1964), making them the most abundant type of photoreceptors in adult amphioxus. It was noted initially that most of the DO look slightly to the right side to be oriented to light coming from the right side (Hesse, 1898). Franz (1923) provided detailed analysis of orientation of DO on transversal and longitudinal sections. DO laying ventrally from neural tube central canal face ventrally, those laying on the left from central canal face upwards slightly to right and those laying on the right side face right downwards. The functional meaning of the asymmetric arrangement is however not clear. The distribution of DO is well correlated with the light intensity necessary to evoke stimulation of adult amphioxus. The anterior region of the neural tube appears to be the most light-sensitive, followed by the posterior part (that being only slightly less sensitive). In contrast, the middle part of the neural tube is about

ten times less sensitive compared to the anterior region (Parker, 1908; Sergeev, 1963). It is generally accepted that DO might be necessary to provide an adult amphioxus with information about how deep its body is buried in the sand, and DO are exclusively adapted to this task (Lacalli, 2004).

Limited information exists about the gene expression profile of DO. Apart from melanopsin, that serves as the best defining marker and key physiological component of amphioxus DO (as well as JC) photoreceptors (Koyanagi *et al.*, 2005), only the gene encoding estrogen-related receptor (ERR) was unequivocally found to be expressed in the two photoreceptors of the first DO and interestingly also in dorsal compartment motoneurons (Bardet *et al.*, 2005). These were shown to be innervated by the 1st DO (Lacalli, 2002). Several studies focused on transcription factors known to be involved in development of vertebrate and invertebrate visual systems, such as the members of the *Drosophila* retinal determination gene network (RDGN) (Davis and Rebay, 2017). Expression of amphioxus RDGN orthologous genes belonging to Pax, Six, Eya and Dach families, respectively, was investigated by whole mount *in situ* hybridization at various stages of embryonic development. Notably, Pax6 expression was not detected in developing first or subsequent DO (Glardon *et al.*, 1998), placing DO among those animal photoreceptive organs whose formation is independent of Pax6 function. Instead, the area from which the first DO develops expresses Pax2/5/8 during the neurula stage (Kozmik *et al.*, 1999). At later developmental stages scarce Pax2/5/8 (Kozmik *et al.*, 1999) and Dach (Kozmik *et al.*, 2007) expression was detected along the neural tube – whether this expression is localized to differentiating pigment or photoreceptor cells of the subsequently developing DO remains to be determined. Transient expression of Six4/5 and Eya was detected in the amphioxus neurula in two cells in the region where the first DO develops (Kozmik *et al.*, 2007). Co-expression analysis with specific markers such as melanopsin is needed to confirm that these cells indeed represent the two developing photoreceptors of the first DO. Expression of genes known from the pigment synthesis cascade in the vertebrate retinal pigment epithelium (namely Mitf, Tyrp-a, Tyrp-b and Tyrosinase) was detected in the area of the pigment cell of the first DO (Vopalensky *et al.*, 2012; Yu *et al.*, 2008) and the black pigment was melanin (Vopalensky *et al.*, 2012). These results indicate that the same cascade is used for the synthesis of the shielding pigment in amphioxus and vertebrates. Moreover it showed that the same pigmentation cascade is used for two distinct photoreceptive organs (the FE and DO) in amphioxus (Vopalensky *et al.*, 2012).

The development of JCs is not as well documented as the development of DO. The first description of JCs was made in adult amphioxus (Joseph, 1904; Ruiz and Anadon, 1991a; Watanabe and Yoshida, 1986; Welsch, 1968). So far, however, no study aimed at identifying their advent in earlier stages. JCs are known to develop in the dorso-caudal part of the CV (Ruiz and Anadon, 1991a). In larvae, JCs are probably located posterior to the LB, while in adults the JCs form a cap above the scarce lamellate cells. About 400-450 JCs are present in the adult amphioxus (Castro *et al.*, 2015). Studies of the ultrastructure of JCs confirmed their rhabdomeric character. JCs are about 15 um in diameter and oval in shape. Their microvilli extend over most of the cell surface and are enclosed by surrounding glial cells. One or two cilia with 9+0 structure emanate from the membrane of each JC, but these are not related to rhabdom structure. Interestingly, notable differences in rhabdom structure were observed between dark-adapted and light-adapted JCs. In dark-adapted JCs, the microvilli are thinner, more numerous and more regularly arranged compared to light

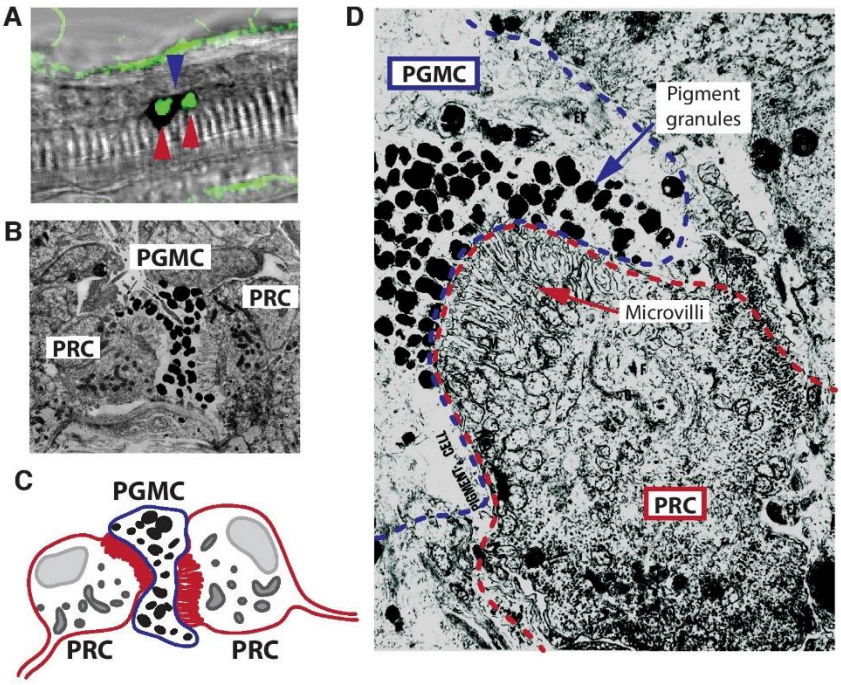

Fig. 7. Melanopsin expression in amphioxus dorsal ocelli (or Hesse organs) and ultrastructure of dorsal ocellus (DO). (A) *Detail of melanopsin expression in 1st dorsal ocellus in 2 days old* B. floridae *larvae. Red arrowhead points to photoreceptor cell, blue arrowhead points to pigment cell. Two photoreceptor cells forming the first dorsal ocelli are visible.* **(B)** *Electron microscopical photo of 1st DO of 12.5 days old larva of* B. floridae. *Photo used and adapted with permission of the publisher from Kozmik (2008).* **(C)** *Scheme of 1st DO based on photo in B.* **(D)** *ultrastructure of DO in adult* B. belcheri. *Except for 1st DO other DO are formed by one photoreceptor and one adjacent pigment cell. Borders of photoreceptor cell are marked with dashed red light. Borders of pigment cell are marked with dashed blue line. Microvilli in photoreceptor cell and pigment granules in pigment cell are highlighted. Photo used and adapted with permission of the publisher from Nakao (1964).*

adapted JCs. Gross morphological changes were accompanied by changes of vesicle content in the cytoplasm. Similar changes in rhabdom structure and content of cytoplasmic granules were observed in photoreceptors of several invertebrate species (Arikawa *et al.*, 1987; Arikawa *et al.*, 1988; Hariyama *et al.*, 2001; Sakura *et al.*, 2003). Noticeably, the above-mentioned changes were shown to appear even in specimens kept in constant darkness, and are therefore likely regulated by circadian rhythm pathways rather than a direct response to light intensity. In case of JCs, however, no information is available about the effect of the light/dark cycle on rhabdom structure. It is noteworthy that while the LB disaggregates during development, the number of JCs and DO seems to increase. This would point to a switch of roles for maintenance of circadian rhythms from LB in larvae to JCs and/or DO in adult amphioxus. With the primary role of DO proposed to be in providing information about the vertical position of amphioxus within a burrow, the JCs seem to play the lead role in directing circadian rhythms in the adult amphioxus.

DO photoreceptor cells are described as having a single basal axon. The data from larvae showed that projections from the first DO are ipsilateral (Lacalli, 2002), whereas in adult amphioxus the projections from the DO are contralateral (Castro *et al.*, 2006). Amphioxus larvae exhibit two different swimming modes – slow undulatory swimming involved mainly in vertical diurnal migration, and rapid muscular movement for escape (Guthrie, 1975; Lacalli and Kelly, 2003). Two different muscle types are probably involved in these reactions – superficial muscles involved in the slow swimming mode and deep muscle fibers responsible for the fast mode of swimming (Lacalli and Candiani, 2017; Lacalli, 2002). Tracking the axons of the first DO showed that they probably target exclusively dorsal compartment motoneurons involved in innervation of superficial fibers. The first DO is thus probably involved in controlling the slow swimming mode (Lacalli, 2002). However physiological recordings are needed to confirm this.

In JCs, some kind of axonal projections were detected but their exact terminals were not found (Welsch, 1968). More recent EM survey of juvenile amphioxus for JCs axon did not provide any positive results. It is, however, still possible, that JCs develop their processes later in development.

In contrast to FE photoreceptors, where at least two distinct ciliary opsins are present and the molecular details of the downstream cascade are not entirely resolved, the situation in DO and JC photoreceptors is better known. As stated above, melanopsin is the only opsin expressed in both classes of amphioxus rhabdomeric photoreceptive organ – JCs and DO (Koyanagi *et al.*, 2005). Amphioxus melanopsin was shown to be bistable (Koyanagi *et al.*, 2005). This means that upon irradiation, 11-*cis*-retinal is converted to all-*trans*-retinal, as is common for most opsins. However, the all-*trans*-retinal is not released from melanopsin, but is converted back to 11-*cis*-retinal after irradiation by absorption of another photon. This is a shared characteristic between all melanopsins and rhabdomeric opsins that have been studied. Amphioxus melanopsin has its maximum absorption in the blue part of the spectrum – between 470 and 485 nm (Gomez Mdel *et al.*, 2009; Koyanagi *et al.*, 2005), similar to vertebrate melanopsins.

The physiology and phototransduction cascade in isolated DO and JCs has been investigated in several studies (Acemel *et al.*, 2016; Angueyra *et al.*, 2012; Ferrer *et al.*, 2012; Gomez Mdel *et al.*, 2009; Nasi and del Pilar Gomez, 2009; Peinado *et al.*, 2015; Pulido *et al.*, 2012). These seminal studies not only confirmed that JCs and DO indeed function as photoreceptors, but also provided comparative data with respect to invertebrate rhabdomeric photoreceptors and ipRGCs. The irradiation of both cell types leads to depolarization and an increase in membrane conductance (Gomez Mdel *et al.*, 2009). This is similar to the physiological changes observed in other invertebrate rhabdomeric photoreceptors and in vertebrate ipRGCs. After irradiation, the phototransduction cascade begins with activation of GNAQ (Bailes and Lucas, 2013; Gomez Mdel *et al.*, 2009; Terakita *et al.*, 2008). In support of this step of the cascade is the fact that GNAQ is co-expressed with melanopsin in both JCs and DO (Koyanagi *et al.*, 2005). The ancient chordate GNAQ gene underwent quadruplication and specialization for various tasks after 2RWGD, as did the genes of the vertebrate GNAT family. Nevertheless, the core of the ipRGC phototransduction cascade (melanopsin activating member of GNAQ family) seems to be the same. The next step of the phototransduction cascade in JCs and DO is the activation of PLC and the hydrolysis of PIP2 to IP3 and DAG. The IP3 branch of PLC signaling was verified, while DAG seems to have minimal or no role in mediation of the conductance change (Angueyra *et al.*, 2012). The situation in ipRGCs is more complicated, since neither IP3 nor DAG appears to be involved in the phototransduction cascade (Graham *et al.*, 2008) (reviewed by Hughes *et al.*, (2012)). Results of several studies suggest that PIP2 itself might act as second messenger in the ipRGC phototransduction cascade (reviewed by Hughes *et al.*, (2012)). On the other hand, in invertebrate rhabdomeric photoreceptors, the detected downstream effectors of phototransduction cascade vary between species as well as within species. Proposed candidates include IP3 (Brown *et al.*, 1984; Fein *et al.*, 1984) or Ca^{2+} (Payne *et al.*, 1986) in *Limulus polyphemus*; DAG or its metabolites, e.g. PUFAs (Chyb *et al.*, 1999; del Pilar Gomez and Nasi, 1998; Delgado *et al.*, 2014) in *Drosophila* or scallop; protons (Huang *et al.*, 2010) and mechanical forces (Hardie and Franze, 2012) in *Drosophila*. The next step of the cascade, namely the role of TRP channels in DO and JCs photoconductance has been confirmed (Pulido *et al.*, 2012) and appears similar to that in invertebrate photoreceptors and ipRGCs. For JCs and DO Na^+ carries a substantial fraction of the photocurrent, while Ca^{2+} contribute only moderately to depolarization, and the role of K^+ appears to be minimal (Pulido *et al.*, 2012). However, it has been shown in JCs and DO that an increase in the level of Ca^{2+} precedes the opening of the Ca^{2+} permeable TRP channels (Peinado *et al.*, 2015). This also appears to occur in ipRGCs (Graham *et al.*, 2008). Moreover the release of Ca^{2+} from internal stores in the ER has been detected in both JCs and DO (Angueyra *et al.*, 2012). The opening of the TRP channels is thus probably mediated by an increase in the level of intracellular Ca^{2+} (Peinado *et al.*, 2015), but more data are needed to confirm this. In sum, the reconstructed phototransduction cascade in JCs and DO seems to be as follows: melanopsin – GNAQ – IP3 – Ca^{2+} increase – opening of TRP channels – Na^+ and Ca^{2+} influx (Fig. 8). Moreover, presence of S-arrestin, involved in attenuation of phototransduction cascade in visual photoreceptors of invertebrates (Lieb *et al.*, 1991) and vertebrates (Pfister *et al.*, 1985) as well as in ipRGCs (Cameron and Robinson, 2014), has been reported in both JCs and DO (Mirshahi *et al.*, 1985; van Veen *et al.*, 1986). Because of discrepancies in descriptions of the phototransduction cascade in ipRGCs and invertebrate photoreceptors, it would be premature to assess which one is more similar to the cascade

present in JCs and DO.

Despite similarities in the overall design among rhabdomeric-type phototransduction cascades of vertebrates and invertebrates (including amphioxus) notable differences exist in the light sensitivity of the corresponding photoreceptors. Vertebrate ipRGCs do not have elaborate membrane protrusions (Sand *et al.*, 2012) of the kind found in rhabdomeric photoreceptors, leading to less efficient photon capture. In agreement with this finding, ipRGCs are less sensitive than most invertebrate visual photoreceptors (Do and Yau, 2015). Amphioxus JCs and DO exhibit a photosensitivity somewhere between ipRGCs and invertebrate photoreceptors. It is estimated that JCs and DO express melanopsin at levels comparable to typical rhabdomeric photoreceptors, yet the gain of the photocascade upon irradiation is lower indicating that differences in phototransduction cascades are responsible for overall efficiency. In fact, although the TRP channels seems not to be the limiting factor, the number of TRP channels activated per photon was shown to be lower in DO and JC compared to invertebrate photoreceptors (Ferrer *et al.*, 2012). The single photon sensitivity of JCs and DO is similar to that of ipRGCs. Nevertheless, due to their more elaborate morphology (typical rhabdomeric membrane protrusions) JCs and DO are overall more sensitive than ipRGCs, so they can provide better information about light conditions. On the other hand while the response of ipRGCs to illumination decays on the order of seconds (probably an adaptation for their role in control of circadian rhythm), the decay in response of JCs and DO is in the millisecond range (Ferrer *et al.*, 2012). Amphioxus melanopsin-positive photoreceptors thus cannot function as circadian photoreceptors as effectively as ipRGCs. If one would consider amphioxus JCs and DO to resemble the ancestral state of melanopsin expressing photoreceptors in the

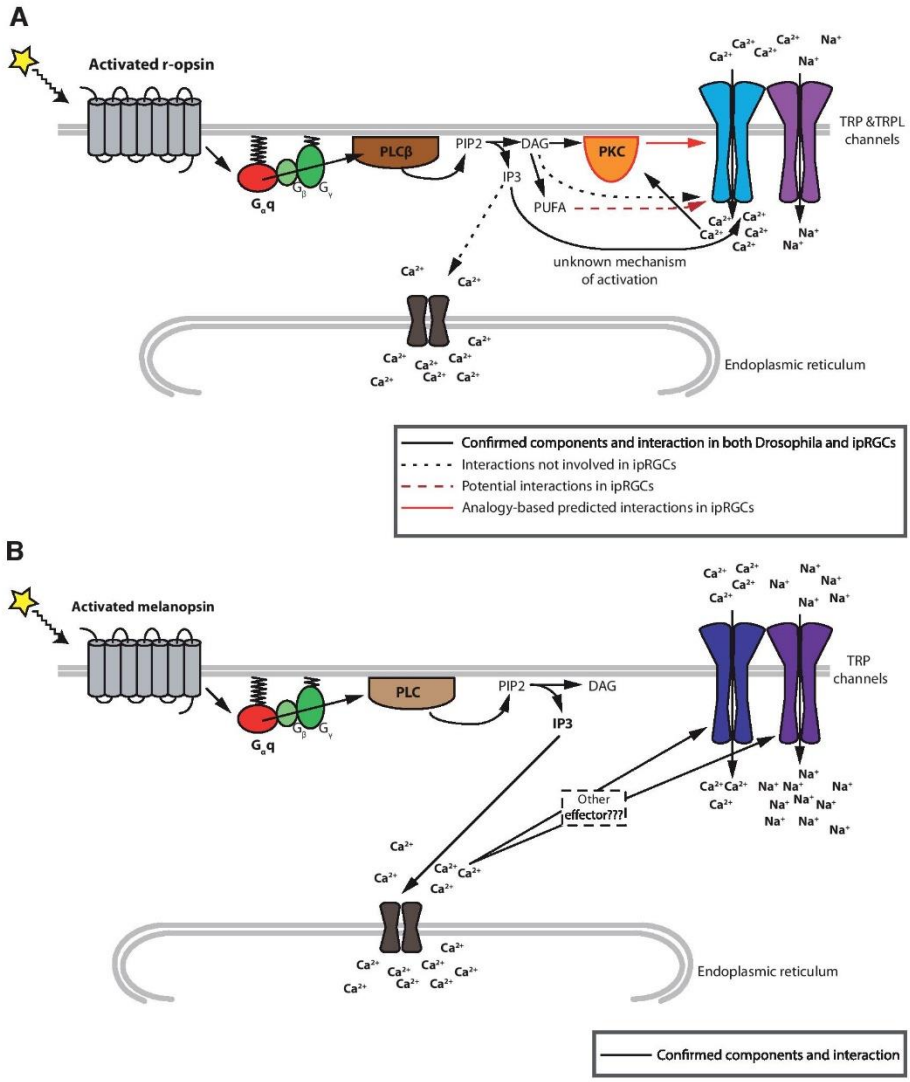

Fig. 8. Phototransduction cascades in *Drosophila* photoreceptors, vertebrate intrinsic photosensitive ganglion cells (ipRGCs) and amphioxus dorsal ocellus (DO) and Joseph cells (JCs). *Comparison of phototransduction cascades for* Drosophila *& ipRGCs and amphioxus rhabdomeric photoreceptors are shown.* **(A)** *Phototransduction cascade in* Drosophila *retinal photoreceptors and vertebrate ipRGCs. After opsins irradiation, member of GNAQ family is activated in both of the presented cell types. Subsequently, PLC activation was shown to be involved in both cases. Next steps in the cascade might, however, differ between* Drosophila *photoreceptors and ipRGCs. Some interactions identified in* Drosophila *photoreceptors were shown not to be involved in phototransduction in ipRGCs (marked with black dotted arrows). For ipRGCs proposed steps in the cascade are shown (marked with red arrow or red dashed arrow).* **(B)** *Phototransduction cascade in amphioxus JCs and DO. Identified components and their connections are shown. The effect of* Ca^{2+} *released from endoplasmic reticulum is still not resolved. Interestingly after the thorough studies performed in past years, the phototransduction cascade of JCs and DO is described more accurately than for* Drosophila *or ipRGCs.*

vertebrate ancestor, then it is clear that relatively modest modifications (loss of membrane protrusions; lower melanopsin expression; difference in phototransduction cascade) were needed to enable them attaining the lower photosensitivity necessary for their role as circadian receptors.

Taken together JCs and DO of amphioxus have a lot in common with both invertebrate rhabdomeric photoreceptors and vertebrate ipRGCs. The homology between JCs and DO and ipRGCs appears to be especially well justified. Based on the differences in their structure and development, there is, however, a possible division of roles between JCs and DO. DO seem to be more important for controlling the proper burrowing of the adult animal. Recently, noncephalic r-opsin positive photoreceptors along the body of the marine annelid *Platynereis dumerilli* were identified (Backfisch *et al.*, 2013). When combined with data from zebrafish, where melanopsin (Opn4)-positive cells were identified in the lateral line organ, it was proposed that DO might be representative of very ancient noncephalic rhabdomeric-type photoreceptors (Backfisch *et al.*, 2013). Additional scenario has been proposed, in which DO are evolutionarily related to vertebrate neural crest cells (Ivashkin and Adameyko, 2013). To test either of these hypotheses, more data are necessary, especially about gene expression profiles of DO. On the other hand, available data support a role of JCs as the main controllers of circadian rhythmicity in adult amphioxus, thus making them, at least functionally, more closely related to ipRGCs. Since it is difficult to find a JC homolog in other chordates and JCs are entirely restricted to amphioxus adults, one still cannot rule out the possibility that they may play a so far unknown role in amphioxus behavior. JCs might, for example, serve as shadow detectors. FE being formed by just a few photoreceptor cells seems to be used mainly in larval stage and not sufficient for the use in adults (even though it might still retain some function there). On the other hand, JCs are abundant in the adult, located in the anterior part projecting outside from the sand and thus exposed to ambient light. Their role might thus lie in detecting the sudden change in illumination (e.g., caused by the approaching predator) or even in monitoring the movement of the passing object (due to their expansion across the anterior body surface). Another question is the evolutionary origin of JCs, whether they are ancestral for chordates, or specific for amphioxus, which could imply the way of life of the chordates' ancestor. If the former is true, then the ancestral chordates were burrowers. Otherwise, burrowing is an innovation and ancestral chordates were Pikaia-like swimmers. Rhabdomeric photoreceptors have been found in the eyes of other extant chordates, salps (Gorman *et al.*, 1971; McReynolds and Gorman, 1975). Recently, an analysis of the brain and eyes of salp *Thalia democratica* was performed (Braun and Stach, 2017). It was documented that *T. democratica* eyes are positioned in the brain region that might be homologous to amphioxus CV (with its Di-Mesencephalic characteristics). It is not clear whether salp´s eyes are homologous to JCs or not. If so, they would probably represent ancestral chordate photosensitive organs, or at least an example of the chordate´s potential to make rhabdomeric receptors from the dorsal midbrain (necessary for various tasks). In this case, the lamellate cells (whose number in the adult stays the same as in larva´s compact LB) might then still be active in the regulation of circadian rhythm in adults.

Conclusion

Here, we have reviewed available information on photoreception in amphioxus. Starting with general observations on light-guided behavior of the animals we examined subjects as diverse as anatomy, morphology, physiology, gene expression profiles and molecular pathways underlying photoreception, in the four distinct photoreceptive organs of amphioxus, namely the FE, LB, DO and JCs. We were especially concerned with possible homologies of amphioxus photoreceptive organs to their vertebrate counterparts. The possible role put forward for amphioxus photoreceptive organs is summarized in Table 2. However, when looking more closely at the proposed homologies, it is becoming clear that more experimental data is desirable to strengthen them. The proposed homology between amphioxus FE and vertebrate lateral eyes stands on solid grounds, being based so far on the FE gene expression fingerprint and EM analysis. Data about the physiology of FE photoreceptors, the phototransduction cascade they utilize, and their development are, however, missing. In addition, information about the FE connectome (projecting neurons) is needed. The homology between the LB and the vertebrate pineal gland is mainly based on the striking morphological similarity between their photoreceptors and location of the LB at the dorsal part of the CV. To corroborate such homology,

TABLE 2

OVERVIEW OF PUTATIVE FUNCTION AND PROPOSED HOMOLOGY FOR PARTICULAR AMPHIOXUS PHOTORECEPTIVE ORGANS

Photoreceptive organ	Putative function	Proposed homology	References
Frontal eye	Orientation of larvae while hovering in water column during feeding		Stokes and Holland, 1995
		Vertebrate lateral eyes	Kemna, 1904; Lacalli *et al.*, 1994; Vopalensky *et al.*, 2012
Lamellar body	Circadian rhythmicity (in larva and/or adult)		Wicht and Lacalli, 2005; This study
		Vertebrate pineal organ	Eakin, 1968; Ruiz and Anadon, 1991b
Joseph cells	Circadian rhythmicity (in adult)		This study
	Changes in ambient light intensity		This study
		Vertebrate ipRGCs	Koyanagi *et al.*, 2005; Gomez *et al.*, 2009
		Ancestral chordate cerebral rhabdomeric photoreceptors	This study
Dorsal ocelli	Negative phototaxis of adults		Hesse, 1898; Parker, 1908; Guthrie, 1975
	Regulation of larval swimming modes (1st DO)		Lacalli, 2002
	Adjusting height in the sand burrow		Lacalli, 2004
		Vertebrate ipRGCs	Koyanagi *et al.*, 2005; Gomez *et al.*, 2009
		Ancestral bilaterian non-cephalic rhabdomeric type photoreceptors	Backfisch *et al.*, 2013; This study
		Neural crest cells of vertebrates (neuroepithelial progenitors of the DOs)	Ivashkin and Adameyko, 2013

additional data about LB development, physiology and especially gene expression will be needed. It is considerably more difficult to ascribe vertebrate homology to JCs and DO. Homology of amphioxus JCs to ipRGCs, especially to the population of ipRGCs involved in circadian rhythm control, seems modestly supported on the basis of JC physiology and the lack of closely associated pigment. It is likely that they function as non-directional photoreceptors, possibly involved in controlling the circadian rhythm in adult amphioxus. We put forward hypotheses proposing homologies of the DO to three vertebrate systems: ipRGCs, melanopsin-positive lateral line cells, and neural crest cells, respectively. We anticipate that future work will allow us to discriminate amongst these scenarios.

In conclusion, the four classes of amphioxus photoreceptive organs represent an exciting model for evolutionary studies. They not only serve as a window into the ancestral chordate condition but also provide an insight into the evolution of vertebrate photoreception.

Acknowledgement

This work was funded by the Czech Science Foundation (17-15374S). We acknowledge the Microscopy Centre - Light Microscopy Core Facility, IMG ASCR, Prague, Czech Republic, supported by grants (Czech-Bioimaging – MEYS LM2015062), "Centre of Model Organisms" OPPK (CZ.2.16/3.1.00/21547) and "Biomodels for health" (LO1419), for their support with the confocal imaging presented herein.

We are grateful to Nicholas D. Holland, Trevor D. Lamb, Dan-Eric Nilsson and Thurston Lacalli for their insightful comments and suggestions on the earlier version of this manuscript.

References

ACEMEL, R.D., TENA, J.J., IRASTORZA-AZCARATE, I., MARLETAZ, F., GOMEZ-MARIN, C., DE LA CALLE-MUSTIENES, E., BERTRAND, S., DIAZ, S.G., ALDEA, D., AURY, J.M. *et al.*, (2016). A single three-dimensional chromatin compartment in amphioxus indicates a stepwise evolution of vertebrate Hox bimodal regulation. *Nat Genet* 48: 336-341.

ALBUIXECH-CRESPO, B., LOPEZ-BLANCH, L., BURGUERA, D., MAESO, I., SANCHEZ-ARRONES, L., MORENO-BRAVO, J.A., SOMORJAI, I., PASCUAL-ANAYA, J., PUELLES, E., BOVOLENTA, P. *et al.*, (2017). Molecular regionalization of the developing amphioxus neural tube challenges major partitions of the vertebrate brain. *PLoS Biol* 15: e2001573.

ANGUEYRA, J.M., PULIDO, C., MALAGON, G., NASI, E. and GOMEZ MDEL, P. (2012). Melanopsin-expressing amphioxus photoreceptors transduce light via a phospholipase C signaling cascade. *PLoS One* 7: e29813.

ARENDT, D., TESSMAR-RAIBLE, K., SNYMAN, H., DORRESTEIJN, A.W. and WITTBRODT, J. (2004). Ciliary photoreceptors with a vertebrate-type opsin in an invertebrate brain. *Science* 306: 869-871.

ARIKAWA, K., KAWAMATA, K., SUZUKI, T. and EGUCHI, E. (1987). Daily changes of structure, function and rhodopsin content in the compound eye of the crab Hemigrapsus sanguineus. *J Comp Physiol A* 161: 161-174.

ARIKAWA, K., MORIKAWA, Y., SUZUKI, T. and EGUCHI, E. (1988). Intrinsic control of rhabdom size and rhodopsin content in the crab compound eye by a circadian biological clock. *Experientia* 44: 219-220.

BACKFISCH, B., VEEDIN RAJAN, V.B., FISCHER, R.M., LOHS, C., ARBOLEDA, E., TESSMAR-RAIBLE, K. and RAIBLE, F. (2013). Stable transgenesis in the marine annelid Platynereis dumerilii sheds new light on photoreceptor evolution. *Proc Natl Acad Sci USA* 110: 193-198.

BAILES, H.J. and LUCAS, R.J. (2013). Human melanopsin forms a pigment maximally sensitive to blue light (lambdamax approximately 479 nm) supporting activation of G(q/11) and G(i/o) signalling cascades. *Proc Biol Sci* 280: 20122987.

BARDET, P.L., SCHUBERT, M., HORARD, B., HOLLAND, L.Z., LAUDET, V., HOLLAND, N.D. and VANACKER, J.M. (2005). Expression of estrogen-receptor related receptors in amphioxus and zebrafish: implications for the evolution of posterior brain segmentation at the invertebrate-to-vertebrate transition. *Evol Dev* 7: 223-233.

BASSETT, E.A. and WALLACE, V.A. (2012). Cell fate determination in the vertebrate retina. *Trends Neurosci* 35: 565-573.

BERTRAND, S. and ESCRIVA, H. (2011). Evolutionary crossroads in developmental biology: amphioxus. *Development* 138: 4819-4830.

BISCONTIN, A., FRIGATO, E., SALES, G., MAZZOTTA, G.M., TESCHKE, M., DE PITTA, C., JARMAN, S., MEYER, B., COSTA, R. and BERTOLUCCI, C. (2016). The opsin repertoire of the Antarctic krill Euphausia superba. *Mar Genomics* 29: 61-68.

BOVERI, T. (1904). Ueber die phylogenetische Bedeutung der Sehorgane des Amphioxus. *Zool. Jahrb. Supplement* 7: 409-428.

BOWMAKER, J.K. and WAGNER, H.J. (2004). Pineal organs of deep-sea fish: photopigments and structure. *J Exp Biol* 207: 2379-2387.

BOZZO, M., MACRI, S., CALZIA, D., SGARRA, R., MANFIOLETTI, G., RAMOINO, P., LACALLI, T., VIGNALI, R., PESTARINO, M. and CANDIANI, S. (2017). The HMGA gene family in chordates: evolutionary perspectives from amphioxus. *Dev Genes Evol* 227: 201-211.

BRAUN, K. and STACH, T. (2017). Structure and ultrastructure of eyes and brains of Thalia democratica (Thaliacea, Tunicata, Chordata). *J Morphol.* 278:1421-1437. (doi: 10.1002/jmor.20722).

BROWN, J.E., RUBIN, L.J., GHALAYINI, A.J., TARVER, A.P., IRVINE, R.F., BERRIDGE, M.J. and ANDERSON, R.E. (1984). myo-Inositol polyphosphate may be a messenger for visual excitation in Limulus photoreceptors. *Nature* 311: 160-163.

CAMERON, E.G. and ROBINSON, P.R. (2014). beta-Arrestin-dependent deactivation of mouse melanopsin. *PLoS One* 9: e113138.

CANDIANI, S., MORONTI, L., RAMOINO, P., SCHUBERT, M. and PESTARINO, M. (2012). A neurochemical map of the developing amphioxus nervous system. *BMC Neurosci* 13: 59.

CASTRO, A., BECERRA, M., MANSO, M.J. and ANADON, R. (2015). Neuronal Organization of the Brain in the Adult Amphioxus (Branchiostoma lanceolatum): A Study With Acetylated Tubulin Immunohistochemistry. *J Comp Neurol* 523: 2211-2232.

CASTRO, A., BECERRA, M., MANSO, M.J., SHERWOOD, N.M. and ANADON, R. (2006). Anatomy of the Hesse photoreceptor cell axonal system in the central nervous system of amphioxus. *J Comp Neurol* 494: 54-62.

CHIN, T.G. (1941). Studies on the Biology of the Amoy Amphioxus *Branchiostoma belcheri* Gray. *Philippine J. Science* 75: 369-421.

CHYB, S., RAGHU, P. and HARDIE, R.C. (1999). Polyunsaturated fatty acids activate the *Drosophila* light-sensitive channels TRP and TRPL. *Nature* 397: 255-259.

CONNAUGHTON, V. (2005). Glutamate and Glutamate Receptors in the Vertebrate Retina. *Kolb H, Fernandez E, Nelson R, editors. Webvision: The Organization of the Retina and Visual System [Internet]. Salt Lake City (UT): University of Utah Health Sciences Center; 1995-. Available from: https://www.ncbi.nlm.nih.gov/books/NBK11526/ (updated 2007).*

COSTA, G. (1834). *Annuario zoologico. Cenni Zoologici ossia descrizione sommaria delle specie nuove di animali discoperti in diverse contrade del regno nell´ anno 1834 (cited from Willey 1894).* Azzolino, Napoli.

CROZIER, W.J. (1917). The photoreceptors of amphioxus. *Contrib. Bermuda Biol. Stn. Res. (reprinted from Anat Rec vol. 11, 1916)* 4: 3.

DARWIN, C. (1859). *On the Origin of Species by Means of Natural Selection, or the Preservation of Favoured Races in the Struggle for Life.* John Murray, London.

DAVIS, T.L. and REBAY, I. (2017). Master regulators in development: Views from the *Drosophila* retinal determination and mammalian pluripotency gene networks. *Dev Biol* 421: 93-107.

DEL PILAR GOMEZ, M. and NASI, E. (1998). Membrane current induced by protein kinase C activators in rhabdomeric photoreceptors: implications for visual excitation. *J Neurosci* 18: 5253-5263.

DELGADO, R., MUNOZ, Y., PENA-CORTES, H., GIAVALISCO, P. and BACIGALUPO, J. (2014). Diacylglycerol activates the light-dependent channel TRP in the photosensitive microvilli of *Drosophila melanogaster* photoreceptors. *J Neurosci* 34: 6679-6686.

DO, M.T. and YAU, K.W. (2015). Intrinsically Photosensitive Retinal Ganglion Cells. *Physiol Rev.* 90: 1547-1581.

EAKIN, R.M. and WESTFALL, J.A. (1962a). Fine structure of photoreceptors in Amphioxus. *J Ultrastruct Res* 6: 531-539.

EAKIN, R.M. and WESTFALL, J.A. (1962b). Fine Structure of Photoreceptors in the Hydromedusan, Polyorchis Penicillatus. *Proc Natl Acad Sci USA* 48: 826-833.

FEIN, A., PAYNE, R., CORSON, D.W., BERRIDGE, M.J. and IRVINE, R.F. (1984). Photoreceptor excitation and adaptation by inositol 1,4,5-trisphosphate. *Nature*

311: 157-160.

FERRER, C., MALAGON, G., GOMEZ MDEL, P. and NASI, E. (2012). Dissecting the determinants of light sensitivity in amphioxus microvillar photoreceptors: possible evolutionary implications for melanopsin signaling. *J Neurosci* 32: 17977-17987.

FEUDA, R., ROTA-STABELLI, O., OAKLEY, T.H. and PISANI, D. (2014). The Comb Jelly Opsins and the Origins of Animal Phototrasduction. *Genome Biol Evol* 6: 1964-1971.

FRANZ, V. (1923). Haur, Sinnesorgane und Nervensystem der Akranier. *Z Naturwiss* 13: 401-526.

FUENTES, M., BENITO, E., BERTRAND, S., PARIS, M., MIGNARDOT, A., GODOY, L., JIMENEZ-DELGADO, S., OLIVERI, D., CANDIANI, S., HIRSINGER, E. *et al.,* (2007). Insights into spawning behavior and development of the European amphioxus (Branchiostoma lanceolatum). *J Exp Zool B Mol Dev Evol* 308: 484-493.

GLARDON, S., HOLLAND, L.Z., GEHRING, W.J. and HOLLAND, N.D. (1998). Isolation and developmental expression of the amphioxus Pax-6 gene (AmphiPax-6): insights into eye and photoreceptor evolution. *Development* 125: 2701-2710.

GOMEZ MDEL, P., ANGUEYRA, J.M. and NASI, E. (2009). Light-transduction in melanopsin-expressing photoreceptors of Amphioxus. *Proc Natl Acad Sci USA* 106: 9081-9086.

GONG, J., YUAN, Y., WARD, A., KANG, L., ZHANG, B., WU, Z., PENG, J., FENG, Z., LIU, J. and XU, X.Z. (2016). The C. elegans Taste Receptor Homolog LITE-1 Is a Photoreceptor. *Cell* 167: 1252-1263 e1210.

GORMAN, A.L., MCREYNOLDS, J.S. and BARNES, S.N. (1971). Photoreceptors in primitive chordates: fine structure, hyperpolarizing receptor potentials, and evolution. *Science* 172: 1052-1054.

GRAHAM, D.M., WONG, K.Y., SHAPIRO, P., FREDERICK, C., PATTABIRAMAN, K. and BERSON, D.M. (2008). Melanopsin ganglion cells use a membrane-associated rhabdomeric phototransduction cascade. *J Neurophysiol* 99: 2522-2532.

GUTHRIE, D.M. (1975). The Physiology and Structure of the Nervous System of Amphioxus (the Lancelet) *Branchiostoma Lanceolatum* Pallas. *Symp Zool Soc Lond (Protochordates)* 36: 43-80.

HARDIE, R.C. and FRANZE, K. (2012). Photomechanical responses in *Drosophila* photoreceptors. *Science* 338: 260-263.

HARIYAMA, T., MEYER-ROCHOW, V.B., KAWAUCHI, T., TAKAKU, Y. and TSUKAHARA, Y. (2001). Diurnal changes in retinula cell sensitivities and receptive fields (two-dimensional angular sensitivity functions) in the apposition eyes of Ligia exotica (Crustacea, Isopoda). *J Exp Biol* 204: 239-248.

HAUG, M.F., GESEMANN, M., LAZOVIC, V. and NEUHAUSS, S.C. (2015). Eumetazoan cryptochrome phylogeny and evolution. *Genome Biol Evol* 7: 601-619.

HESSE, R. (1898). Untersuchungen über die Organe der Lichtempfindung bei niederen Thieren. IV. Die sehorgane des Amphioxus. *Z Wiss Zool* 63: 456-464.

HOLLAND, L.Z. (2017). *Invertebrate Origins of Vertebrate Nervous Systems.*

HOLLAND, L.Z., ALBALAT, R., AZUMI, K., BENITO-GUTIERREZ, E., BLOW, M.J., BRONNER-FRASER, M., BRUNET, F., BUTTS, T., CANDIANI, S., DISHAW, L.J. *et al.,* (2008). The amphioxus genome illuminates vertebrate origins and cephalochordate biology. *Genome Res* 18: 1100-1111.

HOLLAND, L.Z. and YU, J.K. (2004). Cephalochordate (amphioxus) embryos: procurement, culture, and basic methods. *Methods Cell Biol* 74: 195-215.

HOLLAND, N.D. (2011). Spawning periodicity of the lancelet, *Asymmetron lucayanum* (Cephalochordata), in Bihimi, Bahamas. *Ital J Zool* 78: 478-486.

HOLLAND, N.D. and HOLLAND, L.Z. (2010). Laboratory spawning and development of the Bahama lancelet, Asymmetron lucayanum (cephalochordata): fertilization through feeding larvae. *Biol Bull* 219: 132-141.

HUANG, J., LIU, C.H., HUGHES, S.A., POSTMA, M., SCHWIENING, C.J. and HARDIE, R.C. (2010). Activation of TRP channels by protons and phosphoinositide depletion in *Drosophila* photoreceptors. *Curr Biol* 20: 189-197.

HUGHES, S., HANKINS, M.W., FOSTER, R.G. and PEIRSON, S.N. (2012). Melanopsin phototransduction: slowly emerging from the dark. *Prog Brain Res* 199: 19-40.

IVASHKIN, E. and ADAMEYKO, I. (2013). Progenitors of the protochordate ocellus as an evolutionary origin of the neural crest. *Evodevo* 4: 12.

JELGERSMA, G. (1906). Der Ursprung des Wilbeltierauges. *Morphol. Jahrb.* 35: 377-394.

JOSEPH, H. (1904). Über eigentümliche Zellstrukturen im Zentralnervensystem von Amphioxus. *Verh Anat Ges. Ergänzungsh.* z. Bd. 25: 16-26.

KEMNA, A. (1904). Les structures cerebrales dorsales chez les vertebres inferieurs. *Ann. Soc. R. Zool. Belg.* 39: 196-201.

KOHL, C. (1890). Einige Bemerkungen über Sinnesorgane des Amphioxus lanceolatus. *Zoologischer Anzeiger* 13: 182-185.

KOJIMA, K., YAMASHITA, T., IMAMOTO, Y., KUSAKABE, T.G., TSUDA, M. and SHICHIDA, Y. (2017). Evolutionary steps involving counterion displacement in a tunicate opsin. *Proc Natl Acad Sci USA* 114: 6028-6033.

KOLB, H. (2011). Neurotransmitters in the Retina by Helga Kolb. *Kolb H, Fernandez E, Nelson R, editors. Webvision: The Organization of the Retina and Visual System [Internet]. Salt Lake City (UT): University of Utah Health Sciences Center; 1995-. Available from: http://webvision.med.utah.edu/book/part-iv-neurotransmitters-in-the-retina-2/part-iv-neurotransmitters-in-the-retina/ (updated 2011).*

KOYANAGI, M., KUBOKAWA, K., TSUKAMOTO, H., SHICHIDA, Y. and TERAKITA, A. (2005). Cephalochordate melanopsin: evolutionary linkage between invertebrate visual cells and vertebrate photosensitive retinal ganglion cells. *Curr Biol* 15: 1065-1069.

KOYANAGI, M., TERAKITA, A., KUBOKAWA, K. and SHICHIDA, Y. (2002). Amphioxus homologs of Go-coupled rhodopsin and peropsin having 11-cis- and all-trans-retinals as their chromophores. *FEBS Lett* 531: 525-528.

KOZMIK, Z. (2008). The role of Pax genes in eye evolution. *Brain Res Bull* 75: 335-339.

KOZMIK, Z., HOLLAND, N.D., KALOUSOVA, A., PACES, J., SCHUBERT, M. and HOLLAND, L.Z. (1999). Characterization of an amphioxus paired box gene, AmphiPax2/5/8: developmental expression patterns in optic support cells, nephridium, thyroid-like structures and pharyngeal gill slits, but not in the midbrain-hindbrain boundary region. *Development* 126: 1295-1304.

KOZMIK, Z., HOLLAND, N.D., KRESLOVA, J., OLIVERI, D., SCHUBERT, M., JONASOVA, K., HOLLAND, L.Z., PESTARINO, M., BENES, V. and CANDIANI, S. (2007). Pax-Six-Eya-Dach network during amphioxus development: conservation *in vitro* but context specificity in vivo. *Dev Biol* 306: 143-159.

KRAUSE, W. (1888). Die Retina. II. Die Retina der Fische. *Int Monatssch Anat Physiol* 5: 132-148.

KUME, K., ZYLKA, M.J., SRIRAM, S., SHEARMAN, L.P., WEAVER, D.R., JIN, X., MAYWOOD, E.S., HASTINGS, M.H. and REPPERT, S.M. (1999). mCRY1 and mCRY2 are essential components of the negative limb of the circadian clock feedback loop. *Cell* 98: 193-205.

KUTTA, R.J., ARCHIPOWA, N., JOHANNISSEN, L.O., JONES, A.R. and SCRUTTON, N.S. (2017). Vertebrate Cryptochromes are Vestigial Flavoproteins. *Sci Rep* 7: 44906.

LACALLI, T. and CANDIANI, S. (2017). Locomotory control in amphioxus larvae: new insights from neurotransmitter data. *Evodevo* 8: 4.

LACALLI, T.C. (1996). Frontal eye circuitry, rostral sensory pathways and brain organization in amphioxus larvae: evidence from 3D reconstructions. *Philos. Trans. Royal Soc. B: Biol. Sci.* 351: 243-263.

LACALLI, T.C. (2002). The dorsal compartment locomotory control system in amphioxus larvae. *J Morphol* 252: 227-237.

LACALLI, T.C. (2004). Sensory systems in amphioxus: a window on the ancestral chordate condition. *Brain Behav Evol* 64: 148-162.

LACALLI, T.C. (2008). Basic features of the ancestral chordate brain: a protochordate perspective. *Brain Res Bull* 75: 319-323.

LACALLI, T.C. and KELLY, S.J. (2003). Ventral neurons in the anterior nerve cord of amphioxus larvae. I. An inventory of cell types and synaptic patterns. *J Morphol* 257: 190-211.

LACALLI., T.C., HOLLAND., N.D. and WEST, J.E. (1994). Landmarks in the Anterior Central Nervous System of Amphioxus Larvae. *Phil Trans Roy Soc B Biol Sci* 344: 165-185.

LAMB, T.D. (2013). Evolution of phototransduction, vertebrate photoreceptors and retina. *Prog Retin Eye Res* 36: 52-119.

LAMB, T.D., COLLIN, S.P. and PUGH, E.N., JR. (2007). Evolution of the vertebrate eye: opsins, photoreceptors, retina and eye cup. *Nat Rev Neurosci* 8: 960-976.

LAMB, T.D. and HUNT, D.M. (2017). Evolution of the vertebrate phototransduction cascade activation steps. *Dev Biol.* 431: 77-92.

LAMB, T.D., PATEL, H., CHUAH, A., NATOLI, R.C., DAVIES, W.I., HART, N.S., COLLIN, S.P. and HUNT, D.M. (2016). Evolution of Vertebrate Phototransduction: Cascade Activation. *Mol Biol Evol* 33: 2064-2087.

LARHAMMAR, D., NORDSTROM, K. and LARSSON, T.A. (2009). Evolution of vertebrate rod and cone phototransduction genes. *Phil Trans Roy Soc Lond B Biol Sci* 364: 2867-2880.

LAWRENCE, P.A. and KRASNE, F.B. (1965). Annelid Ciliary Photoreceptors. *Science*

148: 965-966.

LI, G., SHU, Z. and WANG, Y. (2013). Year-Round Reproduction and Induced Spawning of Chinese Amphioxus, *Branchiostoma belcheri*, in Laboratory. *PLoS One* e75461.

LIEB, W.E., SMITH-LANG, L., DUA, H.S., CHRISTENSEN, A.C. and DONOSO, L.A. (1991). Identification of an S-antigen-like molecule in *Drosophila melanogaster*: an immunohistochemical study. *Exp Eye Res* 53: 171-178.

LIEGERTOVA, M., PERGNER, J., KOZMIKOVA, I., FABIAN, P., POMBINHO, A.R., STRNAD, H., PACES, J., VLCEK, C., BARTUNEK, P. and KOZMIK, Z. (2015). Cubozoan genome illuminates functional diversification of opsins and photoreceptor evolution. *Sci Rep* 5: 11885.

MARIN, E.P., KRISHNA, A.G., ZVYAGA, T.A., ISELE, J., SIEBERT, F. and SAKMAR, T.P. (2000). The amino terminus of the fourth cytoplasmic loop of rhodopsin modulates rhodopsin-transducin interaction. *J Biol Chem* 275: 1930-1936.

MCREYNOLDS, J.S. and GORMAN, A.L. (1975). Hyperpolarizing photoreceptors in the eye of a primitive chordate, Salpa democratica. *Vision Res* 15: 1181-1186.

MEVES, A. (1973). Elektronmikroskopische Untersuchungen über die Zytoarchitektur des Gehirns von *Branchiostoma lanceolatum*. *Z Zellforsch Mikrosk Anat* 139: 511-532.

MIRSHAHI, M., BOUCHEIX, C., COLLENOT, G., THILLAYE, B. and FAURE, J.P. (1985). Retinal S-antigen epitopes in vertebrate and invertebrate photoreceptors. *Invest Ophthalmol Vis Sci* 26: 1016-1021.

MULLER, W.E., SCHRODER, H.C., MARKL, J.S., GREBENJUK, V.A., KORZHEV, M., STEFFEN, R. and WANG, X. (2013). Cryptochrome in sponges: a key molecule linking photoreception with phototransduction. *J Histochem Cytochem* 61: 814-832.

NAGEL, W.A. (1896). *Der Lichtsinn augenloser Thiere. Eine biologische Studie*. Fischer, Jena.

NAKAO, T. (1964). On the Fine Structure of the Amphioxus Photoreceptor. *Tohoku J Exp Med* 82: 349-363.

NASI, E. and DEL PILAR GOMEZ, M. (2009). Melanopsin-mediated light-sensing in amphioxus: a glimpse of the microvillar photoreceptor lineage within the deuterostomia. *Commun Integr Biol* 2: 441-443.

NILSSON, D.E. (2013). Eye evolution and its functional basis. *Vis Neurosci* 30: 5-20.

PANTZARTZI, C.P., PERGNER, J., KOZMIKOVA, I. and KOZMIK, Z. (2017). The opsin repertoire of the European lancelet: a window into light detection in a basal chordate. *Int J Dev Biol (accepted)*.

PARKER, G.H. (1908). The Sensory Reactions of Amphioxus. *Proc Amer Acad Arts Sci* 43: 415-455.

PAYNE, R., CORSON, D.W. and FEIN, A. (1986). Pressure injection of calcium both excites and adapts Limulus ventral photoreceptors. *J Gen Physiol* 88: 107-126.

PEINADO, G., OSORNO, T., GOMEZ MDEL, P. and NASI, E. (2015). Calcium activates the light-dependent conductance in melanopsin-expressing photoreceptors of amphioxus. *Proc Natl Acad Sci USA* 112: 7845-7850.

PFISTER, C., CHABRE, M., PLOUET, J., TUYEN, V.V., DE KOZAK, Y., FAURE, J.P. and KUHN, H. (1985). Retinal S antigen identified as the 48K protein regulating light-dependent phosphodiesterase in rods. *Science* 228: 891-893.

PLACHETZKI, D.C., DEGNAN, B.M. and OAKLEY, T.H. (2007). The origins of novel protein interactions during animal opsin evolution. *PLoS One* 2: e1054.

PORTER, M.L., BLASIC, J.R., BOK, M.J., CAMERON, E.G., PRINGLE, T., CRONIN, T.W. and ROBINSON, P.R. (2012). Shedding new light on opsin evolution. *Proc Biol Sci* 279: 3-14.

PROVENCIO, I., JIANG, G., DE GRIP, W.J., HAYES, W.P. and ROLLAG, M.D. (1998). Melanopsin: An opsin in melanophores, brain, and eye. *Proc Natl Acad Sci USA* 95: 340-345.

PULIDO, C., MALAGON, G., FERRER, C., CHEN, J.K., ANGUEYRA, J.M., NASI, E. and GOMEZ MDEL, P. (2012). The light-sensitive conductance of melanopsin-expressing Joseph and Hesse cells in amphioxus. *J Gen Physiol* 139: 19-30.

RAMIREZ, M.D., PAIRETT, A.N., PANKEY, M.S., SERB, J.M., SPEISER, D.I., SWAFFORD, A.J. and OAKLEY, T.H. (2016). The Last Common Ancestor of Most Bilaterian Animals Possessed at Least Nine Opsins. *Genome Biol Evol* 8: 3640-3652.

RIVERA, A.S., OZTURK, N., FAHEY, B., PLACHETZKI, D.C., DEGNAN, B.M., SANCAR, A. and OAKLEY, T.H. (2012). Blue-light-receptive cryptochrome is expressed in a sponge eye lacking neurons and opsin. *J Exp Biol* 215: 1278-1286.

RUIZ, M.S. and ANADON, R. (1991a). Some considerations on the fine structure of rhabdomeric photoreceptors in the amphioxus, Branchiostoma lanceolatum (Cephalochordata). *J Himforsch* 32: 159-164.

RUIZ, S. and ANADON, R. (1991b). The fine structure of lamellate cells in the brain of amphioxus (Branchiostoma lanceolatum, Cephalochordata). *Cell Tiss Res* 263: 597-600.

SAKURA, M., TAKASUGA, K., WATANABE, M. and EGUCHI, E. (2003). Diurnal and circadian rhythm in compound eye of cricket (Gryllus bimaculatus): changes in structure and photon capture efficiency. *Zoolog Sci* 20: 833-840.

SAND, A., SCHMIDT, T.M. and KOFUJI, P. (2012). Diverse types of ganglion cell photoreceptors in the mammalian retina. *Prog Retin Eye Res* 31: 287-302.

SATIR, P. and CHRISTENSEN, S.T. (2008). Structure and function of mammalian cilia. *Histochem Cell Biol* 129: 687-693.

SCHOMERUS, C., KORF, H.-W., LAEDTKE, E., MORET, F., ZHANG, Q. and WICHT, H. (2008). Nocturnal Behavior and Rhythmic *Period* Gene Expression in a Lancelet, *Branchiostoma lanceolatum*. *J Bio Rhyth* 23: 170-181.

SERGEEV, B.F. (1963). The sensory reactions of *Amphioxus* and the effects of anesthesia *(In Russian). Fiziol. Zh. SSSR (cited in Guthrie, 1975)* 49: 60-65.

SHEARMAN, L.P., SRIRAM, S., WEAVER, D.R., MAYWOOD, E.S., CHAVES, I., ZHENG, B., KUME, K., LEE, C.C., VAN DER HORST, G.T., HASTINGS, M.H. *et al.*, (2000). Interacting molecular loops in the mammalian circadian clock. *Science* 288: 1013-1019.

STOKES, M.D. and HOLLAND, N.D. (1995). Ciliary Hovering in Larval Lancelets (=Amphioxus). *Biol Bull* 188: 231-233.

SUZUKI, D.G., MURAKAMI, Y., ESCRIVA, H. and WADA, H. (2015). A comparative examination of neural circuit and brain patterning between the lamprey and amphioxus reveals the evolutionary origin of the vertebrate visual center. *J Comp Neurol* 523: 251-261.

SWAROOP, A., KIM, D. and FORREST, D. (2010). Transcriptional regulation of photoreceptor development and homeostasis in the mammalian retina. *Nat Rev Neurosci* 11: 563-576.

TERAKITA, A. (2005). The opsins. *Genome Biol* 6: 213.

TERAKITA, A., KAWANO-YAMASHITA, E. and KOYANAGI, M. (2012). Evolution and diversity of opsins.. *Memb Transp Signal* 1: 104-111.

TERAKITA, A., KOYANAGI, M., TSUKAMOTO, H., YAMASHITA, T., MIYATA, T. and SHICHIDA, Y. (2004). Counterion displacement in the molecular evolution of the rhodopsin family. *Nat Struct Mol Biol* 11: 284-289.

TERAKITA, A., TSUKAMOTO, H., KOYANAGI, M., SUGAHARA, M., YAMASHITA, T. and SHICHIDA, Y. (2008). Expression and comparative characterization of Gq-coupled invertebrate visual pigments and melanopsin. *J Neurochem* 105: 883-890.

TSUKAMOTO, H., TERAKITA, A. and SHICHIDA, Y. (2005). A rhodopsin exhibiting binding ability to agonist all-trans-retinal. *Proc Natl Acad Sci USA* 102: 6303-6308.

VAN DER SCHALIE, E. and GREEN, C.B. (2005). Cryptochromes. *Curr Biol* 15: R785.

VAN VEEN, T., ELOFSSON, R., HARTWIG, H.G., GERY, I., MOCHIZUKI, M., CENA, V. and KLEIN, D.C. (1986). Retinal S-antigen: immunocytochemical and immunochemical studies on distribution in animal photoreceptors and pineal organs. *Exp Biol* 45: 15-25.

VOPALENSKY, P., PERGNER, J., LIEGERTOVA, M., BENITO-GUTIERREZ, E., ARENDT, D. and KOZMIK, Z. (2012). Molecular analysis of the amphioxus frontal eye unravels the evolutionary origin of the retina and pigment cells of the vertebrate eye. *Proc Natl Acad Sci USA* 109: 15383-15388.

WATANABE, T. and YOSHIDA, M. (1986). Morphological and histochemical studies on Joseph cells of amphioxus, Branchiostoma belcheri Gray. *Exp Biol* 46: 67-73.

WEBB, J.E. (1969). On the feeding and behavior of the larva of *Branchiostoma lanceolatum*. *Marine Biol.* 3: 58-72.

WELSCH, U. (1968). [The ultrastructure of the cells of Joseph in the brain of Amphioxus]. *Z Zellforsch Mikrosk Anat* 86: 252-261.

WICHT, H. and LACALLI, T.C. (2005). The nervous system of amphioxus: structure, development and evolutionary significance. *Canadian J. Zool.* 83: 122-150.

WICKSTEAD, J.H. and BONE, Q. (1959). Ecology of Acraniate Larvae. *Nature* 184: 1849-1851.

WILLEY, A. (1894). *Amphioxus and the Ancestry of the Vertebrates*. Macmillan, New York.

WILLIAMS, N.A. and HOLLAND, P.W.H. (1996). Old head on young shoulders. *Nature* 383.

YU, J.K., MEULEMANS, D., MCKEOWN, S.J. and BRONNER-FRASER, M. (2008). Insights from the amphioxus genome on the origin of vertebrate neural crest. *Genome Res* 18: 1127-1132.

6.6 The role of transposable elements in functional evolution of amphioxus genome: the case of opsin gene family

In the past, it was widely accepted that three Cephalochordate genera, *Epigonichthys*, *Asymmetron* and *Branchiostoma* diverged about 120 mya[28] (approximately the time of appearance of first mammals). Ever since their first appearance, cephalochordate morphology seemed to be unmodified and hence they were considered as slowly evolving both on morphological and genomic level. Recent data, however, showed that cephalochrodates represent a shallow branching subphylum in which the genera diverged about 45 mya[106]. This is similar to the divergence time between mouse and rat[106]. Previous mistaken predictions of the divergence time were probably partly caused by lack of genomic data of other than *Branchiostoma* species and partly due to gene prediction errors[107]. It is still accepted, that cephalochordates split from the vertebrate ancestor about 500 mya, meaning that their genome rate evolution is rather small when compared to vertebrates. Yet, it was documented that some gene families in amphioxus underwent rapid diversification, e.g. genes involved with development and function of the immune system[108].

In our study we focused on comparison of the opsin family in *B. floridae*, *B. lanceolatum* and *B. belcheri*. We documented the expansion of particular opsin subfamilies (Go and Amphiop6 groups) in all studied species and interestingly spotted some species specific duplications and losses of opsin genes, that even have functional meaning. We hypothesize that both duplications and losses could be caused by homologous recombination via sequences of transposable elements located closely to opsin genes. We base this assumption on extensive bioinformatic analysis of transposable elements in parts of *B. floridae*, *B. lanceolatum* and *B. belcheri* genome. Additionally we corrected previously wrongly annotated opsin genes of *B. floridae* and identified one new opsin gene omitted in previous *B. floridae* genomic study[16].

We believe that our data document that the amphioxus genome might not be as slowly evolving as predicted recently and can serve as another example of how “junk” DNA can be used during the course of evolution.

My contribution to this work: I cloned all problematic parts (not sequenced or mistakenly annotated) of *B. floridae* opsins. I performed qRT-PCR expression analysis of all *B. floridae* opsins. I contributed to writing of methods and results sections of the manuscript.

Article

The role of transposable elements in functional evolution of amphioxus genome: the case of opsin gene family

Chrysoula N. Pantzartzi[1], Jiri Pergner[2], Zbynek Kozmik[1,2,*]

[1]Laboratory of Eye Biology, Institute of Molecular Genetics of the ASCR, v.v.i., Division BIOCEV, Prumyslová 595, 252 50 Vestec, Czech Republic

[2]Department of Transcriptional Regulation, Institute of Molecular Genetics of the ASCR, v.v.i.,

Videnska 1083, 14220,Prague 4, Czech Republic

***** Author for Correspondence**:** Zbynek Kozmik, Institute of Molecular Genetics of the ASCR, v.v.i., Videnska 1083, 14220, Prague, Czech Republic, +420 241062110, kozmik@img.cas.cz

Abstract

Transposable elements (TEs) are able to jump to new locations (transposition) in the genome, usually after replication. They constitute the so-called selfish or junk DNA and take over large proportions of some genomes. Due to their ability to move around they can change the DNA landscape of genomes and are therefore a rich source of innovation in genes and gene regulation. Surge of sequence data in the past years has significantly facilitated large scale comparative studies. Cephalochordates have been regarded as a useful proxy to ancestral chordate condition partially due to the comparatively slow evolutionary rate at morphological and genomic level. In this study, we used opsin gene family from the three *Branchiostoma* species as a window into cephalochordate genome evolution. We compared opsin complements in terms of family size, gene structure and sequence allowing us to identify gene duplication and gene loss events. Furthermore, analysis of the opsin containing genomic loci showed that they are populated by TEs. In summary, we provide evidence of the way transposable elements may have contributed to the evolution of opsin gene family and to the shaping of cephalochordate genomes in general.

Key words: transposable elements, gene duplication, genome shaping

Introduction

Transposable elements (TEs) are complicated biological entities able to replicate and jump to new locations (transposition) in the genome. Rather simple models have been defined to study their dynamics[1], while their classification is also problematic. The first TEclassification system[2], distinguishes two classes of TEs, based on the transposition intermediate: RNA (class I or retrotransposons) and DNA (class II or DNA transposons), which follow a “copy-and-paste” and “cut-and-paste” mechanism, respectively. This system was later modified in order to include bacterial, non-autonomous TEs (such as the Miniature Inverted Repeat Transposable Elements - MITEs) and other types of TEs that couldn’t fall in any of these two categories. Curcio and Derbyshire [3] categorized transposons according to the way they move, determined by their transposase proteins. A hierarchical classification system for eukaryotic TEs has been proposed by Wicker, et al. [4], which takes into account not only the replication strategy but also the structure of the encoded proteins and of the non-coding domains, the presence and size of the target site duplication (TSD) and even some phylogenetic data.

It was long ago speculated that TEs can "control the time and type of activity of individual genes"[5], or in other words they play key role in a variety of gene regulatory networks and lately there is accumulating information in favor of this theory (revised by Chuong *et al.*[6] and Bourque[7]). This can be achieved either by the insertion of TEs in the proximity of genes and consequently the generation of new regulatory elements[7] or the emergence of new regulatory proteins[8]. In fact, TEs occupy a large proportion of the regulatory control regions (revised by Feschotte[8]). On one hand, TEs alter gene expression (activate or inactivate genes); on the other hand they promote inversions and deletions of chromosomal DNA, they can create new genes (or exons), or serve as illegitimate recombination hotspots. Consequently, they contribute to the shaping of the genome’s architecture, its evolution and the emergence of genetic innovations[9-12]. TE-associated chromosomal rearrangements can be driven by two mechanisms, in particular via homologous recombination[13] or by an alternative transposition process[14].

TEs are main components of eukaryote and prokaryote genomes and they are known to occupy large portions of vertebrate, invertebrate and plant genomes in particular[15-19]. Longterminal repeat retrotransposons (LTRs) are the predominant order of TEs in plants[20], whereas the Non-LTR TEs are the most commonly encountered in the human genome[21] and *Alu* repetitive elements, in particular, are known to generate deletions, duplications and complex genomic rearrangements[22].

The subphylum Cephalochordata, a.k.a. amphioxus or lancelets, have been regarded as a key animal group for understanding the origin of vertebrates, and a useful proxy to the ancestral chordate condition. This is in part due to the presumed slow evolutionary rate within the cephalochordate lineage both at the morphological and the genomic level. Cepahlochordata are comprised of the three genera, namely *Branchiostoma*, *Asymmetron* and *Epigonychtys*[23]. It was recently found that Cephalochordata preserve a high TE diversity in comparison to modern vertebrates[24]. In fact, a comparative analysis of TEs in various genomes has revealed that they constitute 28% of *B. floridae* genome[25]. Amphioxus TEs belong to more

than 30 superfamilies, which are highly heterogeneous as generally none of their members are drastically more abundant than others, and none of the TEs seems to have suffered any massive expansion[26]. The phylogenetic relationship within the extant amphioxus lineage was investigated[27] providing divergence time estimates and suggesting a rather recent diversification within *Branchiostoma* genus, with divergence time similar e.g. to that between rodents belonging to *Muridae* family (mouse and rat)[28].

Whole genome comparative study of *B. belcheri* and *B. floridae* indicated high rate of proteome diversification[24], which might however be explained at least in some cases by the gene prediction errors[29].

In order to provide an insight into the possible role of TEs in cephalochordate genome evolution we focused on the opsin gene family, a member of the G-Protein Coupled Receptor (GPCR) gene superfamily. Opsins play crucial role in light detection in animals and their number differs significantly among species, with no apparent correlation to the overall level of body plan sophistication. Opsins classification, interfamily relationships and evolution of animal vision have been the studied extensively [30-39]. Opsins can be roughly clustered into four major groups, namely the ciliary opsins expressed in ciliary photoreceptors (C-type), the rhabdomeric opsins expressed in rhabdomeric photoreceptors (R-type), the Group 4 opsins, and the Cnidarian opsins. Members of the three major groups were recently identified in the European lancelet[40], whereas similar studies in the past were focused on the opsin complements of the Florida and Chinese lancelets[41-43]. By using manually curated and experimentally confirmed opsin complement of three *Branchiostoma* species, namely *B. lanceolatum* (Pallas 1774), *B. floridae* (Hubbs 1922) and *B. belcheri* (Gray 1847), we have identified gene duplication and loss events. Extrapolating from opsin gene family as an example, we try to address the question of how transposable elements may have been involved in the gene gain/losses and shaping of the *Branchiostoma* genus genome.

Materials and Methods

Gene Prediction, alignments, synteny and phylogenetic analysis

We analyzed both available *Branchiostoma floridae* genome assemblies, i.e. v1.0 through JGI, where two haplotypes are present (http://genome.jgi.doe.gov/Brafl1/Brafl1.home.html) and v2.0 through NCBI (http://www.ncbi.nlm.nih.gov/assembly/GCF_000003815.1/), from which most of the allelic scaffolds have been eliminated and is therefore a non-redundant mosaic of v1.0. All previously annotated opsin genes[41] were validated through BLAST, Genscan[44] and SpliceView[45] analyses. In order to detect putative opsin homologs that were not previously reported, we conducted extensive keyword and BLAST searches. Newly identified opsin containing genomic loci were subjected to Genscan and SpliceView for *de novo* gene prediction. In the case of discrepancies between database gene models and our *in silico* analysis, PCR amplification of the "suspicious" regions was performed, followed by cloning and sequencing (see paragraph "Cloning and Sequencing of Opsin Gene

Fragments/Transcripts"). Additionally, we thoroughly queried the *B. belcheri*HapV2(v7h2) and the v18h27.r3_ref_genome assemblies, available at the **Chinese Lancelet (Amphioxus) Genome Sequencing project** webpage (http://genome.bucm.edu.cn/lancelet/), applying both keyword and BLAST searches. In order to investigate the phylogenetic relationships of previously annotated and newly identified amphioxus opsins and thus establish orthology of opsin genes, a Maximun Likelihood tree was constructed according to Pantzartzi *et al.*[40]. The same dataset was used and it was enriched with *B. floridae* and *B. belcheri* sequences (Supplementary File 1, Supplementary Table 1). For each opsin gene, orthologs from the three *Branchiostoma* species were aligned using ClustalO[46] and visualized using BoxShade. In the case of orthologs absent from one or two species, we used Circoletto[47], in order to investigate synteny conservation and visualize sequence similarity among syntenic scaffolds from the *Branchiostoma* species. E-value for the BLAST run was set to e^{-20}.

Transposable Elements Analysis

Genomic scaffolds containing opsins and those expected to contain opsin genes based on synteny analyses were screened for repetitive elements using Censor[48] in the RepBase database[49]. NCBI Accession numbers for *B. floridae* scaffolds used are NW_003101565 (Bf_scaffold6), NW_003101418 (Bf_scaffold_187), NW_003101537 (Bf_scaffold_36), NW_003101507 (Bf_scaffold_98) and NW_003101409 (Bf_scaffold_196). The genomic regions used were: Bf_scaffold_6: 305,868-729,662 or 305,868-547140 (Comparison of Narrow Regions, CNR); Bf_scaffold_187: 4,135,366-4,628,754 or 4,135,366-4,378,895 (CNR); Bl_Sc0000005: 5,300,000-7,300,000 or 6,885,201-7,300,000 (CNR); Bb_scaffold48: 1-2,523,832 or 1,200,000-2,523,832 (CNR); Bf_scaffold_36: 4,567,754-4,488,902, Bf_scaffold_98: 4,107,000-4,213,900, Bl_Sc0000154: 143,384-219,100, Bl_Sc0000040: 850,000-1,050,000, Bb_Sc0000263: 1-200,000; Bb_scaffold123: 447,402-528,601; Bf_scaffold_196: 2,792,247-2,817,466, Bl_Sc0000011: 2,118,981-2,146,160; Bb_Sc0000116: 763,100-794,099.

Animal Collection

B. floridae embryos were collected in Old Tampa Bay (Florida, USA, no permission required for amphioxus collection). Housing of animals and *in vivo* experiments in the present study were performed in accordance with guidelines established by the Institute of Molecular Genetics and in compliance with national guidelines (ID#12135/2010-17210). All animal works were also conducted according to the National Institute of Health standards as underlined by the "Guide for Care and Use of Laboratory Animals". Gametes were obtained and embryos raised, as previously described[50]. Staging of all collected embryos was performed according to Hirakow and Kajita[51], specimens from late neurula (N3), larvae (L1-L3) and adult stage were collected and frozen in RNAlater® Stabilization Solution (ThermoFisher Scientific), under light conditions.

RNA Isolation / cDNA Preparation

Total RNA was isolated from *B. floridae* embryos stored in RNAlater® Stabilization Solution using the Trizol reagent (Ambion). To avoid genomic DNA contamination, isolated RNA was treated with DNaseI and purified on RNeasy Mini Kit (Qiagen) column. Random-primed cDNA was prepared from 250ng of RNA in a 20 µl reaction using SuperScript VILO cDNA Synthesis kit (Invitrogen).

Cloning and Sequencing of Opsin Gene Fragments/Transcripts

For validation of the *in silico* predicted gene models, cloning and sequencing of opsin gene fragments and complete transcripts from *B. floridae* was performed, according to Pantzartzi *et al.*[40]. Primers used are included in Supplementary Table 2.

qRT-PCR

Primers used are provided in Supplementary Table 2. Experiments and analysis of results were performed according to Pantzartzi *et al.*[40]. TBP was used as the housekeeping gene.

Results

Identification, classification and genome organization of opsin genes in the *Branchiostoma* genus

We initially performed a thorough comparative analysis of the opsin gene repertoires of three cephalochordate species. We used the recently reported genes from *B. lanceolatum*[40] together with previously reported genes from *B. floridae* and *B. belcheri*[41-43] many of which had to be re-predicted and some were *de novo* identified in the current study (Supplementary Table 1). Final transcripts and encoded proteins for newly characterized and modified opsins from *B. floridae* and *B. belcheri* as well as details on gene organization and genomic location are provided in Supplementary File 1. Orthology of identified genes was validated by synteny and phylogenetic analysis (Supplementary Fig. 1).The alignments of orthologs for each opsin gene from the three *Branchiostoma* species are provided in Supplementary File 1. Orthologs have the same number of exons; the sole exceptions are *op7* and *op20*. Orthologous exons have almost identical size, however, pronounced changes are observed in the size of the last exon. Furthermore, there is a great similarity among orthologs in terms of sequence, with the Cterminus being the most variable. Evidently, opsin genes are spread over 16 genomic regions (scaffolds) in *B. floridae* and 14 in *B. belcheri* (Supplementary Fig. 2).Phylogenetic analysis (SupplementaryFig.1) in combination with the arrangement of opsin genes in the genomes of the three species (Supplementary Fig. 2)supports the fact that the majority of opsin genes are represented by an ortholog in all three species (Table 1). This is not the case for *op6*, *op12b*, *op13b*, and *op17b*, which seem to be the result of a gene duplication.

We further analyzed the opsin expression pattern across different developmental stages (Supplementary Fig.3) of *B. floridae*. Onset of several opsin genes expression starts at L1 stage, in which frontal eye and lamellar body (ciliary photoreceptive organs) start to

develop. In agreement with *B. lanceolatum*[40], the majority of the *B. floridae* opsins show most predominant expression in L2/3 stages, where all of the known amphioxus photoreceptor organs are differentiated. Nevertheless, differences are observed between the two species in regard to the onset of expression of *op13a*. Interestingly, *op6*, a gene detected only in *B. floridae,* follows a distinct pattern in regard to the other two neuropsins (i.e. *op7* and *op8*), for which expression patterns are the same for both *B. floridae and B. lanceolatum*.

Transposable elements and opsin genes in the *Branchiostoma* genus

Differences have been noted among the three *Branchiostoma* species in regard both to the structure and the number of opsin genes (Table 1 and Supplementary File 1). Since transposable elements (TEs) have been vastly implicated in gene structure alteration as well as gene duplications and losses, we scanned scaffolds containing altered genes against RepBase to locate TEs populating these regions; for opsin orthologs that are absent from one or two *Branchiostoma* species (Table 1), we found the syntenic scaffolds and also scanned them against RepBase.

The beginning of forth exon of *Bl_op2* is occupied by small repeated sequences, a fact that leads to elongation of the third cytoplasmic loop (Supplementary File 1). Noticeably, the fifth intron of *Bl_op8* highly resembles a satellite locus from *Salmo salar* (SAT-11_SSa in RepBase). In fact, the beginning of the last exon is one of the repeat units. It is also worth mentioning that the last exon of *Bl_op16* is longer in size than the respective exons from the *B. floridae* and *B. belcheri* orthologs due to palindromic repeats at its end (Supplementary File 1). *Bl_op16* is flanked by a truncated and a complete copy of the DNA transposon Ginger2-1 and the non-autonomous DNA transposon Harbinger-N11 (data not shown).

Comparison of the syntenic scaffolds related to *op6* is portrayed in Fig.1. High similarity is observed among the genomic regions containing *op7* in *B. floridae*, *B. lanceolatum* and *B. belcheri*(Fig.1A). Similarity is also observed between the genomic regions flanking *op6* in *B. floridae* and *B. lanceolatum*Sc0000005 and *B. belcheri*scaffold48, however, there are no traces of *op6* in the other two species. Some of the immediately flanking genes of *Bf_op6* have their orthologs in *B. lanceolatum* (only one seems to be eliminated, namely Bf210534), but are duplicated in the latter, with more striking example that of Bf73045 (Fig.1B). Duplication of other genomic fragments in the region where *Bl_op6* was supposed to be is also evident. Numerous families of transposable elements and simple repeated sequences of varying size (265bp) have been detected within and in the proximity of the duplicated genes and genomic fragments in Bl_Sc0000005 (see Supplementary Fig.4A for names of TEs). A similar case of duplicated genomic fragments populated by transposable elements is also observed in *B. belcheri*. What is even more appealing is the number and type of transposable elements within *Bf_op6* and *Bf_op7* genes and in their vicinity (Supplementary Fig.4B). No other conservation at genomic level is observed between *B. floridae* scaffolds 6 and 187, apart from the opsin genes and various transposable elements, as shown in Supplementary Fig.4B.

Differences are observed among the three species in regard to *op12* and *op13* copies (Table 1,Fig.2 and Supplementary Fig. 2). In general, these genes exhibit high sequence similarity and contain the same number of exons. Size of the exons is almost identical, with a

strikingly smaller last exon in *Bb_op12b*(Supplementary File1). Comparison of scaffolds bearing *op12a*, *op12b* and *op13a* from the three species (Fig.2A) shows that there is high conservation in opsin genes as well as in their flanking regions. However, no significant similarity exists in the intergenic regions of *op12a* and *op13a*. Interestingly, opsin genes in *B. belcheri* are flanked by complete copies of DNA transposons (Supplementary Fig.4C). The absence of *op13b*ortholog from *B. floridae* and *B. belcheri* is evident from the comparison of syntenic scaffolds (Fig. 2B). On the other hand, scaffolds containing the *B. lanceolatumop13a* and *op13b* paralogs (Fig.2C, Supplementary Fig.4C) show a high degree of similarity only in the genic regions and their immediate neighborhood which does not extend further in the region of *Bl_op12a*. The region of similarity is bordered by simple repeats as well as complete or partial copies of TEs.

Another example of putative gene duplication and loss event is that of *op17a* and *op17b* (Fig.3). Using the neighboring genes of *Bf_op17a* we detected the syntenic scaffold in *B. belcheri*. Comparison of the three scaffolds shows conservation in the flanking regions but no traces of a *Bb_op17a*gene. Instead, in the region where *Bb_op17a* is expected to be, there are copies of retrotransposons[52] (Supplementary Fig.4D). *Bl_op17a* and *Bl_op17b*genes are as well flanked by autonomous and non-autonomous transposons.

To summarize our previous findings, we could say that independent events of gene duplications and losses occurred during the evolution of *Branchiostoma* opsins (Fig.4A).Taking into account the higher similarity between *B. lanceolatum and B. belcheri* regions, the almost identical structure of *Bf_op6* and *Bf_op7* and the presence of common transposable elements within and outside these two genes, we could conclude that *op6* is the result of a duplication event in *B. floridae*, after its split from *B. lanceolatum*. However, we cannot rule out the possibility that *op6* existed in the common ancestor of the *Branchiostoma* species and it was eliminated in the lineages of *B. lanceolatum* and *B. belcheri*. We could also conclude that*Bb_op12a* and *Bl_op13a* were independently duplicated in *B. belcheri* and *B. lanceolatum*. Finally, we assume that *op17a* was lost in *B. belcheri* and *op17b* is the result of a gene duplication only in *B. lanceolatum* (Fig.4A). Figure4B outlines what the ancestral state could have been for each of the duplicated/lost genes and the putative mechanisms through which gene gains and losses took place. Complete and partial copies of TEs identified in the vicinity of opsin genes probably served as illegitimate spots for recombination, leading to misalignment, unequal crossover and hence duplication of an opsin gene, as in the case of *op12* and *op13*, or caused crossing over of the same chromosome, leading to the deletion of *op17* in *B. belcheri*.

Discussion

Cephalochordates are often used as a proxy to the ancestral chordates. This is in large part due to the presumed slow evolutionary rate of their genomes. In this study we used the *Branchiostoma* opsin gene family as an example of how TEs can shape cephalochordate genomes, by deleting or creating new genes, by altering the number and size of exons or influencing their expression patterns. We further reconstructed the evolutionary history of

opsin family in the *Branchiostoma* genus, via comparison of primary sequence, structure and expression patterns of opsin genes from three cephalochordate species.

The species-specific duplicates *Bl_op13a* and *Bl_op13b*differ in their spatial (tissuespecific) but overlap in their temporal expression patterns and are already detected at an earlier stage than *B. floridae* (Pantzartzi *et al.*[40] and SupplementaryFig.3). The first one is indicative of subfunctionalization, where the two genes seem to have optimized for specific tasks in tissues with different type of photoreceptor cells (ciliary and rhabdomeric), while the latter implies that *Bl_op13a* underwent neofunctionalization, due to which expression is triggered at an earlier stage. The relatively large size of the Go group and the retention in the genome of the duplicated opsins (*Bb_op12b* and *Bl_op13b*) could be an indication of fine tuning between these opsins in order for specific photoreception-related tasks to be fulfilled. Similarly, retention of *Bf_op6*and *Bf_op7*in the genome of *B. floridae* could be attributed to subfunctionalization, since changes are noted in their temporal expression pattern (Supplementary Fig. 3B).

The role of transposable elements (TEs) in shaping the genome and promoting evolution has been the focus of many studies, and what was formerly characterized as "junk"or "selfish DNA" is gaining more and more value and functional importance[53]. TEs may act in the same or completely different way, depending on selection forces. This is nicely exemplified by the ParaHox loci in *Ciona*, amphioxus and vertebrates[54,55]. ParaHox cluster in *Ciona* has lost the tight organization present in chordates and this degeneration could be attributed to the invasion of TEs in the locus, specifically of MITEs[55]. On the other hand, even though the amphioxus ParaHox cluster was found to be a hotspot for TE insertion, selection constraints probably inhibit this disruptive elements from influencing the ParaHox locus[54]. Another example of how TEs may influence the gene structure is that of *PRHOXNB* gene, for which the gain of an intron was reported, in which the miniature inverted-repeat transposable element (MITE) LanceletTn-2 was detected[56].

An increase in the number of opsin gene has been previously reported for various species, owing either to local gene duplications[57] or whole genome duplications[58]. In some cases, the number or structure of opsin genes seems to be shaped under the influence of TEs[5961]. The presence of an incomplete *Alu* element upstream the human middle wavelength sensitive (MW) opsin gene may imply that *Alu* elements have been involved in the initial gene duplication responsible for the MW and long-wavelength sensitive (LW) genes in the Old World primates and the high frequency of gene loss and gene duplication within the opsin gene array[60]. It is suggested that unequal crossover is the mechanism through which this duplication occurred[60]. In the swordtail fish, *Xiphophorus helleri*, one of the four LW copies was found to be the result of a retrotransposition event[59]. On the other hand, the loss of function of the *Takifugu rubripes* RH2-2 gene is reported to follow a transposon-induced deletion that truncated the N-terminal of the protein[61].

We have provided information about how TEs might have led to gene duplications and losses in the *Branchiostoma* opsin family, or alterations in the number and size of exons. In fact, the *Branchiostoma* opsin family could serve as an example of how TEs can play an important role in the shaping of a gene family and of the genome per se, through gene gain

and loss events due to unequal cross-over or moving of genes between different loci in the genome (Fig. 5). Moreover, TEs may also lead to neofunctionalization of duplicate genes, which typically occurs by the acquisition of new regulatory elements. Overrepresentation of transcription factor binding sites is evident for TEs residing in promoter regions of not only human genes[11], but of amphioxus as well[62]. Retention of *Branchiostoma* gene copies in the genome and differences in their spatiotemporal expression pattern, together with the presence of different types of TEs, could also imply that TEs were not implicated only in the birth or death of opsin genes but in their control as well.

References

1 Lankenau, D. & Volff, J. N. *Transposons and the Dynamic Genome*. Springer-Verlag Berlin Heidelberg, (2009).

2 Finnegan, D. J. Eukaryotic transposable elements and genome evolution. *Trends Genet.* **5,** 103-107 (1989).

3 Curcio, M. J. & Derbyshire, K. M. The outs and ins of transposition: from mu to kangaroo. *Nat. Rev. Mol. Cell Biol.* **4,** 865-877; 10.1038/nrm1241 (2003).

4 Wicker, T. *et al.* A unified classification system for eukaryotic transposable elements. *Nat Rev Genet* **8,** 973-982; 10.1038/nrg2165 (2007).

5 McClintock, B. Controlling elements and the gene. *Cold Spring Harb. Symp. Quant. Biol.* **21,** 197-216 (1956).

6 Chuong, E. B., Elde, N. C. & Feschotte, C. Regulatory activities of transposable elements: from conflicts to benefits. *Nat. Rev. Genet.* **advance online publication**; 10.1038/nrg.2016.139 (2016).

7 Bourque, G. Transposable elements in gene regulation and in the evolution of vertebrate genomes. *Curr. Opin. Genet. Dev.* **19,** 607-612; 10.1016/j.gde.2009.10.013 (2009).

8 Feschotte, C. Transposable elements and the evolution of regulatory networks. *Nat. Rev. Genet.* **9,** 397-405; 10.1038/nrg2337 (2008).

9 Feschotte, C. The contribution of transposable elements to the evolution of regulatory networks. *Nat. Rev. Genet.* **9,** 397-405; 10.1038/nrg2337 (2008).

10 McVean, G. What drives recombination hotspots to repeat DNA in humans? *Phil. Trans. R. Soc. B.* **365,** 1213-1218; 10.1098/rstb.2009.0299 (2010).

11 Thornburg, B. G., Gotea, V. & Makalowski, W. Transposable elements as a significant source of transcription regulating signals. *Gene* **365,** 104-110; 10.1016/j.gene.2005.09.036 (2006).

12 Feschotte, C. & Pritham, E. J. DNA transposons and the evolution of eukaryotic genomes. *Annu. Rev. Genet.* **41,** 331-368; 10.1146/annurev.genet.40.110405.090448 (2007).

13 Arguello, J. R., Fan, C., Wang, W. & Long, M. *Origination of chimeric genes through DNA-level recombination*. Karger, (2007).

14 Gray, Y. H. It takes two transposons to tango: transposable-element-mediated chromosomal rearrangements. *Trends Genet.* **16,** 461-468 (2000).

15 Canapa, A., Barucca, M., Biscotti, M. A., Forconi, M. & Olmo, E. Transposons, genome size, and evolutionary insights in animals. *Cytogenet. Genome Res.* **147,** 217239; 10.1159/000444429 (2015).

16 Joly-Lopez, Z. & Bureau, T. E. Diversity and evolution of transposable elements in *Arabidopsis*. *Chromosome Res.* **22,** 203-216; 10.1007/s10577-014-9418-8 (2014).

17 Kaminker, J. S. *et al*. The transposable elements of the *Drosophila melanogaster* euchromatin: a genomics perspective. *Genome biology* **3,** research0084.00810084.0082; 10.1186/gb-2002-3-12-research0084 (2002).

18 Mahillon, J. & Chandler, M. Insertion Sequences. *Microbiol. Mol. Biol. Rev.* **62,** 725774 (1998).

19 Mills, R. E., Bennett, E. A., Iskow, R. C. & Devine, S. E. Which transposable elements are active in the human genome? *Trends Genet.* **23,** 183-191; 10.1016/j.tig.2007.02.006 (2007).

20 Baucom, R. S. *et al*. Exceptional diversity, non-random distribution, and rapid evolution of retroelements in the B73 maize genome. *PLoS Genet.* **5,** e1000732; 10.1371/journal.pgen.1000732 (2009).

21 Cordaux, R. & Batzer, M. A. The impact of retrotransposons on human genome evolution. *Nat. Rev. Genet.* **10,** 691-703; 10.1038/nrg2640 (2009).

22 Gu, S. *et al*. Alu-mediated diverse and complex pathogenic copy-number variants within human chromosome 17 at p13.3. *Hum. Mol. Genet.* **24,** 4061-4077; 10.1093/hmg/ddv146 (2015).

23 Bertrand, S. & Escriva, H. Evolutionary crossroads in developmental biology: amphioxus. *Development* **138,** 4819-4830; 10.1242/dev.066720 (2011).

24 Huang, S. *et al*. Decelerated genome evolution in modern vertebrates revealed by analysis of multiple lancelet genomes. *Nat. Commun.* **5,** 5896; 10.1038/ncomms6896 (2014).

25 Chalopin, D., Naville, M., Plard, F., Galiana, D. & Volff, J. N. Comparative analysis of transposable elements highlights mobilome diversity and evolution in vertebrates. *Genome Biol. Evol.* **7,** 567-580; 10.1093/gbe/evv005 (2015).

26 Canestro, C. & Albalat, R. Transposon diversity is higher in amphioxus than in vertebrates: functional and evolutionary inferences. *Briefings in functional genomics* **11,** 131-141; 10.1093/bfgp/els010 (2012).

27 Igawa, T. *et al*. Evolutionary history of the extant amphioxus lineage with shallowbranching diversification. *Sci. Rep.* **7,** 1157; 10.1038/s41598-017-00786-5 (2017).

28 Kim, E. B. *et al*. Genome sequencing reveals insights into physiology and longevity of the naked mole rat. *Nature* **479,** 223-227; 10.1038/nature10533 (2011).

29 Banyai, L. & Patthy, L. Putative extremely high rate of proteome innovation in lancelets might be explained by high rate of gene prediction errors. *Sci. Rep.* **6,** 30700; 10.1038/srep30700 (2016).

30 Porter, M. L. *et al*. Shedding new light on opsin evolution. *Proceedings. Biological sciences / The Royal Society* **279,** 3-14; 10.1098/rspb.2011.1819 (2012).

31 Liegertova, M. *et al*. Cubozoan genome illuminates functional diversification of opsins and photoreceptor evolution. *Scientific reports* **5,** 11885; 10.1038/srep11885 (2015). 32 Terakita, A. The opsins. *Genome biology* **6,** 213; 10.1186/gb-2005-6-3-213 (2005).

33 Shichida, Y. & Matsuyama, T. Evolution of opsins and phototransduction. *Phil Trans R Soc B.* **364,** 2881-2895 (2009).

34 Feuda, R., Hamilton, S. C., McInerney, J. O. & Pisani, D. Metazoan opsin evolution reveals a simple route to animal vision. *Proc. Natl. Acad. Sci. USA* **109,** 18868-18872; 10.1073/pnas.1204609109 (2012).

35 Plachetzki, D. C., Degnan, B. M. & Oakley, T. H. The origins of novel protein interactions during animal opsin evolution. *PLoS One* **2,** e1054; 10.1371/journal.pone.0001054 (2007).

36 Peirson, S. N., Halford, S. & Foster, R. G. The evolution of irradiance detection: melanopsin and the non-visual opsins. *Philosophical transactions of the Royal Society of London. Series B, Biological sciences* **364,** 2849-2865; 10.1098/rstb.2009.0050 (2009).

37 D'Aniello, S. *et al*. Opsin evolution in the Ambulacraria. *Marine Genomics* **24, Part 2,** 177-183; 10.1016/j.margen.2015.10.001 (2015).

38 Ramirez, M. D. *et al*. The last common ancestor of most bilaterian animals possessed at least 9 opsins. *Genome Biol Evol.* **8,** 3640-3652; 10.1093/gbe/evw248 (2016).

39 Suga, H., Schmid, V. & Gehring, W. J. Evolution and functional diversity of jellyfish opsins. *Curr. Biol.* **18,** 51-55 (2008).

40 Pantzartzi, C. P., Pergner, J., Kozmikova, I. & Kozmik, Z. The opsin repertoire of the European lancelet: a window into light detection in a basal chordate. *Int. J. Dev. Biol. (accepted)*; 10.1387/ijdb.170139zk (2017).

41 Holland, L. Z. *et al*. The amphioxus genome illuminates vertebrate origins and cephalochordate biology. *Genome research* **18,** 1100-1111; 10.1101/gr.073676.107 (2008).

42 Koyanagi, M., Kubokawa, K., Tsukamoto, H., Shichida, Y. & Terakita, A. Cephalochordate melanopsin: evolutionary linkage between invertebrate visual cells and vertebrate photosensitive retinal ganglion cells. *Curr. Biol.* **15,** 1065-1069; 10.1016/j.cub.2005.04.063 (2005).

43 Koyanagi, M., Terakita, A., Kubokawa, K. & Shichida, Y. Amphioxus homologs of Go-coupled rhodopsin and peropsin having 11-*cis*- and all-*trans*-retinals as their chromophores. *FEBS Lett.* **531,** 525-528 (2002).

44 Burge, C. & Karlin, S. Prediction of complete gene structures in human genomic DNA. *J. Mol. Biol.* **268,** 78-94; 10.1006/jmbi.1997.0951 (1997).

45 Rogozin, I. B. & Milanesi, L. Analysis of donor splice sites in different eukaryotic organisms. *J. Mol. Evol.* **45,** 50-59 (1997).

46 Sievers, F. *et al*. Fast, scalable generation of high-quality protein multiple sequence alignments using Clustal Omega. *Mol. Syst. Biol.* **7,** 539; 10.1038/msb.2011.75 (2011).

47 Darzentas, N. Circoletto: visualizing sequence similarity with Circos. *Bioinformatics* **26,** 2620-2621; 10.1093/bioinformatics/btq484 (2010).

48 Kohany, O., Gentles, A. J., Hankus, L. & Jurka, J. Annotation, submission and screening of repetitive elements in Repbase: RepbaseSubmitter and Censor. *BMC Bioinformatics* **7,** 474; 10.1186/1471-2105-7-474 (2006).

49 Bao, W., Kojima, K. K. & Kohany, O. Repbase Update, a database of repetitive elements in eukaryotic genomes. *Mobile DNA* **6,** 11; 10.1186/s13100-015-0041-9 (2015).

50 Holland, L. Z. & Yu, J. K. Cephalochordate (amphioxus) embryos: procurement, culture, and basic methods. *Methods in cell biology* **74,** 195-215 (2004).

51 Hirakow, R. & Kajita, N. Electron microscopic study of the development of amphioxus, *Branchiostoma belcheri tsingtauense*: the neurula and larva. *J. Anat.* **69,** 1-13 (1994).

52 Permanyer, J., Albalat, R. & Gonzalez-Duarte, R. Getting closer to a pre-vertebrate genome: the non-LTR retrotransposons of *Branchiostoma floridae*. *International journal of biological sciences* **2,** 48-53 (2006).

53 Muotri, A. R., Marchetto, M. C., Coufal, N. G. & Gage, F. H. The necessary junk: new functions for transposable elements. *Hum. Mol. Genet.* **16 (R2),** R159-R167; 10.1093/hmg/ddm196 (2007).

54 Osborne, P. W. & Ferrier, D. E. Chordate Hox and ParaHox gene clusters differ dramatically in their repetitive element content. *Mol. Biol. Evol.* **27,** 217-220; 10.1093/molbev/msp235 (2010).

55 Ferrier, D. E. & Holland, P. W. *Ciona intestinalis* ParaHox genes: evolution of Hox/ParaHox cluster integrity, developmental mode, and temporal colinearity. *Mol Phylogenet Evol.* **24,** 412-417 (2002).

56 Xing, F. *et al*. Characterization of amphioxus *GDF8/11* gene, an archetype of vertebrate *MSTN* and *GDF11*. *Dev. Genes Evol.* **217,** 549-554; 10.1007/s00427-007-0162-3 (2007).

57 Matsumoto, Y., Fukamachi, S., Mitani, H. & Kawamura, S. Functional characterization of visual opsin repertoire in Medaka (*Oryzias latipes*). *Gene* **371,** 268-278; 10.1016/j.gene.2005.12.005 (2006).

58 Porath-Krause, A. J. *et al*. Structural differences and differential expression among rhabdomeric opsins reveal functional change after gene duplication in the bay scallop, *Argopecten irradians* (Pectinidae). *BMC Evol*. *Biol*. **16,** 250; 10.1186/s12862-0160823-9 (2016).

59 Watson, C. T., Lubieniecki, K. P., Loew, E., Davidson, W. S. & Breden, F. Genomic organization of duplicated short wave-sensitive and long wave-sensitive opsin genes in the green swordtail, *Xiphophorus helleri*. *BMC Evol*. *Biol*. **10,** 87-87; 10.1186/14712148-10-87 (2010).

60 Dulai, K. S., von Dornum, M., Mollon, J. D. & Hunt, D. M. The evolution of trichromatic color vision by opsin gene duplication in New World and Old World primates. *Genome research* **9,** 629-638 (1999).

61 Neafsey, D. E. & Hartl, D. L. Convergent loss of an anciently duplicated, functionally divergent RH2 opsin gene in the fugu and *Tetraodon* pufferfish lineages. *Gene* **350,** 161-171; 10.1016/j.gene.2005.02.011 (2005).

62 Holland, L. Z. & Short, S. Gene duplication, co-option and recruitment during the origin of the vertebrate brain from the invertebrate chordate brain. *Brain Behav*. *Evol*. **72,** 91105; 10.1159/000151470 (2008).

Competing financial interests: The authors declare no competing financial interests.

Figures

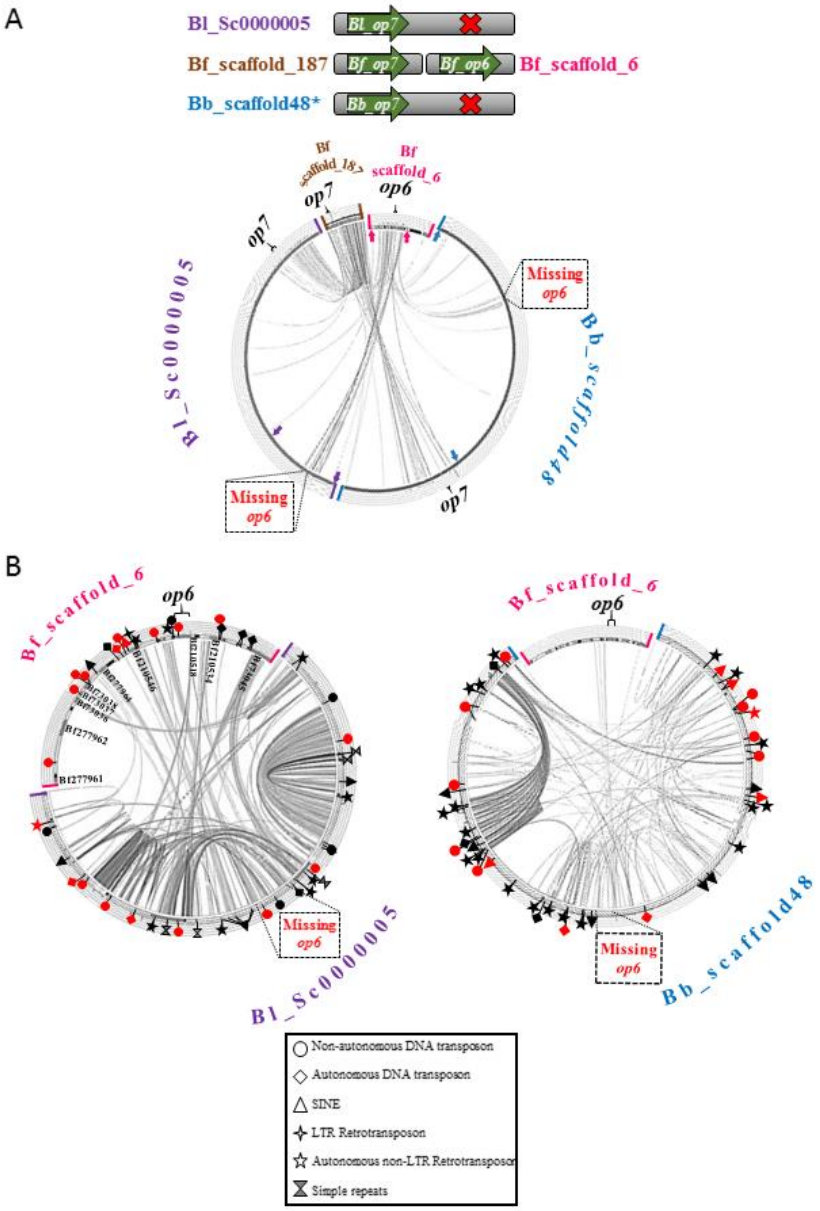

Fig.1. Comparison of genomic loci containing or lacking *op6* and *op7*.

(A) Comparison of the *op6*containing Bf_scaffold_6 and the *op7*containing Bf_scaffold_187 with the Bl_Sc0000005 and the Bb_scaffold48 that apparently contain only *op7* and lack *op6*. (B) Comparison of more narrow regions of Bf_scaffold_6 (delimited by arrows in (A)), with Bl_Sc0000005 (left) and Bb_scaffold48 (right). A high degree of duplicated regions was observed for *B. lanceolatum*, with the most striking example that of Bf73045 (left). Duplicated regions were also observed for *B. belcheri*(right). Red and black (complete and partial copies based on the RepBase database) symbols mark the position of simple tandem repeats and various families of Transposable Elements (TEs) (see key legend for explanation and Supplementary Fig.4A for TE names). For the sake of clarity, predicted *B. floridae* gene models are listed only in the internal part of the Bf_scaffold_6in (B). Ribbons connecting syntenic scaffolds under comparison denote similarity at genomic level.

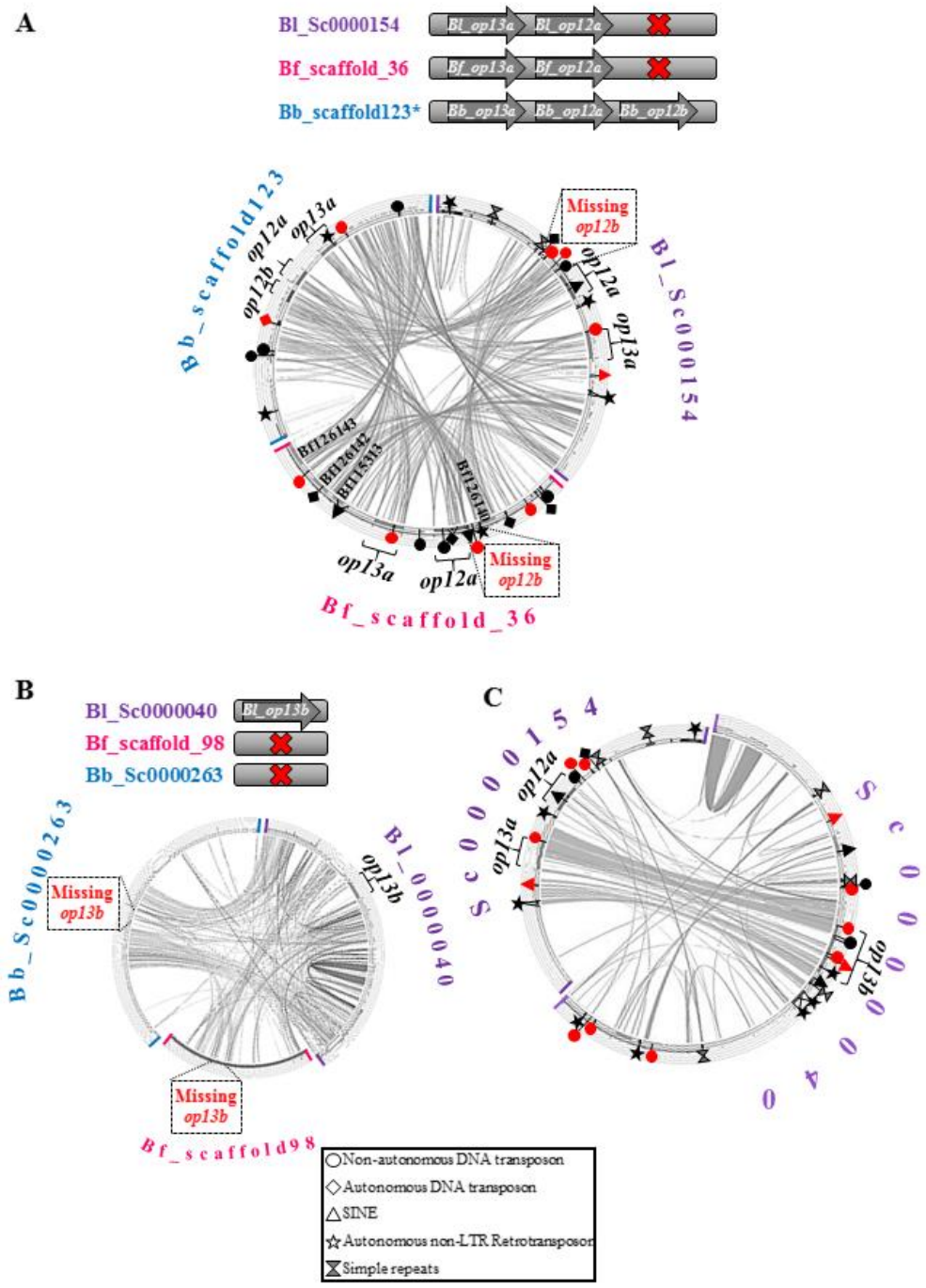

Fig.2. Comparison of genomic loci containing or lacking *op12a*, *op12b*, *op13a* and *op13b* opsins.

(A) Comparison of Bl_Sc0000154 with Bf_scaffold_36 and Bb_scaffold_23 (B) Comparison of *B. lanceolatum* scaffold containing the *op13b* gene with the syntenic scaffolds from *B. floridae* (Bf_scaffold_98) and *B. belcheri* (Bb_Sc0000263). (C): Comparison of *B. lanceolatum* scaffolds bearing opsins *op13a* (Sc0000154) and *op13b* (Sc0000040). Red and black (complete and partial copies based on the RepBase database) symbols mark the position of simple tandem repeats and various families of transposable elements (TEs) (see key legend for explanation and Supplementary Fig.4B and C for TE names). Predicted *B. floridae* gene models are listed in the internal part of the scaffolds.

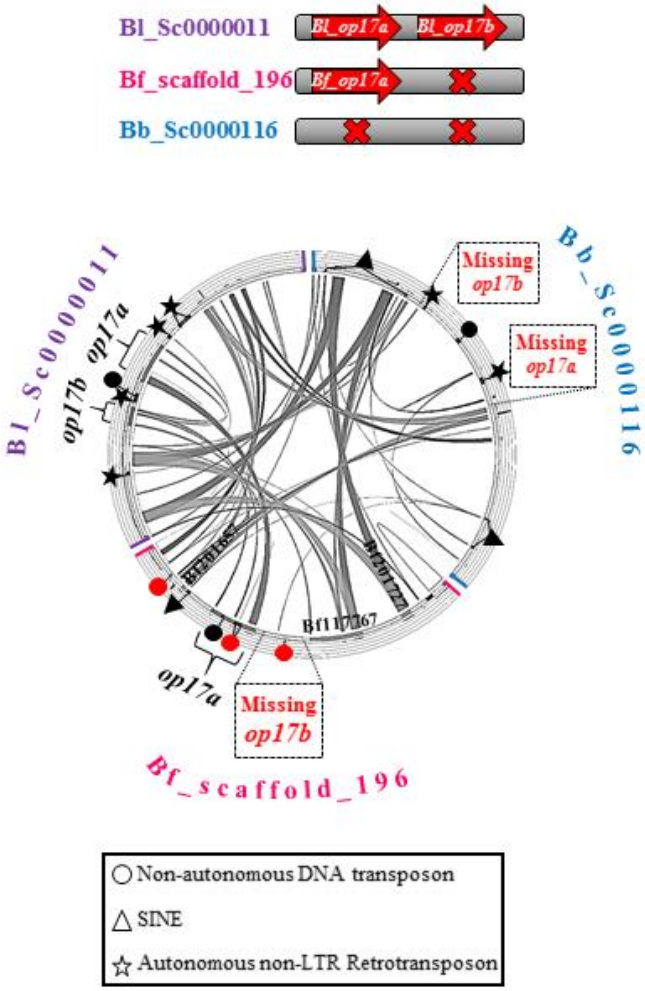

Fig.3. Comparison of genomic loci containing or lacking *op17a* and *op17b* opsins. Comparison of the *op17a* and *op17b* containing scaffold from *B. lanceolatum* with the *op17a*containing B. *floridae* scaffold and the syntenic scaffold from *B. belcheri* that obviously lacks both *op17a* and *op17b*. A clear conservation of the genomic regions is observed. Red and black (complete and partial copies based on the RepBase database) symbols mark the position of various families of transposable elements (TE) (see key legend for explanation and Supplementary Fig.4D for TE names). Predicted *B. floridae* gene models are listed in the internal part of the scaffolds.

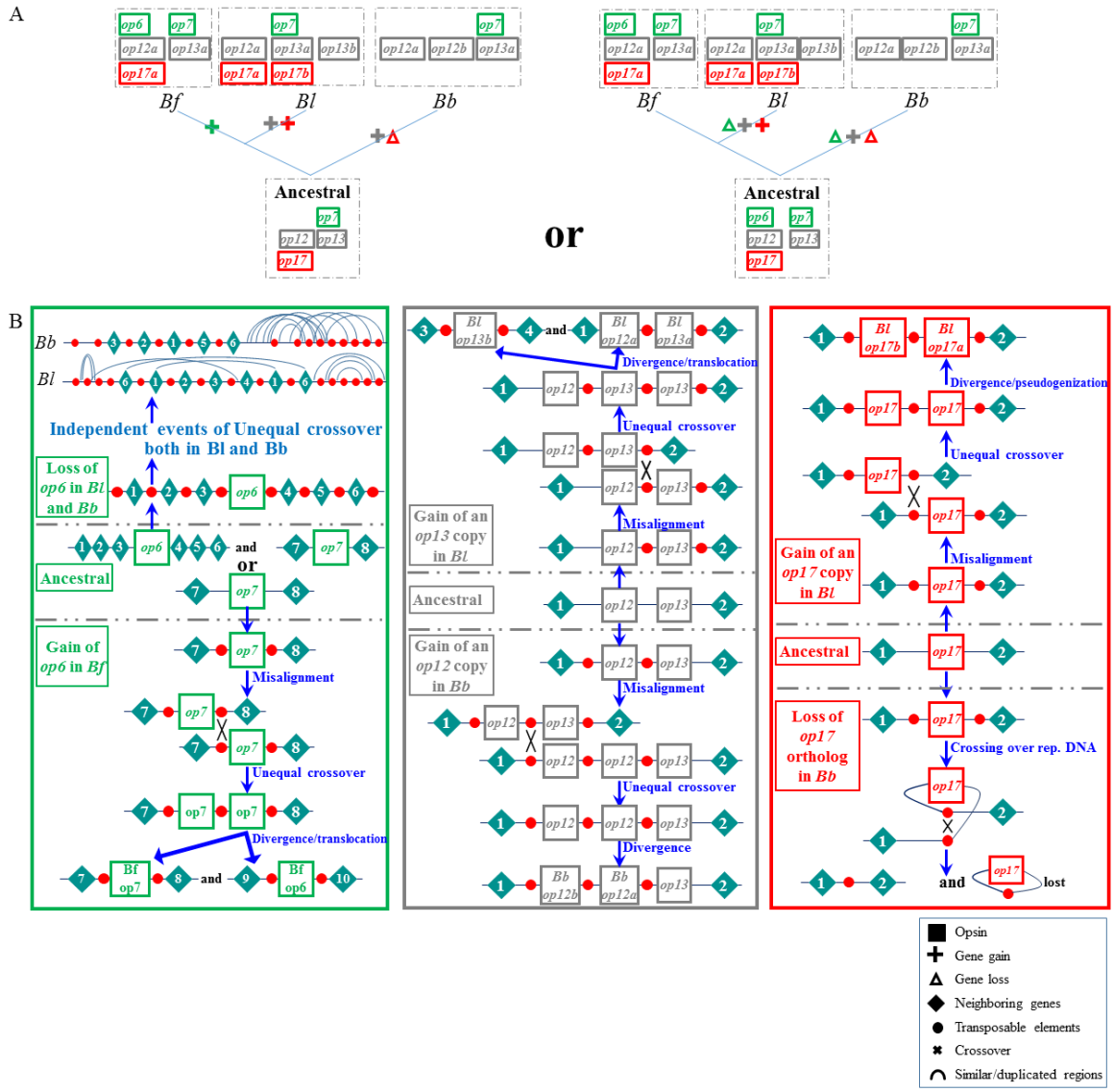

Fig.4. Reconstruction of the evolutionary history of opsin family in the *Branchiostoma* genus.

(A) Schematic representation of gene gains and losses in the lineages of *B. lanceolatum, B. floridae and B. belcheri*. (B) *op6* was either lost independently in the lineages of *B. lanceolatum* and *B. belcheri* or duplicated in *B. floridae*, due to misalignment and unequal cross-over events, where Transposable Elements (TEs) were used as illegitimate recombination hotspots. Likewise, *Bb_op12b* and *Bl_op13b* were duplicated independently only in the genomes of *B. belcheri* and *B. lanceolatum,* respectively. Finally, *Bl_op17b* was duplicated in the genome of *B. lanceolatum* and later was rendered non-functional, whereas recombination over transposable elements eliminated *Bl_op17a* from the *B. belcheri* genome.

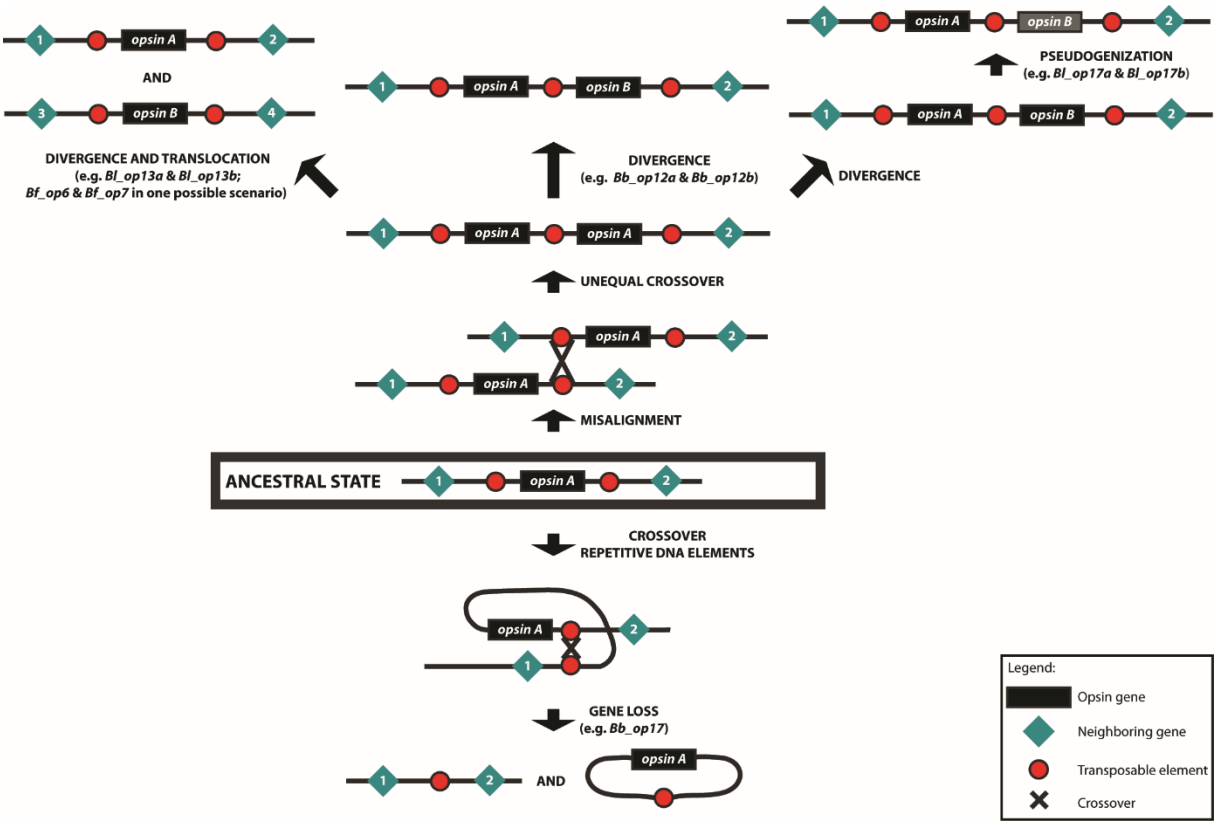

Fig.5. Suggested mechanisms for the evolution of a gene family, under the effect of Transposable Elements, as exemplified by the opsin family in the *Branchiostoma* genus

Supplementary figures

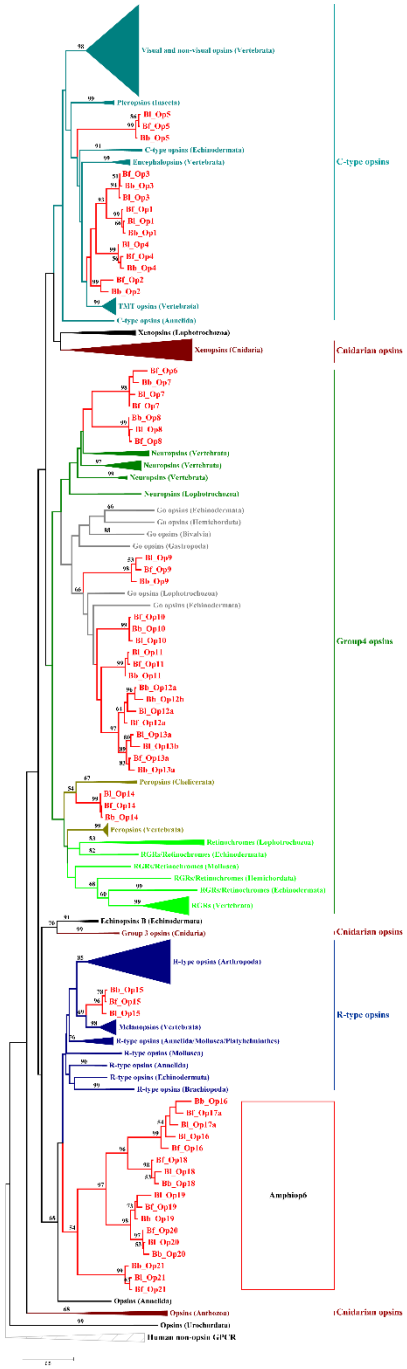

Supplementary fig.1. Molecular Phylogenetic analysis of opsins by Maximum Likelihood method.

The evolutionary history of opsin proteins was inferred by using the Maximum Likelihood method based on the Le_Gascuel_2008 model. The tree with the highest log likelihood is shown. Bootstrap values are shown (only values>50) either at the nodes or above the branches in the case of non-expanded subgroups (Neuropsins). A discrete Gamma distribution was used to model evolutionary rate differences among sites (2 categories). The tree is drawn to scale, with branch lengths measured in the number of substitutions per site. The analysis involved 827 amino acid sequences. There were a total of 419 positions in the final dataset (third cytoplasmic loop was excluded).

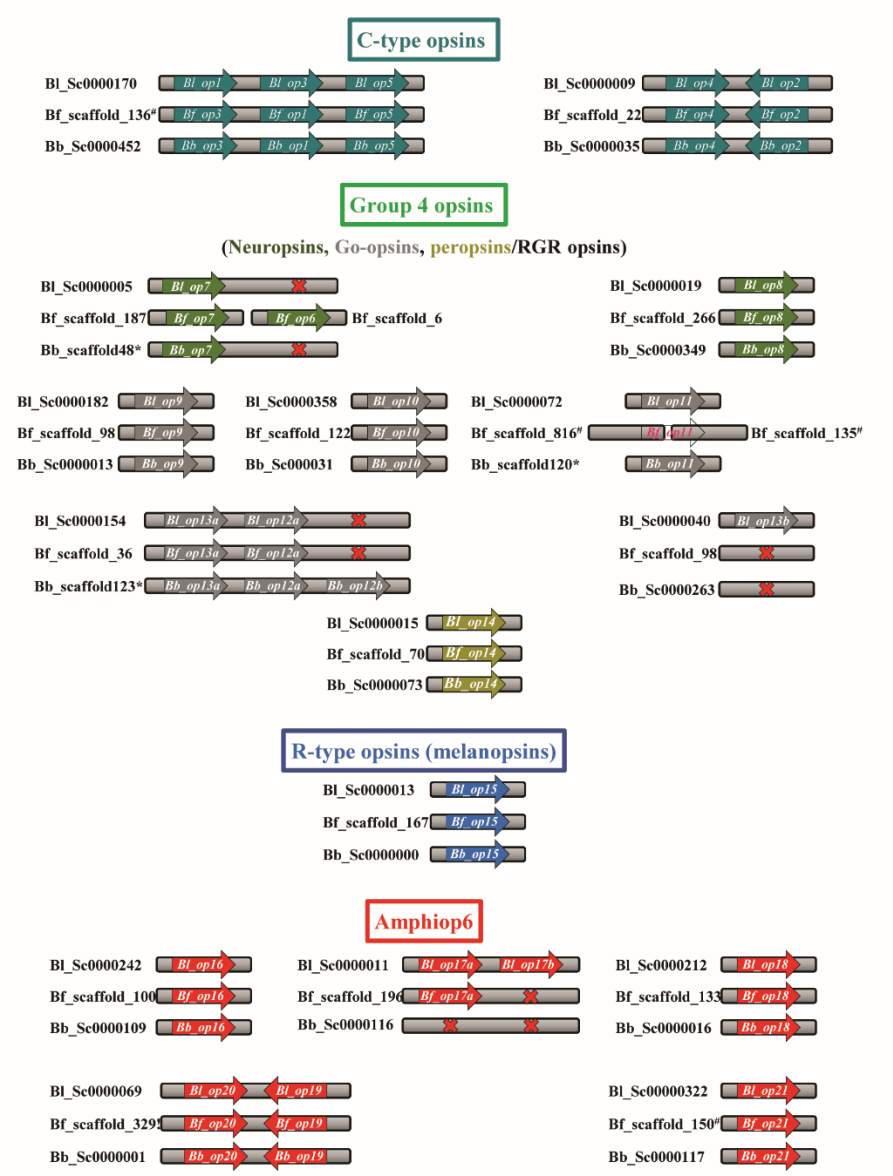

Supplementary Fig.2. Opsin containing genomic loci from *Branchiostoma* genus.

The genomic loci from *Branchiostoma lanceolatum* (Bl), *B. floridae* (Bf) and *B. belcheri* (Bb) containing opsin genes or lacking opsin genes (red x) but exhibiting synteny conservation to either of the other two respective opsin loci are depicted. Scaffold numbers for *B. floridae* correspond to v2.0 genome assembly in NCBI; # scaffolds correspond to the v1.0 genome assembly in JGI; † problem with genome assembly, see Supplementary File 1. Scaffold numbers for *B. belcheri* correspond to HapV2 genome assembly; * scaffolds refer to the r3refgenome assembly. Groups are colored based on their phylogenetic position (see supplementary Figure 1)

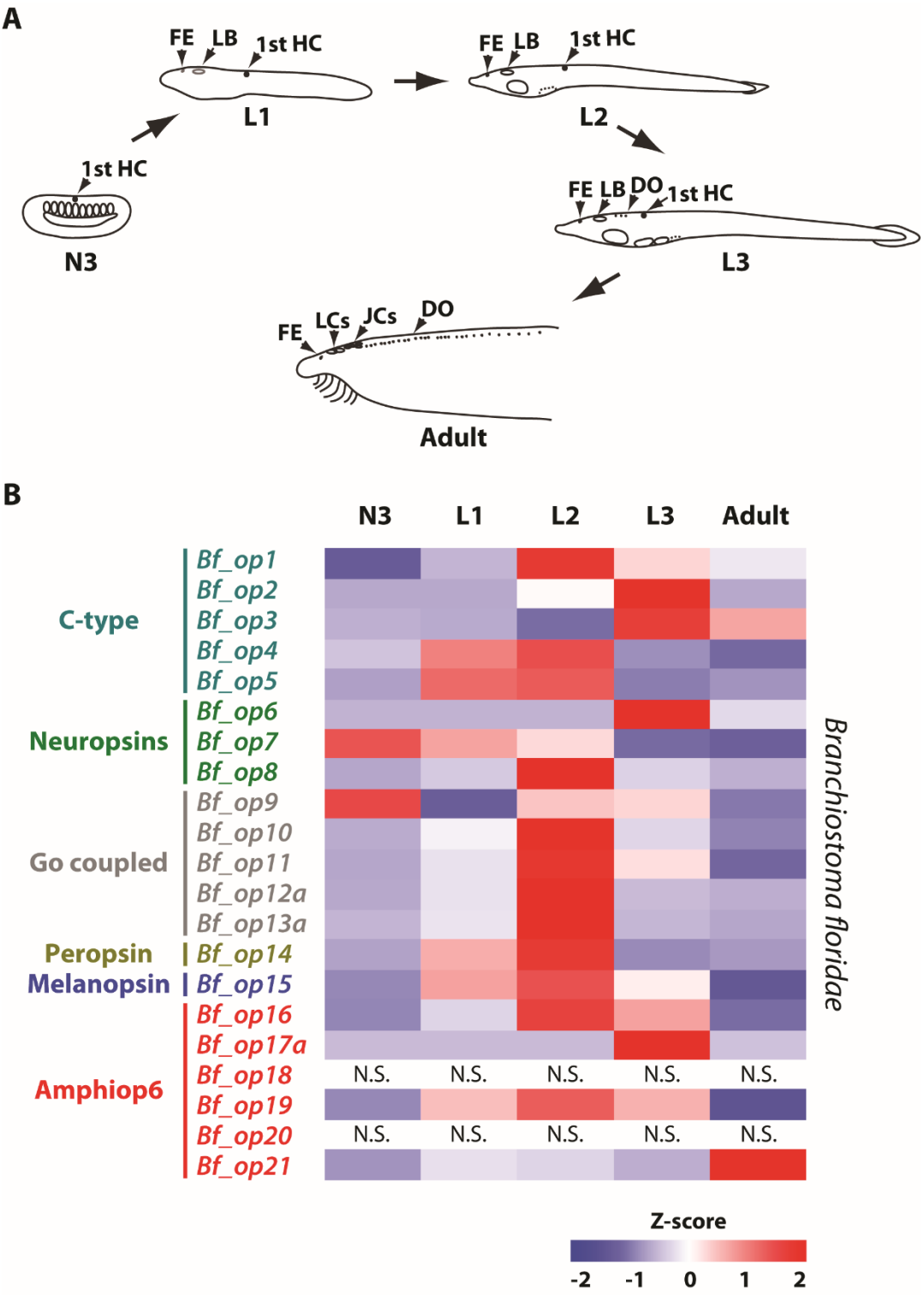

Supplementary Fig.3. mRNA expression levels of individual B. floridae opsins across different developmental stages.

(A) Schematic drawing of developmental stages (N3, L1, L2, L3, adult), in which detection of opsin genes expression was performed. Staging was determined according to Hirakow and Kajita (1994) (see Materials and Methods). 1st HC: 1st Hesse cell, FE: frontal eye, LB: lamellar body, DO: dorsal ocelli, JCs: Joseph cells. (B) Heat map displaying expression of opsin genes across different developmental stages. Opsin genes expression was detected by qRT-PCR and normalized to expression of TBP (B. floridae). Each row represents particular opsin gene expression in various developmental stages. Blue color represents expression below row average, white color represents average row expression, red color expression above row

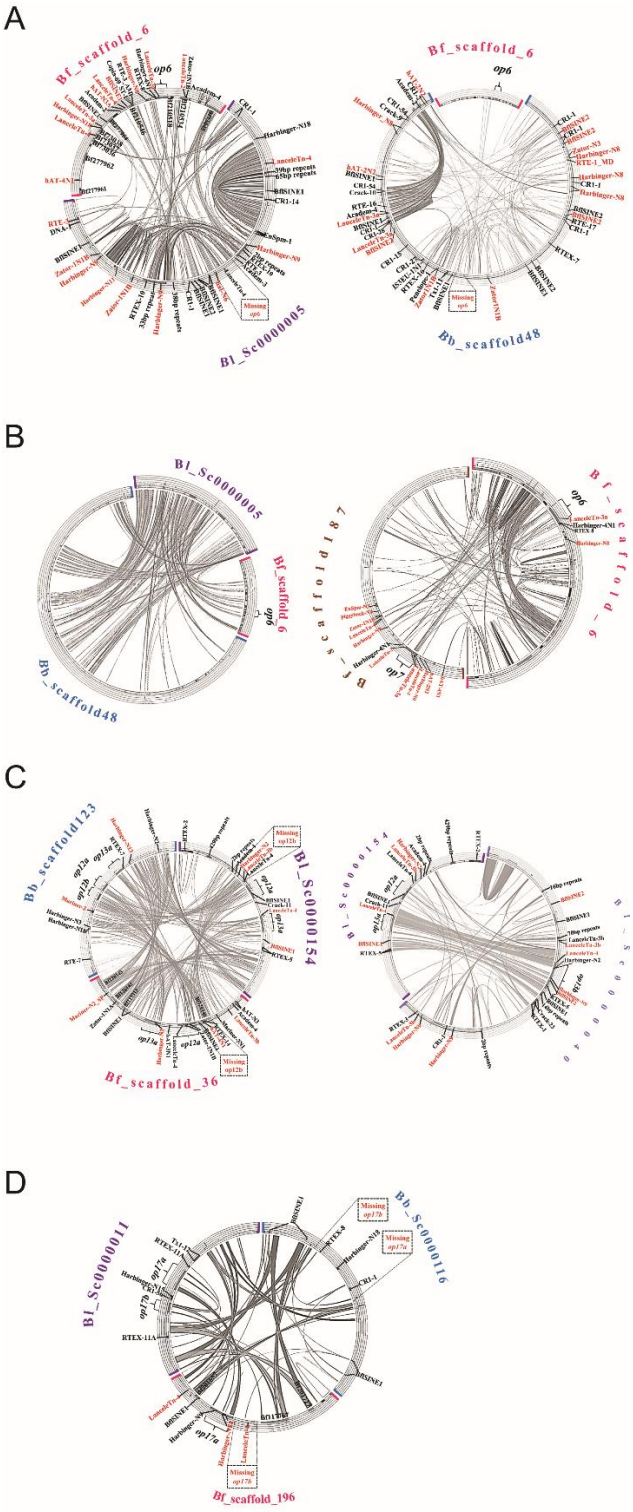

Supplementary Figure 4. Transposable elements and Branchiostoma opsin genes.
(A) Comparison of genomic regions of Bf_scaffold_6 with Bl_Sc0000005 (left) and Bb_scaffold48 (right), same as in fig.1. (B) Comparison of the op6-containing Bf_scaffold_6 with Bl_Sc0000005 and Bb_scaffold48 (left) and with Bf_scaffold_187 (right). Similarity between B. lanceolatum and B. belcheri scaffolds seems to be larger than of either of these with B. floridae. For B. floridae, similarity is observed in the genic region of op6 and op7 but not so much in the flanking regions. (C) Left: Comparison of Bl_Sc0000154 with Bf_scaffold_36 and Bb_scaffold_23, as in fig. 2. Right: Comparison of B. lanceolatum scaffolds bearing opsins op13a (Sc0000154) and op13b (Sc0000040). (D) Comparison of the op17a-containing Bf_scaffold_196 with Bl_Sc0000011 and Bb_Sc0000116, as in fig.3. Simple tandem repeats and various transposable elements (TE) are marked in red and black letters (complete and partial copies based on the Rep-Base database). Predicted B. floridae gene models are listed in the internal part of the scaffolds.

7. Discussion

This PhD. thesis and the scientific papers, it was built upon, are focused on the evolution of light reception and photoreceptive organs of amphioxus. Special emphasis was put on comparison of amphioxus frontal eye and opsins with their vertebrate counterparts.

Molecular fingerprint of developing amphioxus frontal eye resembles the fingerprint of developing vertebrate retina

Evolution of the vertebrate eye was always considered as one of the main obstacles for accepting Darwin´s theory about evolution by the matter of natural selection. Even Darwin admitted, that the vertebrate eye seems to be an organ of extreme perfection and it will be difficult to explain its evolution by the means of natural selection[62]. The problem of explaining the evolution of vertebrate eye is even so complicated, that some creationists take it as the proof, showing that the whole theory of evolution by the means of natural selection is incorrect. Several studies were trying to address this topic, but the main problem always was in finding a proper extant model organism to study.

Amphioxus´ position as the most basally branching chordate, makes it a useful proxy for studies dealing with the evolution of vertebrate specific traits. Amphioxus frontal eye is formed of only nine pigment cells and six photoreceptors with ciliary morphology in a 12.5 days old *B. floridae* larvae[94]. Photoreceptor cells are arranged in a single row, which means, that amphioxus frontal eye does not have image forming capacity. This makes it the simplest cephalic eye among chordates. Even the ocellus of *Ciona* (belonging to the urochordate subphylum) larvae seems to be composed of more photoreceptor cells (about 30)[109]. Urochordates´ tadpole-like larvae are similar to larvae of other chordates, but adults look very differently, being a vase-like benthic filter feeders. Moreover, urochordates genomes belong to one of the fastest evolving genomes among Metazoans[110]. These raise a question about how *Ciona* larval ocellus can be similar to the eye of a putative chordate ancestor. On the other hand, amphioxus body plan and genome evolve slowly[106]. Its frontal eye might, thus, be a reasonable starting point for seeking the ancestral chordate eye status.

Position and ultrastructure of the amphioxus frontal eye made it rational candidate for the homolog of vertebrate lateral eye already in early 1990s[94] based on EM analysis, but gene expression data were still missing. Studies with some interesting expression data, however, followed soon. First of all amphioxus *Otx* was shown to be expressed in the developing cerebral vesicle[102]. Other clues about the genetic similarity of the program driving the development of amphioxus frontal eye and vertebrate eyes came from a study showing the expression of *Pax6* gene in the anterior part of the cerebral vesicle[7]. Later, expression of amphioxus genes belonging to the Retinal Determination Gene Network (RDGN)[111], namely *Pax2/5/8*, *Six3/6*, *Eya* and *Dach*, was detected in the anterior cerebral vesicle[46,103].

The above mentioned studies were, however, done on various developmental stages and gene expression patterns were obtained by ISH, which by itself is not able to give precise information about single cell expression patterns. We, therefore, focused in our study on showing expression of genes important for development of the vertebrate eye on single cell resolution in a single developmental stage – 2 days old larvae. In this stage, the frontal eye

pigment spot is already present (meaning the cells in frontal eye might be already terminally differentiated or finishing their development) and the larvae are small enough to be scanned through the whole width of the body on confocal microscope.

Our results confirmed expression of Pax2/5/8 and Otx proteins in the developing pigment cell. This was in agreement with the role of these genes in the developing vertebrate retinal pigmented epithelium (RPE). We also showed Mitf expression in the frontal eye pigment cell. Mitf was, interestingly, detected also in the developing pigment cell of the 1st dorsal ocellus, rhabdomeric photoreceptive organ. Chemical inhibition of melanin synthesis proved, that pigment cells in both the frontal eye and the 1st dorsal ocellus contain melanin. This means, that amphioxus uses the same pigmentation program in two morphologically and genetically distinct photoreceptive organs.

Next, we detected expression of Otx and Pax4/6 in photoreceptors of developing frontal eye. Gene *OTX2* is necessary for proper development of vertebrate photoreceptors[112]. On the other hand *PAX6* was shown to be involved in the development of retinal progenitors in mouse, but does not have a direct effect on photoreceptor development from undifferentiated retinal progenitor cells[113]. Similar is the situation in the development of *Drosophila* photoreceptors, where *PAX6* orthologs are necessary for determination of eye development, but are not involved in differentiation of photoreceptors from progenitors. Of interest is the expression of amphioxus *Rx* in frontal eye photoreceptors. We were able to detect its expression in earlier stages (about 1 day old larvae) by ISH. Amphioxus *Rx* mRNA was detected in very anterior tip of the cerebral vesicle, where photoreceptors would later develop. Immunofluorescent staining of 2 days old larvae showed Rx expression only in more posteriorly located Row3 and Row4 cells, putative homologs of vertebrate interneurons (*this will be discussed in detail later in the text*). It thus seems, that amphioxus *Rx* is necessary for early specification of photoreceptors and might thus act in parallel to *Otx* and *Pax4/6*. *OTX* and *PAX4/6* might then be necessary for later development of photoreceptors, e.g. opsin expression, while action of *Rx* would not be required in later stages. Protein alignment and function of amphioxus Rx shows, it is probably homologous to vertebrate Rax. In vertebrates Rax was also shown to be expressed in developing retinal progenitors and acts upstream of Pax6 and Otx[114]. Slightly confusing is the fact that a gene called *C-RX* can be found in the mouse genome and is also active in eye development. *C-RX* is, however, necessary only for development of photoreceptors and not interneurons and acts in the developing retina downstream of *PAX6* or *OTX2*[112]. Moreover, vertebrate *C-RX* is more homologous to *OTX* genes.

While frontal eye photoreceptors seem to be homologous with vertebrate photoreceptors, data about putative interneurons in amphioxus frontal eye are ambiguous. Our analysis uncovered serotonin positive projections of Row2 cells of frontal eye (neurons located just posteriorly to frontal eye photoreceptors) leading to presumptive amphioxus tegmentum (visual processing center). Distinct population of amacrine cells in vertebrate retina was shown to be serotonin positive [115]. This could mean, that Row2 cells serve as interneurons homologous to vertebrate ganglion cells (based on termination in tegmentum) or amacrine cells (based on serotonin positivity). Previous EM analysis failed to follow Row2

projections precisely. Neurites that probably came from Row2 cells, appeared, however, not to form synaptic connection with other neurons, but ended with diffuse irregular terminals[116]. Additionally, Row2 processes are lateral, while most ganglion cells send their neurites contralaterally[116]. This seems, nevertheless, necessary mainly for proper spatial vision, which could definitely not be achieved by amphioxus frontal eye. Requirement for contralateral projections might thus not be essential for amphioxus interneurons.

Except for the aforementioned serotonin the Row2 cells did not express any of the examined genes. On the other hand, other amphioxus putative visual interneurons, Row3 (located posteriorly to Row2 cells) and Row4 cells (located posteriorly to Row3 cells), were Pax4/6 and Rx positive. As mentioned earlier both *RAX* and *PAX6* are necessary for proper development of retinal progenitors that give rise also to interneurons in the mouse. Besides this fact, two other arguments support the hypothesis that Row3 and Row4 cells might be putative homologs of vertebrate interneurons: 1. We documented glutamate positivity for both Row3 and Row4 cells[54]. In vertebrate retina, glutamate positivity was shown for bipolar and ganglion cells. 2. Row4 cells send contralateral processes[116], which is typical for ganglion cells. All presented results are, nevertheless, not sufficient for final decision of whether Row2, Row3 or Row4 cells serve as interneurons in amphioxus and which of the interneuron population they are homologous to.

The results of our as well as other studies, about the molecular fingerprint of amphioxus frontal eye pigment cell, photoreceptors and putative interneurons and their comparison with vertebrate counterparts are summarized in Fig.8. In total, it seems, that homology between amphioxus pigment cell and vertebrate RPE, and homology between amphioxus frontal eye photoreceptors and vertebrate retinal photoreceptors stands on solid grounds. Prof. Lacalli, who provided thorough EM analysis of amphioxus cerebral vesicle in early 1990s and since then follows all new data about amphioxus CNS[94,116], stated in his comment on our work: "There is still a big evolutionary gap to bridge between this tiny eye *(of amphioxus – note of the author of this thesis)*, lacking image forming capabilities, and vertebrate eyes, but at least that bridge is now firmly anchored at both ends."[65] What remains to be addressed is the identity of amphioxus interneurons. It will be worth focusing in the future research on the expression of amphioxus orthologs of other genes, known to be involved in the development of vertebrate interneurons. This goal is, however, quite tempting. Preparation of antibodies directed against chosen proteins is not difficult, as we have shown in our study[117]. The whole problem of deciphering the expression profile of Row2-4 cells in amphioxus, yet, stands on the assumption, that the set of genes necessary for development of retinal interneurons, would be at least in part ancestral to all chordates. Here might come the problem with the obvious simplicity of amphioxus frontal eye when compared with eyes of other extant chordates. Amphioxus frontal eye seems to be necessary only for providing information about presence or absence of light. Stimuli from amphioxus frontal eye might easily be transmitted through Rox2 cells, even if they would lack synapses, to putative tegmentum. The signal from Row2 cells to processing neurons in tegmentum might be transmitted, for example, by using non-synaptic connections similar to previously identified the so called juxta-reticular junctions in some parts of amphioxus cerebral vesicle[118,119]. This type of neuronal connection lacks

synaptic vesicles and yet seems to be working. This is, however, pure speculation and more data will be necessary to solve this issue.

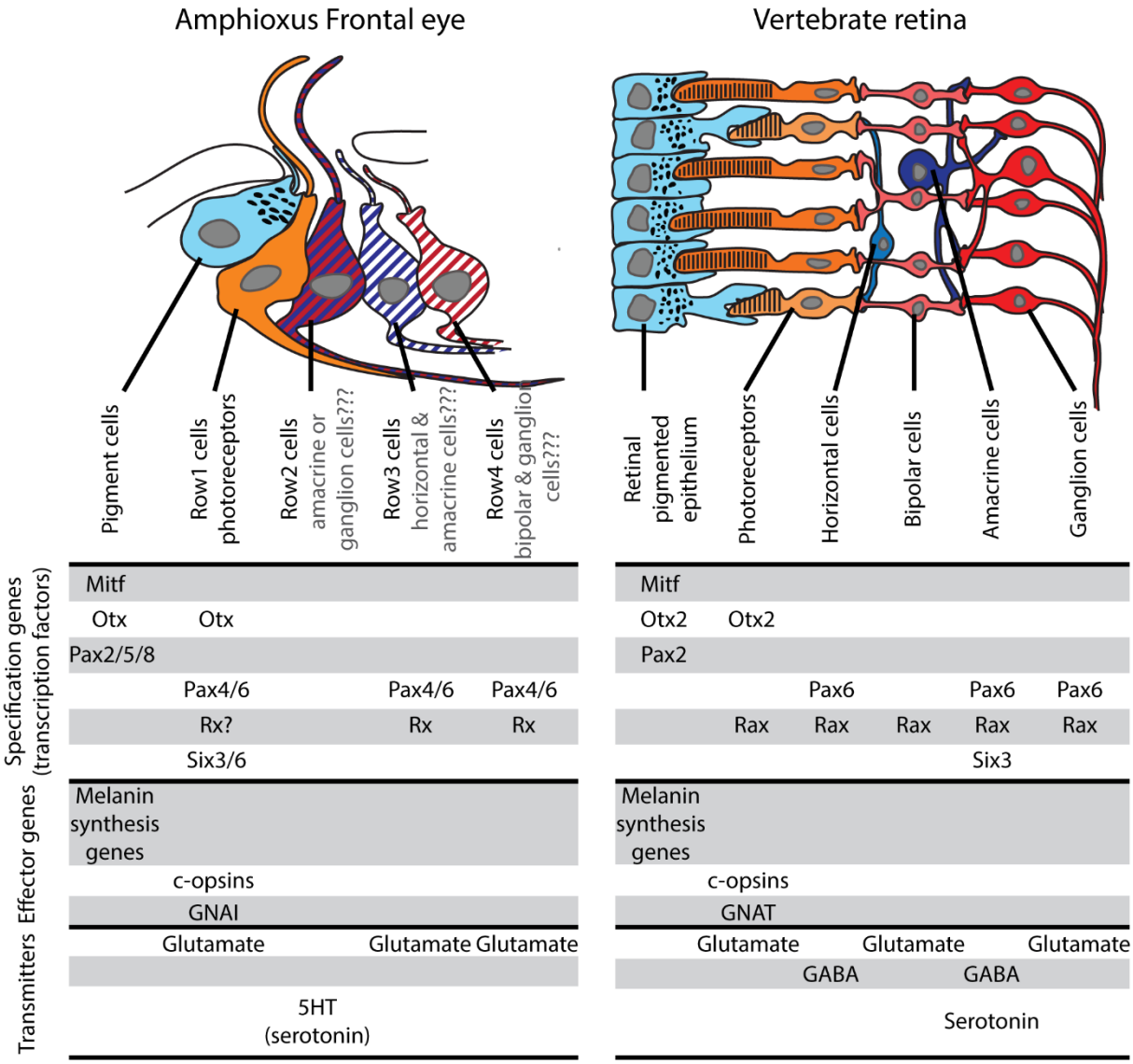

Fig.8 Schematic comparison of molecular fingerprint of amphioxus frontal eye and vertebrate retina (adapted from Pergner and Kozmik[54])

Proposed homologies between particular cell types in the amphioxus frontal eye and vertebrate retina are shown. For specification genes, only homeobox transcription factors are shown (only exception is Mitf, a member of basic helix-loop-helix transcription factors). Expression data for other than homeobox transcription factors in amphioxus frontal eye are missing in the literature. For proposed homologies between putative interneurons in amphioxus and vertebrate interneurons, data from EM analysis were also taken into account. Data for expression of amphioxus genes were taken from Kozmik, et al.[46], Kozmik, et al.[103] and Vopalensky, et al.[59]. EM data were taken from Lacalli[116]. Data for molecular fingerprint of vertebrate retinal cell types were taken from Bassett and Wallace[120], Kolb[115] and Swaroop, et al.[121]. GNAI and GNAT is alternative designation of $G_{\alpha}i$ and $G_{\alpha}t$ respectively.

Neural circuitry of amphioxus frontal eye probably represents ancestral chordate state

Despite the difficulties in finding the homology between the amphioxus frontal eye neurons and vertebrate retinal interneurons, our data opened a discussion about how the ancestral chordate visual circuitry looked like and what the vertebrate novelties in transmitting and processing visual inputs are. Our results showing the terminals of Row2 cells leading to putative amphioxus tegmentum (visual processing center), were later confirmed also by Candiani*, et al.*[105]. In 2015 Suzuki*, et al.*[122] compared the visual circuitry of larval and adult lamprey with visual circuitry of *B. lanceolatum*. Eyes of the larval lamprey are relatively simple, with only bi-layered retina and miss lens, being instead covered with translucent skin. During metamorphosis the eyes changed in the way, they resemble eyes of other vertebrates in having transparent lens and three neuronal layers in the retina. These changes influence also projecting neurons. In the larval lamprey the visual projecting neurons terminate in the Pax6 positive pretectal part of the brain. In adult lamprey, new visual projecting neurons develop, terminating in Pax2 and Engrailed (En) positive mesencephalon. Suzuki*, et al.*[122] proposed an evolutionary scenario, saying that development of photoreceptors in Otx and Pax6 positive brain region (in amphioxus and both larval and adult lamprey) and projections leading to Pax6 positive prosencephalic part of the brain (in amphioxus and lamprey larva) would represent ancestral chordate trait. The situation found in adult lamprey, projecting neurons terminating in mesencephalic tegmentum, would represent a vertebrate specific character. Recent study by Albuixech-Crespo*, et al.*[39], however, negated this hypothesis. The authors showed, that amphioxus cerebral vesicle does not evince only prosencephalic like characteristics (more specifically diencephalic), but also mesencephalic characters with hardly distinguishable borders. In this case, Row2 neurites would end in the mesencephalic part of the amphioxus cerebral vesicle, similarly as projecting neurons in adult lamprey. We took the analysis by Albuixech-Crespo*, et al.*[39] into account and added our proposition that this circuitry would represent the ancestral chordate state and situation found in larval lamprey would be an example of non-differentiated state[54]. Both scenarios are compared in Fig.9. The scenario by Albuixech-Crespo*, et al.*[39] seems to be more probable, mainly because of the depth of the analysis and amount of data collected. One must admit, that their thorough analysis was done only on one chosen developmental stage (late neurula) and may not cover changes that could occur in cerebral vesicle during later development and transition from neurula to larva. Yet, their scenario is also in concordance with the hypothesis raised by Holland[47] about existence of simple brain organizing centers in the amphioxus cerebral vesicle and thus arguing for the presence of prosencephalic and mesencephalic parts of cerebral vesicle (this was mentioned already in section 3.2.1 and shown in Fig.3 of this thesis).

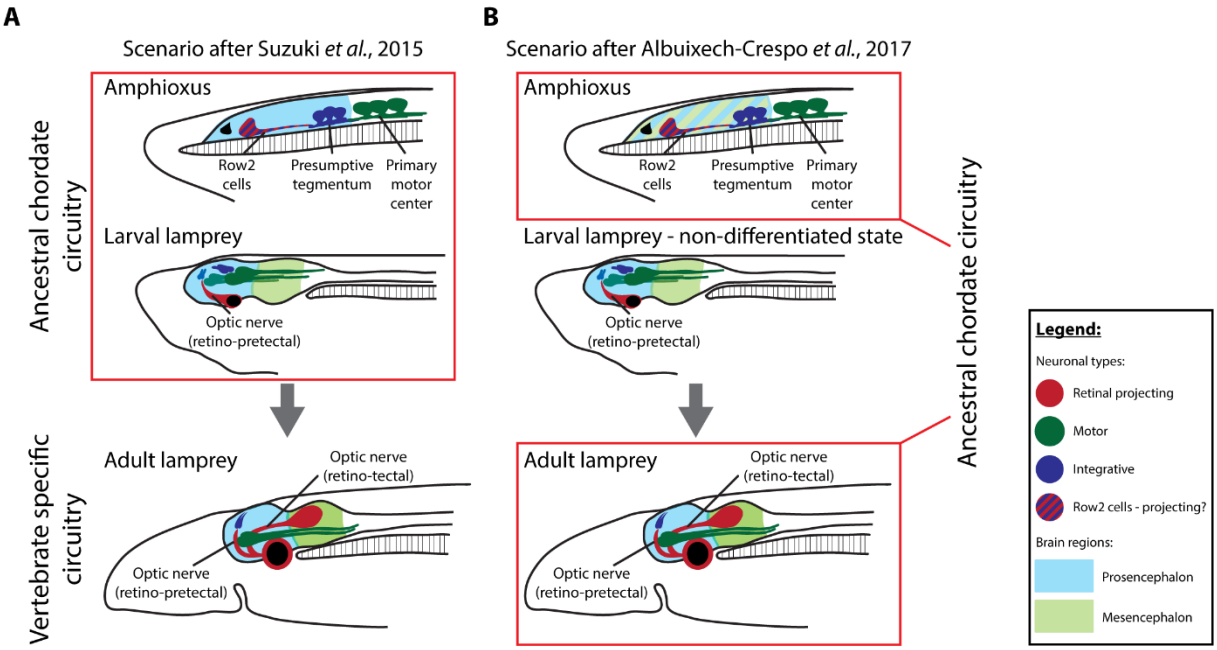

Fig.9 Hypotheses about evolution of ancestral visual circuitry (taken from Pergner and Kozmik[54])

In amphioxus, photoreceptors develop in Otx and Pax6 positive region and putative visual projecting neurons terminate in Pax6 positive region. In the larval lamprey the situation is similar as in amphioxus with photoreceptors arising in Otx and Pax6 positive region and optic nerve processes terminating in Pax6 positive brain region. On the other hand, in the adult lamprey optic nerve ends in mesencephalic region defined by expression of Pax2 and En. According to scenario proposed by Suzuki, et al.[122] ancestral chordate visual circuitry is the one where visual projecting neurons send their processes to Pax6 positive region of prosencephalon. This hyphothesis was built upon assumption that amphioxus cerebral vesicle is homologous to vertebrate prosencephalon and does not have mesencephalic character. More recent scenario by Albuixech-Crespo, et al.[39] takes into account data showing, that amphioxus cerebral vesicle evince characters of pros- and mesencephalon with hardly distinguishable borders. Based on these results the authors proposed that amphioxus visual circuitry might be similar to that of vertebrates, beginning with photoreceptors in prosencephalic part of the brain and terminating in mesencephalon. We accepted[54] this scenario in our work and added the suggestion that this circuitry might thus be ancestral to all chordates and circuitry of larval lamprey represents a not terminally differentiated state.

Vertebrate phototransduction cascade – variation on ancestral chordate themes

Our results uncovered expression of two distinct c-type opsins in amphioxus frontal eye photoreceptor cells[59]. Next, we detected expression of $G_{\alpha}i$, but not $G_{\alpha}o$ nor $G_{\alpha}q$ in the frontal eye photoreceptors[59]. Given that gene for transducing $G_{\alpha}t$ arose via tandem duplication of $G_{\alpha}i$ gene after split of cephalochordate (or maybe even urochordate) and vertebrate lineage[81,82], this gave some clues about ancestral chordate phototransduction cascade in visual ciliary photoreceptors. Lamb and Hunt[82] came up with a hypothesis on how phototransduction cascade in amphioxus might look like. This cascade starts with a c-type opsin and continues

through activation of $G_{\alpha}i$. This part is based on experimental data. Next steps are just hypothetical. $G_{\alpha}i$ would inhibit adenylate cyclase, which would result, together with constant action of phosphodiesterase, in decrease of intracellular cAMP, closure of CNG channels and probably end in cell hyperpolarization. Vertebrate phototransduction cascade starts with a c-type opsin and $G_{\alpha}t$ activation. Next, phosphodiesterase is activated, leading to decrease of cGMP levels and closure of CNG channels, resulting in cell hyperpolarization (both cascades are compare in Fig.10). Whether the amphioxus phototransduction cascade works as proposed and what the benefits of vertebrate specific phototransduction cascade are, needs to be determined. We assume, that we could gain some information from checking the coupling between amphioxus c-opsins and $G_{\alpha}i$ by the use of the modified cell-line based assay from our study about *T. cystophora* opsins[123].

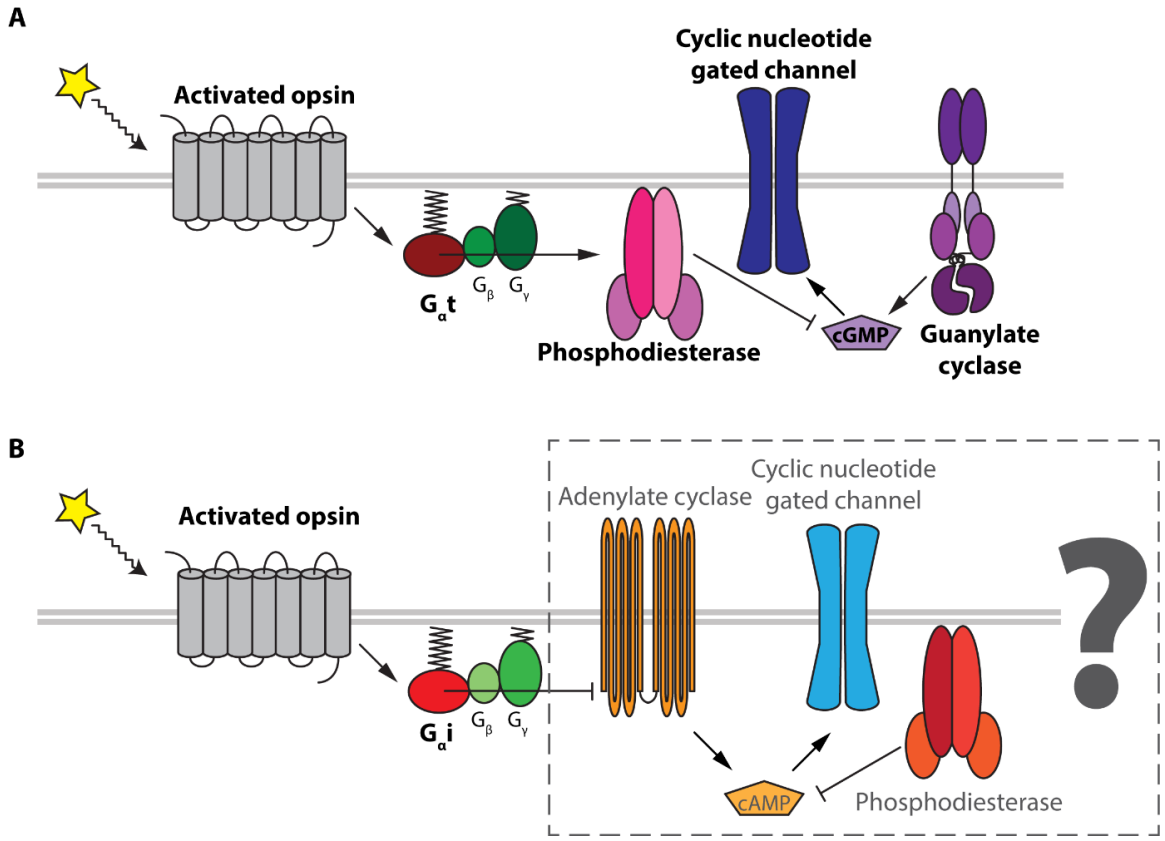

Fig.10 Comparison of the phototransduction cascade in ciliary photoreceptors of vertebrates and amphioxus (taken from Pergner and Kozmik[54])

A – *Phototransduction cascade in vertebrate ciliary photoreceptors. After excitation, the opsin activates $G_{\alpha}t$ (transducin). Next, phosphodiesterase is activated, which results in decrease of intracellular levels of cGMP, despite constant activity of guanylate cyclase. Due to the decrease of cGMP level, CNG channels are closed, which leads to photoreceptor hyperpolarization.*

B – *Proposed phototransduction cascade in amphioxus frontal eye photoreceptors. So far only presence of a c-type opsin and $G_{\alpha}i$ was shown in amphioxus. The rest of the proposed cascade is just speculation. After stimulation, the opsins activates $G_{\alpha}i$. $G_{\alpha}i$ inhibits adenylate cyclase, which leads, together with constant activity of phosphodiesterase, to intracellular cAMP decrease. Next, CNG channels are closed which results in cell hyperpolarization. This was proposed by Lamb and Hunt[82].*

Amphioxus opsins – cornerstones for studies of vertebrate-specific opsin adaptations

Marine animals usually have in their genome and express more opsin genes than terrestrial ones[88,123,124]. This is probably caused by the need of light responses in various conditions, mostly different depths, which results in rapid changes in light intensities. Amphioxus is not an exception to this rule. We have documented both redundancy and specificity in the use of opsins in different developmental stages and tissues of amphioxus. Our results imply, that amphioxus needs light stimuli for various physiological processes and not only for vision and regulation of circadian rhythms.

We identified 21 opsin genes plus one opsin pseudogene in the genome of *B. lanceolatum* and have corrected previous prediction of opsin genes in *B. floridae* to 21 functional opsin genes. In our studies we also documented expansion of some opsin groups in the genomes of three amphioxus species, namely *B. floridae*, *B. lanceolatum* and *B. belcheri*. Most notable was the expansion of Amphiop6 and Go opsins. The role of these opsins in amphioxus light-guided behavior remains to be examined. Some clues about the utilization of Go opsins for fine spectral tuning of photoreceptors came recently from the annelid *Platynereis dumerilii*[125]. Appart from the r-type opsins, one Go opsin was shown to be also expressed in *Platynereis* visual rhabdomeric photoreceptors. The authors showed, that animals with knocked-out Go opsin had reduced phototaxis to source of cyan light, which might be necessary, for example, for diurnal migration of *Platynereis* larvae[125]. Performing knock-outs in amphioxus is however still difficult and performing such complicated study will be challenging.

Previous studies showed that amphioxus opsins might be crucial for understanding the evolution of specific biochemical properties of vertebrate opsins[93,126,127]. Main focus was put mainly on switch of counterion position from E181 to E113. This switch seems to be a key event in the evolution of vertebrate opsins properties. The vertebrate opsins with counterion E113 are up to 50 times more efficient in activating the downstream signaling cascade than other opsins with counterion E181[126]. Opsins with counterion E113 also evince significant decrease of noise activity in dark. Additionally, loss of restriction on maintaining glutamate at position 181 enabled the switch to H181 and thus enabled the evolution of a red-sensitive opsin. All these facts were shown by mutational studies of the amphioxus, tunicate and vertebrate opsins[126,127] (results of both studies are summarized in Fig.10). The study in amphioxus was, however, done in 2004 and no amphioxus opsin with E or D at position 113 was then taken into account. Our data show, that several amphioxus opsin have D/E113 and most of them have D/E83 in their sequence. Whether these act as counterions needs to be addressed. Moreover amphioxus opsins were shown to be able to bind not only *11-cis*-retinal, but also all-*trans* retinal[128]. Vertebrate opsins show negligible binding affinity to all-*trans* retinal and higher affinity to *11-cis* retinal, which results in easier and faster recovery of the opsin after light stimulation[128]. Again this study was done before identification of more amphioxus opsins and mainly identification of other amphioxus c-type opsins might be jumping-off point for studies showing, whether this is really a vertebrate specific novelty.

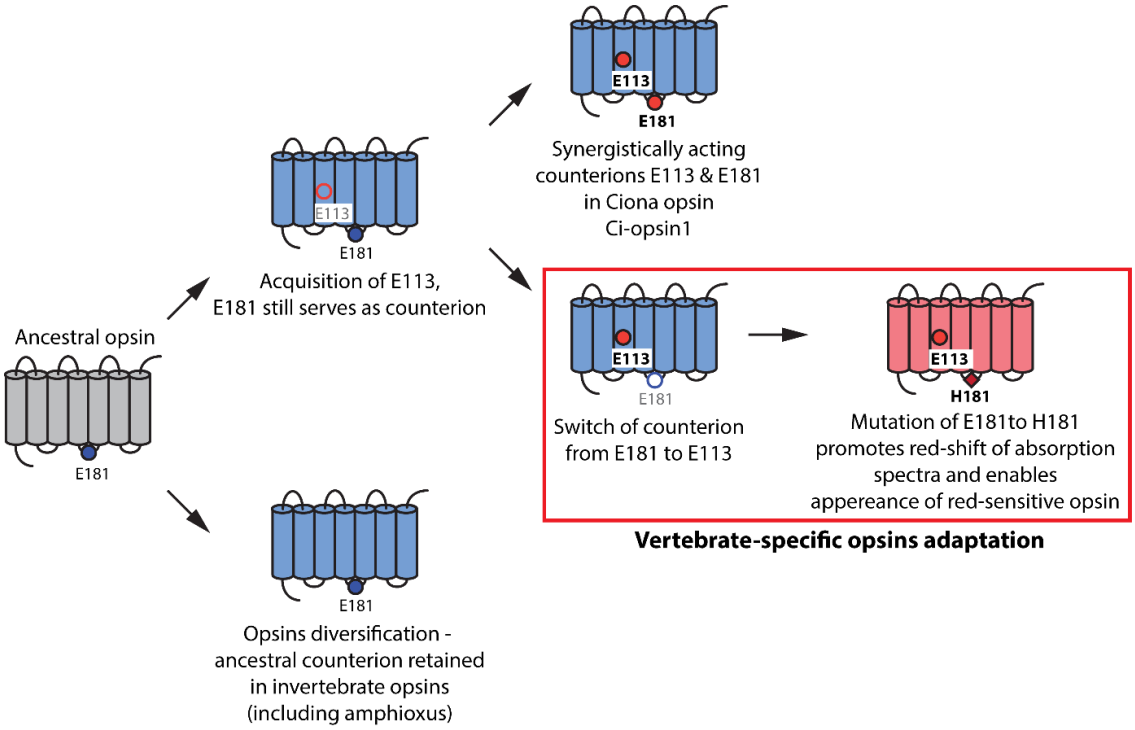

Fig.10 Gain of new properties of vertebrate opsins by switching of counterion position (taken from Pergner and Kozmik[54])
Proposed scenario for evolution of counterion position is shown. In most of the so far explored opsins, E181 serves as the counterion. In vertebrate c-type opsins, E113 serves as the counterion. This means, that ancestral opsin probably possessed counterion at position E181. Recently it was shown, that E113 and E181 serve as synergistically acting counterions in Ciona *opsin. This is in agreement with proposed evolutionary scenario – first E appeared at position 113 in olfactores´ (urochordates and vertebrates) ancestor opsins. Then a switch of counterion from E181 to E113 appeared. Lost constrains on aa present at position 181 led to change to histidine (H) and enabled a red-shift of vertebrate opsin sensitivity.*
Scheme adapted from Terakita, et al.[129] with addition of data from Kojima, et al.[127]

Of special interest might be the tripeptide variability of amphioxus opsins. Our analysis showed minor variation in tripeptide motif between more opsins of the same group, for example N (S/N/K) Q motif found in four amphioxus c-type opsins. On the other hand amphioxus Go opsins are highly variable in regard to their tripeptide sequence, having SEV, HKK, NQR, SKA or NSK tripeptides. What is the functional consequence of this variability needs to be addressed. Our data on *Tripedalia* opsins showed, that tripeptide sequence might not be crucial for opsin G_{α} subunit coupling (as in bovine rhodopsin), but rather might influence duration and intensity of opsin´s response to stimulation.

8. Conclusions

In this thesis I presented data on the photoreception and photoreceptive organs in the basal chordate amphioxus. Our investigations took advantage of a broad palette of methodological approaches used in our lab and other laboratories at the Institute of Molecular Genetics in Prague, as well as the possibility of working with live amphioxus in the laboratory at the Observatoire Océanologique de Banyuls sur mer. We were thus able to perform comprehensive analyses of various aspects of amphioxus photoreceptive organs and proteins involved in phototransduction cascade. The results can be summarized in several points:

- We were able to define the molecular fingerprint of developing amphioxus frontal eye. We showed that orthologs of genes involved in the development of vertebrate photoreceptors and RPE are also utilized for the development of amphioxus frontal eye. Moreover amphioxus frontal eye photoreceptors use similar, but not exactly the same, phototransduction cascade as photoreceptors in vertebrate eye. The difference can be explained by the need of additional improvement of ancestral chordate photoreceptors to be able to provide faster and more precise responses to light stimulation. This was enabled by the appearance of new G_{α} subunit of trimeric G proteins, the so called transducing, in the lineage leading to vertebrates. Presented data strengthen previously proposed homology between amphioxus cephalic visual organ, the frontal eye, and vertebrate lateral eye.

- We presented the advantages of the use of “home-made” antibodies raised specifically against proteins of a non-model organism, in evo-devo studies. We expect that our data will be jumping-off point for broadening the methodological toolkit

- We published the complete opsin repertoires of two amphioxus species *B. floridae* and *B. lanceolatum*. Amphioxus genome contains a large number of opsins, as is usual for marine organisms. Our expression analysis showed, that the opsins may be utilized for various functions, since some evinced for example highest expression rate in gonads and others in tissues around mouth or in tail fin, where no presence of photoreceptive cells was previously documented.

- We have used a cell-line based assay to document the biochemical properties of cnidarian opsins. We uncovered two opsins that signal via a G_{α}s-cAMP signaling cascade. Moreover we documented, for the first time, utilization of this cascade for vision guided behavior. Our assay can be modified to provide information about opsin coupling to other G_{α} subunits. This would allow checking of biochemical properties of more opsins in one standardized procedure.

9. References

1 Fernald, R. D. The evolution of eyes. *Brain, behavior and evolution* **50**, 253-259 (1997).

2 Hill, R. E. *et al.* Mouse small eye results from mutations in a paired-like homeobox-containing gene. *Nature* **354**, 522-525, doi:10.1038/354522a0 (1991).

3 Quiring, R., Walldorf, U., Kloter, U. & Gehring, W. J. Homology of the eyeless gene of Drosophila to the Small eye gene in mice and Aniridia in humans. *Science* **265**, 785-789 (1994).

4 Halder, G., Callaerts, P. & Gehring, W. J. Induction of ectopic eyes by targeted expression of the eyeless gene in Drosophila. *Science* **267**, 1788-1792 (1995).

5 Chow, R. L., Altmann, C. R., Lang, R. A. & Hemmati-Brivanlou, A. Pax6 induces ectopic eyes in a vertebrate. *Development* **126**, 4213-4222 (1999).

6 Gehring, W. J. & Ikeo, K. Pax 6: mastering eye morphogenesis and eye evolution. *Trends in genetics : TIG* **15**, 371-377 (1999).

7 Glardon, S., Holland, L. Z., Gehring, W. J. & Holland, N. D. Isolation and developmental expression of the amphioxus Pax-6 gene (AmphiPax-6): insights into eye and photoreceptor evolution. *Development* **125**, 2701-2710 (1998).

8 Arendt, D., Tessmar, K., de Campos-Baptista, M. I., Dorresteijn, A. & Wittbrodt, J. Development of pigment-cup eyes in the polychaete Platynereis dumerilii and evolutionary conservation of larval eyes in Bilateria. *Development* **129**, 1143-1154 (2002).

9 Blackburn, D. C. *et al.* Isolation and expression of Pax6 and atonal homologues in the American horseshoe crab, Limulus polyphemus. *Developmental dynamics : an official publication of the American Association of Anatomists* **237**, 2209-2219, doi:10.1002/dvdy.21634 (2008).

10 Piatigorsky, J. A Genetic Perspective on Eye Evolution: Gene Sharing, Convergence and Parallelism. *Evolution: Education and Outreach* **1**, 403-414.

11 Delsuc, F., Brinkmann, H., Chourrout, D. & Philippe, H. Tunicates and not cephalochordates are the closest living relatives of vertebrates. *Nature* **439**, 965-968, doi:10.1038/nature04336 (2006).

12 Bertrand, S. & Escriva, H. Evolutionary crossroads in developmental biology: amphioxus. *Development* **138**, 4819-4830, doi:10.1242/dev.066720 (2011).

13 Willey, A. Amphioxus and the Ancestry of the Vertebrates. (1894).

14 Jandzik, D. *et al.* Evolution of the new vertebrate head by co-option of an ancient chordate skeletal tissue. *Nature* **518**, 534-537, doi:10.1038/nature14000 (2015).

15 Putnam, N. H. *et al.* The amphioxus genome and the evolution of the chordate karyotype. *Nature* **453**, 1064-1071, doi:10.1038/nature06967 (2008).

16 Holland, L. Z. *et al.* The amphioxus genome illuminates vertebrate origins and cephalochordate biology. *Genome research* **18**, 1100-1111, doi:10.1101/gr.073676.107 (2008).

17 Acemel, R. D. *et al.* A single three-dimensional chromatin compartment in amphioxus indicates a stepwise evolution of vertebrate Hox bimodal regulation. *Nature genetics* **48**, 336-341, doi:10.1038/ng.3497 (2016).

18 Huang, S. *et al.* Discovery of an Active RAG Transposon Illuminates the Origins of V(D)J Recombination. *Cell* **166**, 102-114, doi:10.1016/j.cell.2016.05.032 (2016).

19 Fuentes, M. *et al.* Insights into spawning behavior and development of the European amphioxus (Branchiostoma lanceolatum). *Journal of experimental zoology. Part B, Molecular and developmental evolution* **308**, 484-493, doi:10.1002/jez.b.21179 (2007).

20 Li, G., Shu, Z. & Wang, Y. Year-Round Reproduction and Induced Spawning of Chinese Amphioxus, *Branchiostoma belcheri*, in Laboratory. *PloS one* **e75461**, doi:10.1371/journal.pone.0075461 (2013).

21 Holland, L. Z. & Yu, J. K. Cephalochordate (amphioxus) embryos: procurement, culture, and basic methods. *Methods in cell biology* **74**, 195-215 (2004).

22 Holland, N. D., Holland, L. Z. & Heimberg, A. Hybrids between the Florida amphioxus (Branchiostoma floridae) and the Bahamas lancelet (Asymmetron lucayanum): developmental morphology and chromosome counts. *The Biological bulletin* **228**, 13-24, doi:10.1086/BBLv228n1p13 (2015).

23 Holland, N. D. & Holland, L. Z. Laboratory spawning and development of the Bahama lancelet, Asymmetron lucayanum (cephalochordata): fertilization through feeding larvae. *The Biological bulletin* **219**, 132-141, doi:10.1086/BBLv219n2p132 (2010).

24 Kozmikova, I. & Kozmik, Z. Gene regulation in amphioxus: An insight from transgenic studies in amphioxus and vertebrates. *Marine genomics* **24 Pt 2**, 159-166, doi:10.1016/j.margen.2015.06.003 (2015).

25 Huang, S. *et al.* Decelerated genome evolution in modern vertebrates revealed by analysis of multiple lancelet genomes. *Nature communications* **5**, 5896, doi:10.1038/ncomms6896 (2014).

26 Suzuki, M. M. & Satoh, N. Genes expressed in the amphioxus notochord revealed by EST analysis. *Developmental biology* **224**, 168-177, doi:10.1006/dbio.2000.9796 (2000).

27 Yang, K. Y. *et al.* Transcriptome analysis of different developmental stages of amphioxus reveals dynamic changes of distinct classes of genes during development. *Scientific reports* **6**, 23195, doi:10.1038/srep23195 (2016).

28 Yue, J. X., Yu, J. K., Putnam, N. H. & Holland, L. Z. The transcriptome of an amphioxus, Asymmetron lucayanum, from the Bahamas: a window into chordate evolution. *Genome biology and evolution* **6**, 2681-2696, doi:10.1093/gbe/evu212 (2014).

29 Oulion, S., Bertrand, S., Belgacem, M. R., Le Petillon, Y. & Escriva, H. Sequencing and analysis of the Mediterranean amphioxus (Branchiostoma lanceolatum) transcriptome. *PloS one* **7**, e36554, doi:10.1371/journal.pone.0036554 (2012).

30 Kozmikova, I., Candiani, S., Fabian, P., Gurska, D. & Kozmik, Z. Essential role of Bmp signaling and its positive feedback loop in the early cell fate evolution of chordates. *Developmental biology* **382**, 538-554, doi:10.1016/j.ydbio.2013.07.021 (2013).

31 Soukup, V. *et al.* The Nodal signaling pathway controls left-right asymmetric development in amphioxus. *EvoDevo* **6**, 5, doi:10.1186/2041-9139-6-5 (2015).

32 Li, G. *et al.* Cerberus-Nodal-Lefty-Pitx signaling cascade controls left-right asymmetry in amphioxus. *Proceedings of the National Academy of Sciences of the United States of America* **114**, 3684-3689, doi:10.1073/pnas.1620519114 (2017).

33 Le Petillon, Y. *et al.* Nodal/Activin Pathway is a Conserved Neural Induction Signal in Chordates. *Nature ecology & evolution* **1**, 1192-1200, doi:10.1038/s41559-017-0226-3 (2017).

34 Kozmikova, I. & Yu, J. K. Dorsal-ventral patterning in amphioxus: current understanding, unresolved issues, and future directions. *Int. J. Dev. Biol.*, 601 - 610, doi:10.1387/ijdb.170236ik (2017).

35 Panopoulou, G. D., Clark, M. D., Holland, L. Z., Lehrach, H. & Holland, N. D. AmphiBMP2/4, an amphioxus bone morphogenetic protein closely related to Drosophila decapentaplegic and vertebrate BMP2 and BMP4: insights into evolution of dorsoventral axis specification. *Developmental dynamics : an official publication of the American Association of Anatomists* **213**, 130-139, doi:10.1002/(SICI)1097-0177(199809)213:1<130::AID-AJA13>3.0.CO;2-6 (1998).

36 Yong, L. W., Bertrand, S., Yu, J. K., Escriva, H. & Holland, N. D. Conservation of BMP2/4 expression patterns within the clade Branchiostoma (amphioxus): Resolving interspecific discrepancies. *Gene expression patterns : GEP* **25-26**, 71-75, doi:10.1016/j.gep.2017.06.004 (2017).

37 Kaji, T., Reimer, J. D., Morov, A. R., Kuratani, S. & Yasui, K. Amphioxus mouth after dorso-ventral inversion. *Zoological letters* **2**, 2, doi:10.1186/s40851-016-0038-3 (2016).

38 Wicht, H. & Lacalli, T. C. The nervous system of amphioxus: structure, development and evolutionary significance. *Canadian Journal of Zoology* **83**, 122-150 (2005).

39 Albuixech-Crespo, B. *et al.* Molecular regionalization of the developing amphioxus neural tube challenges major partitions of the vertebrate brain. *PLoS biology* **15**, e2001573, doi:10.1371/journal.pbio.2001573 (2017).

40 Guthrie, D. M. The Physiology and Structure of the Nervous System of Amphioxus (the Lancelet) *Branchiostoma Lanceolatum* Pallas. *Symposia of the Zoological Society of London (Protochordates)* **36** (1975).

41 Parker, G. H. The sensory reactions of amphioxus. *Proceedings of the American Academy of Arts and Sciences* **43**, 415-455, doi:10.2307/20022358 (1908).

42 Lacalli, T. C. Basic features of the ancestral chordate brain: a protochordate perspective. *Brain research bulletin* **75**, 319-323 (2008).

43 Holland, L. Z. Chordate roots of the vertebrate nervous system: expanding the molecular toolkit. *Nature reviews. Neuroscience* **10**, 736-746, doi:10.1038/nrn2703 (2009).

44 Takahashi, T. The evolutionary origins of vertebrate midbrain and MHB: insights from mouse, amphioxus and ascidian Dmbx homeobox genes. *Brain research bulletin* **66**, 510-517, doi:10.1016/j.brainresbull.2005.03.013 (2005).

45 Murakami, Y., Uchida, K., Rijli, F. M. & Kuratani, S. Evolution of the brain developmental plan: Insights from agnathans. *Developmental biology* **280**, 249-259, doi:10.1016/j.ydbio.2005.02.008 (2005).

46 Kozmik, Z. *et al.* Characterization of an amphioxus paired box gene, AmphiPax2/5/8: developmental expression patterns in optic support cells, nephridium, thyroid-like structures and pharyngeal gill slits, but not in the midbrain-hindbrain boundary region. *Development* **126**, 1295-1304 (1999).

47 Holland, L. Z. Evolution of new characters after whole genome duplications: insights from amphioxus. *Seminars in cell & developmental biology* **24**, 101-109, doi:10.1016/j.semcdb.2012.12.007 (2013).

48 Pani, A. M. *et al.* Ancient deuterostome origins of vertebrate brain signalling centres. *Nature* **483**, 289-294, doi:10.1038/nature10838 (2012).

49 Wickstead, J. H. & Bone, Q. Ecology of Acraniate Larvae. *Nature* **184**, 1849-1851 (1959).

50 Chin, T. G. Studies on the Biology of the Amoy Amphioxus *Branchiostoma belcheri* Gray. *The Philippine Journal of Science* **76** (1941).

51 Parker, G. H. The Sensory Reactions of Amphioxus. *Proceedings of the American Academy of Arts and Sciences* **43**, 415-455 (1908).

52 Schomerus, C. *et al.* Nocturnal Behavior and Rhythmic *Period* Gene Expression in a Lancelet, *Branchiostoma lanceolatum*. *Journal of Biological Rhythms* **23**, 170-181, doi:10.1177/0748730407313363 (2008).

53 Holland, N. D. Spawning periodicity of the lancelet, *Asymmetron lucayanum* (Cephalochordata), in Bihimi, Bahamas. *Italian Journal of Zoology* **78**, 478-486 (2011).

54 Pergner, J. & Kozmik, Z. Amphioxus photoreceptors - insights into the evolution of vertebrate opsins, vision and circadian rhythmicity. *Int. J. Dev. Biol.*, 665-681, doi:doi: 10.1387/ijdb.170230zk (2017).

55 Stokes, M. D. & Holland, N. D. Ciliary Hovering in Larval Lancelets (=Amphioxus). *Biological Bulletin* **188**, 231-233 (1995).

56 Webb, J. E. On the feeding and behavior of the larva of *Branchiostoma lanceolatum*. *Marine Biology* **3**, 58-72, doi:10.1007/BF00355593 (1969).

57 Costa, G. Annuario zoologico. Cenni Zoologici ossia descrizione sommaria delle specie nuove di animali discoperti in diverse contrade del regno nell´ anno 1834. *cited from Willey 1894* (1834).

58 Hesse, R. Untersuchungen über die Organe der Lichtempfindung bei niederen Thieren. IV. Die sehorgane des Amphioxus. *Zeitschrift für Wissenschaftliche Zoologie*, 456-464 (1898).

59 Vopalensky, P. *et al.* Molecular analysis of the amphioxus frontal eye unravels the evolutionary origin of the retina and pigment cells of the vertebrate eye. *Proceedings of the National Academy of Sciences of the United States of America* **109**, 15383-15388, doi:10.1073/pnas.1207580109 (2012).

60 Bozzo, M. *et al.* The HMGA gene family in chordates: evolutionary perspectives from amphioxus. *Development genes and evolution* **227**, 201-211, doi:10.1007/s00427-017-0581-8 (2017).

61 Lacalli, T. C. Sensory systems in amphioxus: a window on the ancestral chordate condition. *Brain, behavior and evolution* **64**, 148-162, doi:10.1159/000079744 (2004).

62 Darwin, C. On the Origin of Species by Means of Natural Selection, or the Preservation of Favoured Races in the Struggle for Life. (1859).

63 Joseph, H. Über eigentümliche Zellstrukturen im Zentralnervensystem von Amphioxus. *Verhandlungen der Anatomischen Gesellschaft* (1904).

64 Kohl, C. Einige Bermerkungen über Sinnesorgane des Amphioxus lanceolatus. *Zoologischer Anzeiger* **13**, 182-185 (1890).

65 Lacalli, T. C. Looking into eye evolution: amphioxus points the way. *Pigment Cell & Melanoma Research* **26**, doi:10.1111/pcmr.12057 (2012).

66 Terakita, A. The opsins. *Genome biology* **6**, 213, doi:10.1186/gb-2005-6-3-213 (2005).

67 Rivera, A. S. *et al.* Blue-light-receptive cryptochrome is expressed in a sponge eye lacking neurons and opsin. *The Journal of experimental biology* **215**, 1278-1286, doi:10.1242/jeb.067140 (2012).

68 Muller, W. E. *et al.* Cryptochrome in sponges: a key molecule linking photoreception with phototransduction. *The journal of histochemistry and cytochemistry : official journal of the Histochemistry Society* **61**, 814-832, doi:10.1369/0022155413502652 (2013).

69 Gong, J. *et al.* The C. elegans Taste Receptor Homolog LITE-1 Is a Photoreceptor. *Cell* **167**, 1252-1263 e1210, doi:10.1016/j.cell.2016.10.053 (2016).

70 Kutta, R. J., Archipowa, N., Johannissen, L. O., Jones, A. R. & Scrutton, N. S. Vertebrate Cryptochromes are Vestigial Flavoproteins. *Scientific reports* **7**, 44906, doi:10.1038/srep44906 (2017).

71 Feuda, R., Rota-Stabelli, O., Oakley, T. H. & Pisani, D. The comb jelly opsins and the origins of animal phototransduction. *Genome biology and evolution* **6**, 1964-1971, doi:10.1093/gbe/evu154 (2014).

72 Fredriksson, R., Lagerstrom, M. C., Lundin, L. G. & Schioth, H. B. The G-protein-coupled receptors in the human genome form five main families. Phylogenetic analysis, paralogon groups, and fingerprints. *Molecular pharmacology* **63**, 1256-1272, doi:10.1124/mol.63.6.1256 (2003).

73 Hauser, A. S., Attwood, M. M., Rask-Andersen, M., Schioth, H. B. & Gloriam, D. E. Trends in GPCR drug discovery: new agents, targets and indications. *Nature reviews. Drug discovery* **16**, 829-842, doi:10.1038/nrd.2017.178 (2017).

74 Palczewski, K. & Orban, T. From atomic structures to neuronal functions of g protein-coupled receptors. *Annual review of neuroscience* **36**, 139-164, doi:10.1146/annurev-neuro-062012-170313 (2013).

75 Palczewski, K. *et al.* Crystal structure of rhodopsin: A G protein-coupled receptor. *Science* **289**, 739-745 (2000).

76 Terakita, A. The opsins. *Genome biology* **6**, 213, doi:10.1186/gb-2005-6-3-213 (2005).

77 Porter, M. L. *et al.* Shedding new light on opsin evolution. *Proceedings. Biological sciences* **279**, 3-14, doi:10.1098/rspb.2011.1819 (2012).

78 Sakmar, T. P., Franke, R. R. & Khorana, H. G. Glutamic acid-113 serves as the retinylidene Schiff base counterion in bovine rhodopsin. *Proceedings of the National Academy of Sciences of the United States of America* **86**, 8309-8313 (1989).

79 Marin, E. P. *et al.* The amino terminus of the fourth cytoplasmic loop of rhodopsin modulates rhodopsin-transducin interaction. *The Journal of biological chemistry* **275**, 1930-1936 (2000).

80 Choe, H. W. *et al.* Crystal structure of metarhodopsin II. *Nature* **471**, 651-655, doi:10.1038/nature09789 (2011).

81 Lamb, T. D. *et al.* Evolution of Vertebrate Phototransduction: Cascade Activation. *Molecular biology and evolution* **33**, 2064-2087, doi:10.1093/molbev/msw095 (2016).

82 Lamb, T. D. & Hunt, D. M. Evolution of the vertebrate phototransduction cascade activation steps. *Developmental biology*, doi:10.1016/j.ydbio.2017.03.018 (2017).

83 Lamb, T. D. Evolution of phototransduction, vertebrate photoreceptors and retina. *Progress in retinal and eye research* **36**, 52-119, doi:10.1016/j.preteyeres.2013.06.001 (2013).

84 Fernald, R. D. Casting a genetic light on the evolution of eyes. *Science* **313**, 1914-1918, doi:10.1126/science.1127889 (2006).

85 Kojima, D. *et al.* A novel Go-mediated phototransduction cascade in scallop visual cells. *The Journal of biological chemistry* **272**, 22979-22982 (1997).

86 Koyanagi, M. *et al.* Jellyfish vision starts with cAMP signaling mediated by opsin-G(s) cascade. *Proceedings of the National Academy of Sciences of the United States of America* **105**, 15576-15580, doi:10.1073/pnas.0806215105 (2008).

87 Plachetzki, D. C., Degnan, B. M. & Oakley, T. H. The origins of novel protein interactions during animal opsin evolution. *PloS one* **2**, e1054, doi:10.1371/journal.pone.0001054 (2007).

88 Suga, H., Schmid, V. & Gehring, W. J. Evolution and functional diversity of jellyfish opsins. *Current biology : CB* **18**, 51-55, doi:10.1016/j.cub.2007.11.059 (2008).

89 Plachetzki, D. C., Fong, C. R. & Oakley, T. H. The evolution of phototransduction from an ancestral cyclic nucleotide gated pathway. *Proceedings. Biological sciences* **277**, 1963-1969, doi:10.1098/rspb.2009.1797 (2010).

90 Feuda, R., Hamilton, S. C., McInerney, J. O. & Pisani, D. Metazoan opsin evolution reveals a simple route to animal vision. *Proceedings of the National Academy of Sciences of the United States of America* **109**, 18868-18872, doi:10.1073/pnas.1204609109 (2012).

91 Pisani, D. *et al.* Genomic data do not support comb jellies as the sister group to all other animals. *Proceedings of the National Academy of Sciences of the United States of America* **112**, 15402-15407, doi:10.1073/pnas.1518127112 (2015).

92 Whelan, N. V. *et al.* Ctenophore relationships and their placement as the sister group to all other animals. *Nature ecology & evolution* **1**, 1737-1746, doi:10.1038/s41559-017-0331-3 (2017).

93 Koyanagi, M., Terakita, A., Kubokawa, K. & Shichida, Y. Amphioxus homologs of Go-coupled rhodopsin and peropsin having 11-cis- and all-trans-retinals as their chromophores. *FEBS letters* **531**, 525-528 (2002).

94 Lacalli., T. C., Holland., N. D. & West, J. E. Landmarks in the Anterior Central Nervous System of Amphioxus Larvae. *Philosophical Transactions of the Royal Society B: Biological Sciences* **344**, 165-185 (1994).

95 Nakao, T. On the Fine Structure of the Amphioxus Photoreceptor. *The Tohoku journal of experimental medicine* **82**, 349-363 (1964).

96 Meves, A. Elektronmikroskopische Untersuchungen über die Zytoarchitektur des Gehirns von *Branchiostoma lanceolatum*. *Zeitschrift fur Zellforschung und mikroskopische Anatomie* **139**, 511-532 (1973).

97 Eakin, R. M. & Westfall, J. A. Fine structure of photoreceptors in Amphioxus. *Journal of ultrastructure research* **6**, 531-539 (1962).

98 Welsch, U. [The ultrastructure of the cells of Joseph in the brain of Amphioxus]. *Zeitschrift fur Zellforschung und mikroskopische Anatomie* **86**, 252-261 (1968).

99 Watanabe, T. & Yoshida, M. Morphological and histochemical studies on Joseph cells of amphioxus, Branchiostoma belcheri Gray. *Experimental biology* **46**, 67-73 (1986).

100 Ruiz, M. S. & Anadon, R. Some considerations on the fine structure of rhabdomeric photoreceptors in the amphioxus, Branchiostoma lanceolatum (Cephalochordata). *Journal fur Hirnforschung* **32**, 159-164 (1991).

101 Ruiz, S. & Anadon, R. The fine structure of lamellate cells in the brain of amphioxus (Branchiostoma lanceolatum, Cephalochordata). *Cell and tissue research* **263**, 597-600 (1991).

102 Williams, N. A. & Holland, P. W. H. Old head on young shoulders. *Nature* **383**, doi:10.1038/383490a0 (1996).

103 Kozmik, Z. *et al.* Pax-Six-Eya-Dach network during amphioxus development: conservation in vitro but context specificity in vivo. *Developmental biology* **306**, 143-159, doi:10.1016/j.ydbio.2007.03.009 (2007).

104 Kozmik, Z. *et al.* Assembly of the cnidarian camera-type eye from vertebrate-like components. *Proceedings of the National Academy of Sciences of the United States of America* **105**, 8989-8993, doi:10.1073/pnas.0800388105 (2008).

105 Candiani, S., Moronti, L., Ramoino, P., Schubert, M. & Pestarino, M. A neurochemical map of the developing amphioxus nervous system. *BMC neuroscience* **13**, 59, doi:10.1186/1471-2202-13-59 (2012).

106 Igawa, T. *et al.* Evolutionary history of the extant amphioxus lineage with shallow-branching diversification. *Scientific reports* **7**, 1157, doi:10.1038/s41598-017-00786-5 (2017).

107 Banyai, L. & Patthy, L. Putative extremely high rate of proteome innovation in lancelets might be explained by high rate of gene prediction errors. *Scientific reports* **6**, 30700, doi:10.1038/srep30700 (2016).

108 Yuan, S., Ruan, J., Huang, S., Chen, S. & Xu, A. Amphioxus as a model for investigating evolution of the vertebrate immune system. *Developmental and comparative immunology* **48**, 297-305, doi:10.1016/j.dci.2014.05.004 (2015).

109 Horie, T., Orii, H. & Nakagawa, M. Structure of ocellus photoreceptors in the ascidian Ciona intestinalis larva as revealed by an anti-arrestin antibody. *Journal of neurobiology* **65**, 241-250, doi:10.1002/neu.20197 (2005).

110 Lemaire, P. Evolutionary crossroads in developmental biology: the tunicates. *Development* **138**, 2143-2152, doi:10.1242/dev.048975 (2011).

111 Davis, T. L. & Rebay, I. Master regulators in development: Views from the Drosophila retinal determination and mammalian pluripotency gene networks. *Developmental biology* **421**, 93-107, doi:10.1016/j.ydbio.2016.12.005 (2017).

112 Brzezinski, J. A. & Reh, T. A. Photoreceptor cell fate specification in vertebrates. *Development* **142**, 3263-3273, doi:10.1242/dev.127043 (2015).

113 Klimova, L. & Kozmik, Z. Stage-dependent requirement of neuroretinal Pax6 for lens and retina development. *Development* **141**, 1292-1302, doi:10.1242/dev.098822 (2014).

114 Zagozewski, J. L., Zhang, Q., Pinto, V. I., Wigle, J. T. & Eisenstat, D. D. The role of homeobox genes in retinal development and disease. *Developmental biology* **393**, 195-208, doi:10.1016/j.ydbio.2014.07.004 (2014).

115 Kolb, H. Neurotransmitters in the Retina by Helga Kolb. *Kolb H, Fernandez E, Nelson R, editors. Webvision: The Organization of the Retina and Visual System [Internet]. Salt Lake City (UT): University of Utah Health Sciences Center; 1995-. Available from: http://webvision.med.utah.edu/book/part-iv-neurotransmitters-in-the-retina-2/part-iv-neurotransmitters-in-the-retina/ (updated 2011).* (2011).

116 Lacalli, T. C. Frontal eye circuitry, rostral sensory pathways and brain organization in amphioxus larvae: evidence from 3D reconstructions. *Philosophical Transactions of the Royal Society B: Biological Sciences* **351**, 243-263 (1996).

117 Bozzo, M., Pergner, J., Kozmik, Z. & Kozmikova, I. Novel polyclonal antibodies as a useful tool for expression studies in amphioxus embryos. *Int. J. Dev. Biol.*, 793-800, doi:10.1387/ijdb.170259ik (2017).

118 Lacalli, T. C. The dorsal compartment locomotory control system in amphioxus larvae. *Journal of morphology* **252**, 227-237, doi:10.1002/jmor.1101 (2002).

119 Lacalli, T. & Candiani, S. Locomotory control in amphioxus larvae: new insights from neurotransmitter data. *EvoDevo* **8**, 4, doi:10.1186/s13227-017-0067-9 (2017).

120 Bassett, E. A. & Wallace, V. A. Cell fate determination in the vertebrate retina. *Trends in neurosciences* **35**, 565-573, doi:10.1016/j.tins.2012.05.004 (2012).
121 Swaroop, A., Kim, D. & Forrest, D. Transcriptional regulation of photoreceptor development and homeostasis in the mammalian retina. *Nature reviews. Neuroscience* **11**, 563-576, doi:10.1038/nrn2880 (2010).
122 Suzuki, D. G., Murakami, Y., Escriva, H. & Wada, H. A comparative examination of neural circuit and brain patterning between the lamprey and amphioxus reveals the evolutionary origin of the vertebrate visual center. *The Journal of comparative neurology* **523**, 251-261, doi:10.1002/cne.23679 (2015).
123 Liegertova, M. *et al.* Cubozoan genome illuminates functional diversification of opsins and photoreceptor evolution. *Scientific reports* **5**, 11885, doi:10.1038/srep11885 (2015).
124 Biscontin, A. *et al.* The opsin repertoire of the Antarctic krill Euphausia superba. *Marine genomics* **29**, 61-68, doi:10.1016/j.margen.2016.04.010 (2016).
125 Guhmann, M. *et al.* Spectral Tuning of Phototaxis by a Go-Opsin in the Rhabdomeric Eyes of Platynereis. *Current biology : CB* **25**, 2265-2271, doi:10.1016/j.cub.2015.07.017 (2015).
126 Terakita, A. *et al.* Counterion displacement in the molecular evolution of the rhodopsin family. *Nature structural & molecular biology* **11**, 284-289, doi:10.1038/nsmb731 (2004).
127 Kojima, K. *et al.* Evolutionary steps involving counterion displacement in a tunicate opsin. *Proceedings of the National Academy of Sciences of the United States of America* **114**, 6028-6033, doi:10.1073/pnas.1701088114 (2017).
128 Tsukamoto, H., Terakita, A. & Shichida, Y. A rhodopsin exhibiting binding ability to agonist all-trans-retinal. *Proceedings of the National Academy of Sciences of the United States of America* **102**, 6303-6308, doi:10.1073/pnas.0500378102 (2005).
129 Terakita, A., Kawano-Yamashita, E. & Koyanagi, M. Evolution and diversity of opsins. . *WIREs Membrane Transport and Signaling* **1**, 104-111, doi:10.1002/wmts.6 (2012).